Analyzing the Behavior and Reactions of Mercury in the Solid Phase of a Flue-Gas-Desulfurization Sludge

Von der Fakultät für Ingenieurwissenschaften, Abteilung Maschinenbau und Verfahrenstechnik der
Universität Duisburg-Essen
zur Erlangung des akademischen Grades

einer
Doktorin der Ingenieurwissenschaften

Dr.-Ing.

genehmigte Dissertation

von

Isabelle Klöfer
aus
Wiesbaden

Gutachter:

Univ.-Prof. Dr.-Ing. Dieter Bathen

Univ.-Prof. Dr.-Ing. Stefan Panglisch

Tag der mündlichen Prüfung: 11. Dezember 2023

I. Acknowledgements

This work was conducted during my work as scientist at the Institute of Energy and Environmental Engineering e. V.(Iuta) with the funding of the AIF as part of the IGF project 20388 BG.

First and foremost, I would like to thank Prof. Dr. Ing. Dieter Bathen and the Institute of Energy and Environmental Engineering e. V. for their support of this work.

Many thanks also go to my colleagues, my students and laboratory technicians at the Institute of Energy and Environmental Engineering e. V. without whom the work would never have been finished. Furthermore, I would like to thank the industrial partners of the BG Project for their input and the discussions at our six-monthly meetings.

This work was funded by the AIF and I would like to express my gratitude for the possibility of conducting my research.

In addition, I would like to express my thanks to the m3 Mentoring program of the Research Academy Ruhr for the additional support of my work. Especially I would like to thank my mentor, she always had a sympathetic ear and good advice for me.

Finally, I would like to thank my family and friends for their loving support, understanding and believe in me during this adventure.

This work is for my son, for him to see that anything is possible, if you believe in it.

Düsseldorf, 05. January 2024 Isabelle Klöfer

II. Content

III. List of abbreviations

Table 1 List of Latin letters

Figure	Unit	Description
A		Component
A	J	Free Energy
A_m	$kg^{1/2}$ $mol^{-1/2}$	Debye-Hückel constant
a_i		Activity of component i
A		Border of derivation of the interval of X_2
B		Component
c_i	mol L^{-1}	Concentration of component i
c^0	mol L^{-1}	1 mol L^{-1}
c_0	mol L^{-1}	Starting concentration
D	m^2 s^{-1}	Diffusion coefficient
E	V	Electromotive force
e^-		Electron
E^0	V	Electromotive force for standard conditions
E_A	J mol^{-1}	Activation Energy
F	C mol^{-1}	Faraday constant
f_i		Activity coefficient of component i
G	J	Free Enthalpy
G^0	J	Free Enthalpy for standard conditions
H	J	Enthalpy
H_R	J	Reaction Enthalpy
I_m	mol kg^{-1}	Ionic strength calculated with the molality
$J_{molecule}$		Rate of vaporization
K	-	Equilibrium (stability) constant
K		Correction factor for the systematical error
K	mol $s^{-1}L^{-1}$	Reaction velocity constant
M	g mol^{-1}	Molar mass
M	G	Mass
m_i	mol kg^{-1}	Molality of component i
N		Number of samples
N_A	mol^{-1}	Avogadro constant
n_i	Mol	Amount of substance of component i
P	Pa	Pressure

Figure	Unit	Description
p_{eq}	Pa	Equilibrium pressure
Q	J	Potential energy
R	J mol^{-1} K^{-1}	General gas constant
$R_{s/l}$		Reactant
R	mol $s^{-1}L^{-1}$	Reaction rate
S	J K^{-1}	Entropy
S_R	J K^{-1}	Reaction entropy
s(v)		Standard deviation
$s(\bar{v})$		Standard deviation of the mean
T	K	Temperature
T	s	Time
T		Factor to calculate the confidence interval
U	J	Internal energy
$u(x_i)$		Uncertainty
u(y)		Overall uncertainty
V	m^3	Volume
$\bar{v}$		Mean
v_j		Value of component j
W	J	Kinetic energy
Y		Measurand, true value
Y		Best estimate of the Measurand Y
y_i		Molar activity component of component i
$y_{\pm}$		Average activity ion coefficient
x_1		Random error
x_2		Systematical error
x_i		Mole fraction
Z		Number of electrons
z_i		Valance of component i
z_a		Valance of all anions
z_c		Valance of all cations

Table 2 List of Greek letters

Figure	unit	Description
B	g L^{-1}	Mass concentration [1]
β_n		Equilibrium constant cumulative
E		Relative dielectric constant
ε0	$C^2N^{-1}m^{-2}$	Dielectric constant in vacuum
$_i$	J mol^{-1}	Chemical potential of the component i
v_i		Stochiometric coefficient of the component i
Ξ	mol	Extent of reaction
Π		Pi-constant
P	g cm^{-3}	Density of the solvent
Φ	%	Humidity

Table 3 List of abbreviations

Abbreviation	Description
AAS	Atomic-Adsorption-Spectroscopy
Ag	Silver
Al	Aluminum
AOX	Absorbable organic halides
Au	Gold
B	Boron
BimSchG	Bundes-Immissionsschutz Gesetz
Br	Bromine
BREF LCP	Best Available Technique Reference Document for large combustion plants
BVT	Best Available Technique
Ca	Calcium
$CaSO_4$	Gypsum
Cd	Cadmium
Cl	Chlorine
CO_3^{2-}	Carbonate
Cr	Chromium
Cu	Copper
CV AAS	Cold vapor atomic absorption spectroscopy
DeNOx	Denitrification
e.g.	For example

Abbreviation	Description
F	Fluorine
Fe	Iron
(W)FGD	(Wet) Flue Gas Desulfurization
H	Hydrogen
Hal	Halides
Hg(0)	Elemental Mercury
Hg_{aq}	Aqueous mercury
Hg_{el}	Elemental Mercury
Hg_{ox}	Oxidized Mercury
Hg_{S}	Solid Mercury
Hg(t)	Total Mercury
$HgBr_2$	Mercury(II)-bromide
$HgCl_2$	Mercury(II)-chloride
HgF	Mercury(II)-fluoride
HgI_2	Mercury(II)-iodide
$Hg(NO_3)_2$	Mercury(II)-nitrate
HgO	Mercury(II)-oxide
HgO (r)	Mercury(II)-oxide red
HgO (y)	Mercury(II)-oxide yellow
HgS	Mercury(II)-sulfide
$HgSO_3$	Mercury(II)-sulfate
$HgSO_4$	Mercury(II)sulfate
Hg_2Cl_2	Calomel
$Hg_2(NO_3)_2$	Mercury(I)-nitrate
Hg_2O	Mercury(I)-oxide
Hg_2SO_4	Mercury(I)-sulfate
HNO_3	Nitric acid
H_2O	Water
H_2S	Hydrogen sulfide
I	Iodine
IAP	Ion activity product
K	Potassium
L	Ligand
M	Metal
Me	Methyl

Abbreviation	Description
MFC	Mass-flow controller
Mn	Manganese
MO	Molecule orbital
N	Nitrogen
Na	Sodium
Ni	Nickel
O	Oxygen
OH	Hydroxide
ORP	Oxidation reduction potential
Pb	Lead
PFA	Perfluoro-alkoxy polymer
PTFE	Poly-tetra-fluoro-ethylene
Rb	Rubidium
S	Sulfur
Sat. index	Saturation index
SCR	Selective catalyst reduction
Se	Selenium
SHE	Standard hydrogen electrode
Si	Silicon
Sn	Tin
Sr	Strontium
SO_2	Sulfur dioxide
SO_3^{2-}	Sulfite
TDS	Thermo-Desorption
Ti	Titanium
V	Vanadium
VESPR	Valence shell electron pair repulsion
WHO	World Health Organization

IV. List of figures

V. List of tables

VI. Abstract

Toxic mercury emissions are released into the flue gas during coal combustion and are mainly co-treated in the flue gas desulfurization (FGD). In this process mercury(II)-species and SO_2 are washed out of the flue gas and are transferred into the aqueous phase. The aim is to stabilize mercury in the aqueous phase and to transfer it for treatment in a waste water treatment plant, reduce reemissions of the scrubber solution and prevent a carry-over into the gypsum production over the solid phase. Mercury is known to create heavy metal complexes in the scrubber suspension after the absorption. Possible ligands are halides, chloride, bromide and iodine or sulfite. The Hg_g - Hg_{aq} equilibrium can be described by the halides concentration and distribution, the Henry coefficient for possible reemissions, the redox reaction caused by presumably sulfite to elemental mercury and a reemission out of the scrubber solution. The other equilibrium of the aqueous and solid phase of mercury is not that well researched. Different experiments were conducted to better understand the influences on the equilibrium and the resulting mercury species in the solid phase. First, a method was developed to analyze mercury species in a solid sample. This method is based on methods found in literature that thermally decompose mercury samples to identify specific evaporation behavior of the different species. Reported species in FGD gypsum are Hg-halides, HgS, HgO and $HgSO_4$. In difference to the found approaches, the resulting mercury emissions in the developed method were differentiated between possible oxidation states (0 and II). This led to new evaporation information for mercury-halides that was not reported before. Mercury halides only evaporate as oxidized species while all the other species evaporate as elemental mercury. A laboratory scaled FGD scrubber was put into operation, to better understand the reaction path of aqueous mercury into the solid phase and to identify the resulting species. In literature identified indicators and process settings were executed to find the main influences on the different presumed resulting mercury species in gypsum. Most of the influences on the quantitative amount of mercury found in literature, such as halides concentration, sulfite concentration and metal concentration, were confirmed by the experiments. It was not possible to verify the redox potential due to technical restrictions of the experiment. None of the expected mercury species were found in the created samples. This can be explained by the improved mercury analysis due to the specification of the different oxidation states and a slow temperature ramp. The results indicate that a heavy metal precipitation based on pH level changes takes place in the scrubber solution. This indication was confirmed by indicative precipitation experiments. The suspected reaction is a precipitation of $HgSO_3$ to a not known Hg complex.

1. Introduction and motivation

1.1 Background

Mercury is known to be a toxic element, and its emission needs to stop. [2] The WHO considers mercury as one of the top ten chemicals concerning human health. [3] Most of the mercury emissions have an anthropogenic source. The top five sources are small gold mining businesses, coal-powered combustion plants, non-ferrous metal production, cement production and waste treatment plants. [2]

These emissions lead to a worldwide accumulation of mercury and its species in the environment. The recently published UN Mercury Assessment shows significant pollution of mercury in animals, plants, and humans. [4]

There are different political levers to stop anthropogenic emitting mercury emissions. One approach to protect human health from anthropogenic caused mercury emissions is the Minamata Convention. [5]

The goal is to reduce mercury emissions by substituting mercury out of products and production processes and finding a safe and stable final storage. [2]

The European Union is to set new emission ranges for the coal or lignite combustion. Table 4 shows new ranges for mercury emissions for Europe, released in the BREF LCP [6] from 2017.

Table 4 BVT-associated emission values [6] **for mercury emissions in air, thermal capacity ≥ 300 MW_{th} yearly average of over the year taken samples.**

Hard coal [µg m_n^{-3}]		Lignite [µg m_n^{-3}]	
New Plants	Old Plants	New Plants	Old Plants
< 1- 2	< 1- 4	< 1 – 4	< 1 – 7

Those emission values are in comparison to the 13. BImSchV, the German limit values of 30 µg*m_n^{-3} a big change for the coal combustion industries. [7]

To meet those new restrictions, new techniques are needed for the removal of mercury emissions in the flue gas. Because the coal combustion is one of the major emitters of mercury, the reduction of mercury out of flue gas is essential to reach zero anthropogenic mercury emissions. With the German plan to quit all coal-generated energy production until 2038, new techniques need to be found to meet the new limits for mercury emissions today preferably without further investment.

There are different approaches to clean mercury out of a flue gas stream. The main sink is the absorption via flue gas desulfurization (FGD) and later treatment in the wastewater treatment plant. [8] But still, the reaction paths for mercury in FGD are not completely known. To this day, the storage of mercury in the solid phase of the scrubber is still not fully understood. The storage of mercury in gypsum can result in a carry-over of the mercury inventory of an FGD into the gypsum production.
Therefore, it is crucial to investigate the chemical processes in the scrubber sump of an FGD to stabilize mercury in the aqueous solution. The stabilization should not be achieved by adding an additive but by finding the main reactions that cause the reemission of mercury or precipitates into the solid. This work aims to better understand the co-treatment of mercury via FGD and find the main drivers to stabilize Hg_{aq}.

1.2 Mercury in coal combustion

The mercury concentration in coal varies depending on the source and the kind of the coal. Around 95% of the mercury content of the coal is released during combustion into the flue gas.[8]–[10]
After the combustion, there are three main flue gas cleaning steps.

- Denitrification via a $DeNO_x$-SCR (selective catalytic reduction) catalytic reduction of NO_x
- Dedusting via E-Filter or backhouse filter
- Desulfurization via scrubber system [11]

[7]– [9]
Figure 1 shows basic steps of mercury in a power plant and demonstrates the different impacts of the different cleaning steps on it. The values are average concentrations for hard coal combustion. Values inside the boxes show the mercury concentration downstream the described process.

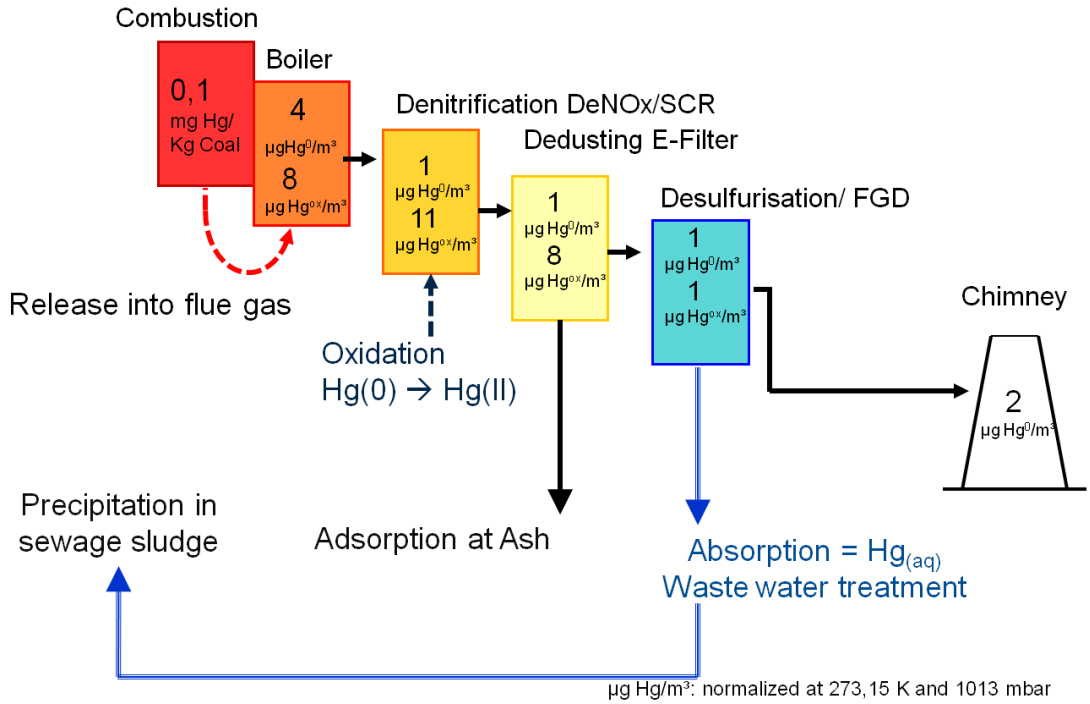

Figure 1 Mercury in a flue gas cleaning process. [12]

After the combustion chamber the main oxidation level of Mercury is 0 due to the high temperatures during combustion. Mercury is converted to the oxidation state +I or +II in the cooling phase. The presence of halides like bromide or chloride increases the conversion to a higher oxidation level as well as a SCR catalyst of the denitrification. [13] It is believed that the main oxidized mercury species in flue gas is mercury chloride but the flue gas can also include mercury bromide if it is added during the combustion process. [14] A part of the mercury content is captured on the fly ash. The fly ash has a five times higher mercury content than the coal, with 10wt% fly ash and a 50 % capture rate. [13]

As Figure 1 shows, that the flue gas desulfurization (FGD) is the main sink for mercury and later treatment in the wastewater treatment plant. It shows how important efficiency is when capturing mercury in FGD since every emission out of FGD ends up in the chimney. There are different technical approaches for a scrubber system. The main one used in coal combustion is a limestone based wet scrubber system. [8]

The main purpose of an FGD is to wash sulfur dioxide out of the flue gas. SO_2 is absorbed and converted via limestone forced oxidation into gypsum as by-product.[14]

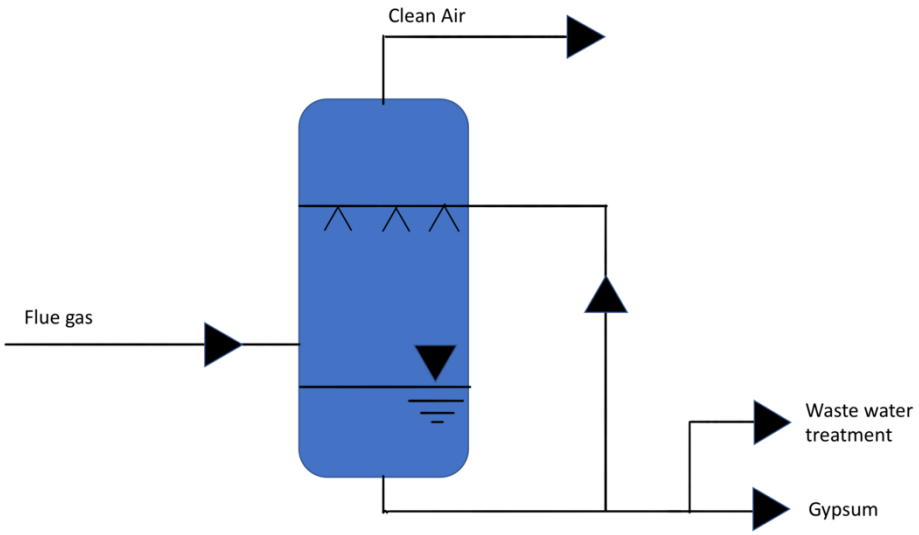

Figure 2 FGD Scheme.

Figure 2 describes the basic operation steps of a scrubber. The flue gas is led counter stream through the spray zone and the droplet separator. Releasing a gas at the top of the column, cleaned of all water-soluble gas impurities. The slurry is collected as sump on the bottom of the reactor. The sump circulates into the spray zone as alkaline liquid. It is possible to add oxidation air in the sump to increase the redox-potential and add lime, as $Ca(OH)_2$ or $CaCO_3$ to create gypsum and to control the pH value inside the operation restrictions. The solubility of lime (low pH values) as well as of SO_2 (high pH values) is dependent on the pH value. [11] The operation pH value lies in the range of 5 - 6. This is the perfect compromise between the solubility of lime and solubility of SO_2.[13]

The reaction of SO_2 with limestone creates gypsum (by-product) that has to be periodically drained out of the system. [14] The drained sludge is further separated in three fractions:

- Liquid phase, which ends up in the wastewater treatment plant or re-circulates into the scrubber.
- Fines fraction, which ends up in the wastewater treatment plant or is re-circulated into the process.
- Gypsum phase that ends up as by-product. [11]

The main operation parameters in the scrubber are:

- The ORP (oxidation-reduction potential),
- pH-value,
- Operating temperature and
- Salts and dissolved solid content. [13]

One of the co-benefits of a scrubber system is the possibility to absorb the remaining oxidized mercury species out of the flue gas. After the absorption process into the aqueous phase of the scrubber, mercury can undergo three different paths:

- Remain in the aqueous phase of the suspension,
- Be adsorbed or precipitated in or at the solid phase,
- Undergo a reaction and reemit out of the suspension. [14]

The aim of the process is to transfer mercury from the liquid-phase into the wastewater treatment plant to precipitate it into the sludge. [15]
A low mercury content in gypsum is preferable as it is used e.g., in agriculture applications or wallboard feedstock. In Germany 50 % of the used gypsum is from FGD. [16]–[18]

For the further investigation of the state of research the focus will be consider following aspects. To optimize the co-treatment of mercury via a FGD, the reaction path of mercury in the scrubber solution needs to be better understood, and the following aspects have to be considered. After the absorption, mercury has different kinds of reaction partners. All of the possible ligands for mercury have other influences on its further behavior in the scrubber system. To understand how mercury reacts with gypsum, the main reaction partners in the solution should be known, including the coordination number, the structure of the created complex and its characteristic behavior. The parameter settings that influence the reactions of mercury in the scrubber system or have an influence on possible ligands have to be considered in further investigations. Whereas the focus of the investigation lies on the Hg_{aq}-Hg_s equilibrium, reactions that influence Hg_{aq} or the Hg_g-Hg_{aq} equilibrium have to be looked at. To detect the formed product in the scrubber sludge it is necessary to further discuss analytic methods to identify possible ways to qualitatively analyze a solid containing an unknown mercury species. The following chapter will discuss the state of research of the different aspects.

1.3 State of research

The following section will investigate the main influences on aqueous mercury after the absorption in a FGD sump, the Hg_{aq}-Hg_g equilibrium and the reactions of Hg_{aq}. It will also discuss the different approaches on how to detect the different kinds of reactions.

Bittig et al. [12] created the Bittig droplet (Figure 5) to describe the different reaction paths of mercury during an absorption, like in a FGD:

- The absorption from the gaseous phase into the aqueous phase following the Henry-Law (Hg_g-Hg_{aq} equilibrium).
- The possible reaction partners/ ligands for the mercury complex in the aqueous phase (stabilization of Hg_{aq}).
- The reduction of oxidized mercury.
- And a possible reemission of Hg(II) and Hg(0) following the Henry-Law (Hg_g-Hg_{aq} equilibrium).

Mercury(II) has an absorption rate in an FGD up to 99 %, but the net removal rate is often smaller because of reemission phenomena's. [14]

Blythe et al. [14] describe as reason for a reemission a chemical redox reaction of mercury(II). Mercury(II) can be reduced into the nearly not soluble elemental form while dissolved in the scrubber suspension and reemits into the flue gas (e.g. equations (1.1),(1.2) and (1.3)).

Schütze et al. [19] describe the oxidation state of mercury emission upstream and downstream of a FGD as following. Upstream the FGD 80 % of the mercury emission can be detected mainly as Hg^{ox}, downstream the FGD, 80 % of the mercury species is Hg^0. They conclude, that the change of oxidation state of mercury emissions is due to reduction mechanisms in the FGD, that are leading to the reemission of mercury. This is in agreement with the Bittig droplet. [12]

Blythe et al. [14], [20] describe the reduction mechanism of absorbed oxidized mercury in a scrubber system via sulfite as following:

$$Hg^{2+} + SO_3^{2-} \rightleftharpoons [HgSO_3] \qquad (1.1)$$

$$[HgSO_3] + SO_3^{2-} \rightleftharpoons [Hg(SO_3)_2]^{2-} \qquad (1.2)$$

$$[HgSO_3] + H_2O \rightleftharpoons Hg^0 \uparrow + SO_4^{2-} + 2H^+ \qquad (1.3)$$

They identified that sulfite reduces Hg_{aq}^{2+} rapidly. To stabilize aqueous mercury and slow down the reduction process, Blythe et al. [20] recommend a higher coordination of the mercury complex via sulfite, chloride, or iodide. Whereas chloride in small concentrations could not stop the mercury reduction, iodide as a strong ligand for mercury could substantially reduce mercury reduction.

They used UV-spectroscopy to measure the reduction of mercury's absorbance in the solution. They measured the reemission of mercury in the gas phase via CV AAS (cold vapor atomic absorption spectroscopy). As conversion for the oxidized mercury species to elemental mercury, they used $SnCl_2$ as reduction agent.

Van Loon et al. [21] also investigated the existence of $HgSO_{3(aq)}$. Van Loon et al. [21], [22] were also able to show that sulfite is a possible ligand of mercury. In their measurement they were able to show that the UV spectrum shifted from an absorbance from around 230 nm to 215 nm by adding NaOH to their solution. This behavior indicates mercury forms a sulfite complex at first, which leaves at a higher pH value the ligand bond to form a free ion in the solution. [22]

The coordination number of $HgSO_{3(aq)}$ is not known, but it is most likely that there is at least one water molecule in the sphere of mercury coordination. This would conclude that sulfite is a mono dentate-ligand. [21], [23]

$Hg(SO_3)_2^{2-}$ is a higher coordinated complex than $HgSO_3$, showing a higher stability than $HgSO_3$. The reaction to $Hg(SO_3)_2^{2-}$ seems only to be inhibited by free SO_3^{2-}. A higher coordination with sulfite than $Hg(SO_3)_2^{2-}$ was excluded. Van Loon et al. assume that possible other ligand for a mixed complex is water.

The reaction of Hg with sulfite is mainly with SO_3^{2-}. It appears that mercury has no affinity to HSO_3^-.[22]

Blythe et al. [20] found evidence that mercury causes a catalytic disproportionation of sulfite:

$$4SO_3^{2-} \rightleftharpoons 3SO_4^{2-} + S^{2-} \qquad (1.4)$$

If this is a true hypothesis, it can be an indication of the formation of HgS in gypsum. [24]

The formation of higher coordinated sulfite complexes was also reported by Heidel [8], who investigated that a high concentration of S(IV) led to irreversible bonds of mercury in a solid phase that seem to be stable at high temperatures.

Wu et al. [25] reported sulfite ions as the primary driver for the reemission of elemental mercury from the FGD sludge. They also found that trace metal ions such as Cr^{3+}, Fe^{2+}, Pb^{2+}, Sn^{2+}, Ni^{2+}, Mn^{2+} influence the reemission of Hg^0 out of the scrubber.

Schütze [19], [26] suspected that the mechanisms or parameter settings that cause a reemission of mercury out of FGD sludge not only to be sulfite. He reported that the disproportionation of $Hg(I)_{2,aq}$ species into Hg(II) and Hg^0 could lead to a reemissions. The reduction of $Hg(II)_{aq}$ to $Hg(I)_{2,aq}$ species caused by the oxidation of metals in the suspension. He suspected other compounds to influence a reemission but also parameter settings such as a high pH value. Unlike the studies conducted by Blythe et al. [20] and van Loon et al.[21], [22], who mainly worked with simplified solutions, Schütze worked with synthetic FGD solutions and a solution from a scrubber.
Not only elemental mercury can reemit out of a scrubber solution. Uncharged mercury-halide- complexes remain in equilibrium with the gas phase, following the Henry law. With an excess of the ligand in solution, anionic mercury complexes can be formed and withdraw mercury from the equilibrium with the gaseous phase. By carrying a charge, the complex will no longer stay in equilibrium with the gaseous phase. [8], [27], [28]

Bittig [27] [12], [29] et al. show that the stabilization impact of halides on Hg_{aq} is mainly independent of the pH value, but their ligand strength and concentration has a significant influence on the resulting mercury complex in solution. For example, increasing the halide concentration to form a higher coordinated mercury complex with a charge makes it possible to remove the complex from the Hg_{aq}-Hg_g equilibrium to stabilize it in the aqueous phase. Furthermore, the ligand strength of the different halides increases with the period of the elements as:
$I^- > Br^- > Cl^-$.
Unfortunately, the volatility of the different mercury-halides complexes also increases with the ligand strength. As a result, the higher volatility can lead to a reemission of mercury caused by a ligand exchange. [28]
Schütze [28] shows in his work that the ligand strength of sulfite and OH^- is different from halides, dependent on the pH value of the scrubber solution.
Determining the right ligand strength and coordination number for mercury is essential to stabilize mercury in solution, because it defines the most likely ligand for mercury and with it the amount of reemissions of mercury caused by an redox reaction or the equilibrium between the gas phase and the aqueous phase.[17], [28]

The strength of sulfite as a ligand for mercury is described via theoretical stability complex constants K (e.g. chapter 2.2.1) as a mono-dentate ligand in comparison to the halides as [27], [30]:

Table 5 Ligand constants for mercury. [27], [30]

Ligand	Cl^-	Br^-	I^-	SO_3^{2-}	
Log K1	6.76	9.05	12.87	22.66	
Log K2	13.16	17.33	23.82	24.07	
LogK3	13.99	18.55	27.6	24.96	
Log K4	15.22	20.01	29.82		

If sulfite is mono-dentate as postulated by van Loon et al. [21], [22] it is in comparison to all halides, the strongest ligand for mercury in a onetime coordinated mercury complex and as strong as iodide as a two times coordinated complex.

For the analysis Schütze [28], Heidel [8], and Blythe et al. [20] measured the reemission of mercury out of solution and measured the resulting mercury concentrations in the solution. Schütze [28] worked with wash bottles filled with the solution to be investigated and flown through with carrier gas. Heidel [8] and Blythe et al. [20] worked with a laboratory-scaled scrubber system. Heidel [8] additionally separated the sump and spray zone to closer analyze the reemission out of the sump and separate it from the absorption capacity of the spray zone. All three measured pH value, ORP, and sulfite concentration. [8], [20], [28] However, Heidel [8] and Schütze [28] only measured the reemission and, therefore, the end of a reaction where elemental mercury indicates a reemission forced by sulfite.

Van Loon et al. [21], [22] and Blythe et al. [20] used a second approach to investigate the reaction of sulfite with mercury. Both studies measure the reaction in the aqueous phase via UV-spectrometer.

Van Loon et al. took a small UV-cuvette and cooled it down to slow down the swift reaction of sulfite with mercury.[21], [22]

The discussed state of research shows the main drivers for reemission phenomena are the vapor pressure of uncharged mercury complexes and the redox reaction of mercury with a sulfite as a ligand.

To reduce such emissions, the Hg_{aq}-Hg_g equilibrium must be influenced to stabilize Hg as Hg_{aq}. The main drivers are:

- Bromide, iodide and chloride and their concentration as free ion in solution,
- Sulfite and its concentration as free ion in solution and
- The pH value

The pH value has no direct influence on Hg_{aq}, but on some of its ligands like OH^- or sulfite.

It should be considered there is a general agreement that sulfite forces a reduction of oxidized mercury. The input and output are known, but the reaction path is still not completely understood. The discussed research showed, that $HgSO_3$ is an unstable complex and it can lead to a redox reaction that causes Hg(0) reemissions. It was shown that the reaction of mercury with sulfite and the stability of the formed complex have a high dependence of the pH value and the free sulfite ion concentration. But it also shows that it is not completely clear, if $HgSO_3$ is a mono-dental complex, and if there are heteroleptic complexes such as $Hg(SO_3)_2Br_2^{4-}$.

It is essential to know what kind of mercury-compound is the most likely to be in solution to identify the possible reaction partners for the next step to Hg_s.

This research needs to first integrate sulfite as ligand in the very good understood mercury-halides system, to be able to add the solid phase to the Bittig droplet. Questions to be answered are:

- Is sulfite a mono-dental ligand for mercury?
- Can mercury form a complex with HSO_3^-?
- Is it possible to stabilize $HgSO_3$ with free halides ions?
- What is the needed concentration of free sulfite to form a higher coordinated mercury sulfite complex?
- Is it possible to create a higher coordination of mercury with sulfite than $Hg(SO_3)_2^{2-}$?

While the first discussed equilibrium of Hg_g-Hg_{aq} is widely researched, it seems that the state of research for the formation of Hg_s and the equilibrium of Hg_{aq}-Hg_s still has some blanks. The following section will discuss the state of research of the known and suspected mechanism for the formation of Hg_s. This section will be focusing on two aspects. First, what kind of parameters force mercury in the solid and what species is expected. The second aspect focuses on the method to assay a mercury species in an unknown solid sample.

Heidel [8] describes that the adsorption of mercury on a particle is reversible. The adsorbed ratio of mercury is decreasing with increasing temperature.

Gansley et al. [31] reported that the presence of sulfite could force mercury into the solid fraction of a scrubber system.

Blythe [14] separates compounds in the scrubber solution and parameter settings that cause mercury to precipitate. He reports that trace elements such as Fe(III) can co-precipitate heavy metals such as mercury, and he suspects the concentration of halides to influence the mercury whereabouts. Next to possible reaction partners, he

also suspects that the redox-potential influences the phase mercury prefers. He postulates that:

- A high redox-potential favors Hg_{aq} and
- A low redox-potential favors Hg_s [14]

Schütze [28] not only reports the redox potential as an influence on the mercury concentration in gypsum, but he also separates between different redox potentials and their influence on how mercury is bound in the scrubber solution. Mercury in the solid phase is more thermal stable at redox potentials E_H> 700 mV. At 200°C, only 15% of the solid-bound mercury reemits. At E_H< 500 mV, 25-40% reemits at 200°C. At redox potentials as high as 700mV, the mercury content was as low as in natural gypsum.

Van Dijen [13] argues for the influence of the ORP on the concentration of mercury in gypsum that at higher ORP levels, the preferred oxidation level of mercury is +II. At lower ORP levels, the formation of Hg(I) species will lead to the precipitation of this species in gypsum.

The ORP also significantly influences present metals in the solution, like Mn or Fe. Both are linked to the concentration of mercury in gypsum.

It also has an effect on the formation of unwanted metal oxides like Cr(VI), Se(VI), Mn(IV), AOX, the evaporation of bromide and iodide, and consumption of compressed air.

Van Dijen also states that the chemistry of mercury in gypsum is still not fully known. It seems that different types of Hg can be present in FGD gypsum. Acid can leach out some of the mercury content. Temperature steps in thermo-desorption process (TDS) show a different amount of mercury release from the gypsum. That can indicate the presence of different kinds of mercury species in the FGD gypsum. [13]

To date, there has been little agreement on the main mercury species to be found in FGD gypsum. [24], [32]–[35]

To analyze the impact of mercury in gypsum, different aspects have to be investigated.

Knuth et al. [36] report that in the gypsum production process, the raw gypsum from the FGD gets dried and calcined at temperatures around 180 °C. This process step can lead to a mobilization of captured mercury and end in its emission if the formed mercury species in gypsum gets volatile at temperatures $\leq$ 180°C .

Rumayor et al. [18], [37] state that depending on the species and oxidation state, the properties and toxicity of mercury vary. The chemical form of mercury in a sample is the key to prediction towards its behavior and characteristics.

This is why it is essential to not only identify the mercury content but also identify the mercury species in a sample. [18], [38]–[41]

Species reported in a FGD gypsum are Hg_2Cl_2, $HgCl_2$, Hg_xBr_n, HgO, $HgSO_4$ and HgS. Also suspected is a complex with iron. The frequency and composition of the mercury species that can be found in gypsum vary dependent on the scrubber system. [24], [32], [33] [34], [35], [42], [43]

Two different approaches can be found in literature to identify the main species in FGD gypsum or wallboard gypsum. The primary research focuses on the analysis of samples of FGD gypsum taken out of a combustion process.

Lee et al. [32] found the same mercury peak in their analysis of different wallboard and gypsum samples and suspect Hg_2Cl_2 or $HgCl_2$ as species. Species such as HgS, HgO, and $HgSO_4$ are excluded.

Rallo et al. [34] investigated FGD gypsum from a co-combustion plant. They found $HgCl_2$ with a maximum peak of 130°C to be the main species in FGD gypsum.

Sedlar et al. [33] suspect as main species mercury-halides such as Hg-Br or Hg-Cl compounds in the gypsum sample. They found a smaller amount of HgO, HgS, and $HgSO_4$.

In comparison, Sui et al. [24] identified HgS as the main species, Hg-halides and HgO as secondary species in FGD gypsum samples. To find a reason for the different species in the gypsum, they analyzed if they could find a correlation of the sulfur and chloride concentration in the coal to the outcome of the species in the gypsum sample, but it was not possible. They suspect that the gypsum species depends on the chloride and sulfur concentration in the scrubber and other conditions like pH value, temperature, or not identified factors. [24]

Córdoba et al. [35] also describe three different species, Hg_2Cl_2, $HgCl_2$, and HgS, identified in gypsum samples via TDS. Other sampling days changed the composition of the species in gypsum. In the first sampling, HgS was the main species. HgS is the product of the reaction of Hg(II) with S^{2-}. The formation of S^{2-} is described as the reduction of SO_4^{2-} by CO. In the second sampling, Hg-Cl species were the main species found. The explanation is that Hg_2Cl_2 meets the saturation limits in the calculated equilibrium as well as HgS.

$HgCl_2$ is believed to adsorb on the gypsum particle or precipitate because the saturation limits were met in the aqueous phase or because of moisture water of the FGD gypsum.

All of the discussed research papers conducted samples out of a FGD process and measured the emissions out of the solid sample with an AAS or AFS analyzer while heating them in a defined temperature program.

The second possible approach or maybe next step is to compare technical FGD gypsum samples with prepared and synthetic gypsum samples.

Pavlin et al. [42] created synthetic gypsum samples by dry and wet mixing of different mercury species with gypsum. Then they mixed all mercury samples (dry and wet) with FeOOH to investigate the influence of Fe on mercury. All measured technical gypsum samples showed one similar evaporation characteristic. The precipitated (wet mixed species) showed only one peak independent from the mercury species used for the precipitation. Because of the small amount of Cl in all gypsum fractions, they consider a Hg-Cl species rather unlikely. They also suspect that Fe influences the desorption characteristic of mercury.

As of today, there is no standardized and valid analytical method to characterize mercury species in a sample. There are only methods to quantify it. [18], [39], [40], [42], [43]

The thermal treatment of a solid sample containing mercury was first applied by Biester et al. for analyzing the mercury contamination in soils. [37], [39], [40], [43]–[47]

Rumayor et al. [18], [43] showed that the method of thermo-desorption (TDS) of a sample containing an unknown mercury species seems to be the fastest solution of analyzing mercury species while gaining a similar quantitative output as standardized procedures, e.g., chemical extraction. They showed [37], [47] that they could identify pure mercury species by their evaporation profile. They also observed no significant interference between mixed species. Their analysis used a thermo-desorption furnace to release the mercury from the solid sample flown through with nitrogen and heated for 50°C min^{-1}. For the oxidation state convention of mercury to measure it via AAS, a PYRO unit was used heating the gas up to 800°C to convert all oxidized mercury species to elemental ones. [37]

Dependent on the analyzer and the measured sample in the literature, different sample preparations, heating rates, sample dwell times, and analysis methods are described, which deliver different results. [39], [40], [42]–[45], [48]

For example, Lee et al. [32] reports a higher flow rate decreases the residence time of the mercury vapor as well as the mercury concentration. For analyzing FGD gypsum samples and dry wallboard samples, they used two different heating ramps of 5 and 1 °C min^{-1}, but preferred the 1 °C min^{-1} ramp. For analyzing the mercury vapor, a continuous measurement with a CV AAS was used. An $SnCl_2$ solution was

used for the conversion of oxidized mercury species to elemental mercury. The mass balance caused some problems because of the detection limit of the CV AAS and the small amount of mercury in the gypsum.

Rallo et al. [34] used an AFS Analyzer from PS Analytical Merlin for measuring the total mercury-content and a heating ramp of 10 °C min^{-1}.

Sedlar et al. [33] worked with a 2.2 °C min^{-1} ramp and for analysis with a CV AAS from Lumex with an additional Pyro-oven that heats the sample to 700 °C.

Sui et al. [24] also used an AAS from Lumex.915+, a high-temperature furnace, for the TDS analysis.

Córdoba et al. [35] used a thermal dissociation oven from PS Analytical for the thermal decomposition of the sample and a SIR Galahad II, an atomic fluorescence spectrometer as an analyzer for the mercury vapor.

Pavlin et al. [42] had a different approach to analyzing their samples via MS in comparison to the other studies.

According to Pavlin et al. [42], using a continuous AAS, the sample matrix, particle size distribution, heating ramp, types of carrier gas and flow rate, sample weight, sampling time, and procedure are all factors to affect the shift of the desorption/ decomposition of mercury species to a different temperature range and peak intensity.

The research to date for analyzing mercury species tends to focus on analyzing one outgoing sample stream speciated in the wanted oxidation state of the mercury. However, these studies do not consider that by speciating the flue gas into total mercury and elemental mercury during one measurement, maybe a new footprint can be found as characteristic evaporation behavior of different mercury species.

Previous studies only have focused on the analysis of mercury species in technical FGD gypsum samples or investigated the correlation between the mercury content in gypsum with different process parameter settings or changing scrubber matrices. The suspected mercury species in FGD gypsum are $HgCl_2$, $HgBr_2$, Hg_2Cl_2, HgS, HgO and $HgSO_4$. The research showed that the main mercury species could change from HgS to a Hg-Cl species in FGD gypsum but to date not known what causes that change. Suspected are pH value and halides concentration.

It was also shown that the ORP influences the amount of mercury and the decomposition temperature of the unknown Hg_s species. Other influences were found in the composition of the scrubber suspension, main factors are:

- Halides concentration,
- Sulfite concentration,
- And other impurities like metal oxides.

What causes the formation of Hg_s and what species can be expected is still not answered.

1.4 Aim of this work

The discussion above shows that the aim of the co-treatment of mercury via FGD is to stabilise mercury in the aqueous phase and precipitate it in the waste water treatment plant. A transition of the mercury content into the by-product gypsum needs to be stopped.
To do so, it is not only necessary to understand the factors that cause mercury to reemit out of a scrubber sump but also find the main drivers that push mercury in, on or into a solid.
It was possible due to extensive literature research to isolate different parameters that could influence the capture of mercury in a gypsum sample. It was also shown, that possible occurring mercury species were identified.
The research shows that two kinds of approaches were done. One is the side of the FGD scrubber system that researched the influences like parameters or sump matrices on the mercury content. The other approach researched how to analyze mercury species in solid samples, such as FGD gypsum samples.
Aim of this work is to combine those two approaches to discover different reaction paths and the main players that cause the transition of aqueous mercury into the solid phase after being absorbed in a FGD system and define the resulting Hg_s species in the gypsum depending on the different FGD settings.
This will be done by creating standardized gypsum samples via a laboratory scaled FGD system and analyze the formed mercury species via a thermo-desorption process.
The first part, since there is no standardized method to investigate different mercury species, will be the development of an analyzing method via thermo-desorption (TDS) based on the systems found in literature. Investigations for mercury species via

thermo-desorption already exist. As an addition, this work will differentiate the evaporating oxidation states of mercury between Hg(0) and Hg(t) during one measurement.
The second part will be the creation of gypsum samples to define the influences of different parameter settings and sump matrices on the mercury content and species in a FGD gypsum.

Due to its complexity, this part will be subdivided into two parts:

1. The investigation of possible Hg_{aq} species depending on the scrubber settings, to define the starting point for the Hg_{aq}-Hg_s equilibrium. Therefore, following steps will be studied:
    - The integration of sulfite as ligand for mercury in the Hg-Halides-System.
    - The investigation without a solid phase to better understand the reaction in aqueous phase.
2. Concerning the investigation of the influences of the main drivers for the mercury concentration in FGD gypsum following settings were identified from literature research:
    - High halides concentration can stabilize mercury aqueous.
    - High sulfite concentration causes the implementation of mercury in gypsum.
    - High ORP levels can force mercury into the aqueous form.
    - Ferrous and other impurities cause an enrichment of mercury in the solid phase.

Because of the complexity of the system, it is only possible to measure the reemission of mercury out of the system, similar to the approaches of Schütze and Heidel. For a better understanding of the reactions the oxidation states of mercury, Hg(0) and Hg(t), will be measured during the experiments.

The main research questions to be answered are:

- What are the main influences on the Hg_{aq}-Hg_s equilibrium?
- What are the main mercury species in gypsum?
- What causes the change of mercury species in the gypsum sample?

Answering those questions ought to lead to a better understanding of mercury in a FGD. And help to actively remove mercury from the flue gas of a coal combustion plant and reduce anthropogenic caused mercury emissions.

2. Theoretical background

This chapter will discuss the theoretical background of this thesis.

2.1 Thermodynamic basics

The equilibrium between the gas phase and the aqueous phase are important to explain reasons for reemission. For further interpretation of the results two different software approaches were chosen to calculate the most plausible Hg_{aq} species and find out which species reaches its saturation limits. The underlying calculations are explained further.

The Hg_g-Hg_{aq} equilibrium

The transition and exchange of a gaseous component like mercury into an aqueous diluted solution can be described via Henry law. Gases and other volatile substances are exchanged at the interface between gas and aqueous phase and result in an absorption equilibrium. The solubility of gases is described by a Henry constant H. Depending on the partial pressure p of a component i above the aqueous phase, it is possible to calculate an equilibrium concentration c in solution as:

$$c_{i,(aq)} = H_i(T) * p_{i,(g)} \tag{2.1}$$

[8], [49]

This constant is a substance specific property and dependent on temperature. The temperature dependency can be described as:

$$H_i(T) = H_i(\theta) * e^{\left(C_i\left(\frac{1}{T}-\frac{1}{\theta}\right)\right)} \tag{2.2}$$

with the reference temperature θ and a substance specific constant C_i.[8]
The Hg_{aq}-Hg_g equilibrium for mercury follows the Law of Henry because of the small concentrations.[49]

Hg_{aq} and Hg_{aq}-Hg_s equilibrium

To investigate the most plausible mercury complex in the scrubber solution equilibrium calculations can be made. In this work, two different calculation programs are used to examine the composition of varying mercury complexes in the scrubber solution.

The first one is called HSC Chemicals and is a program developed by the firm Outokumpu. [50] The second one is called Visual MINTEQ and is a program created by the Royal University of Stockholm. [51]
The two programs calculate the chemical and thermodynamic equilibrium in different ways.
HSC Chemicals [50] is used to create a Pourbaix diagram, which gives an idea of the primary oxidation state and possible mercury species that are the most stable applied in an E-pH value diagram.
The calculation is based on the Nernst equation with the describe the occurring chemical reactions for mercury in solution.

A chemical reaction can be described as an equilibrium between input compounds A and B and product compounds C and D:

$$aA + bB \rightleftharpoons cC + dD \qquad (2.3)$$

[52]
The calculation of the free enthalpy can also be described with the equilibrium constant K of a reaction. With K being calculated as quotient of the sum of the activities of the products divided by the sum of activities of the educts:

$$K = \frac{a_C^{|c|} a_D^{|d|}}{a_A^{|a|} a_B^{|b|}} \qquad (2.4)$$

[53]
The standardised free enthalpy:

$$\Delta G^0 = -2.303\ RT\ \log K \qquad (2.5)$$

[52]
That leads to the free reaction enthalpy described as:

$$\Delta G = \Delta G^0 + RT \ln \frac{a_C^c a_D^d}{a_A^a a_B^b} \qquad (2.6)$$

With the transformation:

$$\Delta G = -zFE \qquad (2.7)$$

For the standardized state:

$$\Delta G^0 = -zFE^0 \qquad (2.8)$$

Where z describes the number of electrons and F is the Faraday constant. The Gibbs equation can be transformed into the Nernst equation.

$$E = E^0 - \frac{2.303\,RT}{zF} \log \frac{a_C^c a_D^d}{a_A^a a_B^b} \qquad (2.9)$$

This transformation makes it possible to describe a chemical equilibrium with the electro chemical potential corrected to the operation temperature. It allows to draw a Pourbaix diagram and describe the most preferred state of metals at different pH values, in aqueous state and at different potentials E.

Pourbaix developed this method to show in an E-pH diagram all information about the thermodynamic stability of metals in different states. It describes a thermodynamic equilibrium without recognizing the reaction rate and kinetics.[52]

The other approach to determine the theoretically most plausible aqueous complexes is a basic calculation via law of mass action. For this calculation, the Visual MINTEQ software was used. Based on the empiric equation of Davies, the activation coefficients are calculated, and with the temperature correction of van't Hoff, all possible components for one pH point and a single temperature are determined. [51] The Davies approach was used because it is most suitable approach available of the software.

The chemical potential for one pure substance is identical with the molar free enthalpy and thereby a function of temperature and pressure. In a mixture, the dependency of all other components has to be considered in the function as well.

For an ideal solution, all molecular interactions are considered as 0. Following in:

$$\mu_i = \mu_i^*(p,T) + RTlnx_i \qquad (2.10)$$

Where x_i is the mole fraction, and * marks the pure substance.

For a non-ideal solution, the mole fraction is replaced with the activity as a corrected concentration:

$$a_i = y_i\, x_i \qquad (2.11)$$

where y_i stands for the activity coefficient and is a function of pressure and temperature.

$$\mu_i = \mu_i^*(p,T) + RTlna_i \qquad (2.12)$$

[53]

The activity of a pure substance can be set as 1. For diluted solution the activity can be described by:

$$a_i = y_i \frac{c_i}{c^0} \qquad (2.13)$$

[53], [54]

For an electrolyte solution the activity coefficient y_i is dependent of the ionic strength. For strongly diluted solutions the Debye-Hückel-Theory is used. The average activity ion coefficient $y_\pm$ can be described as:

$$logy_\pm = -A_m|z_c z_a|\sqrt{I_m} \qquad (2.14)$$

With z_c as valence of the cations and z_a as valence of all anions.

$$A_m(T) = \frac{1}{ln10}\sqrt{2 * 10^3 \pi N_A \rho_{LM}(T)}\left(\frac{e^2}{\pi\varepsilon_0\varepsilon(T)kT}\right)^{\frac{3}{2}} \qquad (2.15)$$

And

$$I_m = \frac{1}{2}\sum_i m_i z_i^2 \qquad (2.16)$$

Whereas ε stands for the dielectric constant, ρ_{LM} describes the density of the solvent. The ionic strength I_m is described with the sum of the molality m_i and the valance z_i of the components i.[54]

The average activity coefficient has to be calculated because it is not possible to define individual activity coefficients via experiment. [53]

The best in the software available approach is the empiric extension of Davies:

$$logy_\pm = -A_m|z_c z_a|\left(\frac{\sqrt{I_m}}{1+\sqrt{I_m}} - 0.3\ I_m\right) \qquad (2.17)$$

[54]

For the determination of temperature dependency of the chemical equilibrium constant K the Van't Hoff equation is used. Where K depends on temperature and the heat of the reaction:

$$\frac{d \ln K}{dT} = \frac{\Delta H_T}{RT^2} \quad (2.18)$$

To calculate the formation of possible Hg_s species Visual MINTEQ uses the saturation index (SI) and the log function of the ion activity product (logIAP). [51]
The precipitation of a species can also be described by the law of mass action. A_aB_b stands for the formed solid.

$$(A_aB_b)_s \rightleftharpoons aA_{aq} + bB_{aq} \quad (2.19)$$

The equilibrium constant K can then be described as

$$K = \frac{a_{A,aq}^{|a|} a_{B,aq}^{|b|}}{a_{AB,s}^{|ab|}} \quad (2.20)$$

[53]
The activity of a solid phase equals 1. The solubility equivalent K_{sp} can be described as:

$$K_{SP} = a_{A,aq}^{|a|} a_{B,aq}^{|b|} \quad (2.21)$$

The variation of the K_{sp} for different species favors algorithmic notation as:

$$pK_{SP} = \log_{10} K_{SP} \quad (2.22)$$

Insoluble:

$$K_{SP} \leq 1 \quad (2.23)$$
$$pK_{SP} \geq 0 \quad (2.24)$$

Soluble:

$$K_{SP} > 1 \quad (2.25)$$
$$pK_{SP} < 0 \quad (2.26)$$

[49], [55]
K_{sp} describes the chemical equilibrium. The real solution does not have to be in an equilibrium. This state is described by the ion activity product (IAP).

$$IAP = a_{A,actual}^{|a|} a_{B,actual}^{|b|} \quad (2.27)$$

The saturation index (SI) describes the ratio between IAP and K_{sp} with:

$$SI = \log_{10}\left(\frac{IAP}{K_{SP}}\right) \quad (2.28)$$

The values can be interpreted as following:
Saturated solution (in equilibrium):

$$K_{SP} = IAP \quad (2.29)$$
$$SI = 0 \quad (2.30)$$

Undersaturated solution:

$$K_{SP} > IAP \quad (2.31)$$
$$SI < 0 \quad (2.32)$$

Supersaturated solution:

$$K_{SP} < IAP \quad (2.33)$$
$$SI > 0 \quad (2.34)$$

[55]

2.2 Complex-chemistry / Reaction of auxiliary group elements

For a better understanding of the possible reaction paths of mercury in a scrubber solution it is of great importance to understand the basic chemical background of mercury and its complex reactions, the characteristics of the different compounds in an FGD solution, molecule structures, the bonds and the affinities to each other.
Mercury has 80 electrons distributed as [Xe] $4f^{14}$ $5d^{10}$ $6s^2$ and stands in the IInd transition group of the periodic table. [56]
Because of its characteristic as transition metal of the IInd transition group and the 6th period mercury tends to sublimate and to form insoluble complexes. [57]
Different approaches can be considered. Mercury forms complexes with halides but also with sulfite, sulfate or hydroxide [57]–[60]. To understand the reaction path, the donor atom of the ligand must be investigated. To consider what bonds can take place, valence electrons and their most likely whereabouts in the molecule play an important role.

2.2.1 Complex structures and reactions

A complex is a compound often formed by transition metals. It always has a complex centrum consisting of a neutral atom or a cation called a central atom. The central atom is surrounded by charged (anion) or neutral one or multi atomic groups, called a ligand. [57]

The number of ligands that are bound on the central atom is called coordination number (CN). The most common coordination numbers are 2, 4, and 6. The corresponding spatial structure can be described as following:[61]

Table 6 Spatial structure for complexes depending on the coordination number. [61]

CN	Spatial structure
2	Linear
4	Tetrahedral, square planar
6	Octahedral

If all ligands are similar, the complex is homoleptic. If not, it is heteroleptic. The process of a formation of a complex can be described as a Lewis-acid-base-reaction. The center is the Lewis acid, and the ligand acts as Lewis base.[57] Complexes dissociate in small amounts in aqueous solutions. Their ion-compounds are also described as masked.[61]

Complexes form covalent bonds between a central element and ligand via orbital overlap of an empty central atom orbital (cation) and a full ligand orbital (anion). The bonding electrons come from the ligands. The spatial order of the ligands can be described by the hybridization of the central atom orbital. [61]

The formation of a complex is expressed as an equilibrium reaction following the law of mass action. The equilibrium constant is calculated as following with M standing for metal and L for ligand [61]:

$$M + L \leftrightharpoons ML \quad K_1 = \frac{c_{ML}}{c_M * c_L} \tag{2.35}$$

$$ML + L \leftrightharpoons ML_2 \quad K_2 = \frac{c_{ML_2}}{c_{ML} * c_L} \tag{2.36}$$

$$ML_2 + L \leftrightharpoons ML_3 \quad K_3 = \frac{c_{ML_3}}{c_{ML_2} * c_L} \tag{2.37}$$

$$ML_3 + L \leftrightharpoons ML_4 \quad K_4 = \frac{c_{ML_4}}{c_{ML_3} * c_L} \tag{2.38}$$

Those constants are called stability constant or complex formation constant. To describe the formation following formulas are applicable [61]:

$$M + L \leftrightharpoons ML \quad \beta_1 = \frac{c_{ML}}{c_M * c_L} \qquad (2.39)$$

$$M + 2\,L \leftrightharpoons ML_2 \quad \beta_2 = \frac{c_{ML_2}}{c_M * c_L^2} \qquad (2.40)$$

$$M + 3\,L \leftrightharpoons ML_3 \quad \beta_3 = \frac{c_{ML_3}}{c_M * c_L^3} \qquad (2.41)$$

$$M + 4\,L \leftrightharpoons ML_4 \quad \beta_4 = \frac{c_{ML_4}}{c_M * c_L^4} \qquad (2.42)$$

or

$$\beta_n = K_1 * K_2 \ldots * K_n \qquad (2.43)$$

The higher the complex constant, the higher is the resistance of the complex. [61]
In literature following ligand constants for mercury can be found:

Table 7 Ligand constants for mercury. [27], [30]

Ligand	**Cl^-**	**Br^-**	**I^-**	**OH^-**	**SO_3^{2-}**
Mono-dentate	yes	yes	yes	yes	yes [62]
log k1	6,76	9,05	12,87	10,3	22,66
log k2	6,4	8,28	10,95	11,4	1,41
log k3	0,83	1,42	3,78	-0,5	0,89
log k4	1,23	1,26	2,23		

Those values can describe the affinity of different ligands to mercury. Chloride with the lowest stability constant will be displaced by bromide if it is available for mercury and so on. But it is also possible that heteroleptic complexes will be formed, depending on the ligand supply in the solution. [27]
For the stability constants for hydroxide and sulfite, it has to be considered that those are dependent on the pH value and change with it.[28]
Complexes of transition metals can undergo three kinds of reactions [23]:

- Oxidation-Reduction
- Substitution and
- Isomerization.

2.2.2 Ligands

Next to the stability constant, the theory of hard and soft acids can explain a central atoms' tendency to prefer one ligand over another. [63]
Central atoms can be separated into two different groups: [63]

- Ions of alkaline, alkaline earth metals, and transition group elements with a high oxidation state and
- Ions of the heavy transition elements like Cu, Ag, or Hg (in both oxidation states)

For the second group, the stability of the different complexes for mercury can be described as:

- O<<S: Sulfur has a much higher tendency to form a complex with mercury than oxygen.
- F< Cl< Br < I: For the halides, it is consistent with the stability constants discussed before. Iodine has the highest tendency to form a complex with mercury compared to the other ligands.

[63]
The terms hard and soft acids as well as bases are introduced for further characterization. Hard acids and bases are small, not polarizable ions, whereas soft bases and acids are big ions with a high tendency to polarize. Therefore, mercury represents a soft acid, and iodine or sulfur are soft bases. [63]
The equilibrium can be explained with equation 2.44 [63]:

$$[\mathrm{BH}]^+ + [\mathrm{MethylHg}]^+ \leftrightharpoons [\mathrm{MethylHgB}]^+ + \mathrm{H}^+ \qquad (2.44)$$

If B is a hard base, the equilibrium lies on the left side. If it is a soft base, the equilibrium lies on the right side.
In competition to that theory, the actual acidity or basicity of the ions must be considered. This means that a strong but hard base can substitute a weak but soft base from a soft acid, as shown in equation 2.71. [63]

$$[\mathrm{OH}]^- + [\mathrm{MethylHgSO_3}]^- \leftrightharpoons [\mathrm{MethylHgOH}] + [\mathrm{SO_3}]^{2-} \qquad (2.45)$$

The higher basic strength of OH^- in comparison to SO_3^{2-} will push the equilibrium of the equation to the right side.

But if there is another hard acid, hard and hard and soft and soft will find each other (see eq.2.46). [63]

$$[\mathrm{MethylHgOH}] + [\mathrm{HSO_3}]^- \leftrightharpoons [\mathrm{MethylHgSO_3}]^- + \mathrm{H_2O} \quad (2.46)$$

In equation 2.46, the hydroxide ion reacts with the strong and hard acid H^+. Further, a central atom can form a hard character due to a coordination of a hard ligand and a soft ligand can contribute a softer character for the Lewis acid. [63]
As an example, for the two complexes BH_3 and BF_3, B^{3+} becomes softer with the coordination with H^- than with F^-. This means BH_3 reacts easier with sulfur than with oxygen, and BF_3 will react the other way around. Also, BH_3F^- will react with BF_3H^- to homiletic complexes BH_4^- and BF_4^-.[63]
The discussed theory is empiric. The following table describes the tendency of the main ligands in FGD to form a hard acid like H^+ and a soft acid like $MeHg^+$ [63]:

Table 8 Basicity of ligands in comparison to a soft and a hard acid. [63]

Base	Binding atom	$pK_{hard}(H^+)$	$pK_{soft}([MeHg]^+)$
Cl^-	Cl	-7.0	5.25
Br^-	Br	-9.0	6.62
I^-	I	-9.5	8.6
OH^-	O	15.7	9.37
SO_3^{2-}	S	6.79	8.11

Table 8 shows that all ligands have a high ambition to react with mercury. OH^- with the highest and Cl^- has the weakest tendency to react with a weak acid like mercury. Sulfite and hydroxide have an even higher affinity to react with H^+. This affinity to H^+ indicates a high dependency on the pH value for both ligands OH^- and SO_3^{2-} to form a Hg-complex. Also, this characteristic shows that the force to form a complex with mercury of the considered three halides is not dependable on the pH value. In conclusion, with a high concentration of H^+ and therefore a low pH value, Iodine is the most likely ligand for mercury. With an increase of the pH value, OH^- becomes the most probable ligand for mercury. This model helps to explain empirically determined stability constants of the different mercury complexes. Nevertheless, it always has to be considered that in an technical FGD process all ligands are in one solution and stand in competition to each other. [8]

2.3 Mercury characteristics, structure and typical behavior

For a better understanding of the behavior of mercury and the interpretation of possible Hg_s species in FGD gypsum, inorganic mercury species are investigated closer.

Except for HgF_2, mercury forms covalent bonds. Hg(II)- compounds have low solubility and are solved as a molecule most of the time. The prior coordination is linear or tetrahedral. [61]

Mercury(I) is bimolecular, mercury (II) monomolecular. Mercury has a positive ORP, high electronegativity, and its first ionization energy is the highest of all the elements in the transition groups of the periodic table. The valence electron configuration with a filled s-orbital leans to the noble gas configuration. The fully occupied s-orbital explains the weak Hg-Hg bond in the elemental state but explains the stable Hg-Hg covalent bound for mercury (I). The high first ionization energy corresponds to the high electronegativity. The stable oxidation state (II) can be explained with the low sum of the ionization energies one and two, and the relatively high sum of the ionization energies one, two and three. This explains partly the high percentage of covalent compounds as Hg-Hg for mercury with the oxidation state one like Hg_2Cl_2 or X-Hg-X for mercury with an oxidation state +II like $HgCl_2$ as a molecular grill. [57] [61] The typical coordination for mercury is linear, similar to the behavior of Ag(I), Cu(I), or Au(I). [61] All mercury(I) species can be a product of Hg(II) and Hg^{el}. [57]

2.3.1 Halides

Mercury halides do not show an ionic character, but the ionization character grows from $HgI_2 < HgBr_2 < HgCl_2$. The dissociation of mercury halides in an aqueous solution is very small and increases in the same pattern as the ionic character. [57] Mercury builds covalent bonds with halides. [61] Mercury(II)chloride melts at 280 °C and evaporates at 303°C. It has covalent bonds as a solid, a gas, and in an aqueous solution. It forms linear Cl-Hg-Cl isolated molecules in all three phases. HgI_2 has an isolated form in the aqueous phase and the gas phase, in the solid state it builds a corner-linked HgI_4 tetrahedron at temperatures < 127 °C. At temperatures > 127 °C, it converts into its yellow form and an isolated covalent molecule form as $HgCl_2$.The structure of $HgBr_2$ is a compromise of the two other halides. The primary molecule is an isolated Br-Hg-Br molecule as for chloride but is surrounded by Br atoms from other $HgBr_2$ molecules, which stabilize this structure by a longer bond. This structure leads to an octahedron of $HgBr_6$ in the solid-state. [57]

Mercury halides react with different impurities in the solution or other possible ligands. In the following, the considered reaction partners: hydroxides, sulfite or sulfate and, metals as contaminants are closer investigated. [58]

Metals like Fe(II)Cl_2 or Cu reduce $HgCl_2$ and oxidize themselves. The reduction happens via Hg_2Cl_2. [58]

It forms HgO (yellow) (HgO(y)) with earth metal oxides like CaO, SrO or MgO and BrO, $HgCl_2$. $Hg(BrO_3)_2$ stays stable up to 140 °C and deflagrates at 155°C mainly as $HgBr_2$. [58]

Aqueous SO_2 reacts with mercury chloride. Diluted sulfuric acid is not reacting with $HgCl_2$. [58]

Hydroxides precipitate $HgCl_2$ to HgO. Mixed complexes may occur. HgO(y) forms a 3HgO * $HgCl_2$ complex with $HgCl_2$. It is possible to shift the precipitation to a higher pH value when adding chlorine to the solution. A 2,500 times higher chloride concentration than mercury concentration is necessary to prevent precipitation. $HgCl_2$* xHgO reacts with the sublimation of $HgCl_2$ until only red HgO stays as solid residue, starting at 100 °C.

Mercury bromide reacts in the same way as $HgCl_2$. Because of the smaller dissociation degree, it needs a higher OH^- concentration than $HgCl_2$. Depending on the concentration, $HgBr_2$ reacts to $HgBr_2$*HgO, HgO or does not precipitate at all.

Carbonates can also precipitate $HgBr_2$ to $HgBr_2$* xHgO, where x depends on the concentration of the solution. The different complexes can be differentiated by color. For example, $HgBr_2$*3HgO has a grayish character and $HgBr_2$* 4HgO has a red-brown coloring. HgI_2 can be produced with HgO and iodine at temperatures between 105-140°C, depending on the present impurities. [58]

Calomel dissociates into $HgCl_2$ and Hg^{el} after heating. The distribution between both species varies with temperature. Figure 3 shows the distribution of Hg(II) and Hg^{el} over the relevant temperatures.

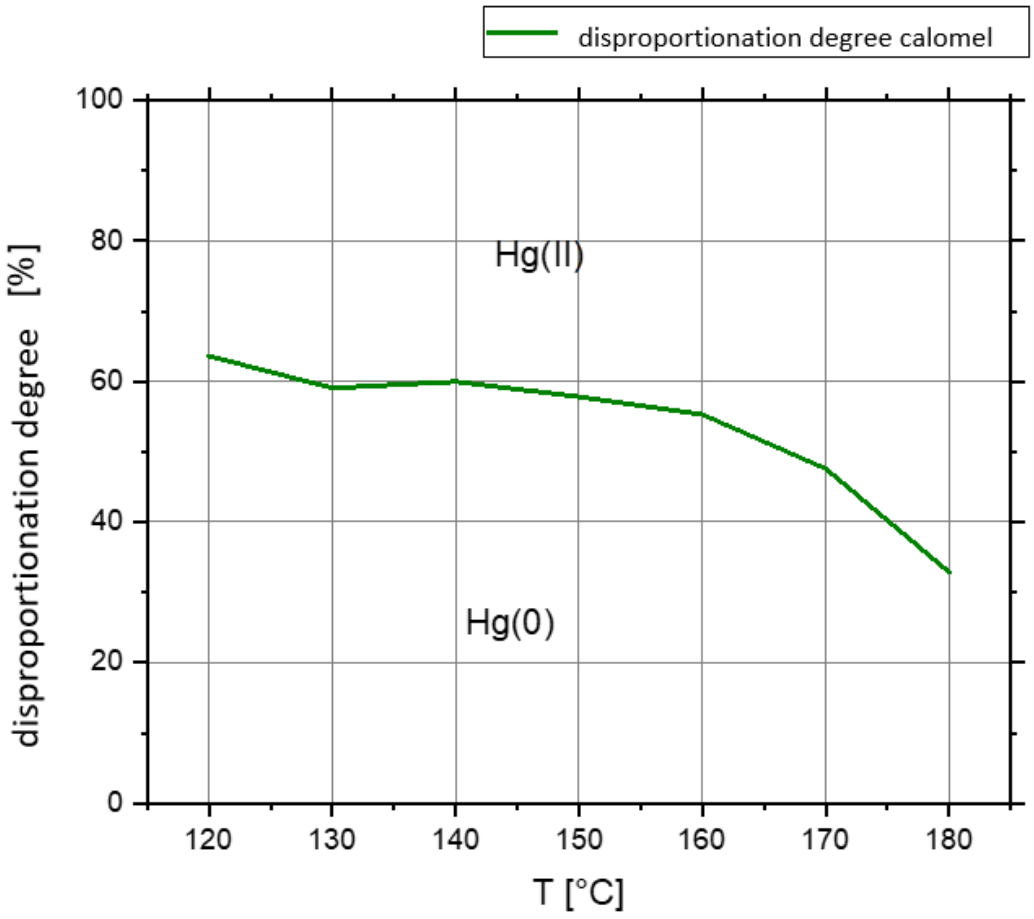

Figure 3 Disproportionation of calomel versus temperature.[58]

One of the formation processes for calomel is the reaction of a $HgCl_2$ solution with SO_2 at 50°C. There are different structures of calomel. It has to be distinguished between the formation of calomel via sublimation or through precipitation. Calomel reacts to Hg_2O with hydroxides. [58]

2.3.2 Oxides

There are two different kinds of mercury(II)oxide, a red one and a yellow one. Those colors appear due to the production process. The red mercury(II)oxide is formed during the thermal decomposition of mercury nitrate, while the yellow-colored oxide is a product of precipitation. Density and crystal structure do not seem to differ, but the precipitation product has a smaller particle size and is harder. In the red form it is more easy to ionize pollutions than in the yellow form. Solutions, as well as solids, change color with the change of temperature. All solids become red at temperatures > 200 °C. [59], [61]

The crystal has a rhombic modification and builds a zigzag chain with Hg and O. It is assumed that by heating HgO, it decomposes into its single compounds and evaporates as elemental mercury and oxygen. The generation of ozone can be observed under certain circumstances. During the evaporation, mercury peroxide can form in the presence of oxygen in the gas phase. HgO decomposes at 431 °C. The presence of Fe_2O_3 (410°C), MnO_2 (225 °C), or CuO (381 °C) can reduce the decomposition temperature of mercury oxide. Al_2O_3, as well as SnO_2, do not trigger any effect. [59]

$$Hg + \frac{1}{2}O_2 \underset{400°C}{\overset{300\text{-}350°C}{\rightleftharpoons}} HgO \qquad (2.47)$$

[61]

Mercury(II)- and mercury(I)oxides are not soluble in water. They hydrolyze into $[Hg(OH)_n]^{n-1}$ complexes. The worst solubility is at a pH value of 7. [59]

$$HgO + H_2O \rightleftharpoons Hg(OH)_2 \qquad (2.48)$$

$$HgO + 2H^+ \rightleftharpoons Hg^{2+} + H_2O \qquad (2.49)$$

[59]

A ligand change can occur in the presence of halides and will form a mercury(II)halide complex. With sulfite, HgO reacts to mercury(II)sulfite and mercury(II)sulfate. Mercury nitrate precipitates to HgO at a pH value of 1.82. Because of the small dissociation degree and therefore a lack of Hg^{2+} a much higher OH^- concentration is needed to precipitate mercury(II)chloride (pH > 5.2) or $HgBr_2$ (pH 7.5-10.4). [58], [59]

Hg_2^{2+} precipitates with KOH to Hg_2O (black). This precipitation product contains the same amount of Hg^{el} as Hg(II)O. The existence of Hg_2O is still under discussion.

$$Hg_2^{2+} + 2OH^- \rightleftharpoons Hg_2O + H_2O \rightleftharpoons Hg\uparrow + HgO\downarrow + H_2O \qquad (2.50)$$

[57], [60]

2.3.3 Sulfide, sulfite and sulfate

There is a theory that Hg_2S is a combination of HgS and elemental mercury. It can be created with Hg^+ and H_2S, similar to Hg_2O.

HgS occurs in red and black. But other than HgO, the red form of HgS has a hexahedral crystal structure while the black HgS a cubic spatial structure. HgS decomposes into elemental Hg and S when heated. The specific decomposition

temperature depends on the formation process of HgS. There are two ways to create HgS. The first is via sublimation and the second is via precipitation. The decomposition starts slowly between 109-210 °C accelerates around 300-310 °C.
Wet HgS oxidizes slowly in air. There is no reaction with bases. [64]
The existence of $HgSO_3$ is still discussed in literature. Gmelin [59] states that it is more realistic that $HgSO_3$ is one component of a blend of different mercury complexes, e.g., 2 HgO*SO_2 or $HgSO_3$*H_2O*0.5 HgO. It can be created with $Hg(NO_3)_2$ and $Na_2(SO_3)$ in a ratio of 1:10.
Better known complexes are Hg_2SO_3*$HgSO_3$*4H_2O and $Hg_4(SO_3)_2$*H_2O. $Hg(HSO_3)_2$ or HgO*2SO_2*H_2O have a high solubility and react under heating to elemental mercury.
The reaction behavior of mercury hydrogen sulfite is - similar to mercury sulfite - very inconsistent. It hydrolyses very fast into elemental mercury and H_2SO_4 or reacts to Hg_2SO_3*$HgSO_3$* 4H_2O and H_2SO_4. It is possible to precipitate this complex with ethanol. [59]
Mercury sulfate decomposes at 700 °C. $HgSO_4$ can also be described as HgO- SO_3- H_2O. The most current pollution is oxygen in a mercury sulfate complex. Mercury sulfate has a rhombic crystal structure. In the crystal, oxygen surrounds Hg. $HgSO_4$ decomposes to $HgSO_4$*HgO. This compound has a high vapor pressure. Therefore, the reaction to $HgSO_4$*2HgO is fast.
The decomposition products of mercury sulfate are dependent on heating time and temperature, as shown in Table 9 [59]:

Table 9 Decomposition of mercury(II) sulfate at different temperatures. [59]

T [°C]	Heating time [h]	Possible species
400	2	$HgSO_4$
500	2	$HgSO_4$; $HgSO_4$*HgO; $HgSO_4$*2HgO
600	1	$HgSO_4$*2HgO; $HgSO_4$*HgO; $HgSO_4$
600	2	No residue
700	0,25	$HgSO_4$*2HgO; $HgSO_4$*HgO; $HgSO_4$ Hg_2SO_4

$HgSO_4$ is formed with concentrated sulfuric acid and elemental mercury.

$$Hg + 2\ H_2SO_4 \rightleftharpoons HgSO_4 + SO_2 + 2\ H_2O \qquad (2.51)$$

In water $HgSO_4$ hydrolyses into alkaline mercury sulfate with a low solubility.

$$3\ HgSO_4 + 2\ H_2O \rightleftharpoons HgSO_4 * 2\ HgO \downarrow + 2\ H_2SO_4 \qquad (2.52)$$

$HgCl_2$ will form via ligand change after the addition of HCl.[64]
Hg_2SO_4 is very sensible to light. It decomposes into Hg, O_2 and SO_2 while heating. The formation of Hg_2SO_4 can be described as:

$$4\ HgO + 2\ SO_2 \rightleftharpoons 2\ Hg + 2\ HgSO_4 \qquad (2.53)$$

And

$$4\ HgSO_4 + 3\ SO_2 \rightleftharpoons 2\ Hg + Hg_2SO_4 + 6\ SO_3 \qquad (2.54)$$

As different from the Hg(II)-species, Hg(I)sulfate is not soluble in water and does not hydrolyze.

2.3.4 Nitrate

$Hg_2(NO_3)_2$ is a non-colored rhombic crystal. In the crystal, mercury has four neighbors:

- Hg,
- two oxides from one nitrate molecule,
- and one oxide from one water molecule.

The formation has a high polarization energy similar to the oxonium ion $[H_2O\text{-}Hg\text{-}Hg\text{-}OH_2]^{2+}$ of mercury.
$Hg_2(NO_3)_2$ is very soluble of low pH values, for example, in diluted HNO_3, but at pH values >1, it quickly forms basic salts. More than 30 different salts are mentioned in literature, e.g., $Hg_2(NO_3)_2 * 2\ H_2O$ (yellow), $Hg_2O * N_2O_5 * 2\ H_2O$, or $3\ Hg_2O * 2\ N_2O_5 * 2\ H_2O$. When adding KOH, Hg_2O will be formed. In the formation of $Hg_2(NO_3)_2$, no disproportionation:

$$Hg_2^{2+} \rightleftharpoons Hg^0 + Hg^{2+} \qquad (2.55)$$

is mentioned. But a $Hg(NO_3)_2$ solution mixed with elemental Hg forms Hg_2^{2+}.
A decomposition of $Hg_2(NO_3)_2$ can be detected at 70 °C. The first mercury evaporation can be measured between 150 °C and 300 °C. The thermal degradation has four steps:

- At ambient temperature, the crystal water evaporates, leaving $Hg_2(NO_3)_2$ as residue.
- The next degradation step is the formation of 3 $Hg_2O * N_2O_5$.
- This is followed by the disproportionation of Hg_2O into HgO as Hg_2O * 2 HgO * N_2O_5 (orange-yellow).
- With a further increase in temperature, the species decompose into their compounds Hg, N, and O.

The rise of temperature is not the only way for decomposition of $Hg_2(NO_3)_2$. It can also decompose under the influence of daylight, ending in $Hg_2O * HgO * N_2O_5$ (yellow).
In solution $Hg_2(NO_3)_2$ dissociates into $^+Hg\text{-}Hg^+$ ions. At c(Hg) > 10^{-5} mol L^{-1} and c(Hg) < 10^{-20} mol L^{-1} solemnly Hg^+ is stable. In between both “species“ are available.
Starting with an increase of the pH value, around pH >1.9 hydrolyses of Hg_2^{2+} begins with:

$$Hg_2^{2+} + H_2O \rightleftharpoons [Hg_2OH^+]_n + nH^+ \qquad (2.56)$$

At pH values >4, hydrolysis can be described as:

$$nNO_3^- + Hg_2^{2+} + H_2O \rightleftharpoons [Hg_2(NO_3)_nOH_{n-1}]^- + H^+ \quad (2.57)$$

At a higher (alkaline) pH value, a mixture from $Hg_2(NO_3)_2$ and Hg_2O will occur. [59]
For $Hg(NO_3)_2$, similar to $Hg_2(NO_3)_2$, the degree of the hydrolyses is not fully known. There is no water-free salt. Even in high acidity solutions, basic salts such as 3 $HgO*N_2O_5$ start to form.
$Hg(NO_3)_2$ forms long transparent crystals that are highly hygroscopic and melt at ambient temperature. Mercury(II)nitrate decomposes from a solid during heating. HgO starts developing at a pH value of 1.85. Hg(II)-nitrate solution with elemental mercury reacts to Hg_2^{2+}.[59]

2.4 Sulfur dioxide

This chapter discusses the reaction of SO_2 in a scrubber system. It starts with the hydrolysis of SO_2. Further reactions follow in the scrubber where the final reaction is the formation of gypsum. Because sulfite is considered one of the ligands for mercury with the highest impact on its oxidation state, its reaction path in the scrubber is considered very important. SO_2 dissolves in water and forms H_2SO_3.

$$SO_2 + H_2O \rightleftharpoons SO_2 * H_2O \rightleftharpoons H_2SO_3 \quad (2.58)$$

The equilibrium lies on the side of hydrated SO_2

$$SO_2 * H_2O \rightleftharpoons H_2SO_3 \, , K \ll 10^{-9} \quad (2.59)$$

As a two protonic acid, it disproportionates in two steps:

$$H_2SO_3 \rightleftharpoons H^+ + HSO_3^- \quad (2.60)$$

$$H^+ + HSO_3^- \rightleftharpoons 2\,H^+ + SO_3^{2-} \quad (2.61)$$

[57]

The equilibrium constants K1 and K2 can be calculated as described in chapter 2.1. Figure 4 shows the change of the main species of the hydrolysis of SO_2 depending on the pH value.

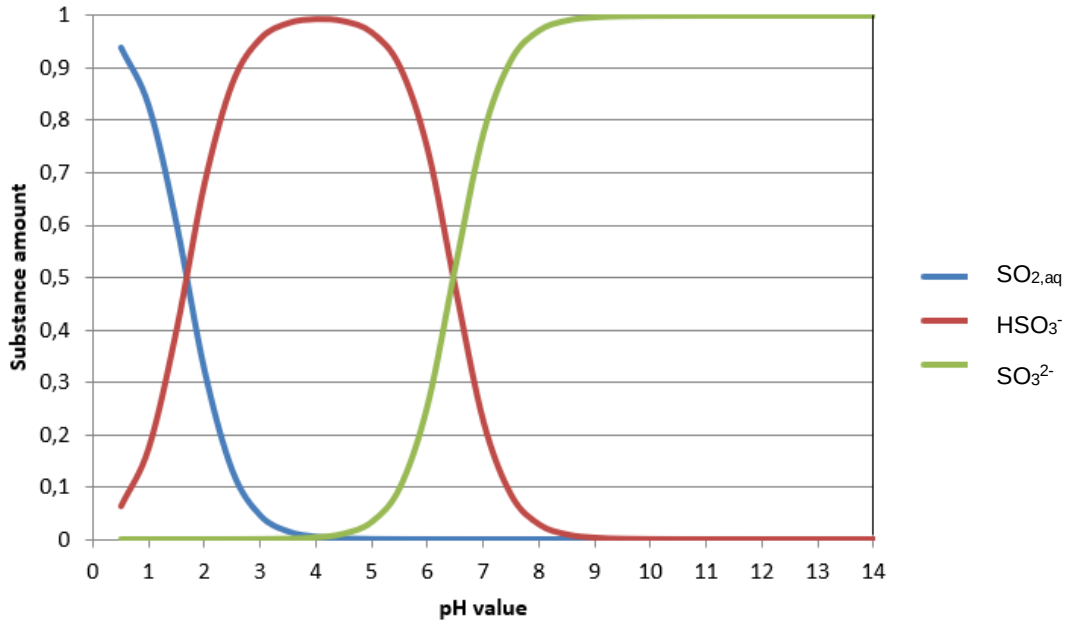

Figure 4 Hydrolysis of sulfite.

Sulfurous(IV) acid tends to oxidize to sulfuric acid and reduce other molecules or elements, such as Hg^{2+}, to elemental Hg.

This behavior is stronger in an alkaline solution than in an acetic one.

$$SO_3^{2-} + 2OH^- \rightleftharpoons SO_4^{2-} + H_2O + 2e^- \; \varepsilon_0 = -0.936\ V \qquad (2.62)$$

$$SO_2 + H_2O \rightleftharpoons SO_4^{2-} + 4\ H^+ + 2e^- \; \varepsilon_0 = +0.158\ V \qquad (2.63)$$

[57]

Sulfite can act as Lewis base and donates an electron via a nucleophilic attack on the Lewis acid.[57]

The absorption rate of SO_2 increases by increasing the pH value, the solubility of limestone restricts this tendency.[15]

The products of the hydrolysis of SO_2 can be described with different tautomers. [65] Guthrie [65] describes SO_2*H_2O as $SO(OH)_2$ with dissociation to $H\text{-}SO_3^-$. The additional protonation on the S-atom could explain the better solubility in water compared to CO_2.

Holleman et al. [57] describe the tautomers of H_2SO_3 as well as HSO_3^- as sulfurous acid and sulfonic acid as well as hydrogen sulfite (SO_3-H) and sulfonate (H-SO_3).

Both tautomers should exist equally in a solution, but only an H-S bond can be found in a complex.[57]

The sulfite as a ligand (SO_3^{2-}) can coordinate mono-dentate with one bond on sulfur or oxygen. It can also act as a bi-dentate ligand via two oxygen molecules or one oxygen and one S bond. Polymeric structures with M-O-S-M bonds are also possible. Such a complex structure is called a bridge, and one character can be a low solubility of the complex. [62]

Sulfur dioxide is known to form O-bound complexes with hard metals and S-bound complexes with soft metals.[57]

SO_2 is washed out of the flue gas, via absorption into water or a suspension of earth alkali hydroxides or a weak base like $CaCO_3$. Inside the scrubber solution SO_2 reacts with $CaCO_3$ to $CaSO_3$ with:

$$CaCO_3 + SO_2 \rightleftharpoons CaSO_3 + CO_2 \qquad (2.64)$$

$CaSO_3$ can be oxidized with oxygen and at pH levels 4.8-5.3 with following reaction:

$$CaSO_3 + \frac{1}{2}O_2 \rightleftharpoons CaSO_4 \downarrow \qquad (2.65)$$

The gypsum suspends in solution and after further treatment steps is used as gypsum for construction. [57]

2.5 Mercury chemistry in FGD-system

To better understand mercury's different reaction paths and behavior, the following chapter will discuss the primary known and discussed reaction possibilities in FGD. The focus is set on the different phases in aqueous solution and solid. The part about mercury in aqueous solution will focus on the main ligands consistency of halides and sulfite and will discuss the influences of parameter settings such as pH value or ORP. The part about mercury in the solid phase considers mercury species that can occur in FGD gypsum and describes ways to analyze a solid sample with an unknown mercury content and species.

2.5.1 Aqueous phase

Mercury has two different oxidation states in flue gas, +II and 0. To be absorbed in a scrubber solution, Hg_g must pass through the boundary of the gas phase and the liquid phase via diffusion. The absorption process follows the Henry law, because of the small concentrations of mercury. After the absorption, mercury does not disproportionate in the aqueous solution and stays in equilibrium with the gas phase. The amount that reemits can be derived from the vapor pressure of the different mercury species. For mercury with the oxidation state (II), the equilibrium lies on the liquid side. For mercury of the oxidation state 0, the equilibrium lies on the gas side. [12]

The main reactions pathways of mercury can be described as following (Figure 5):

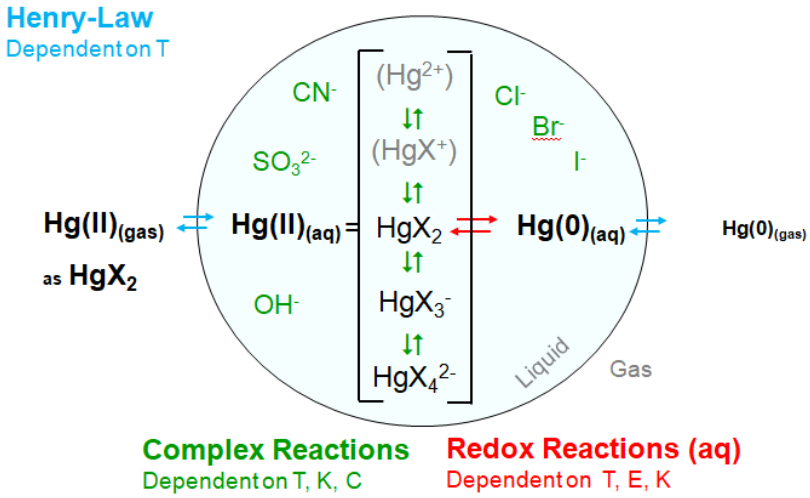

Figure 5 Bittig droplet, description of possible pathways for mercury in a liquid -gas equilibrium. [12]

The blue path describes the absorption of mercury in the aqueous solution and the equilibrium of Hg_{aq} with Hg_g.

Following the Henry law, the temperature (T) impacts the equilibrium between the gas and liquid phase. By increasing the temperature, the concentration of HgX_2 rises in the gas phase. [8]

In the liquid phase, two different reactions can occur. One is the red path of the redox reaction followed by a reemission of elemental mercury. This reaction depends on the temperature (T) the complex constant (K) and the electro chemical potential (E). The other one is the green path and describes a complex reaction with a higher coordination of mercury or a ligand change. Ligands are, e.g., the three halides chlorine, bromine, and iodine, cyanide, hydroxide, and sulfite. [12]

Mercury and halides

The main oxidized mercury species in the flue gas is mercury chloride. It can include mercury bromide from adding bromide salts during the combustion process. [14]

After absorption, mercury starts to react with other components in the scrubber suspension.

For example, a small amount of bromide in the suspension, can have a significant influence on $HgCl_2$. Due to a higher ligand strength, a ligand change will take place. This reaction is mainly dependent on the ligand strength and free ligand concentration. [27]

The ligand strength depending on the stability complex constant (see section 2.2) of the different halides follows the sequence:

$$HgI_2 >> HgBr_2 > HgCl_2 \qquad (2.66)$$

[8], [27], [28]

For the halides system pH value, redox-potential and temperature have a secondary influence on the formed complexes (see section 1.3). [27]

Unfortunately, the volatility of the different mercury-halides complexes also increases with the ligand strength. The described ligand strength and higher volatility can lead to a ligand exchange from the main mercury species in the flue gas $HgCl_2$ in the scrubber solution and lead to higher emission of mercury species of Hg_{aq}^{ox}.[28]

This behavior of HgX_2 explains, that oxidized mercury can be detected behind an FGD scrubber. Hg(II) emissions depend on the ligand due to the Henry coefficient and vapor pressure and the concentration of free ligand in the suspension.[27], [28]

Uncharged mercury-halide- complexes remain in equilibrium with the gas phase, following the Henry law, but with an excess of the ligand in solution, anionic mercury complexes are formed. By carrying a charge, the complex will no longer stay in equilibrium with the gas phase. [8], [27], [28]

Bittig [27] [12], [29], [66] et al. show that the stabilization impact of halides on Hg_{aq} is not dependent on the pH value but on their ligand strength and concentration. It is possible by increasing the halide concentration to form a higher coordinated mercury complex with a charge and remove the complex from the Hg_{aq}-Hg_g equilibrium to stabilize it in the aqueous phase.

Other possible ligands like OH^- are dependent on the pH value. [28]

Bittig [27] was able to show that it needs a much higher free ligand concentration than mercury concentration to build a charged complex. This behavior depends on the ligand stability constant K (see section 2.2). Even with a wide range of values for the different ligand stability constants (see section 2.2), all show a much higher constant for K1 and K2 than for K3 or K4. These constants indicate that for a wide range of free ligand concentrations, mercury halides mainly form an uncharged HgX_2 complex. For mercury chloride, 1mol L^{-1} free chloride is needed to gain a $[HgCl_4]^{2-}$ complex. This concentration differs between the halides for the anionic bromide mercury complex, it is around 10^{-2} mol L^{-1} free bromide, and it is 10^{-3} mol L^{-1} for iodide.

Guthrie showed that mixed halide complexes can be formed. He developed the rule, that halides with lower electronegativity than the one already forming a complex with mercury will lead to a ligand change. Halides with higher electronegativity can be added to the complex. [27] These mixed complexes show a different Henry constant and different evaporation behavior than the homoleptic ones. [28]

Mercury and sulfite

As mentioned in section 1.3 one of the main reactions considered responsible for elemental mercury reemission is the redox reaction of Hg_{aq} and SO_{2aq}.[14] [20]

$$Hg^{2+} + SO_3^{2-} \rightleftharpoons [HgSO_3] \qquad (2.67)$$

$$[HgSO_3] + SO_3^{2-} \rightleftharpoons [Hg(SO_3)_2]^{2-} \qquad (2.68)$$

$$[HgSO_3] + H_2O \rightleftharpoons Hg^0 \uparrow + SO_4^{2-} + 2H^+ \qquad (2.69)$$

Blythe et al.[20] identified a rapid reduction of Hg_{aq}^{2+} to Hg^0 by sulfite. With a higher concentration of sulfite, it was possible to slow down the reaction to Hg^0. Experiments containing chlorides and sulfite showed that a high chloride concentration could also dampen the reaction rate and form a mixed Hg-Cl^--SO_3^{2-} complex. Every addition of chloride in the solution slows down the reduction rate. In comparison, different halides, iodide, and chloride were investigated in solution with mercury and sulfite. Whereas

chloride in small concentrations could not stop the reduction of mercury, iodide as a strong ligand for mercury could substantially reduce the reduction rate of mercury.
The reaction of sulfite with Hg_2^{2+} showed similar results. Hg_2^{2+} disproportionates, resulting in Hg(0) and a Hg(II)-Sulfite complex.

Van Loon et al. [21] show the existence of $HgSO_3$ with a shift of a UV Spectrum from $HgSO_3$ absorption to Hg^+ absorption. In conclusion, Van Loon et al. [21] postulate that the reaction is an intramolecular redox reaction. But because neither Hg^+ nor a sulfite radical can be observed, it is believed that Hg^{2+} is reduced to Hg^0. Hg_2^{2+} is formed via comproportionation of Hg^0 with Hg(II). The reaction rate of the redox reaction is strongly dependent on temperature but independent on a pH value change or soluble oxygen. The results are consistent with the reaction rate of an intra-molecular redox reduction of $HgSO_3$ into Hg(0). The reaction to Hg_2^{2+} is only possible if Hg^{2+} is available in excess.

$$HgSO_{3\,aq} \rightleftharpoons Hg^0 \uparrow + S(VI) \qquad (2.70)$$

$$Hg_{aq}^{2+} + Hg_{aq}^{0} \rightleftharpoons Hg_{2\,aq}^{2+} \qquad (2.71)$$

[21]
The coordination number of $HgSO_3$ is not known, but it is most likely that there is at least one water molecule in the sphere of the coordination of mercury. [21], [23]
As $Hg(SO_3)_2^{2-}$ has a higher coordination for Hg as $HgSO_3$, it shows a higher stability than $HgSO_3$. The reaction to $Hg(SO_3)_2^{2-}$ seems to be inhibited by a limited amount of free SO_3^{2-}.The reaction of Hg with sulfite is mainly with SO_3^{2-}.[22]
Sulfite can act as a ligand via a S- bond or an O- bond. [23], [57], [65] When bonding on the O, the redox reaction is 10^2 times faster than bonding on the S. [13]
It seems that mercury has no affinity to HSO_3^-.[22] This behavior would support the hypothesis that the coordination of mercury is with the lone electron pair of the sulfur. But in the most common tautomer for HSO_3^- the proton occupies this electron pair, so that the sulfur is not accessible for a reaction with mercury. [65] [57]
In an ideal system a higher coordination of $Hg(SO_3)_2^{2-}$ occurs with water ($Hg(SO_3)_2(H_2O)_n^{2-}$), not with an additional SO_3^{2-}. $Hg(SO_3)_2^{2-}$ is formed in an acidic or neutral solution with mercuric ions with excess of HSO_3^-/SO_3^{2-}: The system investigated was air saturated. Van Loon et al [21], [22] were able to show that the UV spectrum shifted from an absorbance from around 230 nm to 215 nm by adding NaOH. This behavior indicates that sulfite of the complex at a higher pH value shifts out of the ligand bond to form a free ion in the solution. [22]

They also suspect a new, coordination for mercury as

$$Hg(0) + SO_2 \rightleftharpoons [Hg(0) * SO_2] \qquad (2.72)$$

[22]

The formation of higher coordinated sulfite complexes was also reported by Heidel [8], who found out that a high concentration of S(IV) led to irreversible bonds of mercury that seem to be stable at high temperatures.

As mentioned in section 1.3 Blythe et al. [20] described a catalytic disproportionation of sulfite caused by mercury. The disproportionation can be described as:

$$4SO_3^{2-} \rightleftharpoons 3SO_4^{2-} + S^{2-} \qquad (2.73)$$

This can be an indication for a possible formation of HgS. [24]

Metals and other impurities

Next to halides and sulfite, other impurities of the FGD matrix but also other process parameters can influence the reaction path of mercury in FGD:

For example, the dosage of Fe(II) can reduce mercury rapidly. Hg_2^{2+} is rapidly oxidized with Fenton reagent, but Fe(III), as well as H_2O_2, do not seem to affect the oxidation state of elemental mercury.[67] Fe(III) showed a different effect on mercury than Fe(II). It raised the redox potential and lowered the Hg^{el} emissions at a pH value of 4 in a scrubber. It could also be shown that a slow dosage and a high oxidation level oxidize Fe(II) into Fe(III) before it can reduce mercury. [26], [28]

The dosage of thiosulfate causes mercury to shift from the liquid phase into the fines fraction of the solid phase. Adding dithionite had the same impact but shifted the mercury concentration in the gypsum part of the solid phase. The mechanisms behind the reactions of thiosulfate and dithionite with mercury are not yet identified. [7]

pH value

Blythe et al. [20] showed in their research that impurities as manganese and calcium increase the reemission of mercury. For the addition of calcium, the increase of mercury reemission was linked to an increase in the pH value.

The most advantageous operation mode to avoid reemission is keeping the oxidation limit high, reducing the sulfite concentration, and keeping the pH value as low as possible.[20]

Bittig showed that mercury and halide reactions are independent of the pH value of the solution [27]. Nevertheless, the state of SO_2 in the solution is dependent on the

pH value. As sulfite is a ligand for mercury, there is an indirect dependency between mercury and the pH value. [8] This behavior can be explained with the reaction formulas and the Nernst equations of the different reactions (e.g. chapter 2.1.1).
Van Loon et al. [21], [22] showed that even if the hydrolysis of SO_2 is dependent on the pH value, the formation constant of $HgSO_3$ is not.
In the experiments by Schütze et al. [10], [26], [28] an increase of the pH value showed an influence on the reemission of elemental mercury. It is significantly higher.
Blythe et al. [20] showed that the relation between mercury reemissions, sulfite concentration, and the pH value is very complex.
They showed that the response of mercury reemissions changes with the sulfite concentration. Therefore, it seems that

- a low sulfite concentration leads to an increase of reemissions but
- a high sulfite concentration seems to lead to a decrease in reemissions.
- A low pH value leads to an increase of reemissions and
- an increase of the pH value leads to a decrease in reemission.

Heidel [8] shows in his work, that at a pH value >8, OH^- has a sufficient high redox potential to reduce $Hg(OH)_2$ to $Hg_2(OH)_2$, resulting in a disproportion into Hg^{el} and $Hg(OH)_2$. At a pH value as high as 8, OH^- is one of the main ligands for mercury. One reason for a high pH value is the possibility of punctual high OH^- concentrations where the lime is added [26], [28]. The solution of lime can lead to punctual, high pH values that are not detected by the global pH measurement.

Redox potential/ ORP level

Dependent on the redox potential of the solution, the oxidation state of mercury can be influenced. At a low redox potential elemental mercury is preferred, at a high potential the oxidized state is the main product. It is also possible that mercury can be kept out of the gypsum but still be stabilized in the FGD sludge. The ORP influences the reaction of mercury, sulfite and sulfate, and other impurities such as manganese, iron, or selenium. An ORP of at least 200-300 mV (Ag/AgCl reference electrode) prevents the reduction from an oxidation state of two to one or zero. Then the oxidation from sulfite to sulfate is also preferred. At this redox potential, 80% of the captured mercury content is in the gypsum. At a potential > 500 mV, 20% of the captured mercury concentration remains in the gypsum. By increasing the ORP in the FGD by adding more oxidizing air into the solution, the ORP is raised, but not the Hg_{aq}

concentration. The Hg_{aq} concentration did not change until L/G and the sludge level were additionally increased. [13]
Schuetze et al. [10], [28] showed that a low redox potential seems to force mercury into the solid phase. Systems operating with a high ORP (>600 mVSHE) stabilize mercury in the liquid phase. It is not clear if the high redox potential is beneficial or if it is the absence of iodide at an ORP this high. However, a high redox potential can also lead to high energy costs, high content of organo-halogen compounds in discharged wastewater, and $Mn(IV)O_2$ clogging sensors.

2.5.2 Solid phase

After the closer investigation of the main influences on stabilizing Hg in a solution, this chapter is about reaction partners and impacts for the formation of Hg_s. Next to the main effects on the formation of Hg_s, the suspected mercury species will be discussed and the possible ways to analyze a solid sample with unknown mercury species in it. The main ingredients of the solid phase are as mentioned in section 2.4:

- Gypsum
- $CaCO_3$ or $Ca(OH)_2$
- $CaSO_3$
- Metals (e.g. Al, Ca, Cu, Fe, Mg, Mn, Na etc.) and
- Halides (mainly Cl but also Br and I)

The impurities depend on the the coal used in the combustion. [26]

Influences on mercury
After pumping the sludge out of the scrubber, the solid phase is treated and separated into three phases:

- liquid
- fines fraction/ fine solids
- and coarse fraction. [14]

Dependent on the dewatering system the fine solids can be recycled into the FGD. [14] The different phases have different particle sizes. The particle size in the coarse fraction is stable, but it varies in the fines fraction. The fraction with the smallest particle size contains the highest mercury content. The main mercury species in gypsum are supposed to be $HgCl_2$ and HgS. The highest mercury concentration is in

the fraction with the highest Fe and Al concentration. This leads to conclude that iron-oxides influence the behavior of mercury in gypsum. [42]
Kairies et al. [68] have shown that the Fe content correlates with the mercury content in gypsum. A range of mercury content of 140 - 1500 µg kg^{-1} dry was detected in gypsum. Both mercury and iron are most present in the slower-settling particles fraction of the FGD slurry.
This conclusion matches with the statement of Blythe [14] that Fe(III) co-precipitates mercury in the fines fraction of the FGD Sludge, and selenium can form insoluble salts with mercury. Schuetze et al. [26] identified Fe(II) as one of the triggers to transfer mercury into the fines fraction of the gypsum.
Gansley et al. [31] showed that the amount of sulfite in the scrubber solution also influences the distribution of mercury in a scrubber. They were able to force mercury in the sludge with a dosage of sulfite. They also found that most mercury was found in the slurry solids, with the highest amount of mercury in the fines.
Lee et al. [32] analyzed FGD gypsum and wallboard samples. All samples showed a peak between 130-150°C. The thermal evolution profile was tested for HgS, HgO, and $HgSO_4$, Hg_2Cl_2, and $HgCl_2$ as possible species. Resulting in Hg_2Cl_2 and $HgCl_2$ to be the most likely species and excluded species as HgS, HgO, and $HgSO_4$.
Sedlar et al. [33] also analyzed technical FGD gypsum samples and found mercury halides to be the main species.
Rallo et al. [34] analyzed technical FGD Gypsum samples out of a co-combustion plant and identified $HgCl_2$ as main species.
Sui et al. found HgS to be the main species in FGD gypsum. Hg-halides, and HgO were found in small amounts in their samples of technical FGD gypsum. [24]
Córdoba et al. [35] found three different species, Hg_2Cl_2, $HgCl_2$, and HgS, in technical gypsum samples. The occurrence of Hg_2Cl_2 and HgS is explained with the saturation limits in the calculated equilibrium. The reaction of HgS is explained due to the reduction of SO_4^{2-} via CO to S^{2-}. S^{2-}reacts with Hg^{2+}_{aq} to HgS. $HgCl_2$ does not reach its saturation limits and is therefore believed to adsorb on the gypsum particle (see section 1.3).

Beatty et al. [69] analyzed mercury species in a gypsum sample by leaching them out of the solid in different experiments. They used five different leaching steps to find different bonding partners for mercury in the solid. They targeted the following compounds:

- water soluble and loosely adsorbed ions

- carbonate and exchangeable ions
- manganese oxides and hydroxides
- iron oxides and hydroxides
- organic matter and sulfide.

The leaching step in which mercury is found provides information about the binding partners or compounds in the vicinity of mercury in the solid.
Beatty et al. found the highest amount of mercury for FGD gypsum in step four. This step dissolves the hydroxide and iron oxides in a solid and forces them to leach out. To conclude, mercury is inoculated, adsorbed, or bound in the regions with hydroxide or iron oxide groups. For wallboard gypsum, the found mercury concentration was equal in steps four and five. This shows that mercury is equally bound on sulfide or organic matter in the researched wallboard gypsum. A low pH value < 1 and a high very specific redox-potential $500 \leq Eh \leq 600$ mV were needed to leach out mercury.
Pavlin et al. [42] did not find HgS in the fine fraction of the FGD sludge. To find possible mercury species, they created samples by mixing mercury species with gypsum. By analyzing these samples via thermo-desorption, only a standard with a FeOOH mixture could reconstruct the measured peak as in the actual FGD gypsum sample. They conclude that an iron-mercurat-complex or iron in the gypsum is responsible for the found evaporation of mercury in their sample. They also postulate that a Hg-Cl compound is very unlikely because of the small chloride concentration detected in the gypsum sample.
However, of all the discussed research approaches, none of them did consider measuring the different possible oxidation states of mercury during the analysis of the sample. It was not possible to find an explanation on what causes the different found mercury species.
Further compounds having an influence on mercury mentioned by v. Dijen [13] are V, Pb, Cr, Se, AOX 6 mg L^{-1}, Mn, Cu. The consumption of compressed air can lead to emissions of Br_2 and I_2 and it can also oxidize sulfite to sulfate.

Analysis of mercury species in a solid

Different aspects can be investigated for analyzing mercury species and the reaction paths of mercury in FGD. Dependent on species and oxidation state, the properties, and toxicity of mercury vary. The chemical form of mercury in a sample is the key to predict its behavior and characteristics. [37] So it is crucial to identify the mercury content and the mercury species in a sample. [38]–[41]

No standardized and valid analytic method to characterize mercury species in a solid sample has been developed yet. [39], [40], [42], [43] One of the fastest methods is the thermo-desorption of a sample. It is possible to analyze mercury species and gain a similar quantitative output as by standardized procedures, e.g., chemical extraction. [43]

With thermo-desorption, a sample is heated in a defined temperature program, and single evaporation peaks can be matched to the characteristic evaporation point of different mercury species. [40] In literature, different approaches are considered for implementing a standardized method for analyzing an unknown sample.

The following main aspects have to be considered for the development of the method:

- Sample preparation,
- Heating rates,
- Sample dwell times,
- Methods of analysis and
- Carrier gas.

Depending on the set parameters, the results of the thermo-desorption deliver different results. [39], [40], [42]–[45], [48]

The following section discusses the individual aspects of the method and their implementation found in the literature, starting with sample preparation.

Table 10 gives an overview of the different approaches made in sample preparation found in literature.

Table 10 Different sample preparations for the Hg - species investigated via TDS found in the literature.

Concentration/Preparation sample	**Sample [mg]**	**Source**
200-1000 µg (Hg) kg^{-1} in the solid sample	40-100	[39]
1 mg(Hg) L^{-1} saturated gypsum solution	1-10	[42]
Dry sample 10mg(Hg) and 5 g (gypsum) mixed (1-2mg Hg g $gypsum^{-1}$)	0.5-1	[42]
Solution 1mg(Hg) sample 1 L of saturated $CaSO_4*H_2O$ (this approach did not work for HgS)	50 ml left to dry and then the precipitation was analyzed	[42]
Wet preparation FeOOH 0.5 g into 100 ml β(Hg)= 1mg L^{-1}	5 mg of the dried solution	[42]
Wet mixed sample was dried for 48 h by 105-110°C		[48]
0.001 M Hg (solid) in 30g quartz powder	10-200 mg	[46]

Rumayor et al. [47] showed, that they could identify pure mercury species by their evaporation profile. They also observed no significant interference of the temperature profiles between solid mixed and solid pure mercury species.
The next step after analyzing different types of mercury species in a sample without impurities is to speciate mercury in a sample with different types of impurities and gypsum and to develop an analyzing guide and standard for them.
Mixing mercury with gypsum can bind it by adsorption on the surface of the gypsum molecule. But this is not the only possible way for mercury to be attached to gypsum. During the FGD process, mercury can be adsorbed on the gypsum particle's surface or be part of the gypsum bulk.[42]

Pavlin et al. [42] tested different approaches for a standard to identify the unknown mercury species found in FGD gypsum. They investigated the presumed components by mixing them in dry and wet state. Results show (e.g., Figure 6) that their standard evaporation profile was not influenced by mixing solid mercury species with dry gypsum. But when mixing mercury species wet with gypsum, only one characteristic peak was found.

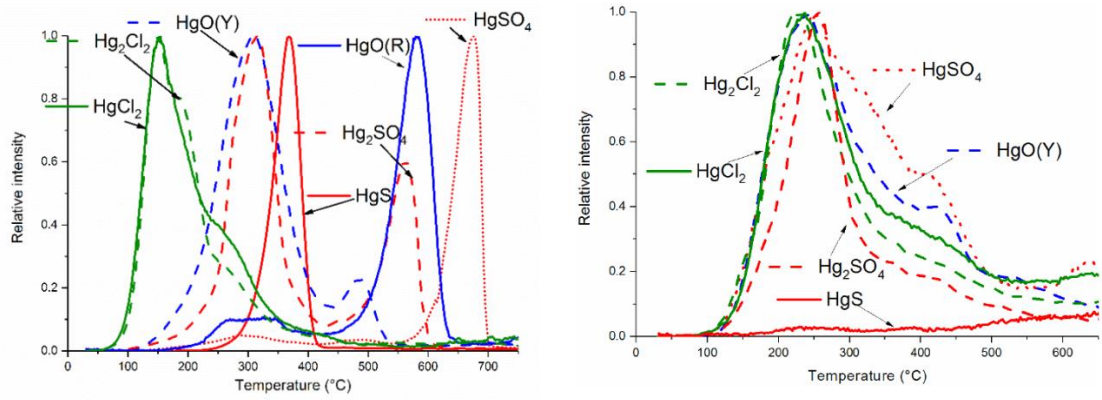

Figure 6 Evaporation profiles by Pavlin et al.[42], comparison of different mercury species mixed dry with gypsum (left) and wet (right).

All FGD gypsum samples showed the same peak between 253-266 °C. The intensity of the peak is correlating with the concentration of mercury in the sample. None of the standards matched that peak.
There are two possible reasons for that:

- None of the compared mercury standards are similar to the actual species or
- The compounds of the gypsum, change the desorption of mercury.

Similar behavior to the evaporation profiles with gypsum was found with the addition of FeOOH (e.g., Figure 7). Whereas the dry mixed components showed a difference in their evaporation for the different species, the wet mixed ones changed their evaporation behavior to one similar peak.

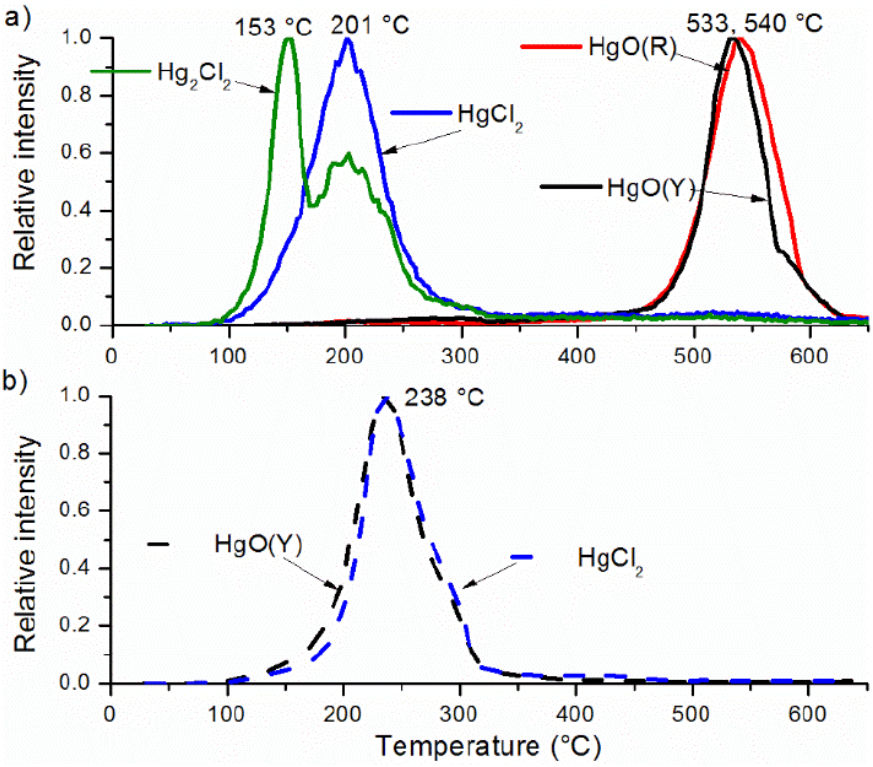

Figure 7 TDS Spectra by Pavlin et al. [42], comparison of mercury species mixed with FeOOH dry(a) and FeOOH in a wet state (b).

It can be seen that the spectra of mercury depend on the iron, so the peaks get more narrow and HgO desorbs at a lower temperature in a wet system. This research shows the influence of impurities on the spectra and the desorption behavior of mercury. The change of a substrate can change the shape and position of a TDS peak. In consideration of the effects of different impurities in the gypsum on the evaporation behavior of mercury, different standards should be produced that consider those aspects. [42]

In literature, different heating programs can be found. Table 11 shows an overview of the different approaches.

Table 11 TDS overview of different temperature programs.

Program	Source
30 s to reach the temperature, 180 s to hold the temperature ramp, before every ramp the oven was cooled down Temperature ramps: 50 °C, 100 °C, 150 °C, 200 °C, 250 °C, 300 °C, 400 °C, 500 °C, 600 °C and 700 °C	[39]
40 °C min^{-1} for 10min (till 400°C) 50 °C min^{-1} for 3.3 min (till 566°C) 80 °C $min^{-1}$for 2 min (till 726 °C)	[43]
Heating to 750 °C in 10 °C min^{-1}	[42]
33 °C min^{-1}	[39]
5 and 7 °C min^{-1} ramps from 200 °C – 650 °C	[48]
0.5 °C s^{-1}	[44]
1 °C min^{-1}	[32]
5 °C min^{-1}	[32]

Depending on the temperature program the characteristic evaporation can be shifted to a different characteristic temperature. A higher flow rate decreases the mercury residence time and concentration to be detected. [32]

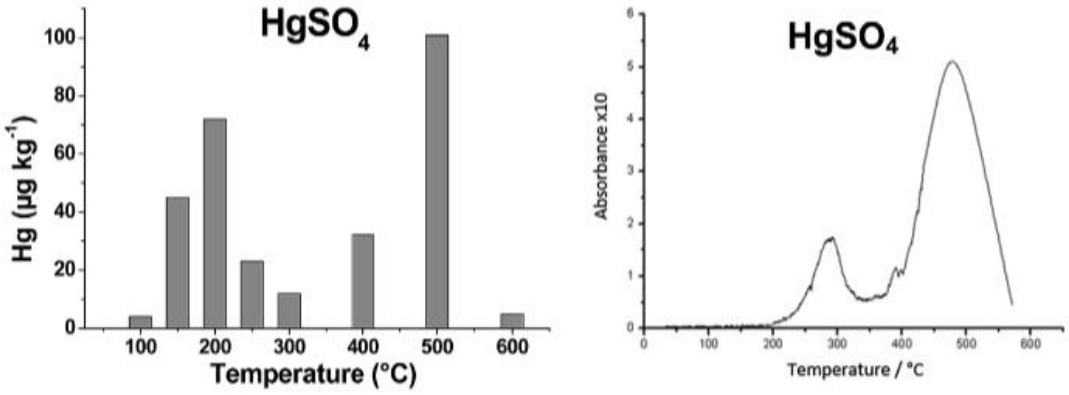

Figure 8 Comparison between different analyzers and heating ramps from Windmöller et al.. [39]

Figure 8 shows the comparison of the measurement of a DMA 80 analyzer stepwise temperature ramp with a gold trap and a continuous measurement via TDAAS, a thermal desorption oven with a constant heating ramp of 33° min^{-1} and analyzed via atomic-adsorption-spectroscopy published by Windmöller et al.[39]. Especially at the beginning of the evaporation, some variations of the mercury signal at specific temperatures dependent on the heating program and analyzer can be seen.
Table 12 shows the influence on the maximum intensity for the mercury evaporations for $HgCl_2$ depending on the heating ramp. It shows a variation of 80°C in the maximum for the evaporation for one species. This comparison shows that it is essential to develop an own standard process and template with the evaporation profiles of the suspected species before analyzing an unknown sample.

Table 12 Comparison of different heating ramps and their influence on the evaporation profile of $HgCl_2$.

Temperature range [°C]	**Temperature of maximum intensity [°C]**	**Temperature ramp [° min^{-1}]**	**Source**
70-220	120	10	[34]
100-350	150	10	[42]
150-350	200	33	[39]
	138	40 (till 400°C)	[47]
Starting 85	145	1	[32]

For the aspect of carrier gas and analytics following possibilities were found in literature.
Table 13 gives an overview on the variety of the different possible carrier gases and analytic methods.

Table 13 Overview of different analysis methods and carrier gases for TDS.

Gas	Flow rate	Method	
Oxygen		DMA	[39]
Nitrogen	200 mL min^{-1}	Homemade TD AAS	[39]
Synthetic air	100 mL min^{-1}	Thermogravimetric and differential thermal analysis	[42]
None	Vacuum	TDS with mass spectroscopy	[42]
Oxygen		DTG derivate thermo-gravimetric Lumex	[48]
N_2		Pyrolysis	[46]
N_2	200 - 2000 ml min^{-1}	CV AAS	[32]
Mercury assessment		DMA	[57]

Table 14 gives an overview of the range of expected evaporation temperatures for the different species.

Table 14 Evaporation temperatures of mercury species. [23], [27], [63]–[65]

Species	Evaporation temperature [°C]
Hg(II) halides	<200; <300
HgS	250 – 400
HgO	300; 460; >400
$Hg(NO_3)_2$	200;280;460
$HgSO_4$	>400; 500-600

The data was only used as orientation because of the different temperature programs, sample preparation and analyzers. The studies varied in their characteristic evaporation temperatures for the different mercury species.

Different to those methods this work differentiates between the evaporating species of mercury Hg(0) and Hg(t) in one measurement via AAS. To make the results

applicable for industrial scrubber systems all Hg-halide species were analyzed as well as mercury sulfate, -sulfite (red), -oxide and -nitrates. [18]

2.5.3 Conclusion for the further investigation

The discussion in literature shows for the Hg_g-Hg_{aq} and Hg_{aq} systems, that the reaction of mercury with sulfite leads to an intra-molecular redox reaction. Van Loon et al. [21] [22] showed that mercury seems to bond with the S-atom of the sulfite and does not form a complex with $HSO3^-$ because of the blocked S. This leads to the conclusion of a coordination number of one for mercury when reacting with one sulfite anion. The concentration of sulfite has an influence on the coordination of mercury. With a concentration > $1*10^{-7}$ mol*L^{-1} of free sulfite anions a two times coordinated complex $Hg(SO_3)_2^{2-}$will occur. Any higher coordination only seems to happen with water. [22]

- For the integration of sulfite as a ligand into the halides system developed by Bittig et al [12] as well as into the Bittig droplet the reaction and coordination of sulfite anions with a mercury cation needs to be clarified.
- The interaction of the three different mercury(II)-halide complexes with sulfite anions in stoichiometric as well as in excess concentration to mercury needs to be investigated. Whereas the reemissions into the gas phase can help interpret the occurring reactions. There it is essential to differentiate between Hg(0) and Hg(ox) emissions.

According to Schuetze [28] the pH value has an influence when working in a Hg-SO_2-H_2O system. Van Loon et al. [21] [22] showed that the pH value has no influence on the complex formation of sulfite. However, it is known that the existence as well as the ligand strength of sulfite is dependent on the pH value. This explains why the influence of the pH-value has to be considered in further investigation. This leads to the following tasks:

- It is necessary to detect the direct influence of pH value on the ligand sulfite and the formation of $HgSO_3$, experiments in a simple system should be considered before expanding the system to a real scrubber system.
- The main ligand for mercury, HSO_3^- or SO_3^{2-} should be determined.

The main influences on the $Hg_{aq} \rightleftharpoons Hg_s$ equilibrium were singled out as following:

- High halides concentration can stabilize mercury aqueous, whilst forming a higher coordinated complex.
- High sulfite concentration causes the implementation of mercury in gypsum.
- High ORP can force mercury into the aqueous form.
- Ferrous and other impurities cause an enrichment of mercury in the solid phase.

The main aspects of the Hg_s species analysis:

- Suspected mercury species in gypsum are:
  - $HgCl_2$, Hg_2Cl_2, HgO, HgS
- Main influence factors for the measurement are:
  - Sample preparation,
  - Heating rates,
  - Sample dwell times,
  - Methods of analysis and
  - Carrier gas.
- The comparison between the evaporation profiles of different approaches is not possible.
- Different mercury species show a species specific evaporation profile.

3. Experimental

This chapter will discuss the different experimental setups, procedures, error analysis and the reproducibility of the experiments. All experiments were conducted under the highest possible safety standards to reduce exposure of mercury to the environment.

3.1 Experimental setup

This work uses two main setups. One is the assay of mercury-containing solids. The goal is to identify unknown mercury species in a solid sample via a thermal decomposition of the sample. Therefore, standards of known mercury species were evaporated to identify their different evaporation behaviors. With those measurements a standard template was generated to help interpret evaporation profiles of samples with unknown mercury species. Then samples with unknown mercury content were measured.

The second setup is a scrubber system. The system was used to better understand the role of sulfur-oxides as ligands for mercury and to produce gypsum samples in pre-defined systems.

The scrubber system was formerly used before by a R&D Lab of Uniper and was purchased for this research project.

3.1.1 Assay of solid mercury samples

Part of this section is published in [18].

To assay solid mercury samples and investigate mercury species in solid samples containing mercury following experimental setup was developed (Figure 9). The system continuously overflows a sample with a carrier gas. The sample put in an oven is heated using a specific program. The evaporated mercury is carried out of the oven via the carrier gas. It is measured with two identical mercury analyzers, to determine the elemental content and the total content of the mercury emissions.

The experimental setup of the assay of solid mercury samples can be structured into four steps:

- Carrier gas
- Oven or thermal decomposition process
- Mercury(t) and Mercury(0) measurement and
- Exhaust gas treatment station

Figure 9 shows the flowsheet of the process.

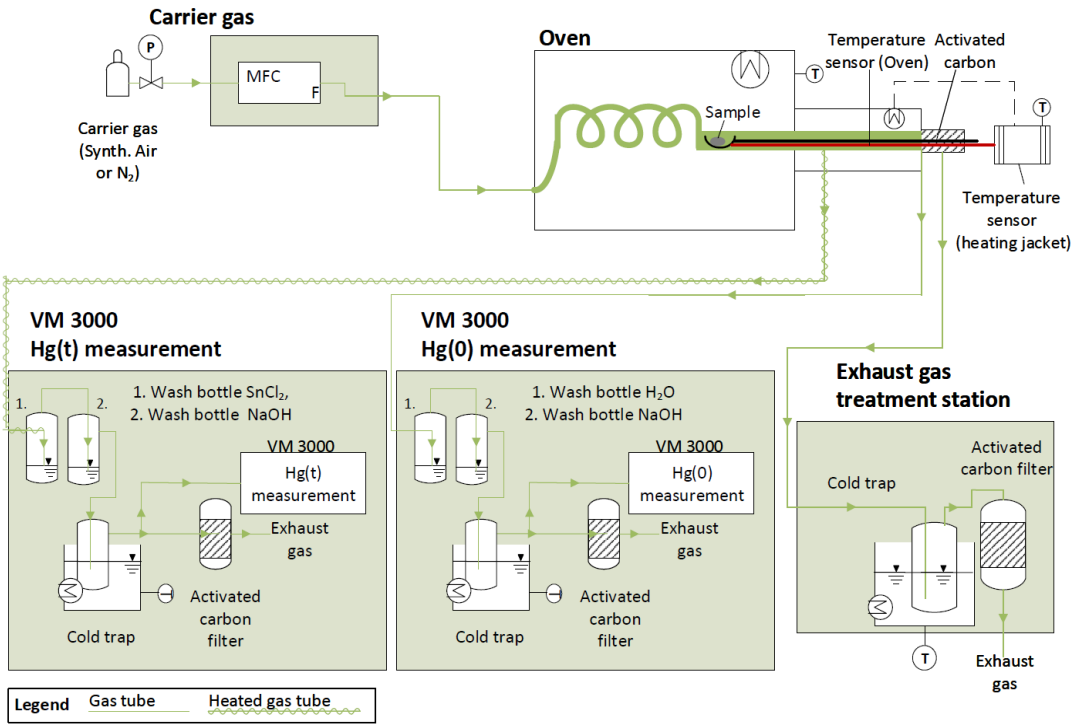

Figure 9 Experimental setup TDS.

The carrier gas is dosed via MFC into the process. Possible carrier gases are nitrogen or air.

The second step of the process is in the oven. It is the center of the process.

The reactor chamber is a quartz glass reactor with a spiral input line inside the tube-shaped oven chamber. Inside the reactor a quartz glass sample holder is placed. The sample holder has a hollow shaft where the thermo-element of the oven is placed. Both the sample and the thermo-element are placed next to each other in the middle of the oven. This set-up guarantees to measure the actual evaporation temperature of the investigated sample.

The correct placement of the reactor, the sample holder and the thermo-element are marked so the setup is always at the same place. The spiral is used to maximize the dwell time of the carrier gas, to guarantee the right temperature of the carrier gas at the point where it meets the sample. After the carrier gas has overflown the sample, the sample stream is separated in two streams for the next step, the measurement of the evaporated mercury emission.

The mercury emissions are measured continuously with a CV AAS (Mercury instruments Model VM3000). Hg(t) and Hg(0) are measured with identical systems for a higher comparability between the results. To avoid cross sensitivities both streams were treated with a sodium hydroxide solution. The Hg(t) stream was led through a

tin(II)chloride solution to reduce all oxidized mercury species to elemental mercury. For the Hg(0) stream a water/HCl or KBr wash bottle was used to compensate the different pressure losses due to two wash bottles in the Hg(t) stream. Upstream the $Sn(II)Cl_2$ wash bottle the sample stream was heated, to minimize mercury losses due to adsorption and condensation. The second and third treatment steps are identical for both measuring lines. In the second step, possible SO_2 pollution is washed out via sodium hydroxide. In the last step, the sample gas is cooled down via cold trap to < 10°C to avoid condensation in the analyzer.

To determine the oxidation rate during the mercury evaporation it is necessary to determine both oxidation states in one sample.

The last step is the flue gas treatment.

After the measurement all outgoing process streams are treated with an iodinated activated carbon before being released to the fume hood.

3.1.2 Creation of standardized solid mercury-gypsum samples via scrubber system

A laboratory scaled flue gas desulfurization process was used to create standardized gypsum samples containing mercury impurities. The experimental setup of the laboratory scaled flue gas desulfurization process is shown in Figure 10 and can be divided into following process steps:

- Carrier gas conditioning (with the Gas mixing station SO_2 generation and the droplet trap)
- FGD scrubber
- Measurement of the sample stream for mercury with two VM 3000 and SO_2 analyzer
- Sampling of the FGD sump
- and the flue gas cleaning

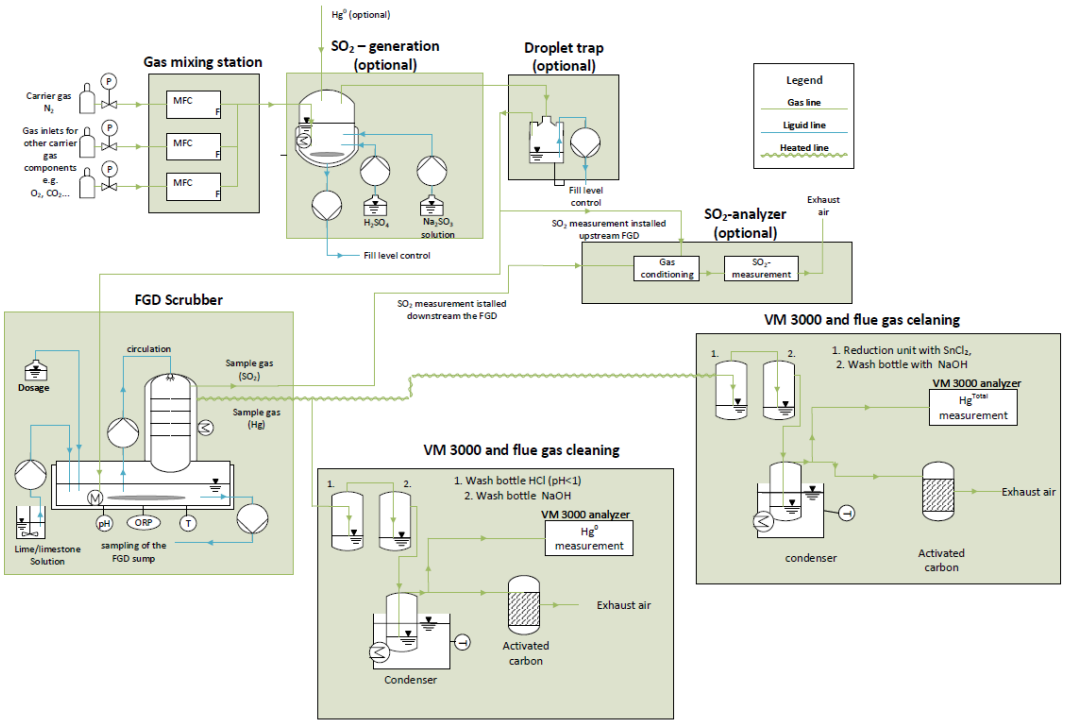

Figure 10 Experimental setup Scrubber.

The different carrier gas components are dosed via MFCs into the process. The correct composition is adjusted by a gas mixing station. It is possible to mix different gases like nitrogen, oxygen, or CO_2. For adding SO_2 to the flue gas, the SO_2 generation can be installed in the process. The SO_2 is produced via the reaction of sulfuric acid and a sodium sulfite solution. To guarantee a stable reaction the components are mixed at 50 °C. The generated SO_2 is stripped out by the flue gas from the gas mixing station.

The two solutions, sulfuric acid and sodium sulfite are pumped via a peristaltic pump into the processing unit. To adjust the SO_2 concentration in the flue gas, the concentration of the two solutions, the flow of the peristaltic pumps, or the diameter of the used hoses can be varied.

The SO_2 concentration is measured downstream of the SO_2 generation to control the process. From SO_2 generation, the flue gas is led through a Woulf's bottle to ensure no drop entrainment. After the Woulf's bottle, the conditioned flue gas is led counter stream through the batch reactor.

The batch reactor can be divided in two parts, the sump and the column. The reactor is the central part of the process.

The whole scrubber system is lined and heated with water to ensure one temperature in the gas washing process.

The conditioned scrubber solution is placed in the sump. The sump reactor has sampling points as well as measurement points. The pH value, ORP, and temperature

of the process are measured continuously in the sump. It is possible to add additional solutions like lime slurry during the procedure via peristaltic pumps to set process conditions and the gypsum growth. It is also possible to sample gypsum via peristaltic pump from the scrubber for later analysis. An additional air dosage is installed to set the ORP conditions. For a better transition of the air into the aqueous phase, the dosing is passed through a glass frit.
The sump solution is stirred and circulated counter stream to the flue gas into the column head. Downstream of the reactor at the head of the column is the sampling point for the measurement of Hg(0) Hg(t) and SO_2 concentration.
The suspension taken out of the scrubber sump was separated via suction filter. The liquid phase was recovered, stabilized and cooled down till further measurement.
The solid phase was washed, weighed, freeze dried, weighed and stored chilled, till further measurement. One sample was not freeze dried and measured the same day.

The mercury sample streams are both passed through three wash bottles each. Depending on the oxidation state of the measured mercury emission the treatment was different.
For the Hg(t) measurement $SnCl_2$ is used to reduce all oxidized mercury species to elemental mercury in the first step. Upstream of the wash bottle the sample gas line is heated to 180°C to avoid losses of Hg by adsorption or condensation.
For the elemental mercury measurement, the first wash bottle is filled with hydrochloric acid (pH 1) to capture all oxidized mercury species.
The second and third treatment steps are identical for both measuring lines. In the second step, possible SO_2 pollution is washed out via sodium hydroxide. In the last step, the sample gas is cooled down to < 10°C to avoid condensation in the analyzer.
For SO_2 measurement, one measurement string was installed downstream of the SO_2 generation and the other one downstream of the scrubber.
To stay within the calibration ranges of the instrument, the string with the more extensive calibration range (0-10.000) was installed upstream of the scrubber and the one with the smaller calibration range (0-1.000) was installed downstream of the scrubber. Both strings are cooled down to avoid condensation in the analyzer. If the flue gas does not contain of SO_2, both measurement strings are set at the head of the column downstream of the FGD to measure possible SO_2 reemissions.
All exhaust gas streams are passed over an activated carbon bed with iodized activated carbon before they are fed into the fume hood.

3.1.3 Analytics

This chapter describes the used analytical methods.

Measurement of mercury and its species in flue gas

Mercury can only be measured as Hg(0). For analyzing mercury in the gas phase, the main method is Atomic-Adsorption-Spectroscopy (AAS) at a wavelength of 253.7nm. A VM3000 laboratory mercury analyzer was chosen for the measurements. This analyzer has one measuring cell and standardizes the measured values at 20°C.
To be able to measure total mercury and elemental mercury two analyzers were used. For measuring total mercury a $SnCl_2$ solution was used to reduce all oxidized species (e.g. [70]) and a NaOH scrubber bottle was used to eliminate cross sensitivities with SO_2.
To generate similar measurement conditions the elemental mercury stream was led through a wash bottle filled with water or hydrochloric acid and sodium hydroxide solution. To eliminate humidity from the gas, both streams were cooled down to below 10 °C. The sample hose upstream the $SnCl_2$ bottle was heated up-to 180°C to minimize adsorption and condensation losses of oxidized mercury species in the tubes.

Mercury analytics in a solid or liquid sample

To close the mercury balance of the scrubber experiments, a mercury analysis of the solid, aqueous and gaseous phase had to be made. For the aqueous and solid phase, a DMA 80 was used. A DMA 80 is a mercury analyzer that thermally decomposes a sample and measures the mercury contents via amalgamation (gold trap) and AAS.

Sulfur dioxide

The SO_2 concentrations were measured with a Rosemont analyzer. It is possible to measure in two strands with different calibration limits. One has a calibration limit of 1,000 mg m^{-3}_n and the other one has a calibration limit of 10,000 mg m^{-3}_n. There is a cross sensitivity because the analyzer measures in a UV-wavelength of the absorption of elemental mercury and the absorption of SO_2 concentration. This was detected in preliminary tests and the measured SO_2 concentration had to be corrected.

pH and Redox potential

The used Ag/ KCl ORP electrode had to be corrected for 50 °C up to 188 mV to correspond to a standard hydrogen electrode (SHE). The pH electrode was calibrated

every day with a two-point calibration between a pH Value of 4 to 7 and checked at a pH level of 5 and 9.

3.2 Experimental procedure

This chapter will give an overview of the realized experiments. It is subdivided into three parts. The two main procedures of the thesis are the procedures to assay a solid sample containing mercury and the procedure to create mercury gypsum samples. The third procedure is a procedure to create precipitated mercury species but has a more indicative measurement character.
For all measurements only glass/quartz glass or PTFE/PFA surfaces and hoses were used to minimize the adsorption of oxidized mercury on surfaces that leads to a low recovery rate, measuring errors in retention time or misinterpretation of the oxidation state of the measured mercury (e.g. DIN EN ISO 12846 [70]). All handling with open mercury samples as well as the next mentioned experimental procedures were conducted under a fume hood.

3.2.1 Procedure to assay mercury in solid samples

Part of this section is published in [18]

The solid mercury samples and the samples containing an unknown mercury species were evaporated to measure the specific evaporation concentrations of mercury of different mercury species at defined conditions.
Different aspects had to be considered for the experimental procedure of the evaporation of the samples. In the state of research different approaches how to evaporate solid mercury samples were identified and are discussed in the previous chapters.

From those approaches, restrictions from the system and first indicative measurements, test conditions were developed.
The procedure can be divided in:

- Preparation of the sample stream conditioning
- Sample Handling:
  - Mercury standards
  - Gypsum samples
  - Precipitation samples
- Evaporation
- Cleaning

The process started with the setup of the mercury emission conditioning. The $SnCl_2$ solution was always freshly prepared. The wash bottles with the sodium hydroxide solution and water were installed in the process. The cooling device was started to dry the sample stream before entering the analyzer.
Sample handling is divided into handling of mercury standards (pure mercury species), the prepared gypsum samples and precipitation samples. The sample size is restricted by the calibration limits of the mercury analyzers. Every pure mercury sample was ground and stored in a new sample storage container to minimize contamination effects. The sample size was 0.5 mg(Hg). For the sample handling a sample holder < 500 mg was used to minimize the weighing error. After weighing the sample, the sample holder was transferred into the bigger sample holder (TDS-sample holder) fitting in the quartz reactor.
The sample was immediately installed in the reactor after the transfer.

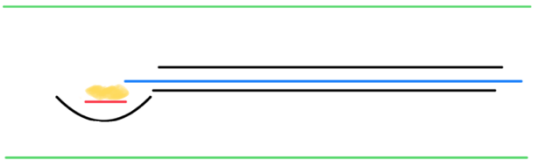

Figure 11 Example of the pure Hg sample inside the reactor.

As can be seen in Figure 11 the sample (yellow) is on the small sample holder (red line), which is put in the TDS sample holder (black lines). Inside the shaft of the TDS sample holder the thermo element of the oven is installed (blue line) next to the sample. The TDS sample holder is placed inside the reactor (green lines).

For the measurement of the gypsum samples the procedure was adapted due to the small mercury content in the samples to a bigger sample size.
At the beginning the gypsum samples were taken out of the refrigerator and weighed, then the TDS-sample holder was filled with gypsum and immediately installed into the reactor. The sample holder was held over a collection vessel which had been weighed before. Both the remaining sample and collection vessel were weighed after installing the sample to determine the sample size.

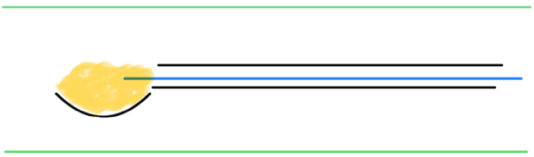

Figure 12 Example of the gypsum sample inside the reactor.

As can be seen in Figure 12 the TDS sample holder (black lines), was filled completely with the sample (yellow) and installed inside the reactor (green lines). Inside the shaft the thermo element of the oven (blue line) was installed, reaching inside the sample.

For the precipitation samples, the samples size varied depending on the mercury concentration in the sample.
After the sample was put into the TDS sample holder, the thermo element was installed. It was put into the shaft of the sample holder and installed next to the sample. Then the TDS sample holder was immediately installed inside the reactor. The volume stream was started and it was controlled that all the wash bottles showed a similar and strong bubble behavior. The cooling temperature of the water trap was controlled to be < 10°C. Then both analyzers were installed into the process. To standardize the measurement the temperature of 30 °C was held for 5 minutes before starting with the heating ramp up to 650 °C.

For the evaporation following conditions were set:

- Temperature ramp of 1°C min^{-1}, boundaries 30-650 °C
- Volume stream 7 l min^{-1}
- Carrier gas: Nitrogen

After an experiment sample holder, wash bottles, collection vessel and spatula were cleaned with HNO_3 solution and VE water before being used again.

3.2.2 Creation of standardized solid mercury-gypsum samples via scrubber system

For the creation of mercury-gypsum samples a laboratory scaled FGD scrubber system was used. Because this scrubber system itself is very complex and has a lot of influences on mercury and its states, two different kinds of experiments were conducted. The first one, a system without a solid phase, was to assure the functionality of the system, better understand the emission measured and the integration of sulfite as ligand into the Hg-Halides-H_2O-System. The second one can be described as the main experimental procedure, were the wanted mercury gypsum samples were created.
The general procedure of the scrubber experiments can be described by the following points:

- Preparation of the sample stream conditioning
- Preparation of needed solution and additives
- Reactor setup
- Calibration and control of the pH and ORP electrodes
- Starting the process
- Test for impurities and leakages
- Starting with the process
- The experiment
- Ending the process
- Cleaning

The first step is the setup of the mercury emission conditioning. The $SnCl_2$ solution was always freshly prepared. The wash bottles with the sodium hydroxide solution and HCl solution were installed in the process. The cooling device was started to dry the sample stream before entering the analyzer.

For the scrubber process additional solutions were needed:

- SO_2 Production:
  - Na_2SO_3 freshly prepared, concentration depending on the wished SO_2 concentration.
  - H_2SO_4, concentration depending on the wished SO_2 concentration.
- Scrubber sump:
  - Sump: the scrubber sump holds 1.4 L and the base was distilled water. The water was prepared freshly for every experiment.
  - Gypsum: To create a gypsum growth a seed crystal has to be added. The weighed portion was diluted with the scrubber water and added into the reactor.
  - Mercury: the needed mercury concentration was added via peristaltic pump of an earlier prepared sample solution.
  - Other salts: Other salts were also diluted with the scrubber water and added into the reactor.
- Limestone:
  - $Ca(OH)_2$ stirred in distilled water
  - $CaCO_3$ stirred in distilled water

The reactor for the SO_2 creation and the scrubber reactor were both washed with distilled water, installed and the heating of the reactor was started. All connection tubes, peristaltic pumps, the sample stream conditioning for the mercury emissions were installed.
Before every measurement the pH electrode and ORP electrode were calibrated or/and tested for a correct functionality.
Then, if needed in the process salts and/or gypsum were diluted in the distilled water and added to the reactor.
To ensure that no impurities were in the system and no leakages occurred during the setup following control points implemented.
The reactor was closed, the pH electrode and ORP electrode were installed and the pH value and ORP level were controlled to ensure no impurities were in the scrubber system. Then the circulation of the sump was started and the pH and ORP value were again checked if they changed to exclude impurities in the scrubber solution.
The carrier gas was then started and the mercury and SO_2 analyzer were installed. It was controlled that all the wash bottles showed a similar and strong bubble behavior and if no mercury emissions or SO_2 emission were detected. Afterwards the process

could be started. If needed, the SO_2 generation was started, and the pH level was set at the wished range. Then mercury was added. After the process reached a close to a steady state the experiment could be started.

Preliminary tests in the aqueous phase

Part of this section is published in [71].

As mentioned above the first measurements were more simplified. The aim of the experiment is to better understand the reaction of mercury in the aqueous phase and to show that the scrubber system is working correctly. The first experiments were conducted without a solid phase.

To integrate and investigate mercury sulfite complexes in the well researched system of aqueous mercury halides an experimental procedure was developed were the ligand and the coordination of mercury can be identified by measuring the gaseous phase.

For the scrubber sump composition different approaches were made. Each experiment was repeated.

- Investigation of the interaction between Hg^{2+} and sulfite:
  $c(Hg(NO_3)_{2aq}) = 5*10^{-5}$ mol L^{-1}
  Dosage of sulfite was added in ratio to the mercury concentration 1:1; 1:10; 1:100; 1:1000. The pH value was regulated via sodium hydroxide solution.
- Investigation of the interaction between Hg-halides and sulfite:
  $c(HgX_{2aq}) = 5*10^{-5}$ mol L^{-1} ; X = Cl, Br, I
  Dosage of sulfite was added in ratio to the mercury concentration 1:1; 1:10; 1:100; 1:1000. The pH value was regulated via sodium hydroxide solution.
- Investigation of the interaction of Hg-halides, sulfite and halides in excess
  $c(HgX_{2aq}) = 5*10^{-5}$ mol L^{-1} ; X = Cl, Br, I
  $c(X^-) = 1$ mol L^{-1}
  Dosage of sulfite was added in ratio to the mercury concentration 1:1; 1:10; 1:100; 1:1000. The pH value was regulated via sodium hydroxide solution.

The starting sump volume was set at 1.4 L. The temperature of the experiments was adjusted at 50 °C. The L/G was set to 10. For the sulfite dosage sulfurous acid was used. For the regulation of the pH-value sodium hydroxide was added.

Main experiments

The main goal of this work is to create a gypsum sample with a mercury content under defined conditions. Therefore, the solid phase needed to be added into the system. The conditions were held similar to the ones without a solid phase, to keep the systems comparable. In addition, gypsum was added into the solution as seed crystal for the gypsum growth. To control the pH value inside the operation limits and to create a gypsum growth $Ca(OH)_2$ or $CaCO_3$ and SO_2 were added into the process. Since there are too many variables that influence the system, the main influences on the $Hg_{aq} \rightleftharpoons Hg_s$ equilibrium were identified as mentioned before. Those are:

- High halides concentration can stabilize mercury in the aqueous phase
- High sulfite concentration causes the implementation of mercury in gypsum
- High ORP can force mercury into the aqueous form
- Ferrous and other impurities cause an enrichment of mercury in the solid phase

Six experiments were planned and carried out to investigate those influences.

The first experiment was executed to investigate the absence of halides and to define the characteristics of the reaction between Hg^{2+}_{aq} and gypsum on the Hg_{aq}-Hg_s equilibrium.

The second experiment was carried out with the typical mercury concentration of FGD. Because of the low mercury content resulting in the gypsum samples, the same experiment was carried out with a decimal power higher in mercury concentration. The gypsum samples of both runs were compared and there was no qualitative change recognizable. Therefore, all following experiments were concluded with a higher mercury concentration to gain higher mercury content in the created gypsum samples and see a clearer change in emissions and reemission in the gas phase. For the fourth experiments a high halides concentration was chosen.

Table 15 shows the different used halide concentrations. With the low concentration mercury will form a two times coordinated HgX_2 halide-complex. With the high concentration mercury will form a HgX_3^- or HgX_4^{2-} as main halide-complex.

Table 15 Overview of the halides concentration in the scrubber suspension.

	Cl^- [mol*L^{-1}]	Br^- [mmol*L^{-1}]	I^- [mmol*L^{-1}]
c (Hal) low	0.03	0.027	0.005
c (Hal) high	0.5	1.2	0.15

For the fifth and sixth experiments, calcium carbonate was used as limestone because of the impurities of natural limestone. All wanted metal and nonmetal impurities needed to recreate a real FGD solution were added with the limestone suspension.
A real scrubber suspension was used in the sixth run to see if equal reactions occur as in the runs with synthetic solutions. A systematic error can be excluded from the process and no influencing factor was overseen. Before adding the solution into the laboratory scaled scrubber system a solid sample (sample 6-0) was taken to see if the mercury species change because of the used scrubber process.

During the experiments gypsum samples were taken at the same time to investigate following influences:

- The investigation of the behavior of the system without any external influence on the system
- The influence of the redox potential: addition of air
- The investigation of the influence of a high sulfite concentration: inoculation of sulfite
- The investigation of the redox potential in coherence with a high sulfite concentration: addition of air

As it is very difficult to determine the sulfite concentration the solution was inoculated with a known sulfite concentration. For the first experiment only the first two steps were conducted because of the duration of the experiment.
To take a gypsum sample the pump ran for one minute before taking a sample to ensure no residues from the sample before. Then the sample was taken, therefor the pump ran for 10 minutes. The sample was then sucked with pressure and a filtrate was taken and stabilized for storage. Then the filtration residue was washed twice and put in an air-tight sealed sample holder. For the third sample a larger sample was taken. All samples were weighed, freeze dried, weighed and stored. For sample three one untreated sample was taken and analyzed at the same day. At the end of one experiment one gypsum sample (sample 5-5) was taken after adding precipitation

agent, to see if HgS can be found in the sample via TDS method. All samples were measured twice via DMA 80 and the TDS method.
Further process parameters were chosen as following:

Table 16 Overview of the composition of the different scrubber solutions.

Exp. No	Hg-Species	β(Hg) [mg(Hg) L^{-1}]	Gypsum	Halides	Metals	Limestone
1	$Hg(NO_3)_2$	10	12 %	No	-	$Ca(OH)_2$
2	$HgCl_2$	1	12 %	Low c(hal)	-	$Ca(OH)_2$
3	$HgCl_2$	10	12 %	Low c(hal)	-	$Ca(OH)_2$
4	$HgCl_2$	10	12 %	High c(hal)	-	$Ca(OH)_2$
5[*1]	$HgCl_2$	10	12 %	Low c(hal)	See $CaCO_3$ Analysis	$CaCO_3$
6[*2]	$HgCl_2$ Real suspension	10 +x	12 %	unknown	Unknown + see $CaCO_3$ analysis	$CaCO_3$

To determine the impurities in the created gypsum selected samples were analyzed via XRF and SEM.

At the end of every experiment, precipitation agent was added into the system. The process was stopped when no mercury emission and SO_2 emission was detected. Then the experimental setup that was in contact with mercury was cleaned with distilled water, HNO_3 Solution, distilled water and then stored filled with distilled water to reduce adhesion of impurities on the walls of the scrubber.

3.2.3 Preliminary precipitation experiments

Precipitation experiments were conducted for a closer investigation to see what kind of mercury species interacts with the solid phase. The general steps that were carried out can be described as:

- Addition of mercury species (solid/or aqueous) in a petri dish.
- Mixing sample with a flocculant (Pural NF/ Al_2O_3)
- Addition of possible influences on the mercury precipitation such as carbonate, sulfite solution etc.
- Precipitate the mercury sample due to a pH change with a NaOH (if no other precipitation agent mentioned) solution.
- Air drying of the precipitated sample

HgS, $Hg(NO_3)_2$ and $HgSO_4$ solids were precipitated with NaOH solution for the first experiments. The first precipitation experiments were conducted without a flocculent and were filtrated. It was not possible to separate the sample and the filter, because of the small particle size. Without flocculent, the samples precipitated in crystals that were very difficult to handle. For further investigations, a flocculent was added to simplify the handling.

The next suspicion was the occurrence of Hg_{aq}^{2+} or Hg_{aq}^{+} due to the influence of sulfite on the Hg_{aq} equilibrium and to interpret the occurring species from the sulfite precipitation experiments. For this experiment $Hg(NO_3)_2$ was diluted with diluted HNO_3. $Hg(NO_3)_2$ was chosen because it is the only mercury species in the investigated mercury species that dissociates into ions in solution. It had to be differentiated between mercury solutions that were prepared days before the precipitation referred as $Hg(NO_3)_{2aq}$ and solutions prepared in the petri dish minutes before the precipitation referred as $Hg(NO_3)_2$.

In literature sulfite and sulfur complexes are often suspected to force mercury into the solid form, $HgSO_4$ as well as $HgSO_3$ precipitation experiments were done. As it is not possible to isolate $HgSO_3$ as a solid the reactions according to Van Loon et al. were recreated and $HgSO_3$ was subsequently precipitated.

The preparation of the sample is described in Table 17. Because of the high mercury concentration of the samples and the possibility of the formation of elemental mercury it was not possible to freeze dry the samples.

The mercury species were distributed in different characteristics:

Hg with sulfur, Hg^{2+} and Hg_2^{2+} with $Hg_x(NO_3)_2$ as input species and Hg-halides if possible, the mercury species were varied in oxidation states.

Following experiments were conducted:

Table 17 Precipitation experiments for the investigation of the main mercury species interacting with the solid phase.

	Hg with sulfur				
Species	Flocculants	Additive	Precipitation Agent	Filtrated	Comment
$HgSO_4$	Pural NF		Deionized H_2O	Yes	Precipitated with water
$HgSO_4$	Pural NF	Washed with $HgCl_2$ $c(HgCl_2)$ = 5 mmol/L	Deionized H_2O	Yes	Precipitated with water
$HgSO_4$	-	-	NaOH-solution	No	
$HgSO_{4aq}$			NaOH-solution		No reaction, no mercury left in the solution
Hg_2SO_4	Pural NF		NaOH-solution	No	
HgS	Pural NF		NaOH-solution	No	No reaction
	$Hg^{2+/+}$				
Species	Flocculants	Additive	Precipitation Agent	Filtrated	Comment
$Hg(NO_3)_2$		HNO_3 diluted,	Deionized H_2O	Yes	Not possible to isolate from filter, solution was prepared in the petri-dish
$Hg(NO_3)_2$	Pural NF	HNO_3 diluted, CO_3^{2-}	Deionized H_2O	Yes	Solution was prepared in the petri-dish
$Hg(NO_3)_2$	Pural NF	Washed with $HgCl_{2,\,aq}$ $c(HgCl_2)$= $5*10^{-3}$ mol L^{-1}	Deionized H_2O	Yes	Solution was prepared in the petri-dish

	$Hg^{2+/+}$				
$Hg(NO_3)_{2aq}$	Pural NF		NaOH-solution	No	Solution with diluted HNO_3 was prepared one week before the experiment
$Hg_2(NO_3)_2$	Pural NF	HNO_3 diluted	NaOH-solution	No	Solution was prepared in the petri-dish
$Hg_2(NO_3)_{2aq}$	Pural NF		NaOH-solution	No	Solution with diluted HNO_3 was prepared one week before the experiment
$Hg(NO_3)_{2aq}$		SO_3^{2-} $c(SO_3^{2-}) < c(Hg^{2+})$ 0.5mmol SO_3^{2-} with 5mmol Hg^{2+}	NaOH-solution	No	Solution with diluted HNO_3 was prepared one week before the experiment. NaOH was added 15 minutes after the sulfite dosage
$Hg(NO_3)_{2aq}$		SO_3^{2-} $c(SO_3^{2-}) = c(Hg^{2+})$ 0.5mmol SO_3^{2-} with 5mmol Hg^{2+}	NaOH-solution	No	Solution with diluted HNO_3 was prepared one week before the experiment. NaOH was added 15 minutes after the sulfite dosage
$Hg(NO_3)_{2aq}$		SO_3^{2-} $c(SO_3^{2-})*5*10^{-7}$ mol $L^{-1} > c(Hg^{2+})$ 20 mmol SO_3^{2-} with 0.5 mmol Hg^{2+}	NaOH-solution	No	Solution with diluted HNO_3 was prepared one week before the experiment. NaOH was added 15 minutes after the sulfite dosage

	Hg-Halides				
Species	Flocculants	Additive	Precipitation Agent	Filtrated	Comment
$HgCl_2$	Pural NF		NaOH-solution	No	
$HgBr_2$	Pural NF		NaOH-solution	No	
HgI_2	Pural NF		NaOH-solution	No	
HgI_2			NaOH-solution	No	
HgI_{2aq}	Pural NF		NaOH-solution	No	$HgCl_2$ diluted in HCl and added NaI
Hg_2Cl_2	Pural NF		NaOH-solution	No	

3.3 Error analysis

Aim of a measurement is to determine the real value. Therefore, measurement equipment needs to be qualified and validated to fulfill the measurement.
During the measurement inevitable deviations from the result occur. This means that every result is an estimation y of the real measurement Y. With this information the measurement inaccuracy can be determined for a process.
Deviations of a measurement can be distinguished in two different kinds of measurement inaccuracies:

- Systematical x_2
- Random/ statistical x_1

The standard deviation can be used to define the random inaccuracy of a measurement.
The systematical inaccuracy can be divided into a known and unknown error. [72]
In this work a new analysis system for solid samples containing mercury was developed. To assure that the new system works solid mercury samples were measured and the advanced measurement inaccuracy was determined. To assure all mercury content in the gypsum samples was found the quantitative amount of mercury was compared to the amount found by an already existing analyzer for solid mercury samples the DMA 80. The advanced measurement inaccuracy (k=2) of the DMA 80 is < 30%. The advanced measurement inaccuracy of the method needs to be calculated to compare those to samples.

The error of the system also shows if the system is usable as an analytical method and shows a low measurement inaccuracy.

3.3.1 Procedure to assay solid mercury samples

Part of this section is published in [18]

To define the error of the system of the developed thermo-desorption method and its applicability, all possible errors must be considered.

As indicator if a measurement was reasonable, the recovery rate of the sample had to be calculated. Influencing parameters are:

- Weighing error at 0.5 mg
- Handling error of the sample
- Handling and setup of the process
- Error of the mercury analyzer
- Error of the balance
- Impurities of the sample
- Error of the mass flow controller/ volume stream metering
- Error of the analyzer

All data measured was corrected to normal conditions (0 °C; 1013 mbar), the evaporation profiles are all normalized to 1 mg Hg. The deviation between the analyzers is also considered. Because not every species has an elemental mercury emission during the evaporation only the Hg(t) can be used as sustainable value for a recovery rate.

The recovery rate was calculated as followed:

$$\frac{\mathrm{m(Hg)_{actual\ value}}}{\mathrm{m(Hg)_{target\ value}}} = \frac{\int_{end}^{start} \beta(Hg(total))dt\ x\ \dot{V}\ \mathrm{x\ error\ (\dot{V})x\ error\ (analyzer)}}{m_{sample}(Hg) x\ error(balance) x\ error(impurity\ of\ sample)} x100 = recovery\ rate \quad (3.1)$$

For reproducibility, all evaporation profiles for every mercury species were measured at least three times. For the evaluation, all recovery rates with an outlier were not further considered. To identify the outliner a Grubbs test with α = 5 % was used.

For the mass flow controller, a derivation of +20% with $\frac{\Delta c}{c}$ was determined. The height of the derivation can be explained that even with the right setting (correct gas density selected, as well as the pre-pressure control was set inside the right boundaries) the

MFC is around 20 years old and not well calibrated. But because the error is steady, and the volume is not a critical parameter it was decided to use the MFC.
The error of the measurement was estimated of 0.4% . This leads to a total systematical error of 20.4% for $m(Hg)_{actual\ value}$. Because this is a steady error the error was considered acceptable.

Calculation of error of the measurement:
The purity of the used mercury species lies between 97-99%. Therefore, an error between 0.5-4 % had to be assumed depending on the measured species. The error of the balance was measured with an examination weight. The error was 0.7%. This results in a maximum error of 3.3 % as error of the sample. This derivation must be considered for the $m(Hg)_{target\ value}$.

Calculation of the random error:
The following assumptions were made for the calculation of the random or statistical error:
For all Hg(t) emissions the remaining recovery rates were normally distributed. Two outliers were identified and are no longer considered. For Hg(0) all recovery rates without the halides measurements were normally distributed. Two outliers were identified and no longer considered.
For further calculation the recovery rates were used to calculate the standardized error of the thermo desorption analysis which includes the errors of the system and the handling of the sample.

Based on DIN 1319-3 [72] the mean $\bar{v}$ of the recovery rates of the different measurements was calculated. With the mean and n as number of measured samples, the standard deviation and standard deviation of the arithmetic mean the measure of uncertainty $s(\bar{v})$ were calculated [73]:

$$x_1 = \bar{v} = \frac{1}{n}\sum_{j=1}^{n} v_j \qquad (3.2)$$

$$s(v) = \sqrt{\frac{1}{n-1}\sum_{j=1}^{n}(v_j - \bar{v})^2} \qquad (3.3)$$

$$u(x_1) = s(\bar{v}) = \frac{s}{\sqrt{n}} \qquad (3.4)$$

The evaluation of Hg(t) showed a mean recovery rate $\bar{v}$(Hg) of 83.17 % with n=50. The standard derivation is determined with $s(v)$ 13.00 % and a standard deviation of the mean $s(\bar{v})$ of 1.84 %.

For elemental mercury only those measurements were used, where only elemental emissions occurred. Concluding that no Hg(0) measurements from Hg-halides evaporations were used.

The evaluation of Hg(0) showed a mean recovery rate $\bar{v}$(Hg) of 91.99 % with n=35. The standard derivation is determined as $s(v)$ 9.55 % and a standard deviation of the mean $s(\bar{v})$ of 1.61 %.

Calculation of the systematical error:

The calculated mean is the estimated value of the expected value with the addition of the systematical error. The systematical error is the difference between the true value (100%) and the estimated value. [74]

This results in a correction factor K for the systematical error x_2 of the system of K=16.83% with:

$$x_2 = -K \tag{3.5}$$

To take the measure of dispersion into account, the standard deviation of the expected value is considered. This results according to [72], [73] in a uncertainty $u(x_{2,Hg(t)})$ of 7.51% (Eq. 3.6).

$$u(x_2) = \frac{a}{\sqrt{3}} \tag{3.6}$$

Where *a* is the border of the deviation of the interval in which X_2 lies.

The overall uncertainty is calculated with:

$$u(y) = \sqrt{u^2(x_1) + u^2(x_2)} \tag{3.7}$$

Resulting in a $u(y_{Hg(t)})$= 7.73%.

With y as the best estimate of the measurand Y defined as:

$$y = x_1 - x_2 = \bar{v} + K \tag{3.8}$$

The advanced measurement uncertainty for the Hg(t) measurement for a k=2 is 15.5%.

From this a confidence interval (Eq. 3.5) of 95 % was calculated with a t = 2,01 with:

$$y - t\ x\ u(y) \leq \mathrm{Y} \geq \mathrm{y} + t\ x\ u(y) \quad (3.9)$$

[72]

All recovery rates of the Hg(t) measurement between 84.46 % - 115.53 % can be considered as a true value of the sample. Only those were used for further interpretation. For elemental mercury with a $x_{2,\ Hg(0)}$ of 8,01 % a u($x_{2,\ Hg(0)}$) of 5,51 % was calculated resulting in a u($y_{Hg(0)}$) = 5.74 % and a confidence interval of 88.22 % - 111.78 % for elemental mercury with a t=2.05.

The ratio between Hg(0) and Hg(t) was calculated as followed:

$$\frac{m(Hg(0))}{m(Hg(t))} * 100 = ratio\ of\ Hg(0) \quad (3.10)$$

For a general statement the average of the Hg(0) ratio was calculated for each species.

3.3.2 Creation of standardized solid mercury-gypsum samples via scrubber system

All mercury concentrations (aqueous and solid) were measured with the DMA 80 with an extended (k=2) measurement inaccuracy < 30 %. All gypsum samples were measured with the DMA 80 and with the in-house designed TDS. The mercury content found for every sample was compared to guarantee that the whole mercury content was detected by the designed TDS process and other mercury species, than those found could be excluded. The extended measurement inaccuracy (k=2) for the TDS method was determined as 15.46 % for Hg(t) and 11.49 % for Hg(0). Because of the small mercury concentrations in samples with a Hg_{max} smaller or equal 15 µg m_n^{-3} a k=3 was set for the used boundaries resulting in an inaccuracy of 23.18 % for Hg(t) and 17.23 % for Hg(0).

The resulting to be considered errors of the scrubber system are discussed in the following section.

The measured error of volume stream for the scrubber system was determined with $\frac{\Delta c}{c}$ as +18 %. This error was considered in the mass balance for the different process streams. Because the deviation is very high, the difference between the real volume stream and the deviation was considered in the target volume stream. The systematical error of the analyzer was also estimated as 0.4 % that concludes in a systematically error of 18.4%.

The SO_2 analyzer was calibrated before the measurements but has a high cross-sensitivity to elemental mercury. The cross sensitivity was calculated with following calculated approximation:

$$\beta(SO_2)_{corrected} = \beta(SO_2)_{measured} - (0.0237 * \beta(Hg(0))_{measured} + 3.8537) \quad (3.11)$$

The pH electrode was calibrated before every experiment. The ORP value was checked with a calibration liquid and was corrected to the ORP of hydrogen (SHE value).

3.3.3 Precipitation experiments

For the precipitation experiments the same inaccuracy as with the other TDS experiments is applicable.

3.3.4 The Hg(0) phenomena

To assure that the measurements of Hg(0) and Hg(t) are comparable, an elemental mercury stream was led through the experimental setup and a deviation was measured. The deviation of the two VM3000 was < 1 %. This deviation was considered in the measurement data. To assure that both strings measured can be compared, HgS was measured with the same oxidation number Hg(0) with both analyzers.

The results showed a deviation of 1.3% between the recovery rates of both measurements.

After the first observatory measurements it became clear that some of the elemental mercury recovery rates were higher than the total mercury recovery rates when measuring mercury species with an oxide group.

To exclude a measurement error with one of the analyzers HgO was measured with both strings measuring Hg(0). The result of the recovery rate showed a deviation of 2%. The analyzers for the Hg(0) and Hg(t) strings were switched so that a analytical problem could be excluded.

Next a possible cross sensitivity was closer investigated. It is known that UV based mercury measurements are cross sensitive to SO_2. Not in all measurements SO_2 was in the flue gas mix. All other possible elements are:

- O, O_2 or O_3 (depending on the split reaction between Hg and oxygen)

- N_2(carrier gas), NO, NO_2, N_2O (reaction of the carrier gas and the oxygen compound)

To exclude a cross sensitivity of nitrogen-based flue gas compound the analyzer VM3000 was installed at the $DeNO_x$ measurement stand. No cross sensitivity with NO_x was measured.

To exclude a reemission out of one of the wash bottles, different wash solutions with high concentration of halide-ions were installed but no change was seen in the emissions.
A system error can be excluded. The statistical analysis showed that Hg(0)/Hg(t) ratios between 1.32 and 0.76 all lie inside the statistical inaccuracy. This shows that the ratio is not a good value to interpret the reaction and it is no longer interpreted for all average ratios of a measurement >50%. All Hg(0) measurements that lie inside the measurement inaccuracy of the system were used for further interpretations. The key component is the Hg(t) recovery rate, because there are more usable measurements. But both emission strings are compared and validated to the actual Hg content (measured with the DMA 80 or use of a pure mercury substance). For the recovery rate, and other comparisons the Hg(t) string was used. For the statistical interpretation of the scrubber system the DMA 80 analyses were used.

3.4 Reproducibility

This chapter will discuss the reproducibility of the experiments.

3.4.1 Procedure to assay a solid sample containing mercury

Part of this section is published in [18].
All TDS measurements were conducted at least three times to verify the reproducibility of the evaporation profiles of the different species. When the recovery rate stayed inside the defined confidence interval it was used to create an average peak for the single species.
Figure 13 (a) shows three evaporation profiles of $HgCl_2$ for standard conditions. All the pictured measurements stayed inside the confidence interval. Figure 13 (b) shows the average peak resulting from the individual measurements for $HgCl_2$. An average was calculated for Hg(0) and Hg(t) but in the case of $HgCl_2$ no Hg(0) emission was detected. This procedure was repeated with every species listed. In the following only average peaks are shown.

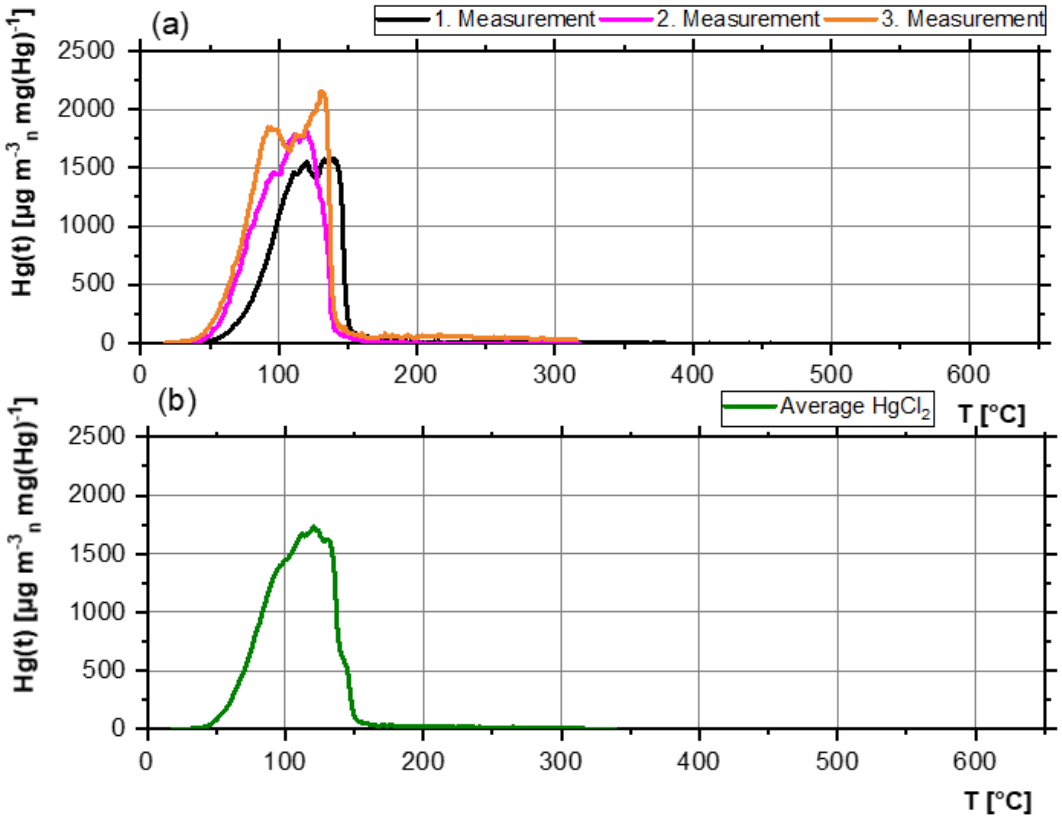

Figure 13 (a): Evaporation profile of $HgCl_2$, standard conditions; (b): Average profile of $HgCl_2$. [18]

3.4.2 Creation of standardized solid mercury-gypsum samples via scrubber system

In every experiment one wet gypsum sample was collected and measured without any further treatment to compare the qualitative outcome of the treated samples. Figure 14 shows a comparison of a freeze-dried sample and the wet gypsum sample. There is no change in the maximum evaporation temperature of both. This shows, that the mercury species is not affected by the treatment.

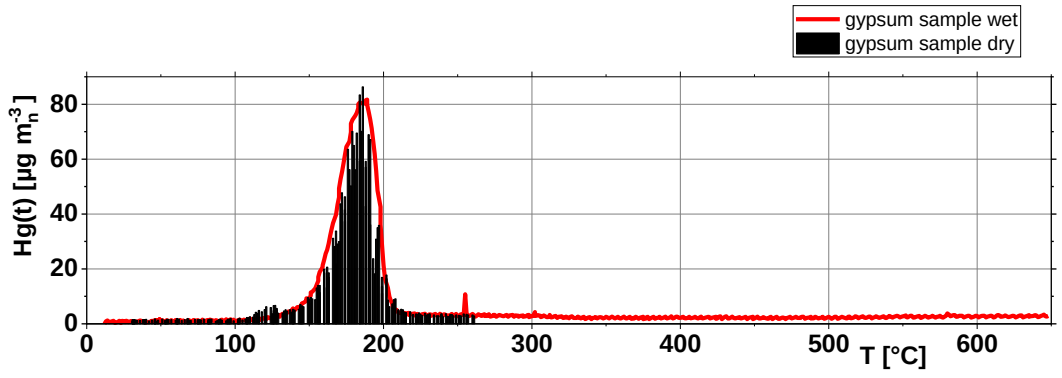

Figure 14 Comparison between freeze-dried sample and wet sample

All gypsum samples were measured at least twice with the TDS method and also measured twice with the DMA 80 for the determination of the Hg^{total} content of the samples. The results were compared to the mercury quantities measured with the TDS method and showed similar results. All further values of the Hg^{total} results are from the DMA 80 measurement as it is a standardized method. All the measurements with the TDS-system showed same evaporation profiles but didn't fit any evaporation profile of the known mercury samples. The gypsum sample with precipitation agent showed a perfect HgS peak. This concludes that it is possible to identify a known species via the mercury standards template developed (see Figure 15).

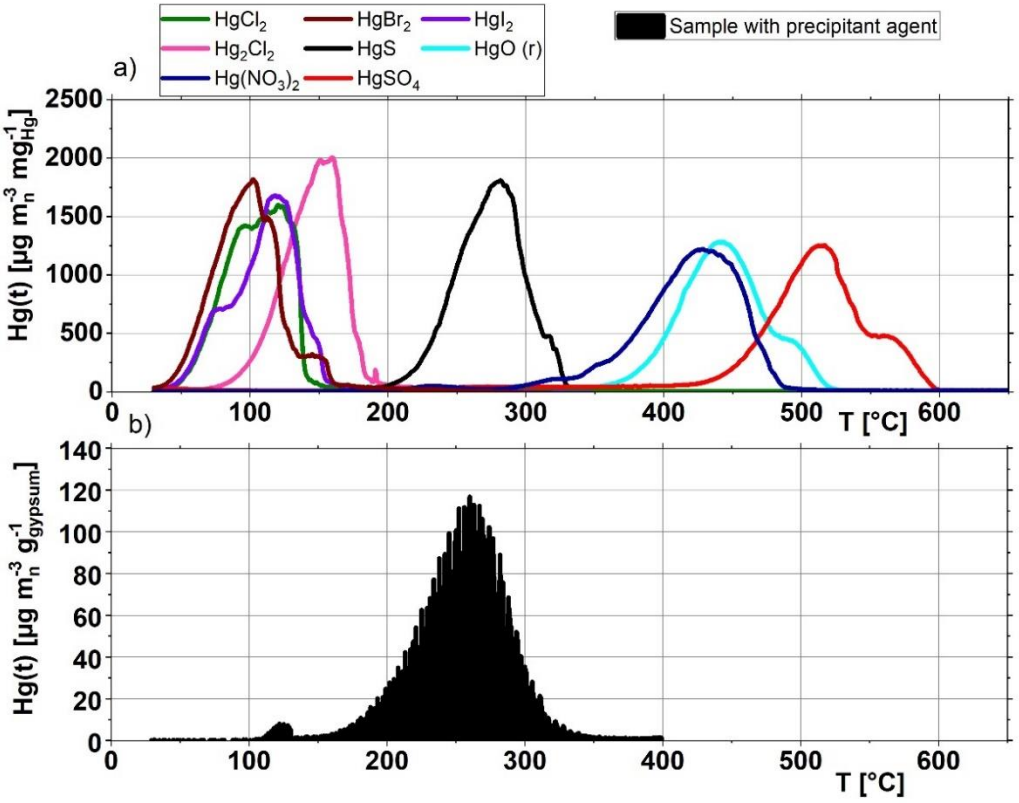

Figure 15 Comparison of the mercury standards with a gypsum sample knowingly containing HgS.

All scrubber tests without the solid phase were repeated twice. It was not possible to repeat the same experiment with exactly the same results, because of different influences on the reaction and the equilibrium of the different species. The effort with respect to needed time for one experiment made it impossible to repeat the experiments more often. Preparation of one experiment could take up to two weeks. Because of the laborious process to clean the scrubber reactor, the experiments were conducted in the order chloride, bromide and iodide. For the experiments with no halides all tubes and seals had to be changed. For all experiments, for every sulfite dosage a mean for Hg(0) and Hg(t) was calculated with both experiments. They

showed no significant deviation to each other. Except for the first dosage peak of the halide free system. There, one measurement was not considered because it was detected via outlier test. The pH value as well as the ORP were measured before and after adding the synthetic scrubber solution to the system. Every other dosage was controlled and checked for reasonableness. This was done to exclude impurities in the scrubber reactor as well as in the used solutions. If a deviation was observed the experiment was stopped, and the system was cleaned again.
Similar challenges occurred for the scrubber experiments. Due to the experiments´ duration and attendance needed it was not possible to repeat the experiments. Therefore, first behavioral aspects between mercury-halides and sulfite anions were detected with experiments without a solid phase. This made it possible to conduct the main aspects in one or two trials and not with single parameter studies.

3.4.3 Precipitation experiments

All precipitation experiments are experiments for the indication of the mercury species precipitating in a scrubber solution. Because of the possible formation of Hg^{el} in the solid, freeze-drying the sample was not an option as a drying process for these experiments.
This led to air drying the sample as only option. Due to the measurements of the samples at different times, it was possible to see the progressing dry states of the samples. Samples that had a chance of drying longer showed more narrow peaks, these results are in conformity with results in literature as well as with the gypsum samples. Even if the evaporation activity appears at the same temperature, the evaporation peaks vary in their appearance.

This characteristic made it impossible for reproducing two measurements. But all precipitated mercury species showed independent from their degree of drying own characteristic evaporation behavior for their species, that could separate them from the other mercury species. Those characteristics were used to identify the active species in the precipitation process of a scrubber.

4 Results and discussion

This chapter sums up the results and discusses the findings to extend the known Hg-Halides-H_2O-System (Bittig droplet) with sulfite as possible ligand for mercury and add the solid phase to the system.

The results start with the investigation of sulfite as a ligand for aqueous mercury and the interpretation of the main driver for the Hg_{aq}-Hg_s equilibrium. Next the correlation of the main influences of the parameter settings and matrix changes in the FGD on the formation of Hg_s will be calculated and argued.

The analysis of the main Hg_s species in the solid fraction of a FGD starts with the results and discussion of the development of the procedure to assay a mercury species in a solid sample.

After the development of the analytical system the results of the evaporation profiles of the gypsum samples containing an unknown mercury species will be evaluated and discussed. For the analysis not only the developed template for the evaporation behavior of solid mercury species will be used but also analyses of the possible elements in the sample were conducted via RFA and SEM analysis and a qualitative analysis of mercury via DMA 80. Based on the findings the first developed evaporation profile had to be extended. Further theoretical calculations were made to see what mercury species is the most likely in a scrubber solution and what are the possible species reaching their saturation limit in FGD like settings. To confirm the developed theory precipitation experiments were conducted and the results are also shown and discussed in this section.

The findings will be merged, resulting in the expansion of the Bittig droplet with the solid phase and the integration of sulfite as ligand.

4.1 Investigation of the main influences on the Hg_{aq}-Hg_s equilibrium

This chapter will concentrate on the Hg_{aq}-Hg_s equilibrium. To investigate the most plausible Hg_{aq}-species interacting in the Hg_{aq}-Hg_s equilibrium. Discussed next will be how to integrate sulfite in the Hg-Halides-H_2O-System visualized in the Bittig droplet. Then the parameter and matrix changes in the FGD, that have an influence on the Hg_{aq}-Hg_s equilibrium will be investigated.

4.1.1 Integration of sulfite in the Hg-Halides-H_2O-System

Part of this section was published in [71]

The first scrubber experiments were conducted without a solid phase. Aim of these experiments is to integrate sulfite as ligand into the mercury halides system to see what role it can take in the $Hg_{aq} \rightleftharpoons Hg_s$ equilibrium and if it can be a possible ligand for the formation of Hg_s. Following questions had to be answered:

- Where is the main coordination on the mercury? Is $HgSO_3$ a two or one times coordinated complex?
- Is sulfite of hydrogen sulfite the main ligand for mercury?
- If it is two times coordinated, what is the characteristic Hg^{ox} emission at 50°C for $HgSO_3$?
- Where does the ligand strength of sulfite fit in the halides system of I > Br > Cl?
- Can a higher sulfite concentration stabilize Hg_{aq} as it is done by halides?
- Can sulfite form a heteroleptic complex with mercury and halides?

The Hg^{2+}-SO_2-H_2O System

The reaction of sulfite as ligand for mercury without any halides in the system is shown in Figure 16. It shows that the main species is elemental mercury. The dosage of H_2SO_3 led to a spontaneous elemental mercury emission > 500 µg m^{-3}. The addition of 1:10 sulfite dosage to the mercury concentration shows an increase up to 3500 µg m^{-3} elemental mercury emissions. With a higher addition of sulfite, the mercury emissions decrease again.

Based on these results following two theses can be postulated:

- The Hg-SO_2-H_2O-System does not generate any oxidized mercury emissions, which means that the mercury(II)sulfite-complex is no relevant Henry component.
- A 1:10 sulfite dosage to mercury causes an increase of the reduction of $Hg(II)_{aq}$ and not a stabilization. This influence decreases with further additions of free sulfite ions into the solution.

Hg-Halides-SO_2-H_2O-Systems

The results of the experiments of the mercury-halides components in a sulfuric system are shown in Figure 17-Figure 19. No differences between HSO_3^- or SO_3^{2-} were detectable, so the results are shown in comparison to the added SO_3^{2-} concentration. There are big differences in the reemission behavior when comparing the three Hg-halides and sulfite addition.

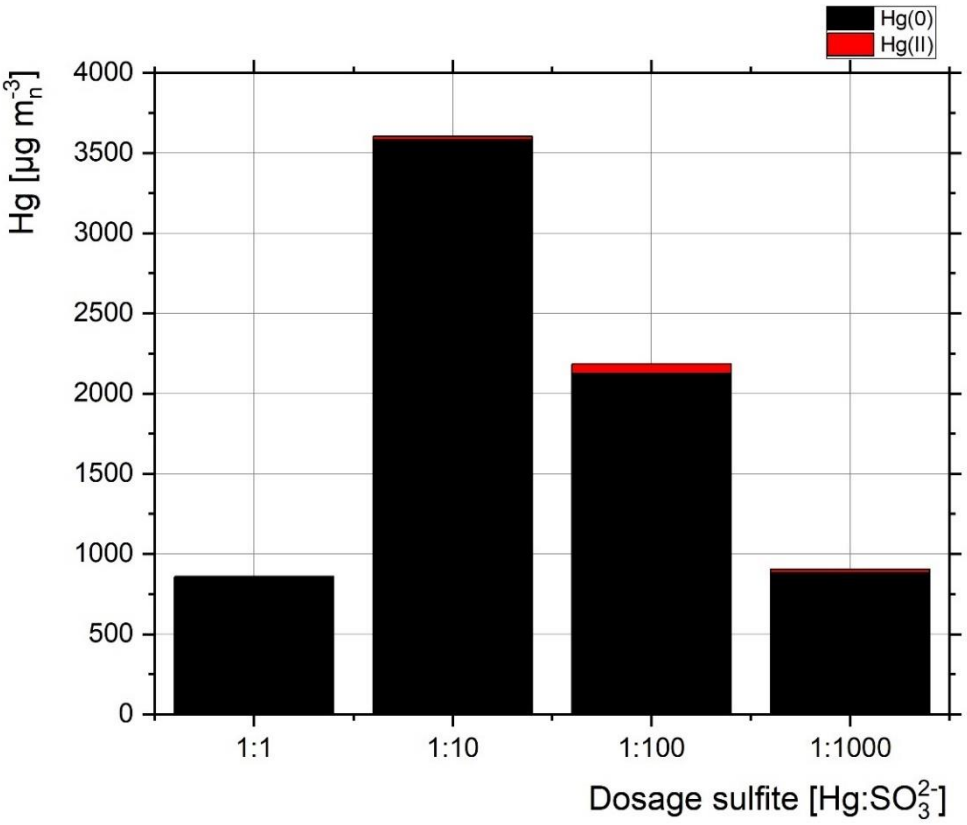

Figure 16 Resulting accumulated Hg-reemission of the Hg-SO_2-H_2O-System after sulfite dosage Hg:SO_3^{2-} of 1:1, 1:10, 1:100 and 1:1000.

Hg-Cl-SO_2-H_2O-System

The first point in the figure is the starting concentration of Hg-emission of the Hg-Halide-H_2O-system. The first dosage shows a spontaneous redox reaction resulting in a high elemental reemission of mercury. The emission is twice as high as the emission of the Hg-SO_2-H_2O-system. The emission increases with the next dosage of sulfite to reach a relation of 1:10 of Hg:SO_3^{2-}. For the 1:100 and 1:1000 dosage of sulfite the elemental emissions of mercury have the same height as in the halides free system. Similar to the halide free system the mercury(II)-emissions are not relevant.

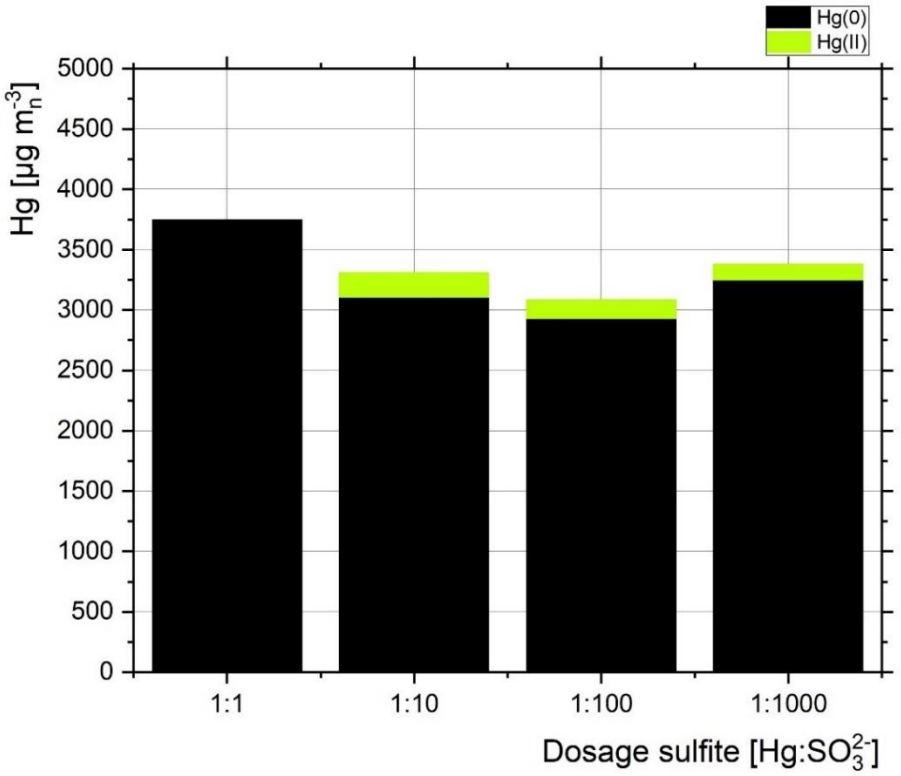

Figure 17 Resulting accumulated Hg-reemission of the Hg-Cl-SO_2-H_2O-System after sulfite dosage Hg:Cl:SO_3^{2-} of 1:2:1, 1:2:10, 1:2:100 and 1:2:1000.

Hg-Br-SO_2-H_2O-System

Similar to the Hg-Cl-SO_2-H_2O-system, the system with bromide shows a big emission raise with the first dosage of sulfite. Different to the systems discussed before the bromide system shows with the first dosage of sulfite a high oxidized mercury emission. This emission is not explainable with the Henry coefficient of $HgBr_2$. Even if the elemental mercury emission stays below the Hg-SO_2-H_2O-system in its concentration, the Hg-total concentration in a stoichiometry of 1:2:1 Hg:Br:SO_3^{2-} lies at > 3 mg m^{-3}_n. Bromide and sulfite show the highest resulting reemission measured. The system stabilizes a little bit more with each following sulfite dosage.

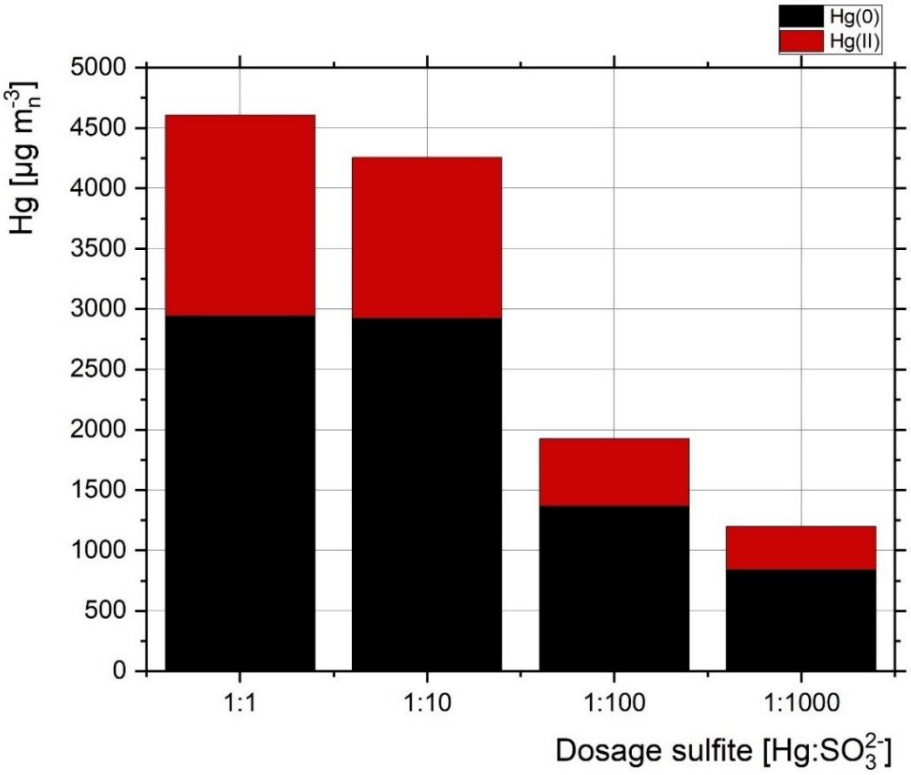

Figure 18 Resulting accumulated Hg-reemission of the Hg-Br-SO_2-H_2O-System after sulfite dosage Hg:Br:SO_3^{2-} of 1:2:1, 1:2:10, 1:2:100 and 1:2:1000.

Hg-I-SO_2-H_2O-System

In comparison to the Systems discussed before the Hg-I-H_2O-system shows a Hg(II) emission in a range of 400-500 µg m^{-3}_n. With the addition of sulfite, the system does not show an extreme reaction as with the other halides. With the dosage of Hg:SO_3^{2-} 1:100 the Hg(0) concentration raises but the Hg(t) concentration stays the same. With the next dosage, the Hg(t) concentration drops from 600 to 300 µg m^{-3}_n, but mostly the oxidized species decreases.

From those experiments following conclusions are drawn:

The Hg-Cl-SO_2-H_2O-system shows the most sensible behavior with sulfite in comparison to the other halides. It was very difficult to set the system into a steady state. The main oxidation state of mercury is elemental. The system shows a similar emission behavior than the system without halides. This leads to the conclusion that sulfite is the preferred ligand for mercury in comparison to chloride.

The Hg-Br-SO_2-H_2O-system shows highest emissions of all systems, not only for elemental but also for oxidized mercury emissions. One reason can be, that bromide and sulfite compete for mercury that leads to an unstable equilibrium resulting in a very high emission. It was not possible to stabilize mercury in this system.

The most stable system is with iodide. But even a strong ligand like iodide cannot prevent an elemental emission caused by a sulfite dosage.

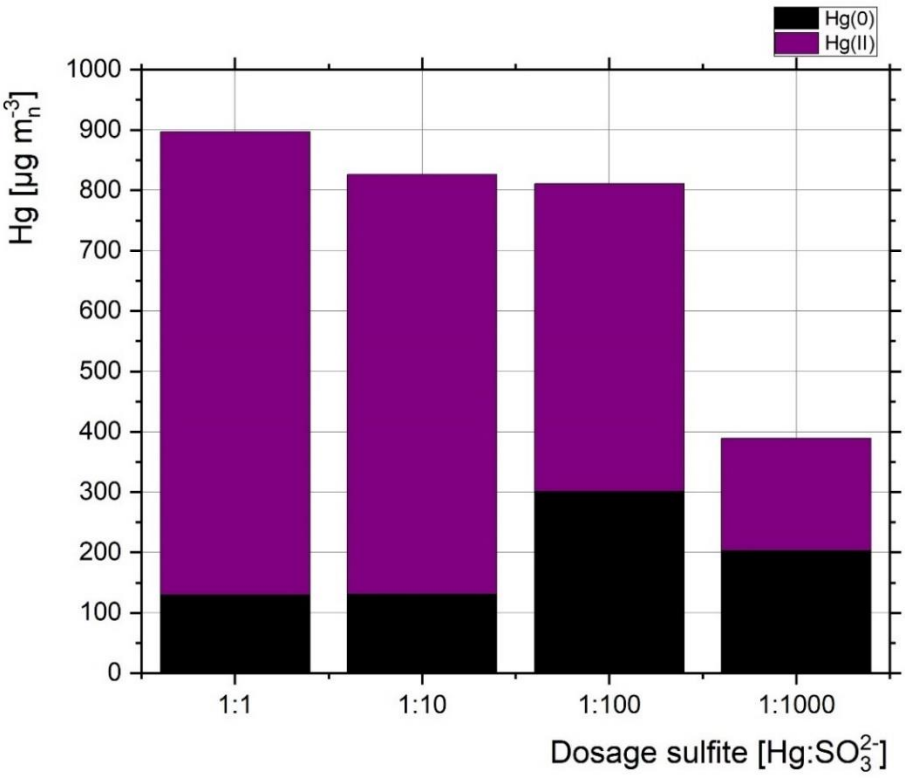

Figure 19 Resulting accumulated Hg-reemission of the Hg-I-SO_2-H_2O-System after sulfite dosage Hg:I:SO_3^{2-} of 1:2:1, 1:2:10, 1:2:100 and 1:2:1000.

One of the main recommendations to prevent Hg-reemissions out of the scrubber sump is the excess of halides in the system. The concentration of the halides was set to 1mol L^{-1} to ensure that for all halides mercury will form a four-times coordinated complex.

The results of the experiments are shown in Figure 20 to Figure 22.

The first most obvious observation in the systems with a halides excess is, that the level of the Hg-reemission concentration drops from mg m^{-3}_n to µg m^{-3}_n. For all systems the Hg(II) emissions stay < 10 µg m^{-3}_n. The Hg-Cl_{excess}-SO_2-H_2O-System shows no elemental reemissions of mercury till the Hg:SO_3^{2-} dosage of 1:100. Even with the higher sulfite dosages the Hg(t)-reemissions stay < 10 µg m^{-3}_n. The systems with an excess of bromide or iodide show an elemental reemission of around 30 µg m^{-3}_n for bromide and around 50 µg m^{-3}_n for iodide.

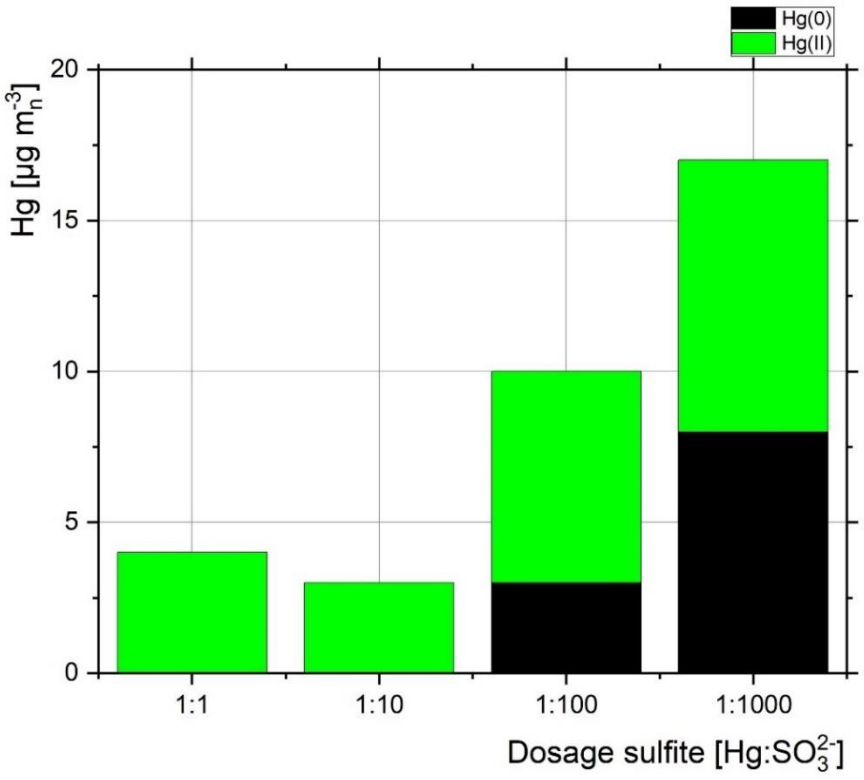

Figure 20 Resulting accumulated Hg-reemission of Hg-Cl-SO_2-H_2O-System with excess Cl^- after the sulfite dosage Hg:SO_3^{2-} of 1:1, 1:10, 1:100, 1:1000.

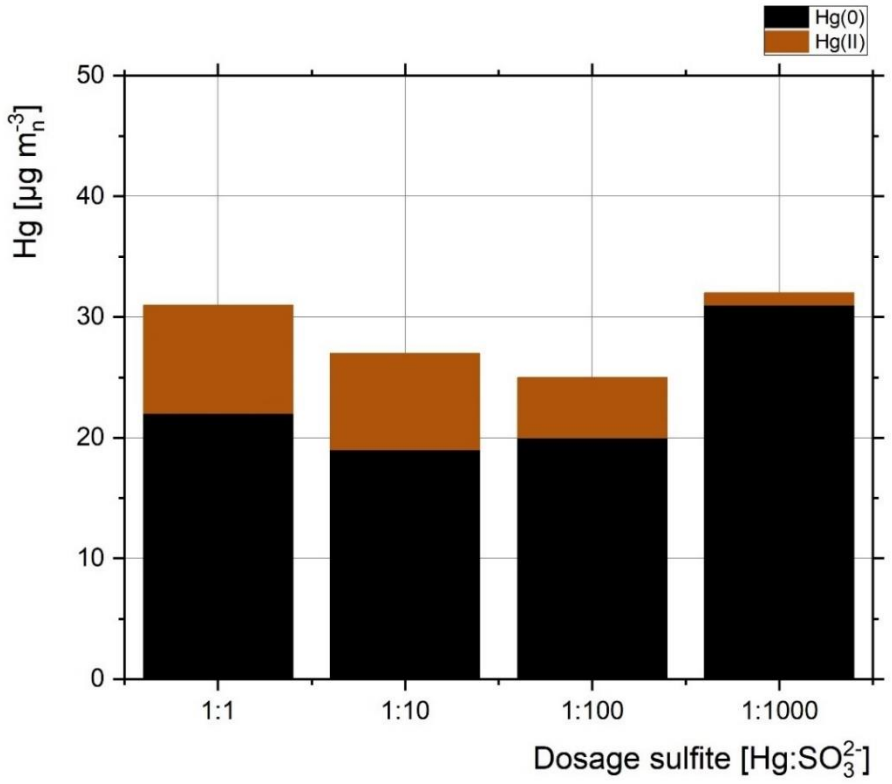

Figure 21 Resulting accumulated Hg-reemission of Hg-Br-SO_2-H_2O-System with excess Br^- after the sulfite dosage Hg:SO_3^{2-} of 1:1, 1:10, 1:100, 1:1000.

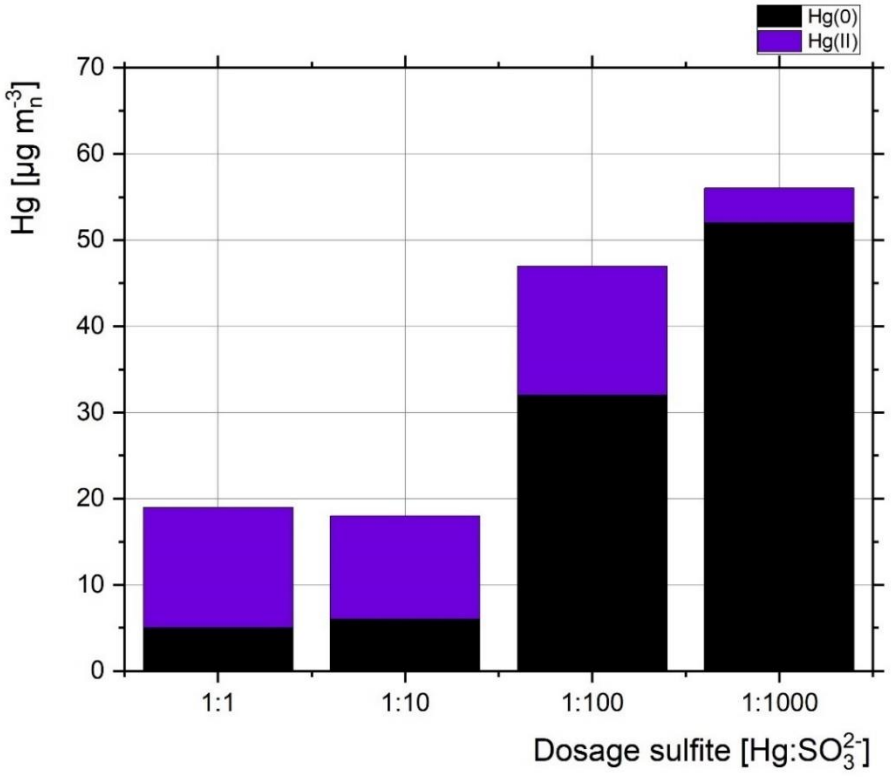

Figure 22 Resulting accumulated Hg-reemission of Hg-I-SO_2-H_2O-System with excess I^- after the sulfite dosage Hg:SO_3^{2-} of 1:1, 1:10, 1:100, 1:1000.

To sum up the results described before:

- The reaction of aqueous mercury and sulfite always leads to an elemental emission.
- Sulfite and bromide in the system in a stoichiometry of Hg:halide:sulfite of 1:2:1, show a similar ligand strength.
- To minimize the elemental reemission of mercury caused by sulfite a sulfite concentration of $Hg:SO_3^{2-}$ of > 1:1000 needs to be present.
- The excess of halides in the system reduces the reemission of mercury noticeably.
- Even in excess of halides the dosage of sulfite causes a destabilization of the system, more noticeably in the bromide and iodide system than in the chloride system. It is possible that the ion diameter is the essential factor in this (iodine 220 pm, bromine196 pm and chlorine 181 pm). [56] That the chloride with the smallest radius can fit in a very packed complex.

  The covalent single bond atom radius for S- and Cl- with103 pm and 99 pm, which are very similar in comparison to iodine with 133 pm or bromine with 114 pm. Hg has radius for a covalent bond of 133 pm. [63]
- The lowest impact of sulfite was detected in the $Hg\text{-}Cl_{excess}\text{-}SO_2\text{-}H_2O$-system. Elemental reemissions were completely repressed till the sulfite dosage of $Hg:SO_3^{2-}$ of 1:100.

4.1.2 Discussion of the impact of sulfite on Hg_{aq} and the integration of sulfite in the Hg-Halides-H_2O-System

Part of this section was published in [71].

Based on the found results following working hypothesis were derived:

1. In an aqueous system diluted sulfite compounds do not act as a Henry compound for mercury. They do not have a vapor pressure over the solution; reemission result as elemental mercury.
2. Sulfite acts most likely as mono-dental ligand for mercury.
3. $HgBr_2$ and $HgSO_3$ with a comparable stoichiometry leads to a maximum of Hg(t)-emission.
4. Sulfite does not lead to a ligand exchange. It reacts with Hg^{2+} and shifts the Hg-halides equilibrium.
5. Chloride in excess is the best solution to stabilize the system. It is assumed that chloride can form because of its small atom radius, a heteroleptic $HgCl_n(SO_3)_n$ complex.
6. Sulfite has an influence on all the created mercury halides complexes, even with iodide as ligand for mercury, a sulfite dosage still has an influence.

Based on this hypothesis the first extension step of the Bittig droplet can be shown in Figure 23:

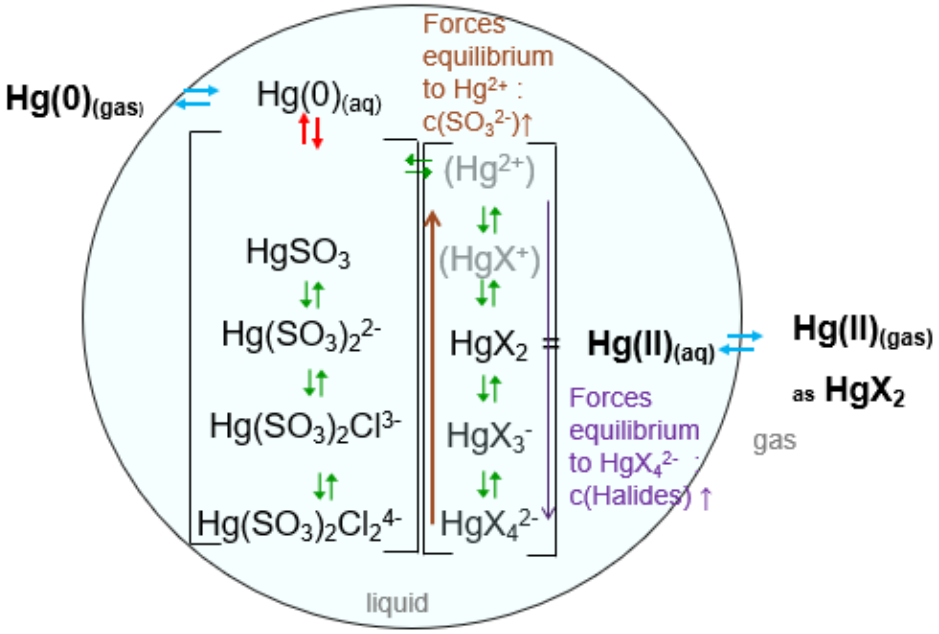

Figure 23 Bittig droplet expanded with sulfite as ligand.

$HgSO_3$ and higher coordination with sulfite as ligand opens a new parallel reaction path for mercury. The only combination with a halide and the formation of a heteroleptic complex can be with chloride in excess, but not with iodide of bromide. The red arrows describe a possible redox reaction, and the formation of elemental mercury that reemits depending on the Henry-Law (blue arrows) into the gas phase. The only other equilibrium with the gas phase is on the side of the HgX_2 halides. It can be concluded that for $HgSO_3$ the only connection to the gas phase is via redox reaction and the formation of Hg(0).

The stability and chemical reactivity of $HgSO_3$ can further be compared with HgX^+ base on the found results and not HgX_2 in the mercury-halides system. This can explain the fast redox reaction with the first sulfite dosages in the system. Concluding that $Hg(SO_3)_2^{2-}$ must be compared with the stability of a HgX_2 mercury(II)halides complex. This statement can be explained with the results of the Hg-Halide-SO_2-H_2O-Systems and the stability constants of the complexes (see Table 18). Whereas Hg: halide: sulfite in a ratio 1:2:1 for bromide, showed an equal strength for $HgBr_2$ compared to $HgSO_3$. Combined with the results in the Hg-I-SO_2-H_2O-System and the existents of elemental mercury emissions, that also support the statement that $HgSO_3$ can be considered as HgX (mono-dental) and $Hg(SO_3)_2^{2-}$ can be compared to the stability of HgX_2.

By doing so the species distribution calculated for the single ligands would show that sulfite as ligand is the strongest ligand for a one-times coordinated complex. As can be seen in Table 18 the stability constants of mercury sulfite in comparison to mercury bromide or - iodide. The Sulfite is the strongest ligand for HgX^+ but not as strong as $HgBr_2$. This can be explained that no coherent value of the stability constant for sulfite can be found.[14], [20], [21], [22]

Table 18 Comparison of the stability constants of mercury sulfite to bromide and iodide, according to the new structure for a T=25° C and starting the formation from Hg^{2+}. Sources for sulfite [21], [22]**, for halides all cumulated K values are from** [27]**.**

Species	K	Species	K	Species$^+$	K
$HgSO_3$	$2.1\ 10^{13}$	HgI^+	$7.14\ 10^{12}$	$HgBr^+$	$1.12\ 10^9$
$Hg(SO3)_2^{2-}$	$2.1\ 10^{23}$	HgI_2	$6.36\ 10^{23}$	$HgBr_2$	$2.08\ 10^{17}$
No further coordination values are known		HgI_4^{2-}	$6.52\ 10^{29}$	$HgBr_4^{2-}$	$9.97\ 10^{20}$

The rule of Guthrie only seems to apply with sulfite and chloride. The addition of the chloride with a higher electronegativity can form with sulfite as ligand a heteroleptic complex.
For a further investigation, the different operation conditions should be measured for a longer time in a steady state. That is not possible in the scale of the experiment.
These results confirm the theories found in literature. The addition of sulfite forces a reemission of elemental mercury. Also as in case of the findings of Blythe et al. it was possible to show that the system can be stabilized with chloride in excess.

4.1.3 Parameter study of main influences on the $Hg_{aq} \rightleftharpoons Hg_s$ equilibrium

This chapter shows and discusses the results of the influence of different parameter settings or matrix changes in the FGD system on the Hg_{aq}-Hg_s equilibrium.

Figure 24 shows all input and output streams of the laboratory scaled FGD starting with the flue gas containing 2000 mg m^{-3}_n SO_2 and 6 vol% O_2. The SO_2 concentration was verified before entering the FGD scrubber. Limestone was also added to the scrubber to set the pH value inside the wanted pH levels and oxygen to influence the ORP level in the scrubber. Outgoing streams are:

- measurement of SO_2,
- cumulated concentration of elemental mercury emission,
- cumulated concentration total mercury and
- mercury concentration of the gypsum sample

The pH value and the ORP level were also measured.

Figure 24 Balance of process streams of the scrubber.

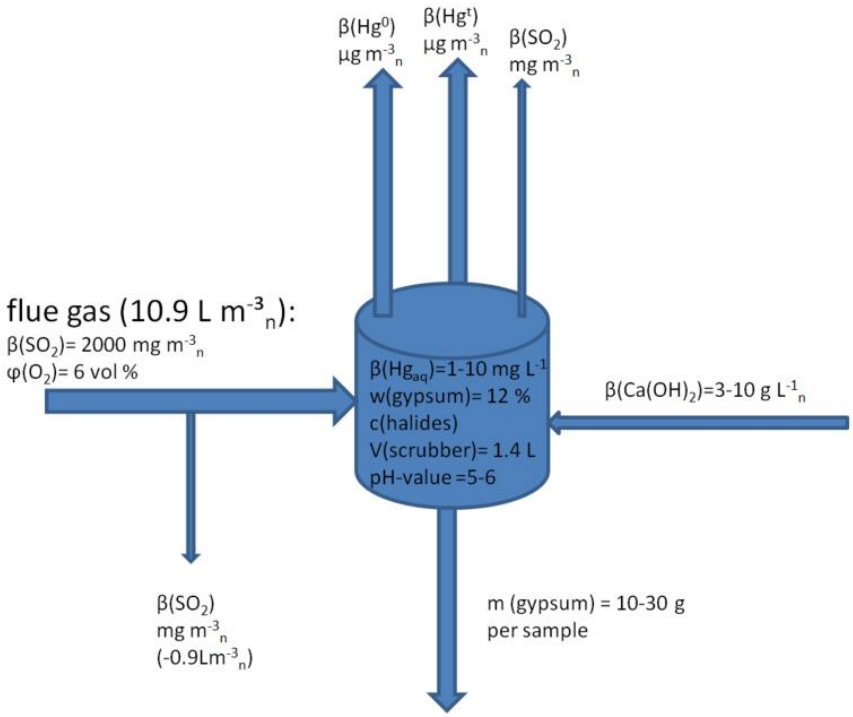

Aim of these experiments was to discover the different process parameters that have a main impact on the storage of Hg in the solid, to stabilize mercury in the aqueous phase and to minimize reemission out of the scrubber. To find correlations between the process parameters and input factors on the researched output factors a multiple regression analysis was used. For all data measured every minute, a mean was calculated to make it possible to compare all impacts to one another.
As Y the following output factors of the different experiment runs were set:

- Hg(0) reemission [µg m^{-3}_n]
- Hg(t) reemission [µg m^{-3}_n]
- Hg(II) reemission [µg m^{-3}_n]
- $Hg_{s,\ cumulated}$ [m (Hg) kg(gypsum)$^{-1}$]
- $Hg_{s,\ difference}$ [m (Hg) kg(gypsum)$^{-1}$]
- β(Hg) [mg (Hg) L^{-1}]

The correlation of the following input factors X and process parameters to the output Y was analyzed:

- $β_{Input}$(Hg) [mg (Hg) L^{-1}]

- pH
- ORP
- Sulfite dosage
- c(Hal) [mol L^{-1}]

To verify the results and the applicability of the system the data had to be normally distributed. The versus fits as well as the versus order of the residuals and unusual observations were checked. All measurements and results can be seen in the Appendix. Compared to all results the first measurement was an outlier and is not further considered.

Table 19 shows the used matrix and Table 20 shows the main influences and the correlation of the single input factors on the chosen output factors.

Table 19 Matrix for multi regression analysis

Hg(0) [µg m^{-3}]	Hg(t) [µg m^{-3}]	Hg(II) [µg m^{-3}]	Hg(t) [mg kg^{-1}] DMA 80 cumulated	Hg(t) [mg kg^{-1}] DMA 80 difference	Hg_{aq} [mg (Hg) L^{-1}] DMA 80	β_{Input} (Hg) [mg L^{-1}]	c(Hal) [mol L^{-1}]	SO_3^{2-}	metals	pH	ORP [mV]
2965	2635	-417	5.25			10	0	no	no	4.7	290
2034	1988	-45	4			10	0	no	no	5.4	299
20.32	25	4.8	1.25	1.25	0.5	1	0.030032	no	no	5.13	203
48	52	3	1.55	0.2	0.5	1	0.030032	no	no	4.9	260
24	28	4.46	1.55	0	0.2	1	0.030032	yes	no	4.9	244
89.9	91.8	1.9	2.4	0.85	0.3	1	0.030032	no	no	4.7	310
220.2	213.66	-6	2.05	2.05	7	10	0.030032	no	no	5.08	223
440	432	-7	3.15	1.1	5.8	10	0.030032	no	no	5.53	276
376	372	-4	5.2	2.05	2.398	10	0.030032	yes	no	5.03	247
336.55	325	-11.06	10.7	5.5	2.3	10	0.030032	no	no	5.27	287
324	351	27	0.99	0.99	7.8	10	0.50135	no	no	5.6	274

Hg(0) [µg m^{-3}]	Hg(t) [µg m^{-3}]	Hg(II) [µg m^{-3}]	Hg(t) [mg kg^{-1}] DMA 80 cumulated	Hg(t) [mg kg^{-1}] DMA 80 difference	Hg_{aq} [mg (Hg) L^{-1}] DMA 80	β_{Input} (Hg) [mg L^{-1}]	c(Hal) [mol L^{-1}]	SO_3^{2-}	metals	pH	ORP [mV]
59	106.4	47	1.4	0.41	6.2	10	0.50135	no	no	5.19	337
159	193.65	34	1.55	0.15	4.5	10	0.50135	yes	no	4.86	285
23.7	76	52	1.6	0.05	3.5	10	0.50135	no	no	5.08	360
604	602	-2	3.05	3.05	4.9	10	0.030032	no	yes	4.9	286
551	552	1	7	3.95	3.6	10	0.030032	no	yes	5.1	327
221	220	-0.8	14.5	7.5	2.5	10	0.030032	yes	yes	5.4	251
196	197	1.3	20	5.5	1.8	10	0.030032	no	yes	5.8	340

Table 20 Overview of output parameter in correlations to the different input factors.

Y	main correlation	second correlation	third correlation	fourth correlation	R^2-Value: The system was described by the parameters to:
Hg(0) reemission [µg m^{-3}_n]	β_{Input}(Hg) [mg (Hg) * L^{-1}] positive	none	none	none	71.54%
Hg(t) reemission [µg m^{-3}_n]	β_{Input}(Hg) [mg (Hg) * L^{-1}] positive	none	none	none	70.98%
Hg(II) reemission [µg m^{-3}_n]	c(Hal) [mol L-1] positive	β_{Input}(Hg) [mg (Hg) * L^{-1}] negative	none	none	94.27%
$Hg_{s, cumulated}$ [m (Hg) kg(gypsum)$^{-1}$]	sulfite dosage positive	pH value positive	metals positive	c(Hal) [mol L-1] negative	91 %
$Hg_{s, difference}$ [m (Hg) kg(gypsum)$^{-1}$]	metals positive	none	none	none	81%
β(Hg) [mg (Hg) L^{-1}]	β_{Input}(Hg) [mg (Hg) * L^{-1}] positive	sulfite dosage negative	none	none	88.49%

Reemissions

The main influence on the reemission is the β_{Input}(Hg) concentration. This factor is positively correlated, meaning with a higher starting mercury concentration in the scrubber suspension a higher reemission can be measured. This is not a surprising result because equilibrium states and Henry coefficients are dependable of this concentration. This result shows that the analysis can describe the system as a necessary prediction.

The more interesting result is the dependency of sulfite and halides concentrations of the system on reemissions.

Hg(II) reemissions are only dependent of the halides concentration. This is no surprising result because only Hg(II)-halides stay in equilibrium with the gas-phase and show a vapor pressure even after being absorbed.

Hg(0) reemission only shows a correlation to the input concentration of mercury. Halides and sulfite concentration show a dependency but with no statistical significance ($p > 0.05$). Both variables have a negative dependency. This means the higher the concentration of possible ligands the smaller the reemission of elemental mercury. This can be explained with a higher coordination of aqueous mercury, which pushes the Hg(II)-halides out of the Hg_g-Hg_{aq} equilibrium and minimizes the possible redox reaction of $HgSO_3$ to elemental mercury and SO_4^{2-}. The chosen parameters only describe the reemission by 70%. This means not all influences on elemental reemissions are captured. The interesting part is, that the suspected main influence of sulfite on the elemental emissions does not have a statistically significant impact on the reemissions. The opposite was suspected before the experiment.

Surprisingly the input concentration of mercury is the only statistically significant influence on the Hg(t) emission. Second and third strongest influences are sulfite and halides concentrations, but the observed correlations are not statistically significant ($p > 0.05$). This is an interesting factor because Hg(0) as well as Hg(II) both seem more dependent to the halides concentration than to the sulfite concentration. This can have the reason that none of the two factors shows a distinct impact on the reemission.

To validate the results for the reemissions, the multiple regression analysis for the gaseous phase was also performed with the full data set (one data point each minute instead of the mean for X´s and Y´s). The main statements of this analysis could be validated.

For Hg(0) and Hg(t) halides (positive) , sulfite (negative) as well as ORP (positive) show a correlation. For Hg(II), in addition to a halides and mercury concentration a dependency on the ORP (positive) and metals (positive) can be found. This fits the

expected statements but the data can only explain the system to 40% (R^2), which is not sufficient for a reliable statement. The versus fit, residual fit and the normal distribution also do not show a good system. An explanation for this could be that it is not perfect to combine a high number of continuous data points with discrete data (yes and no) within one analysis.

Aqueous mercury concentration

To determine the aqueous mercury concentration, the liquid samples taken after each parameter adjustment alongside with the gypsum sample were measured via DMA 80.

The β_{Input}(Hg) concentration shows the strongest influence on the output. This was expected because the concentration in a solution depends on the concentration input. The more surprising factor is the impact of the sulfite concentration. It has a strong influence on the mercury concentration. This value must be considered with caution, because in all the experiments the factor time also has an influence. Sulfite is always added during the third step after an experiment time of at least one hour. This means it is always added when less mercury is in the solution, and therefore this factor could be overrated in the model.

Solid mercury concentration

The solid mercury concentration is the only parameter that is not influenced by the aqueous concentration but by the sulfite concentration, the pH value, metals and halides. The only parameter that is correlated negatively is the halides concentration. This agrees with the starting argument that halides keep mercury out of the solid. The other influences that push mercury in the solid are also identified with this model. Sulfite as well as metals are positively correlated with the mercury concentration in gypsum. The positive correlation of the pH value is interesting. A possible explanation is that if the precipitation of mercury is the key mechanism of mercury ending up as solid it would need, depending on the ligand, a high pH value to precipitate. This is another parameter pointing in the direction of a precipitated mercury in gypsum. Those parameters can describe the model to 91% (R^2).

Because the high influence of the factor time of the concentration of mercury in the samples, the analysis was repeated considering the difference between the Hg-content rather than the absolute values in each sample. There the only statistically correlation is the metal concentration.

ORP

One very important point is that none of the output parameters is dependent of the ORP. This is why it was closer investigated and a correlation between reemissions and ORP was analyzed in more detail. It seems in comparison to the other values, that the influence of the ORP is not high enough to be considered statistically relevant in the main system. For the second calculation with minute values, a correlation could be identified but the system did not show a high R^2 value.

Interpretation and system prediction to stabilize mercury aqueous

None of the output parameters correlated with one another.

The prediction of the system to minimize Hg(0), Hg(t) and Hg(II) emissions is to minimize the Hg_{aq} concentration in the system. The maximization of the Hg_{aq} concentration is achieved by maximizing the halides concentration. For the reduction of mercury in solids, the halides concentration can be raised, sulfite can be minimized as well as metals and the pH value.

4.2 Procedure to assay mercury in solid samples

The first sub chapter will discuss the development of the right parameter settings to stay inside the system and process given restrictions to investigate the evaporation behavior of solid mercury species. The second one will show the found evaporation curves of the different solid mercury species. The last sub chapter will discuss the found results.

4.2.1 Development of the used parameters for the thermo desorption

Part of this section is published in [18].

A measurement process had to be developed to be able to identify different unknown mercury species in a solid. First orientation measurements showed that different aspects had to be considered for the implementation of an experiment. The process had to be improved systematically and therefore following restriction were set:

- The evaporation maximum needs to stay inside the calibration limit of the analyzer.
- It must be possible to conduct at least one measurement per day <12h.
- The process should be low maintenance.
- Only a recovery rate >70% is considered as valid measurement.
- The procedure shall not have an influence on the oxidation state of the evaporating mercury species or the evaporation profile.
- The volume stream needs to be high enough (at least 3 L min^{-1}) to deliver a sufficient volume stream for each mercury analyzer.
- The sample size needs to be manageable and reproducible.
- The process needs to be safe.
- The procedure has to be reproducible and the same for all possible solid mercury species.

As a first step different volume streams and sample sizes were varied. Figure 25 shows 2 mg (Hg) as $HgCl_2$, measured with a temperature ramp of 2 °C min^{-1} and 3 L min^{-1} volume stream.

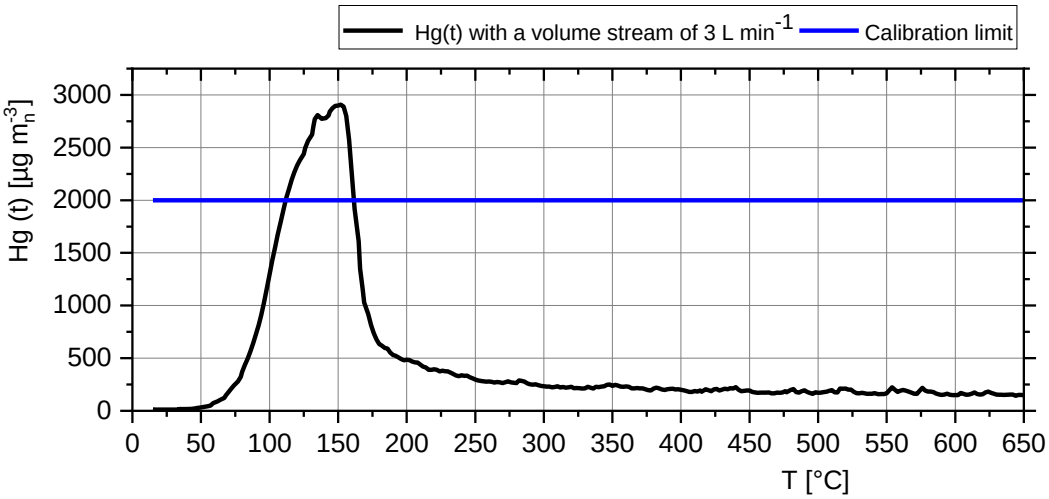

Figure 25 Evaporation profile of $HgCl_2$, 3 L min^{-1} volume stream, 2 °C min^{-1} temperature ramp and 2 mg (Hg) sample size.

Because the calibration limit of the analyzer was not met, the volume stream was set up to 5 L min^{-1} and the result was compared with the measurement with a volume stream of 3 L min^{-1} (Figure 26 (a)). It shows that the change from 3 L min^{-1} to 5 L min^{-1} decreases the retention time for the first evaporation of mercury. The calibration limit was still not met with the increased volume stream. In the next step (Figure 26 (b)) not only the volume stream was increased from 5 L min^{-1} to 7 L min^{-1} but also the sample size was reduced from 2 mg (Hg) to 0.5 mg (Hg).

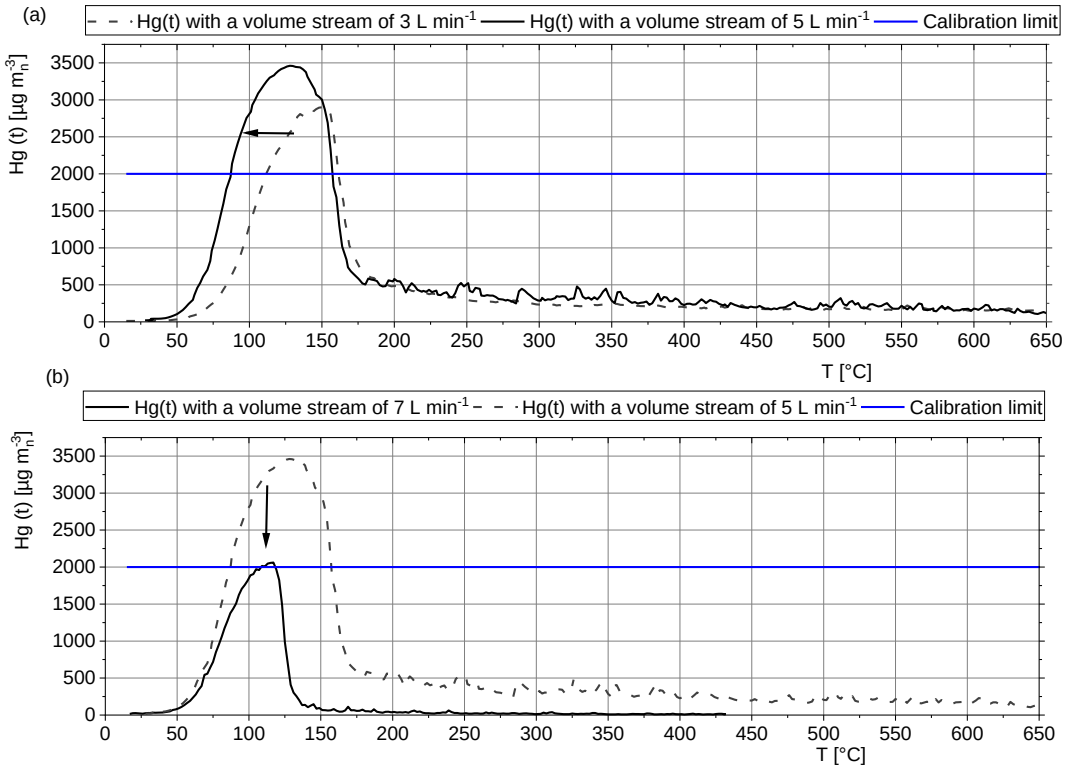

Figure 26 (a) Comparison of evaporation profiles with different volume streams, 2 °C min^{-1} temperature ramp, 2 mg (Hg) sample size (b): Comparison of a evaporation profile of $HgCl_2$ with 5 L min^{-1} volume stream and 0.5 mg(Hg) sample size with 7 L min^{-1} volume stream.

A decrease of retention time cannot be observed. This means that, at a volume stream of 5 L min^{-1} the characteristic retention time for the sample is a substance property and no process property.

Because the retention time does not differ between 5 L min^{-1} and 7 L min^{-1} as well as the temperature for the maximum of the evaporation, 7 L min^{-1} is the best choice for volume stream. 0.5 mg (Hg) was selected as sample size. A smaller sample size is not recommended, because of an too large weighing error.

Different sample holders for a small sample size of 0.5 mg Hg were tested to reduce the weighing error. The sample holder has to:

- have a weight < 500 mg because of the small samples size to minimize the balance mistake but also
- be inert against mercury emissions,
- be inert against high temperatures and
- fit into the sample holder of the reactor.

The sample size of 0.5 mg Hg and a self-cut small glass carrier that was directly inserted into the TDS-sample holder was the choice that led to the highest recovery rate.

But even with a sample size of 0.5 mg (Hg) and a volume stream of 7 L min^{-1} the calibration limits of the analyzer cannot be met. To meet all set restrictions the temperature program was closer investigated.

In literature different approaches of temperature programs are discussed. For a better understanding of the evaporation characteristics two different types of heating programs were tested. One was heating in steps of 50; 80; 100; 120; 150; 200; 250; 300; 400; 500; 600°C. On each step the temperature was held constant until the mercury emissions decreased and stabilized.

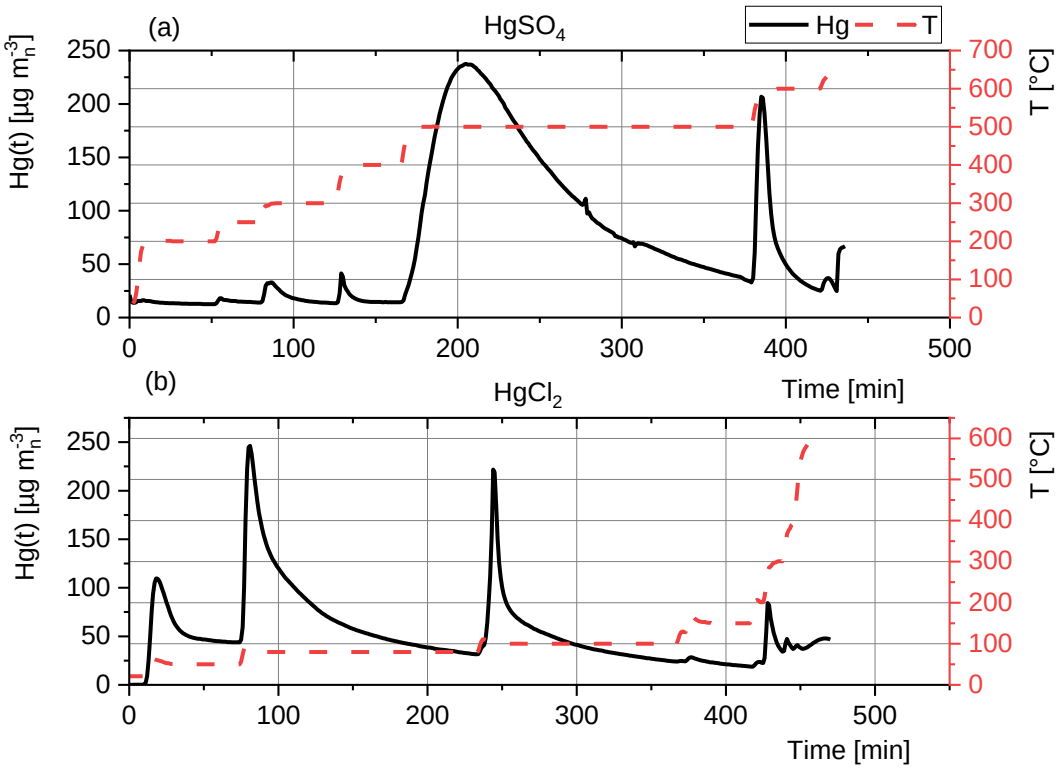

Figure 27 Evaporation profile of (a): $HgSO_4$ and (b): $HgCl_2$ heated by temperature steps.

Figure 27 shows the different evaporation profiles for $HgCl_2$ (Figure 27 (b)) and $HgSO_4$ (Figure 27 (a)). $HgCl_2$ shows no evaporation > 200°C. $HgSO_4$ shows the main evaporation at 500°C. Because $HgSO_4$ was still evaporating at temperatures > 600°C, the temperature program was extended up to 650°C.

A measuring time from up to 1000 minutes can occur for a sample with both species. The process has to be observed for the whole measuring time. Due to the possible long evaporation time and the high personnel effort this method was not feasible.

To meet the set criteria, different temperature ramps were measured, starting with 33°C min^{-1}, 5°C min^{-1}, 2°C min^{-1} and 1°C min^{-1}. 30°C was chosen as starting temperature, for the end-temperature 650 °C was chosen because of the activity of $HgSO_4$ at temperatures > 600°C.

The recovery rate was calculated as integral of total mercury mass over the time (see. Eq. 3.6).

Figure 28 shows the different evaporation profiles of $HgCl_2$ at 2 °C min^{-1} and 1 °C min^{-1}. Due to the increase of dwell time of mercury in the oven, the maximum of the mercury emissions measured was softened and the emission was stretched over time. This made it possible to remain below the calibration limit of the analyzer and leads to a higher recovery rate.

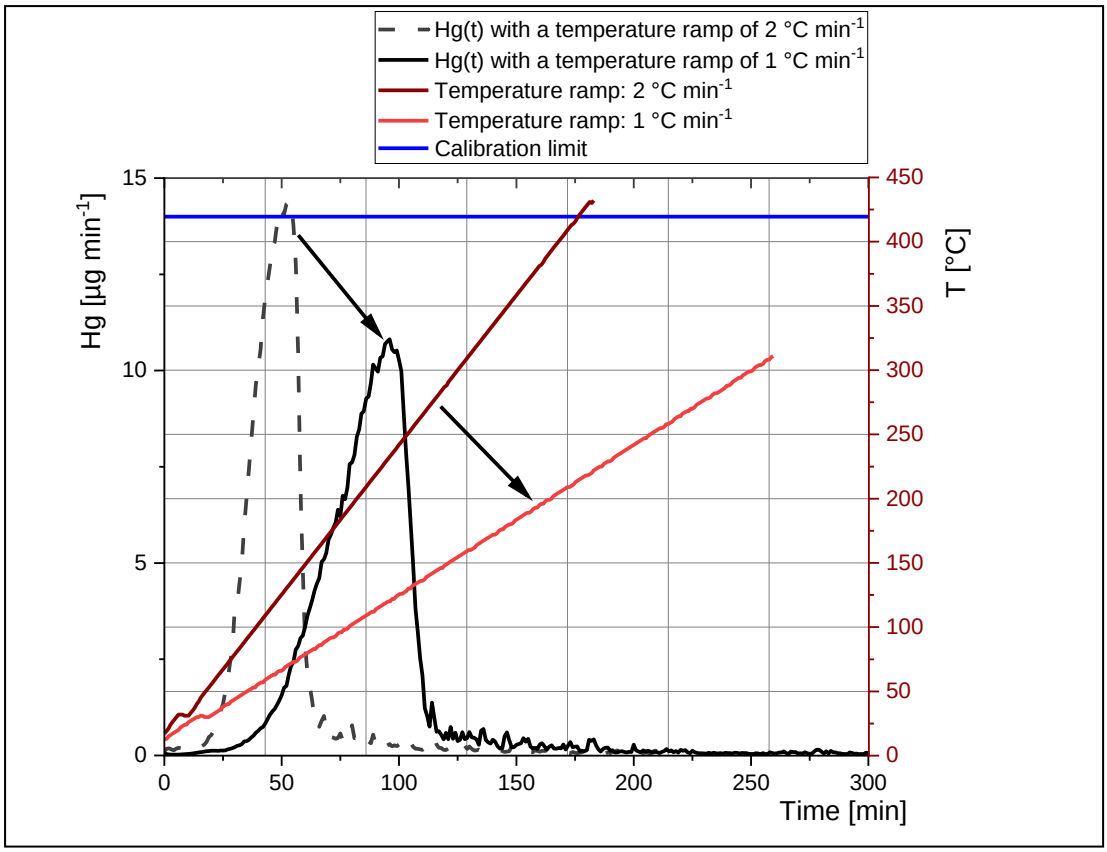

Figure 28 Comparison of the influence of the temperature ramps of 2 °C min^{-1} and 1 °C min^{-1} on the evaporation of $HgCl_2$.

1°C min^{-1} was the only temperature program at which the set boundary conditions for the recovery rate was met, similar to the results to Lee et al. [32]. Also similar to [32] a slower heating rate was not applicable for the set duration of < 12h.

Carrier Gas:

When HgS is heated with oxygen it reacts through HgO to Hg_{el} at about 300°C (eq. 3.8). It is important that the carrier gas does not interact with the species to analyze it. Therefore, nitrogen was chosen as carrier gas and oxygen must not be used. [20]

$$2\,HgS + 3\,O_2 \leftrightarrow 2\,HgO + 2\,SO_2 \leftrightarrow 2\,Hg_{el} + O_2 + 2\,SO_2 \qquad (4.1)$$

[20]

Based on the above, following test conditions for all measurements were chosen:

- Temperature ramp of 1°C min^{-1}, boundaries 30-650 °C
- Sample weight of 0.5 mg (Hg)
- Volume stream of 7 l min^{-1}
- Carrier gas: Nitrogen

It is possible to meet the boundary conditions with those parameters to generate a sustainable baseline. Those conditions are further described as standard conditions. Because of the variation of possible mercury species and the duration of one experiment it was easier to measure both oxidation states at the same time. It also made the results between Hg(t) and Hg(0) more comparable.

Only measurements that stayed in the confidence interval were used for further interpretation.

4.2.2 Evaporation profile for inorganic pure mercury species

Part of this section is published in [18].

Mercury halides

Figure 29 shows the comparison of three different Hg(II)-halides: Iodide, bromide and chloride. It can be shown that all halides evaporate within a similar temperature range starting with 50 °C and ending at 150 °C. None of them shows a distinct peak for Hg(0). The results match with data in literature (e.g. 2.3.1[57],[58])

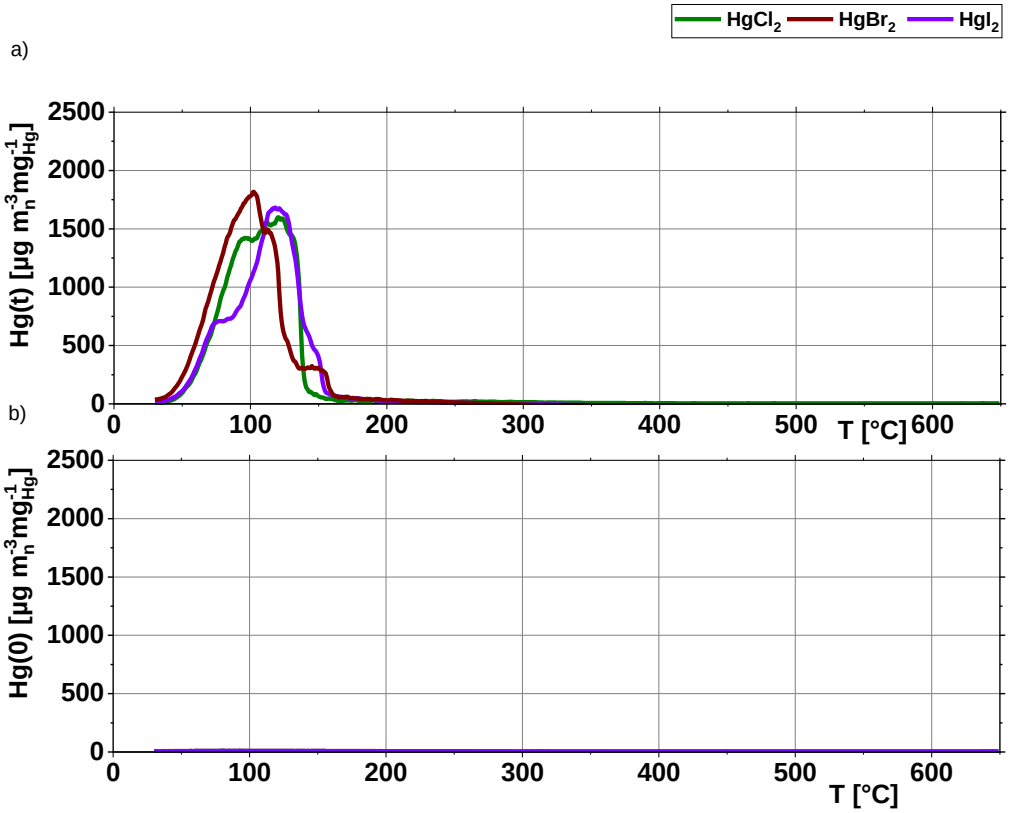

Figure 29 Average measurement Hg(II)-halides, (a): Hg(t); (b): Hg(0), standard conditions.

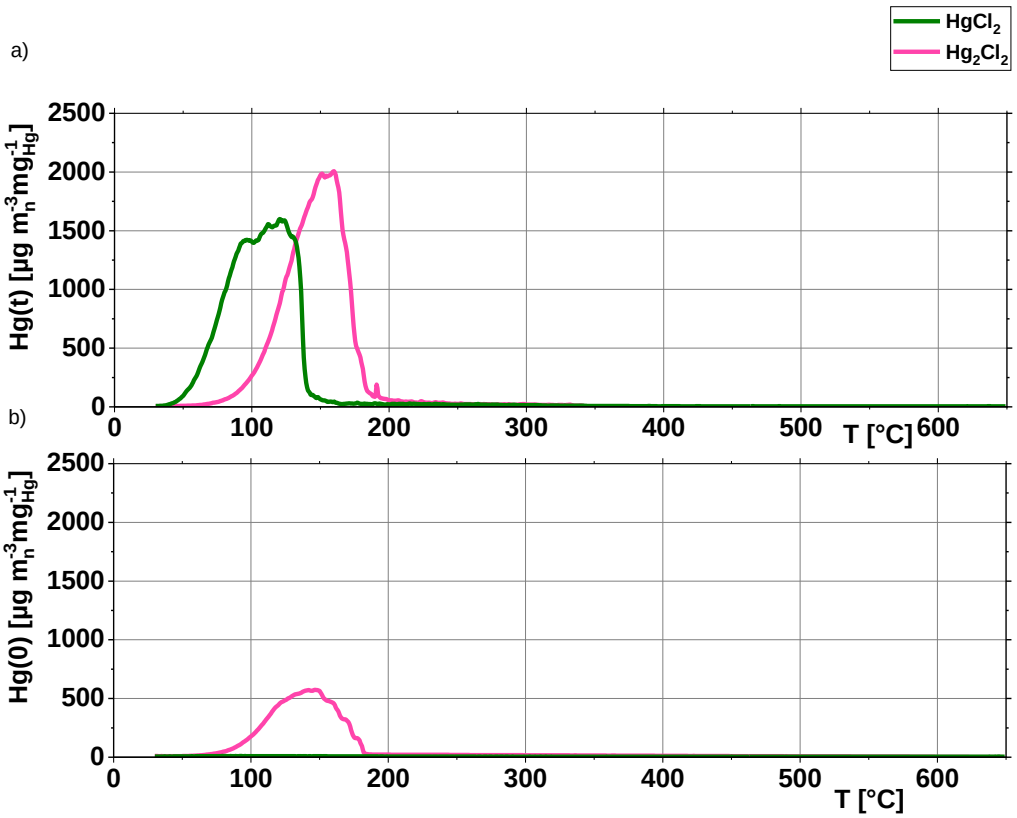

Figure 30 Average measurement Hg_2Cl_2 and $HgCl_2$, (a): Hg(t); (b): Hg(0), standard conditions.

The evaporation profile for Calomel Hg_2Cl_2 (Figure 30) shows an increase of the evaporation temperature in comparison to $HgCl_2$. Hg_2Cl_2 shows a ratio up to 50 % of elemental mercury (Figure 30b). This is around half of the measured Hg(t) concentration.

For the evaporation behavior of mercury-halides following conclusions can be drawn:

- It is not possible to differentiate the different mercury(II)halides with this method.
- It is possible to differentiate between Hg_2Cl_2 and mercury(II)halides.
- All pure mercury(II)-halides sublimate as mercury(II)-emission.
- Hg_2Cl_2 disproportionates into Hg(0) and Hg(II).
- Sublimation energy is smaller than the energy needed to disproportionate Hg(II)halides in their elements. Because of the sublimation of the halides, the characteristic temperature to break the Hg-halide bond is not known but has to be >200°C. This evaporation temperature can only stand for the possibility for Hg-halides to sublimate.

Mercury sulfite

Figure 31 shows the desorption profile of Hg(II)-species with a sulfur compound. The black single peak shows HgS, the red double peak shows $HgSO_4$.

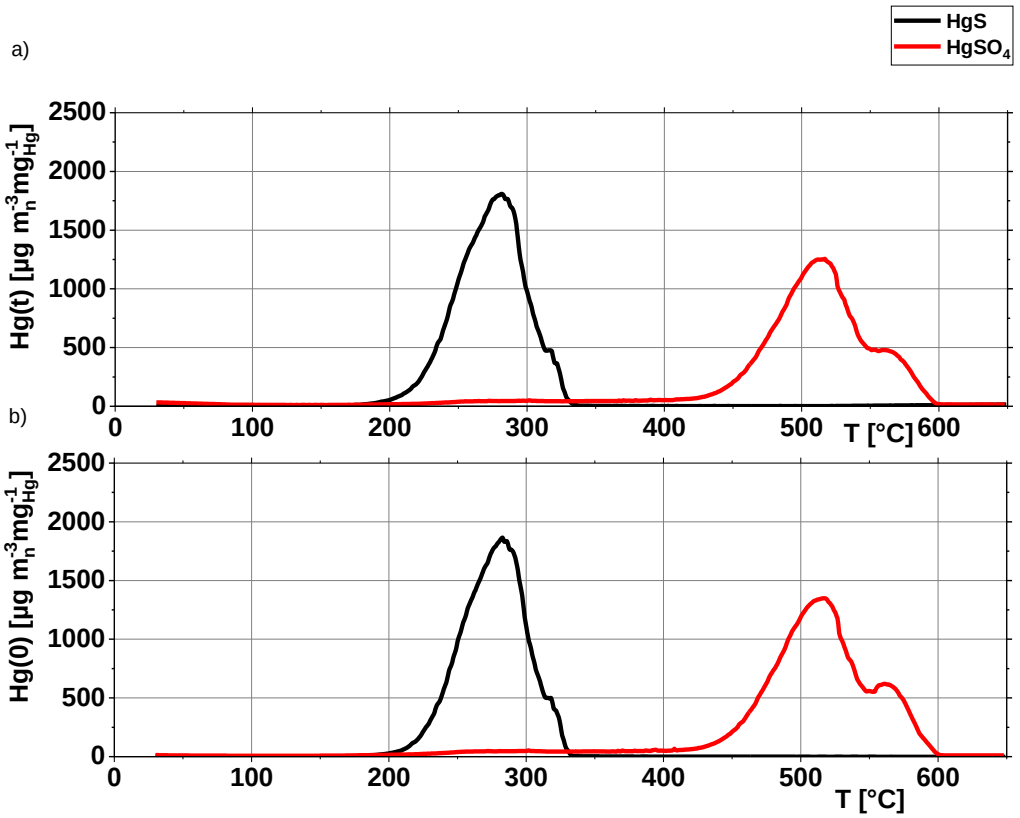

Figure 31 Average measurement of $HgSO_4$ and HgS, (a): Hg(t); (b): Hg(0), standard conditions.

The characteristic desorption profile of HgS can be separated from mercury-halides, $HgSO_4$ and HgO. The peak has similarity to the Hg-halides-peaks at a delta T of 100°C, but is located between 200°C and 300°C. No sulfide peak can be measured after 350°C. In contrast to the desorption profiles of mercury(II)-halides both show a Hg(t) peak which is similar to the Hg(0) peak. This means that all of the measured emissions are elemental mercury.

$HgSO_4$ starts evaporating at temperatures >350°C. It evaporates in a double peak. The two maxima of $HgSO_4$ show the Hg(0) phenomena. The evaporation temperature or behavior shows similarities to the evaporation of -Hg-O- species. This is coherent with the LEWIS structure of SO_4^{2-} that shows no free valence electron pair on the sulfur.

The values found in literature for desorption of HgS (e.g. Table 14) differ from the values measured due to a different temperature program and as a consequence of a slower heating rate and a longer dwell time used in this study. $HgSO_4$ can be

compared with literature values showing a substance property and no characteristic property for the temperature program.

To summarize the evaporation behavior of Hg-S-O_n following points were detected:

- All Hg-emissions measured were Hg(0).
- The molecules decompose into its components before evaporating.
- HgS starts decomposing at 200 °C.
- $HgSO_4$ decomposes via HgO starting at 400 °C.
- $HgSO_4$ behaves like an oxide not like a sulfide, which can be explained with the crystal structure described in literature.

Mercury oxides:

Figure 32 shows all mercury species measured with an oxide compound.

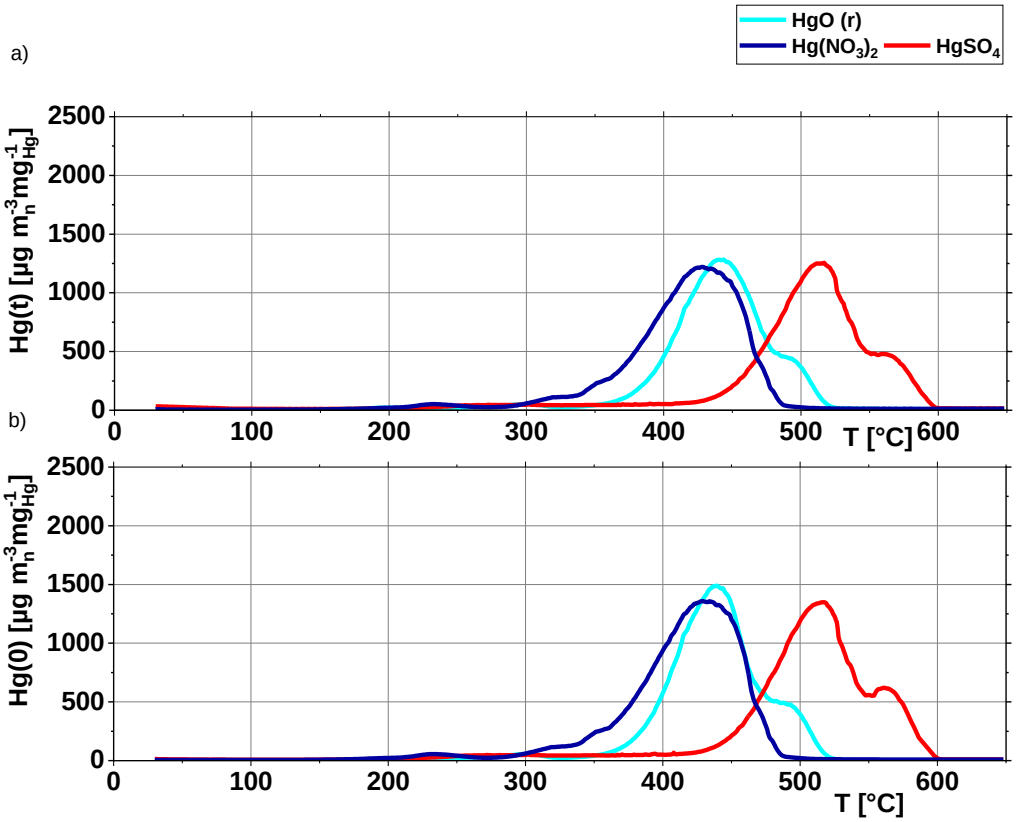

Figure 32 Average measurement Hg-Om-Xn, (a): Hg(t); (b): Hg(0), standard conditions.

Mercury nitrate evaporates at the lowest temperatures starting at 300 °C, followed by HgO at 350 °C and then $HgSO_4$ at 420 °C. The emissions stop in the same order as they started at 490 °C for $Hg(NO_3)_2$; 530 °C for HgO and 620 °C for $HgSO_4$.

Different to Hg-halides and HgS, Hg(II)-oxides start to evaporate at temperatures higher than 300 °C and stretch over 200 °C with the mercury emissions mitigated. All peaks show the before described (eg.3.3.4) Hg(0) phenomena described above.
$HgSO_4$ shows the most characteristic peak structure with a peak maximum of 520 °C and 570 °C and emissions at temperatures >600°C. In literature (eg. Table 9) $HgSO_4$ decomposes into HgO and SO_2. Also HgO is the most common impurity of $HgSO_4$. [64],[59]
If the process is stopped at 500 °C, $HgSO_4$ forms a yellow residue.
It is not yet clarified which atom forms the bond with the mercury. One explanation could be that $[Hg(XO_n)_m]$ has a mercury-oxide-chain that can vary by a $-SO_3$; $-NO_2$ group. The $-NO_2$ group has a destabilizing effect and the $-SO_3$ a stabilizing effect on the complex derived from the evaporation temperatures. This would conclude that mercury with an oxygen atom decomposes to mercury(II)oxide first, before decomposing into further components.
Concerning the evaporation behavior of $Hg\text{-}O_m\text{-}X_n$ following points were detected:

- Evaporation starts at >300 °C
- The peaks are more stretched and dampened than for the other species.
- All emissions show the Hg(0) phenomena discussed in the error analysis.
- The molecule decomposes via HgO into its components before evaporating.

Template for investigation

Figure 33 summarizes the results of the main suspected mercury species in a FGD-gypsum into one template for the investigation of an unknown mercury species. For the investigation of oxidation states of Hg-halides different templates for Hg(0) and Hg(t) need to be considered.

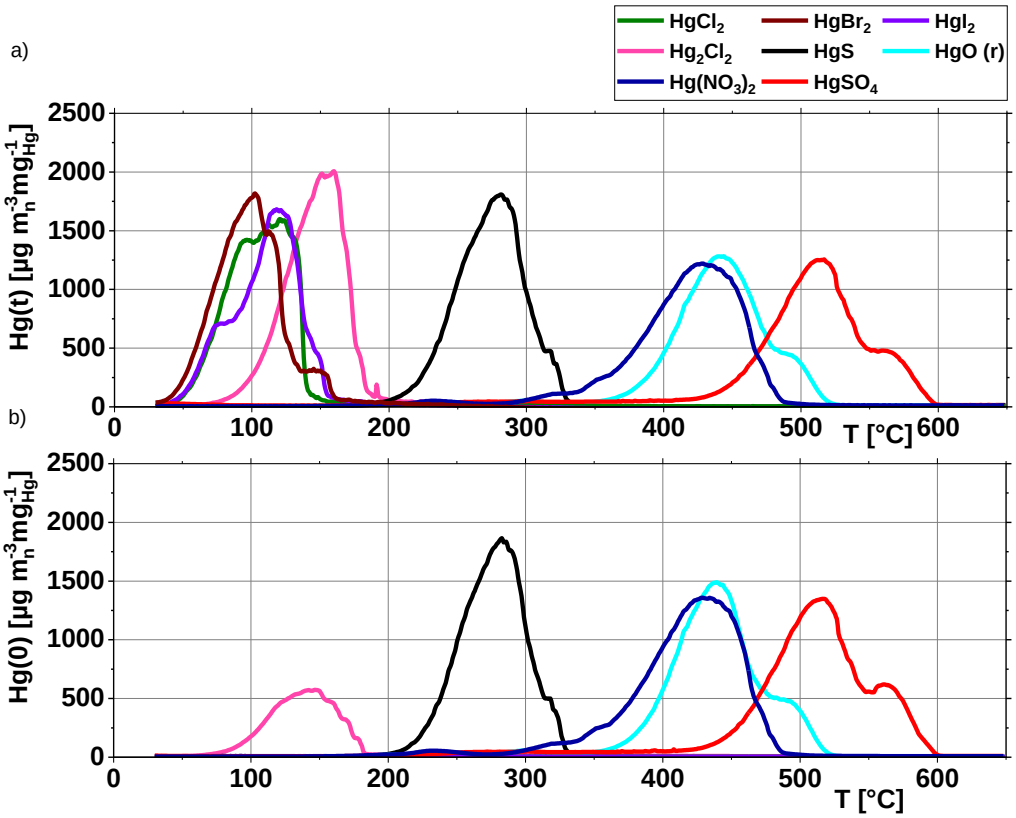

Figure 33 Templates for the investigation of mercury species

4.2.3 Discussion of the procedure to assay mercury in a solid sample

Part of this section is published in [18].

The results show that it is possible to create a standard template of characteristic evaporation behaviors of different inorganic mercury species. It also shows that it was possible to identify a mercury species like HgS in an unknown sample. The following section will discuss the discovered results.

Mercury halides do not evaporate as elemental mercury. They all seem to evaporate within a delta T of 100°C and are gone after 150°C. The results match with the data found in literature. Iodine seems to fall out of the consistent line of evaporation temperatures in literature. The evaporation order of HgI_2, $HgBr_2$ and then $HgCl_2$ is reported.

The elemental mercury concentration increases from HgI_2 with no Hg(0) emissions, to $HgBr_2$ with a Hg(0) recovery rate of 1-2% to $HgCl_2$ recovery rate of 2-5%. Mercury(I)chloride shows a recovery rate of 24-40%. This is around one third of the measured Hg(t) concentration.

It is not possible to differentiate the different mercury(II)halides with this method, but it is possible to identify mercury(I)chloride in the system.

Mercury sulfide can be differentiated from mercury sulfate and mercury oxide. The evaporation peak also has a delta T of 100°C but it evaporates between 200°C and 300°C. No sulfide peak can be detected after 350°C. All emissions are identified as elemental mercury.

Mercury species that have an oxygen atom as a ligand show similar behavior in their evaporation characteristic. The most different characteristic to the other two species is the high evaporation temperature.

The main evaporation starts at temperatures > 300°C. The evaporation profile shows a double peak whereas the maximum emission is not as high as for the species without an oxide chain, but the evaporation happens in a wider temperature range.

This behavior can be explained by the theory that $[Hg(XO_n)_m]$ seems to always have a mercury oxide bond (-Hg-O-) that can vary by a $-SO_3$ or $-NO_2$ compound. Most of those species decompose to a mercury(II)oxide first before decomposing into the single components. This theory is consistent with the crystal structures found in literature where $HgSO_4$ is also described as $Hg\text{-}O\text{-}SO_3$ ([59]). $HgSO_4$ is in literature (e.g chapter 2.3.3) described with a rhombic crystal structure whereas the mercury is surrounded by oxygen. This characteristic can explain the high evaporation temperatures characteristic for an -Hg-O- bond found within the evaporation profiles of $HgSO_4$.

Even if the evaporation profiles of different $[Hg(XO_n)_m]$ show similarities, it is still possible to differentiate them. Mercury sulfate has the most characteristic peak that could be found in preliminary tests as well as in the main tests. The highest activity is measured between 500 and 650°C. It is the only species found that still is active at temperatures above 600 °C.

Experiments showed that it was not always possible to detect this characteristic of mercury sulfate. Some samples drift more into a HgO evaporation characteristic. The explanation is, that mercury sulfate can be polluted with HgO [44] but also can be decreasing into mercury oxides and sulfite while being stored.

HgO evaporates at a temperature between mercury sulfate and mercury sulfide. It has its characteristic evaporation points compliant with the characteristic temperatures found in literature.

All mercury species that do not have a halide as a compound and evaporate above 150°C are mainly evaporating as elemental mercury. All halides show an evaporation as oxidized species. From this fact it can be concluded that mercury halides sublimate when heated and have a vapor pressure as a solid. This is a unique characteristic which was only seen with halides. All other species decompose into their single components.

Following Table can be used to analyze an unknown Hg_s species:

Table 21 Main characteristics of different mercury species (solid).

Temperature [°C]	Hg(t)	Hg(0)	Hg(t):Hg(0) ratio	Likely mercury species
Until 160	Yes	No	1 : 0	Mercury(II) halides
Until160	Yes	Yes	1 : 0.4	Mercury(I) halides
200-300	Yes	Yes	1 : 1	Sulphide
300-500	Yes	Yes	1 : 1	Mercury oxide; Mercury(II) Nitrate
500-550	Yes	Yes	1 : 1	Mercury(II) oxide; Mercury(II) Sulphate
500-650	Yes	Yes	1 : 1	Mercury(II) sulphate

As main conclusions are drawn:

- Mercury(II) halides sublimate as oxidized species below 200°C.
- The temperature needed to split the bond between mercury(II) and the halide compound is not known and not detectable with this method.
- If there is a high elemental mercury concentration below 200°C it is most likely calomel.
- If there is an evaporation between 200 and 300 °C mercury sulfide is in the sample.
- If there is a mercury activity at a temperature higher than 550 °C mercury sulfate is present.

4.3 Investigation of Hg_S in a gypsum sample

After the development of the template for characteristic evaporation profiles for the suspected mercury species in gypsum, the created standardized gypsum samples were measured. Different from the pure solid mercury samples the sample size needed to be adjusted due to the low mercury content in the sample. To assure that all mercury was found the samples were also measured by DMA 80 and the results were compared with the mercury measured via the TDS methods developed in this work.

4.3.1 Evaporation profiles for gypsum samples

The sample size had to be increased because of the small amount of mercury in the gypsum samples. To ensure that all mercury was detected by the developed method, the mercury content was also measured via DMA 80 and compared. Only measurements that stayed inside the inaccuracy limits of the analyzers set in chapter 3.3.1were used for further interpretation. Only one measurement of every setting was used even if more than one stayed inside the limits.
Staying inside the limits means that the adjustment of the sample size did not have an influence on the recovery rate of the developed TDS method and that all containing mercury was found with the developed method. Concluding that the measured results can be used.

All gypsum samples measured showed two identical peaks. Depending on the mercury content it was possible to subdivide the results into three groups.

- Group 1 contains samples with a $Hg(t)_{max}$ concentration < 20 µg m_n^{-3}.
- Group 2 contains samples with a $Hg(t)_{max}$ concentration > 20 µg m_n^{-3} and < 70 µg m_n^{-3}.
- Group 3 contains the samples with a $Hg(t)_{max}$ concentration > 70 µg m_n^{-3}.

Table 22 gives an overview of the used gypsum samples divided in the different groups.

Table 22 Overview Gypsum sample divided in different groups.

Date	Sample	Hg-content mg kg^{-1} DMA 80	Hg-content mg kg^{-1} TDS	Group	Comment
09-Jul-2020	1-1	5.3	5.1	1	
17-Sep-2020	1-2	4.1	2.2	1	
28-Jul-2020	2-1	1.3	1.4	1	
08-Oct-2020	2-2	1.5	0.9	1	
15-Oct-2020	2-3	1.6	1.9	1	
29-Jul-2020	2-4	2.4	2	1	
07-Oct-2020	3-1	2.1	1.3	1	
22-Sep-2020	3-2	3.2	2.1	1	
05-Oct-2020	3-3	5.2	4.3	2	
07-Jul-2020	3-4	11	10.6	2	
13-Aug-2020	4-1	1.0	2.1	1	Very high errors.
20-Aug-2020	4-2	1.4	1	1	
24-Aug-2020	4-3	1.5	0.9	1	
19-Aug-2020	4-4	1.6	2.0	1	
12-Aug-2020	5-1	3.1	2.8	1	

Date	Sample	Hg-content mg kg^{-1} DMA 80	Hg-content mg kg^{-1} TDS	Group	Comment
16-Jul-2020	5-2	7	4.5	2	
17-Aug-2020	5-3	14	9.4	2	
18-Aug-2020	5-4	20	17.5	3	
08-Jul-2020	5-5	73	55.8		HgS Sample
03-08-2020	6-1	8	7.6	2	
24-Sep-2020	6-2	15	12.8	2	
05-Aug-2020	6-3	22	15	3	
11-Aug-2020	6-4	28	24.2	3	
28-Sep-2020	6-5	34	26.1	3	
01-Oct-2020	6-0	4.4	3.9	2	

Figure 34 shows the average of three different evaporation profiles of all measured gypsum samples.

All evaporation profiles show a similar maximum temperature, an elemental emission as well as mercury total emissions. Only the height of the mercury emissions, not the species, which is found, varies dependent on the composition of the scrubber solution.

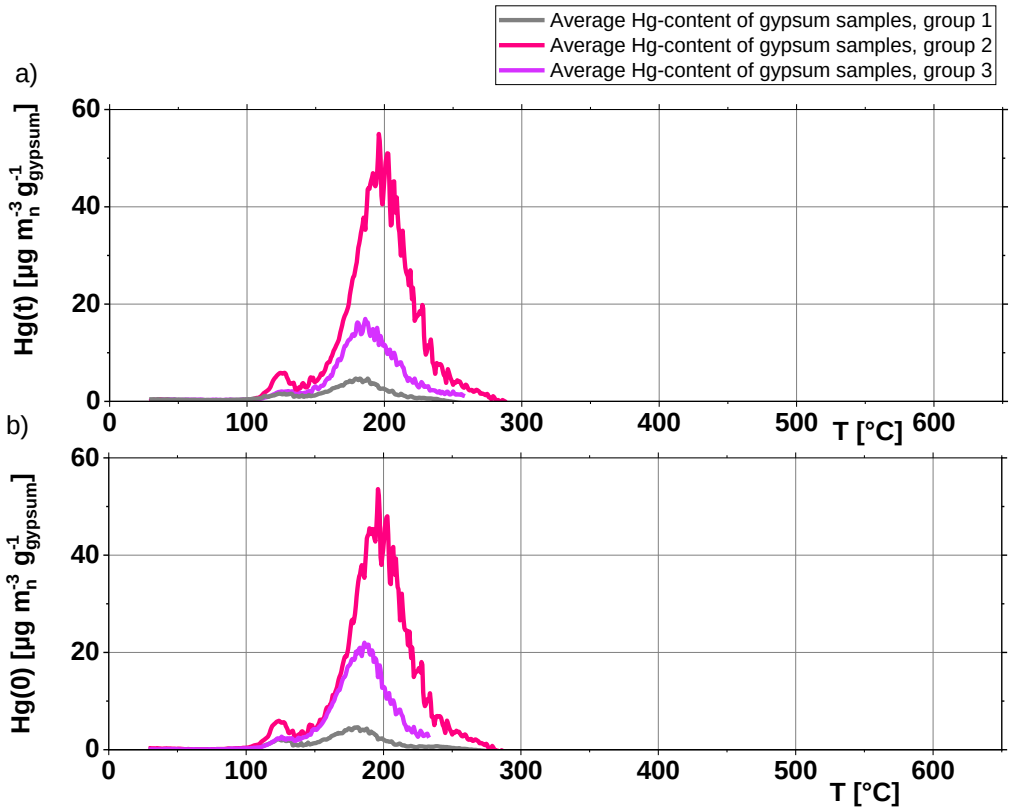

Figure 34 Overview average evaporation profiles of gypsum sample a) Hg(t)-emissions b) Hg(0)-emissions.

To investigate the mercury species found in the gypsum samples the evaporation profile of Hg(t) of the gypsum sample (Figure 35 b)) was compared to the developed Hg(t) template of possible mercury species suspected in gypsum (Figure 35 a)). The main evaporation of the unknown mercury species lies between the evaporation profiles of mercury-halides and mercury sulfite.

To exclude the possibility that the gypsum crystal influences the evaporation profile of the bound mercury, a sulfidic precipitant was added to the scrubber solution and a sample was taken after 30 minutes. The sample was measured as shown in Figure 36. The main peak shifted from 150°C - 200°C to 200°C - 300°C and matches the evaporation profile of the HgS standard.

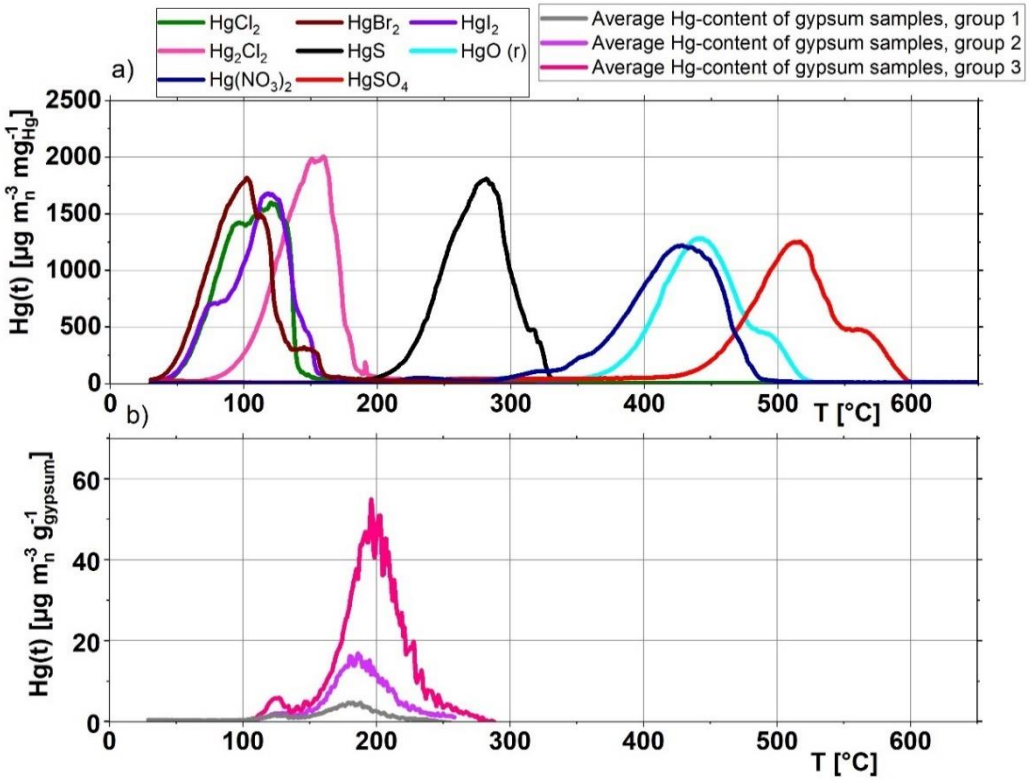

Figure 35 Comparison of a) evaporation profiles of mercury standards with b) evaporation profiles of gypsum samples.

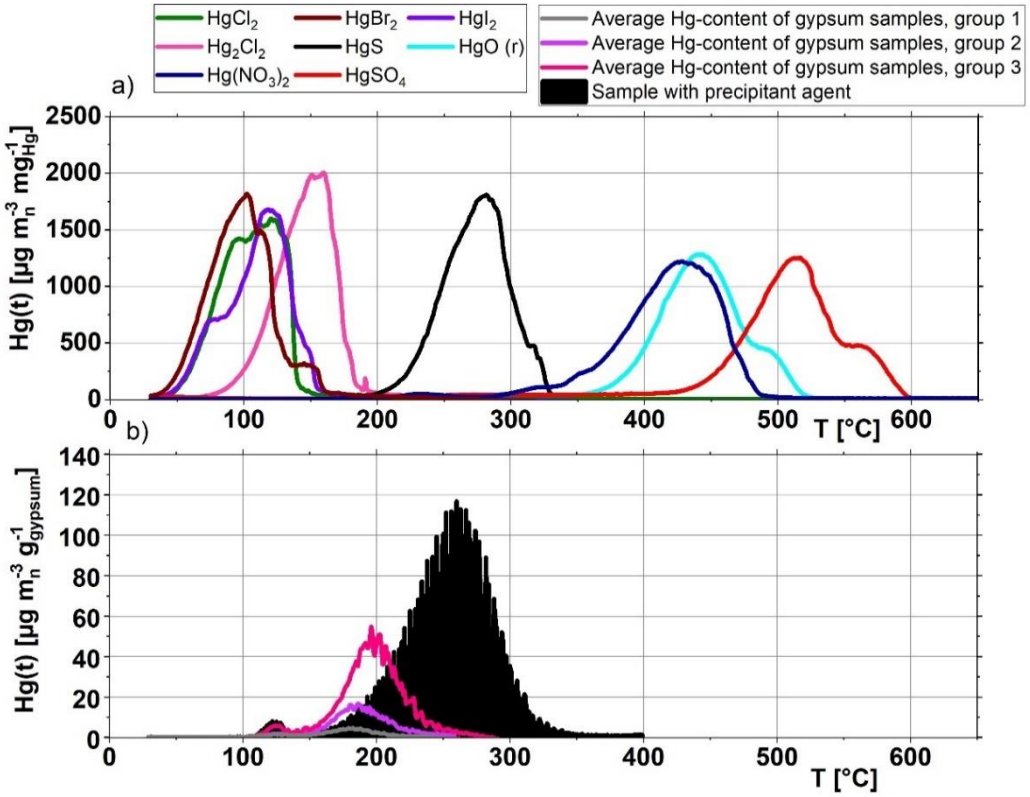

Figure 36 Comparison of a) evaporation profiles of mercury standards with b) evaporation profiles of gypsum samples with one sample measured with precipitant agent.

Following conclusions can be drawn from these results:

- Elemental mercury emissions equal mercury total emissions, so it is possible to exclude the adsorption or inoculation of Hg(II)-halides as main species in gypsum.
- None of the suspected mercury species show a match with the evaporation profile of the gypsum samples.
- It is possible to identify HgS created via sulfuric precipitant in a gypsum sample with the created template.
- The evaporation of Hg(0) of the gypsum also shows the Hg(0) phenomena. For further interpretation the Hg(t) evaporations are used because of the phenomena.

4.3.2 Extended evaporation profile for inorganic pure mercury species

Because none of the expected mercury species could be found in the gypsum samples, the not suspected inorganic mercury species, which can be purchased as solid were measured. Three additional species were purchased:

- HgO(yellow)
- Hg_2SO_4
- Hg_2NO_3

As discussed in chapter 2.3.2, HgO(red) is known to form in a temperature induced process. HgO(y) is the product of precipitation. If Hg_{aq} precipitates in the system HgO(y) and not HgO(r) should occur. All HgO-species transfers into HgO(r) at temperatures > 200°C. [59], [61]
None of the Hg(I)-species with an oxide was yet considered.

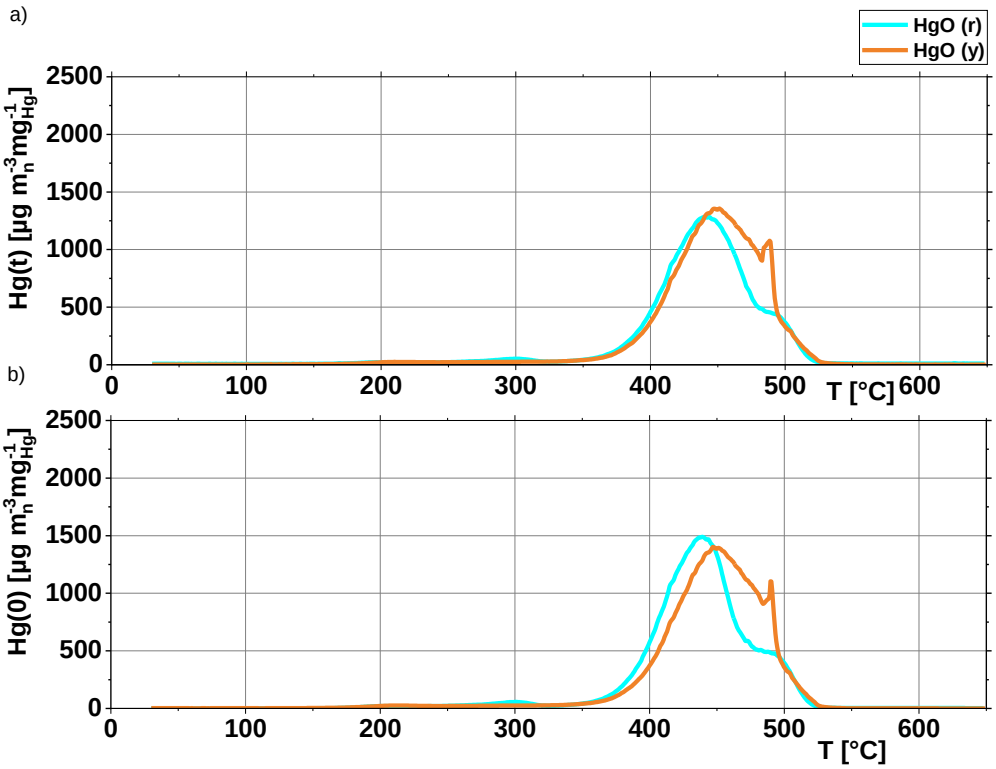

Figure 37 Average measurement HgO (r) and HgO (y), (a): Hg(t); (b): Hg(0), standard conditions.

Figure 37 shows the average evaporation profile of HgO(y) in comparison to HgO(r). No noticeable difference between both species can be detected. But if the figure is zoomed in, both profiles show a small first evaporation at the temperature range of the gypsum samples but the main evaporation starts at 400°C (see Figure 38).

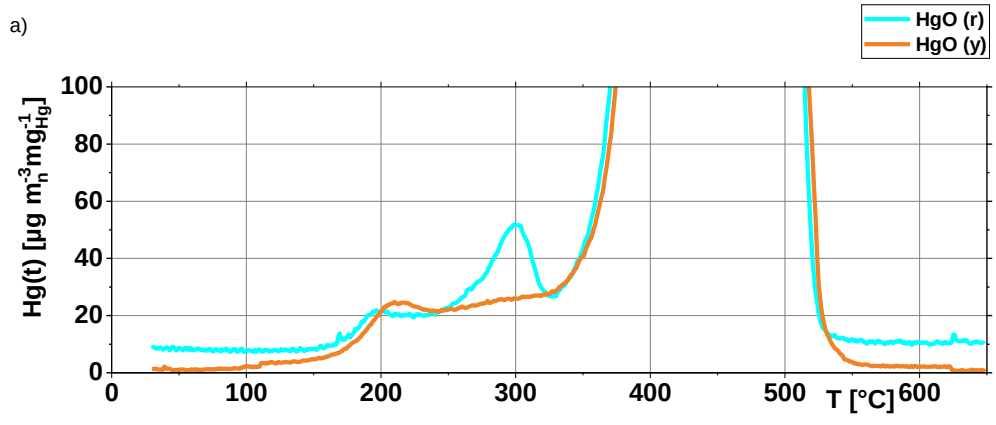

Figure 38 Zoomed in evaporation profile of HgO.

The first signal can be a structural impurity of the crystal. It also fits the temperature range were HgO(y) transfers into HgO(r). HgO(r) has a bigger particle size than HgO(y). It is possible that this transformation is not happening or is not possible in a gypsum sample and leads to a decomposition of the molecule.

Figure 39 shows the Hg_2SO_4 evaporation profile. Hg_2SO_4 decomposes in equal amounts into a HgS and HgO. It means that Hg_2SO_4 has a bond to a sulfur compound different to $HgSO_4$ which is only surrounded by oxygen. No evaporation at temperature ranges of the gypsum samples can be detected.

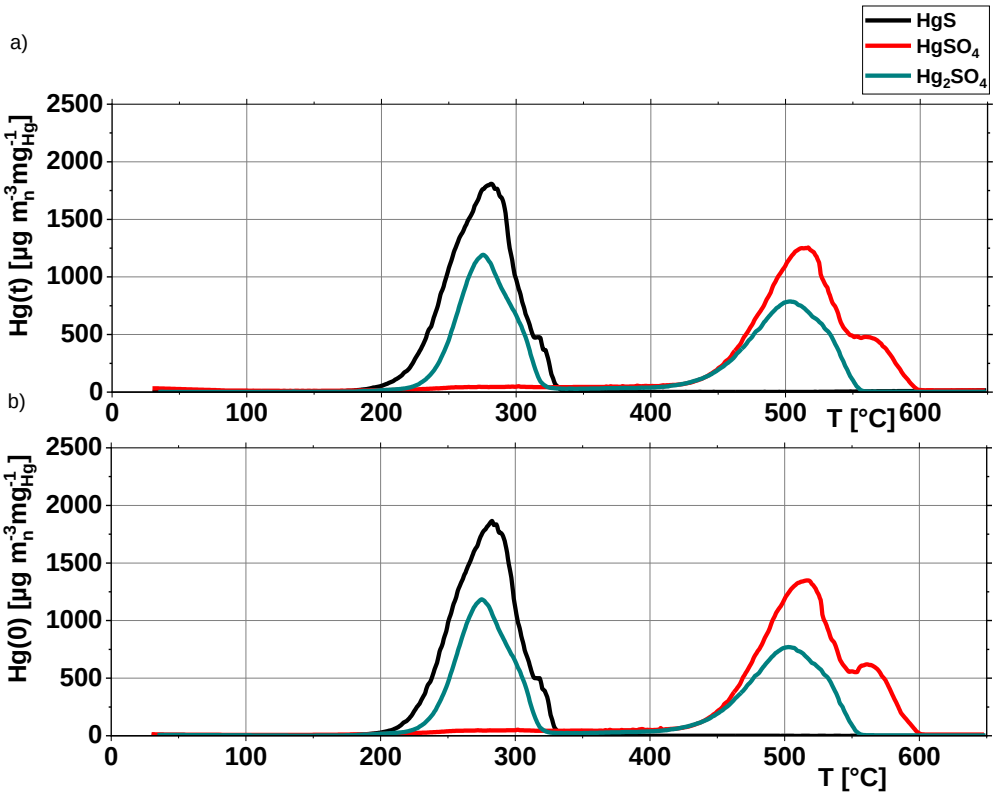

Figure 39 Average measurement of Hg_2SO_4 in comparison to $HgSO_4$ and HgS, (a): Hg(t); (b): Hg(0), standard conditions.

The next possible species is $Hg_2(NO_3)_2$.

Figure 40 shows the evaporation profile of $Hg_2(NO_3)_2$ in comparison to the species with the oxidation state +II. Both evaporation profiles do not strongly differ from one another. There is a small evaporation that starts at the same temperature range as the gypsum samples, but like with the HgO species, the main evaporation starts at 400°C. No other inorganic mercury species was obtainable as pure species.

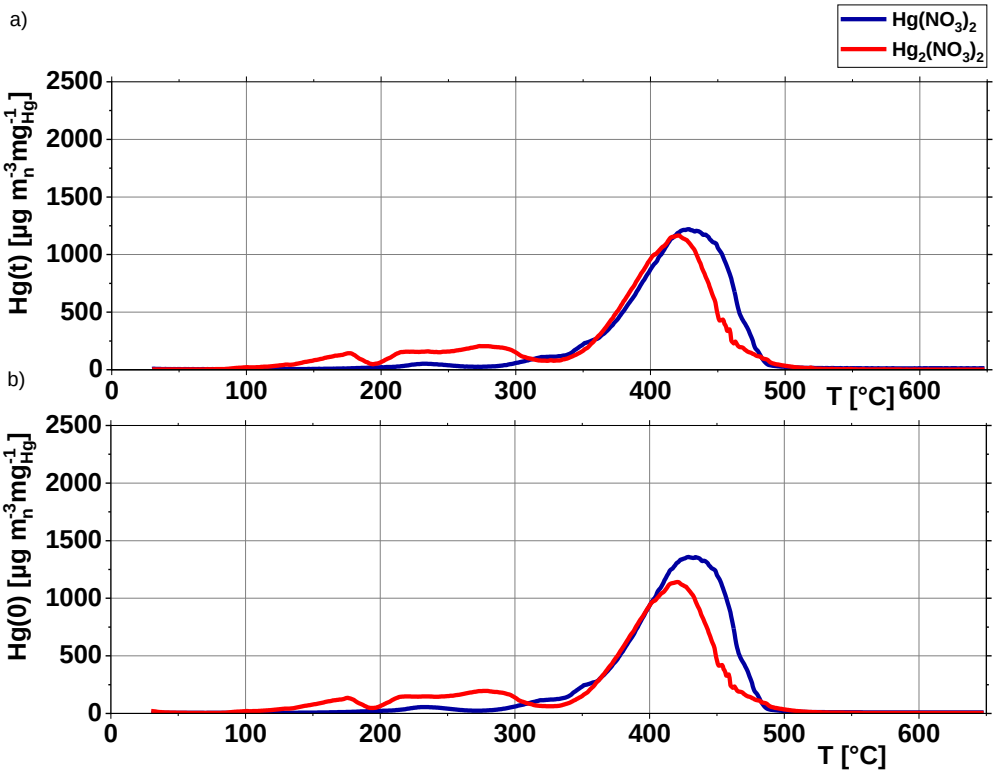

Figure 40 Average measurement of $Hg_2(NO_3)_2$ in comparison to $Hg(NO_3)_2$, (a): Hg(t); (b): Hg(0), standard conditions.

The most plausible theory is that mercury is precipitated in gypsum via OH^- in order of a simple heavy metal precipitation. That could explain the similarities to HgO. For a closer investigation of this theory precipitation experiments were conducted. Aim of the experiments is to define which mercury species is precipitated in the process and therefore influences the equilibrium of Hg_{aq} and Hg_s.

4.3.3 Precipitation experiments

The precipitation experiments all have indicative character. As mentioned in the experimental procedure, it was not possible to freeze dry the precipitated samples because of the possibility that elemental mercury is present. The differently dry states led to different evaporation profiles of one sample. All samples were measured twice, but because of the differently dry states the sample with the sharpest peaks was selected for further comparison and no average was calculated.

Nevertheless, as shown in Figure 41, it was possible to compare the two measurements of one sample, but they weren't similar enough for an average.

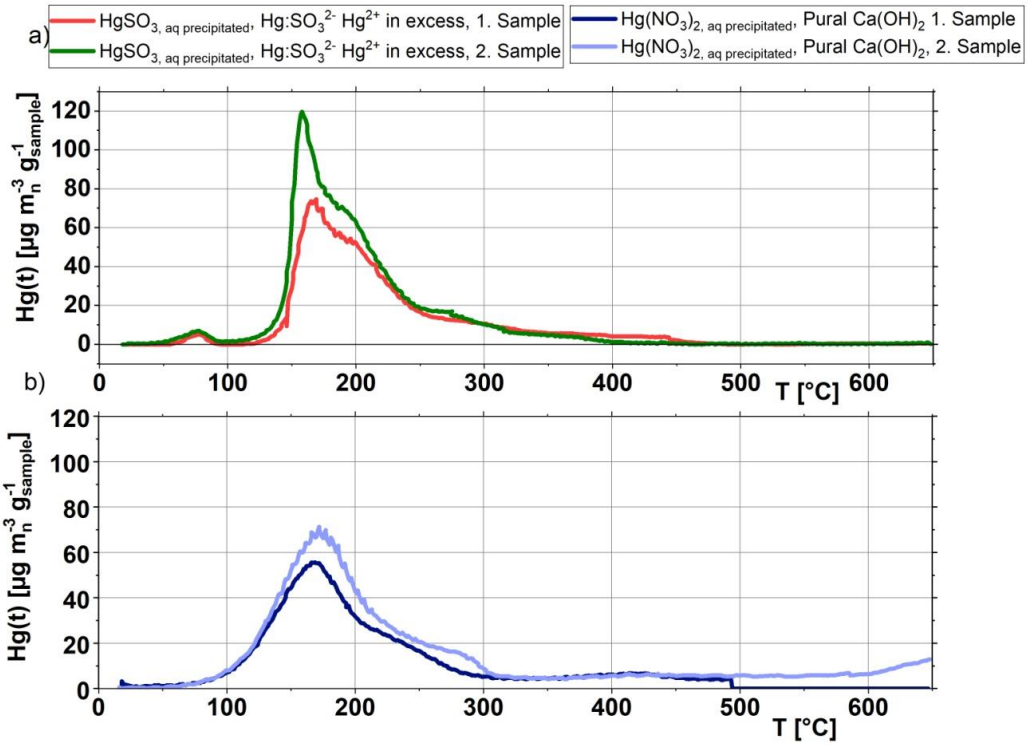

Figure 41 Comparison of two precipitated Hg-species measured twice.

Some of the evaporation profiles showed signals of the species before the precipitation. This was interpreted as a not fully successful precipitation. Even if in all gypsum samples halides could be excluded, Hg-halides were measured to see the reactions of all species and to better understand the process.

The following chapter is divided in sections about the different species:

- Hg-S/ Hg-O-species
- Hg-halides
- Hg^{2+}/Hg^{+}
- $HgSO_3$

Initial Hg-S / Hg-O-species

Figure 42 Precipitated $HgSO_4$ and Hg_2SO_4 species (left).
Figure 43 Precipitation of HgS (right).

HgS and all Hg-O-species in this section were added as solid for the reaction.
HgS did not show any reaction caused by the change of the pH value. All other samples changed their color with the change of the pH value. The $HgSO_4$ samples changed into a yellow residue, which is an indication of the formation of a basic mercury sulfate salt like $HgSO_4$* HgO. Hg_2SO_4 reacted as described in literature into a black residue prospectively due to the formation of elemental mercury and HgO (eg. Eq. 2.50).
The precipitated mercury species with a Hg-S bond showed five different evaporation peaks (see Figure 44):

- 200-300 °C, the typical evaporation area for Hg-S.
- 400-500 °C, the typical evaporation area for Hg-O.
- 500-600 °C, the typical evaporation area for $HgSO_4$.
- < 50 °C, the typical evaporation area for Hg(0).

None of the precipitated species show any evaporation characteristics that is similar to the ones from the gypsum samples.
It was not possible to precipitate HgS. $HgSO_4$ was used as Hg-S-O species because it is the only species possible to precipitate but also obtainable as standard.

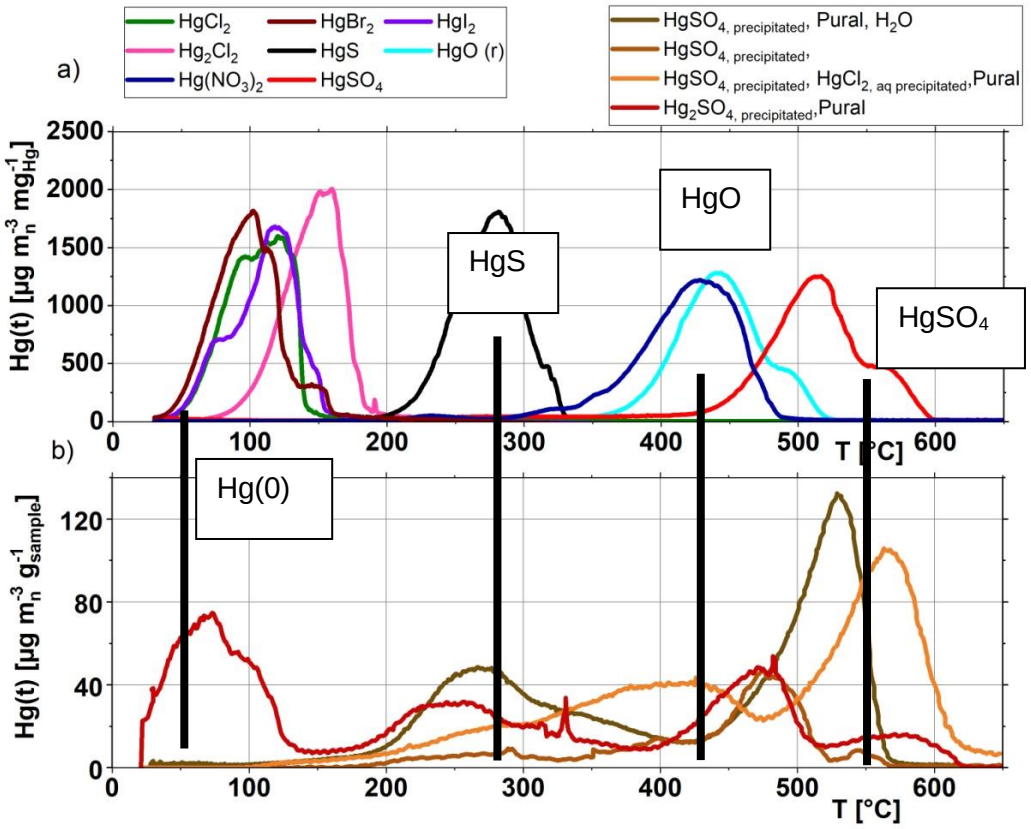

Figure 44 Evaporation profiles of different precipitated $HgSO_4$ and Hg_2SO_4 samples (b) in comparison to the Hg standard template (a).

Initial Hg-Halides-Species

All Hg-Halides were added as solid for the reaction.

$HgCl_2$ and $HgBr_2$ precipitated into a warm yellow residue. With $HgBr_2$ brown freckles could be seen on the surface of the sample. Some of it was seen on the top of $HgCl_2$ but not as much as with bromide as ligand. After air drying the bright yellow color vanished and a grayish nuance occurred.

Figure 45 Freshly precipitated $HgCl_2$ (left).
Figure 46 Freshly precipitated $HgBr_2$ (middle).
Figure 47 Both samples after air drying (right).

During the precipitation of HgI_2, the color changed from bright red, over yellow to grayish yellow that could also be observed at the other halides samples. The sample

with Pural NF showed a grey color from the beginning. The precipitation of Hg_2Cl_2 was characteristic for the precipitation of Hg(I)-solids. A color change to black occurred, which is an indication of the formation of elemental mercury and HgO. The comparison of Hg(0) and Hg(t) emission profiles is different than with the Hg(II)-halides standards (Figure 48).

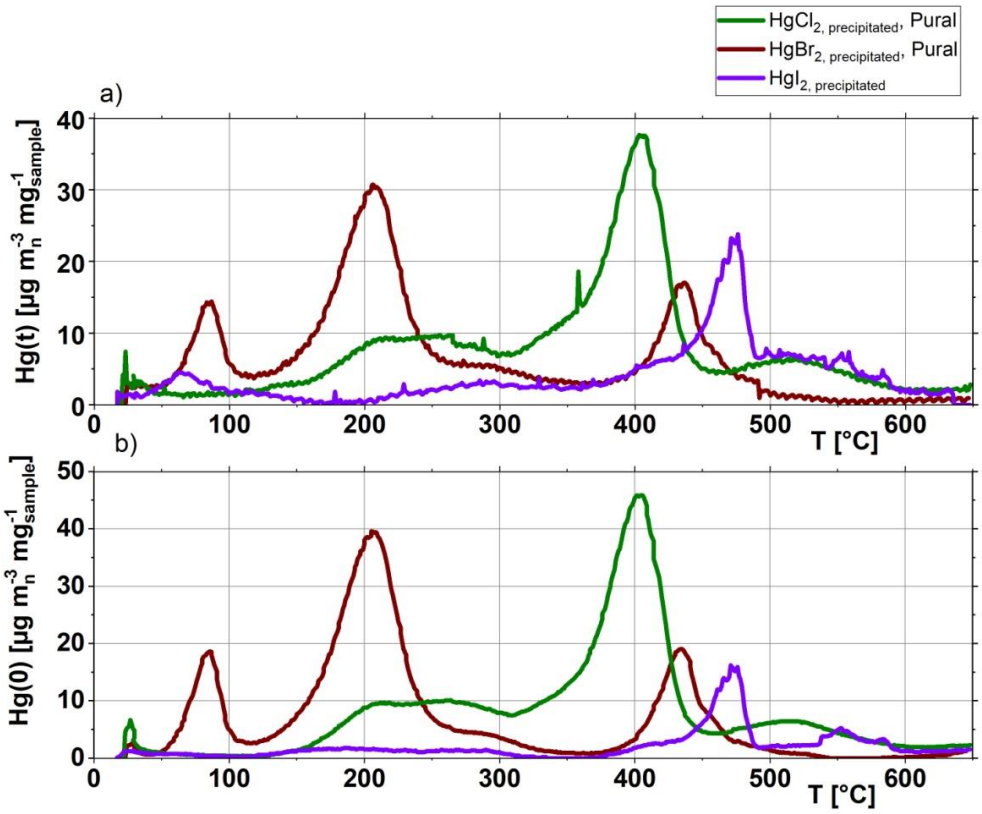

Figure 48 Hg(II)-halides precipitated, (a): Hg(t); (b): Hg(0), standard conditions.

For $HgBr_2$ and $HgCl_2$ the Hg(0) phenomena was detected. In comparison to the other halides, HgI_2 shows Hg(II)-emissions. There is a small peak characteristic for Hg(II)-halides at low temperatures (50-100°C) that is only seen in Figure 48 a) and not b) for HgI_2. It seems that HgI_2 is not fully precipitated.

$HgBr_2$ also has a peak in this low temperature range but different to HgI_2, the evaporation occurs to be elemental mercury. In comparison with the developed template for the identification of mercury species, it can be seen that the starting temperatures are equal to the starting evaporation of Hg(II)-halides (Figure 49) of the discussed peaks around 50°C.

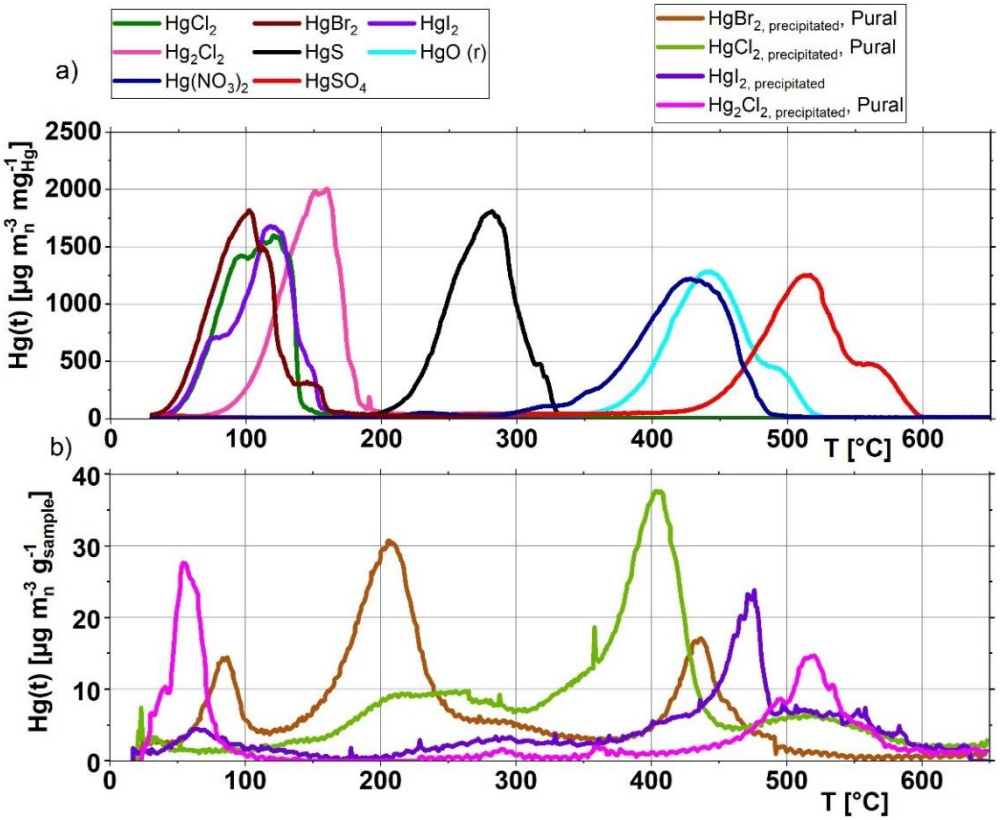

Figure 49 Evaporation profiles precipitated Hg-halides (b), in comparison to mercury standard template (a).

As suspected by the black color, two single peaks are detected during the evaporation of calomel. The first one is <50°C and is an indication of elemental mercury captured in the solid. The second one is around 500°C and shows the formation of a -HgO-X- species.

HgI_2 and $HgCl_2$ show their main evaporation at the temperature ranges of HgO. $HgBr_2$ shows an evaporation in the temperature range of HgO as well as the other two, but the main evaporation is at a lower temperature. $HgCl_2$, HgI_2 and Hg_2Cl_2 show an evaporation in the ranges of $HgSO_4$. It seems that caused by an impurity like crystal water or an OH- ligand the evaporation temperature of HgO is influenced similar to $HgSO_4$.

$HgBr_2$ as well as $HgCl_2$ show a raise of emission at the evaporation temperatures of the gypsum samples. Different to the chloride complex the bromide complex shows a characteristic peak and not only a raise in the baseline of emissions. Figure 50 shows the evaporation profiles of the gypsum samples in comparison to the precipitated Hg-halides. As suspected, $HgBr_2$ lies in the evaporation range of the gypsum samples.

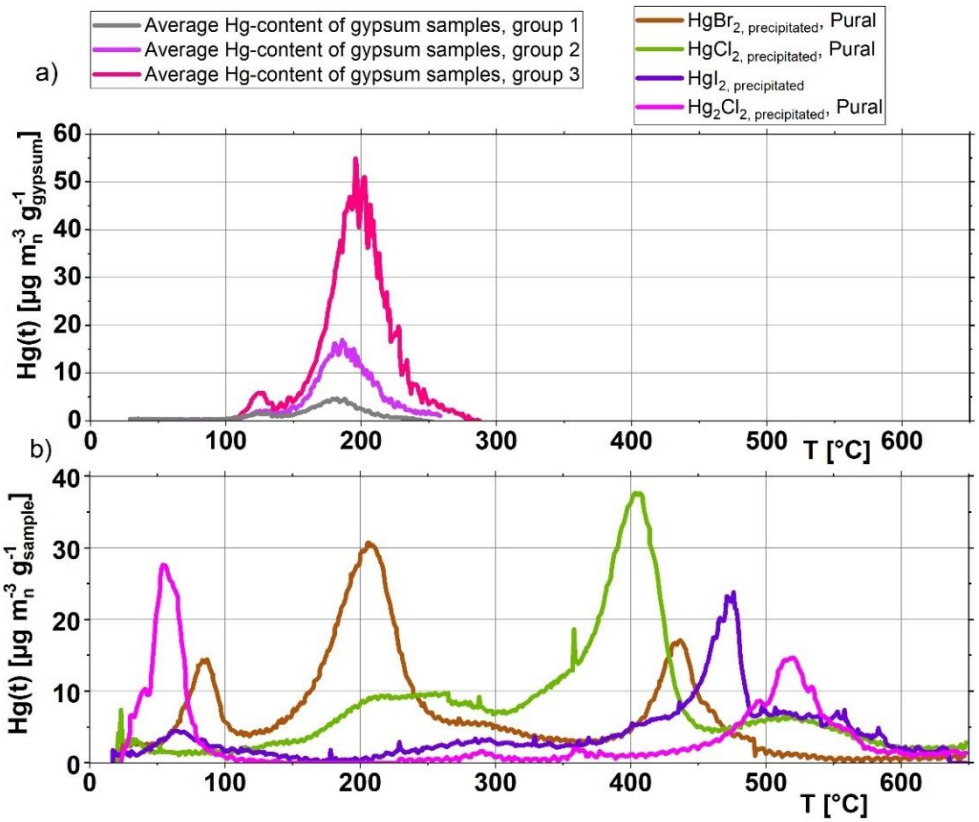

Figure 50 Precipitated Hg-halides (b) in comparison with the evaporation profiles of the gypsum samples (a).

To conclude:

- It is not possible to precipitate HgI_2 completely, even in pH ranges of 14. This means it will not be possible to precipitate HgI_2 in pH ranges of an FGD.
- HgI_2 can be excluded as species found in the gypsum sample.
- Calomel as every precipitated Hg(I)-solid reacted according to theory to Hg(0) and HgO and can also be excluded as possible species.
- $HgBr_{2,precipitated}$ shows a peak at the same temperature range than the species found in the gypsum samples. It still has a peak at a temperature range characteristic for HgO, that cannot be found in the gypsum.
- The evaporation profile of $HgCl_{2precipitated}$ does not have a clear fit with the evaporation profile of the gypsum samples and will be excluded.

Initial $Hg^{2+/+}$ or Hg-N-O-H_2O- Species

Solids

First experiments were conducted with $Hg(NO_3)_2$ solved in diluted HNO_3 shortly before the precipitation. The samples changed their color with the addition of NaOH into yellow. Over time, the color changed into a yellow-gray.

Three main evaporation areas can be singled out of the three precipitated Hg-nitrates. In comparison to the mercury standard template (Figure 51) following conclusion is drawn:

- Between 150°C and 220°C, evaporation range of the gypsum samples
- 400-500°C, evaporation range of Hg-O
- <50°C for $Hg_2(NO_3)_2$, evaporation range of Hg(0).

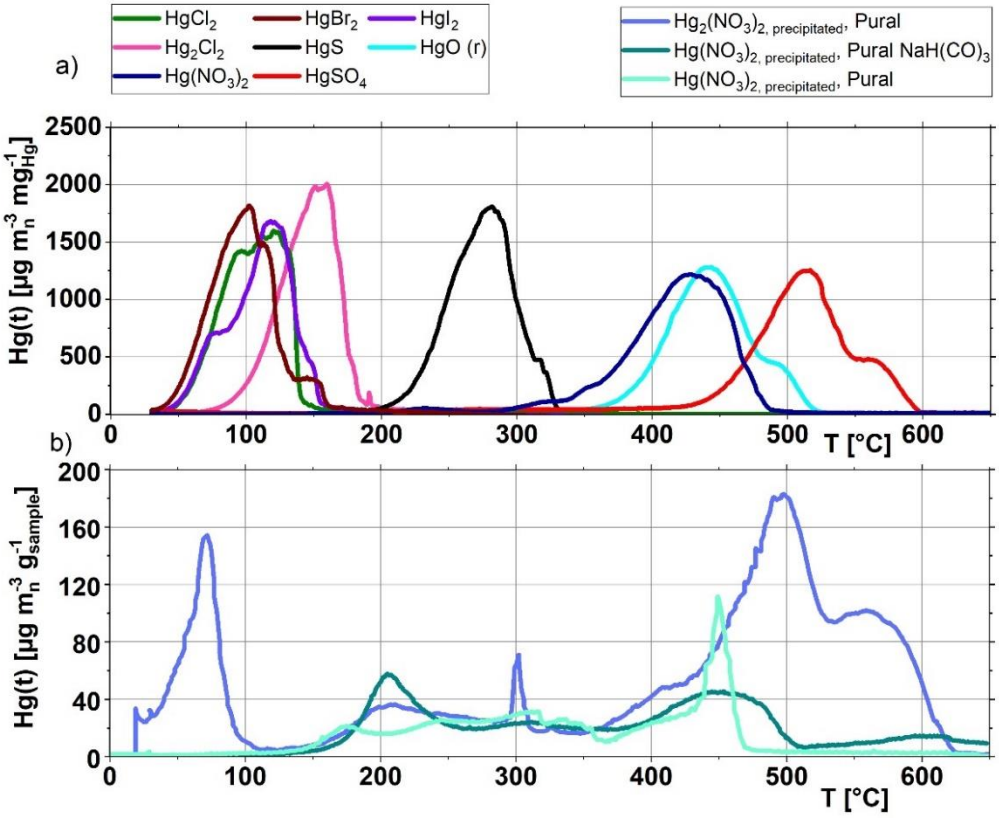

Figure 51 Evaporation profiles of precipitated $Hg_2(NO_3)_2$ and $Hg(NO_3)_2$ (b) in comparison with the mercury standards template (a)

The precipitated Hg(I)-species shows, as expected, a similar evaporation profile than calomel.

In comparison with the gypsum samples it can be seen that the suspected evaporation peaks of $Hg(NO_3)_{2,\ precipitated}$ show a high similarity with the evaporation of the searched species (Figure 52).

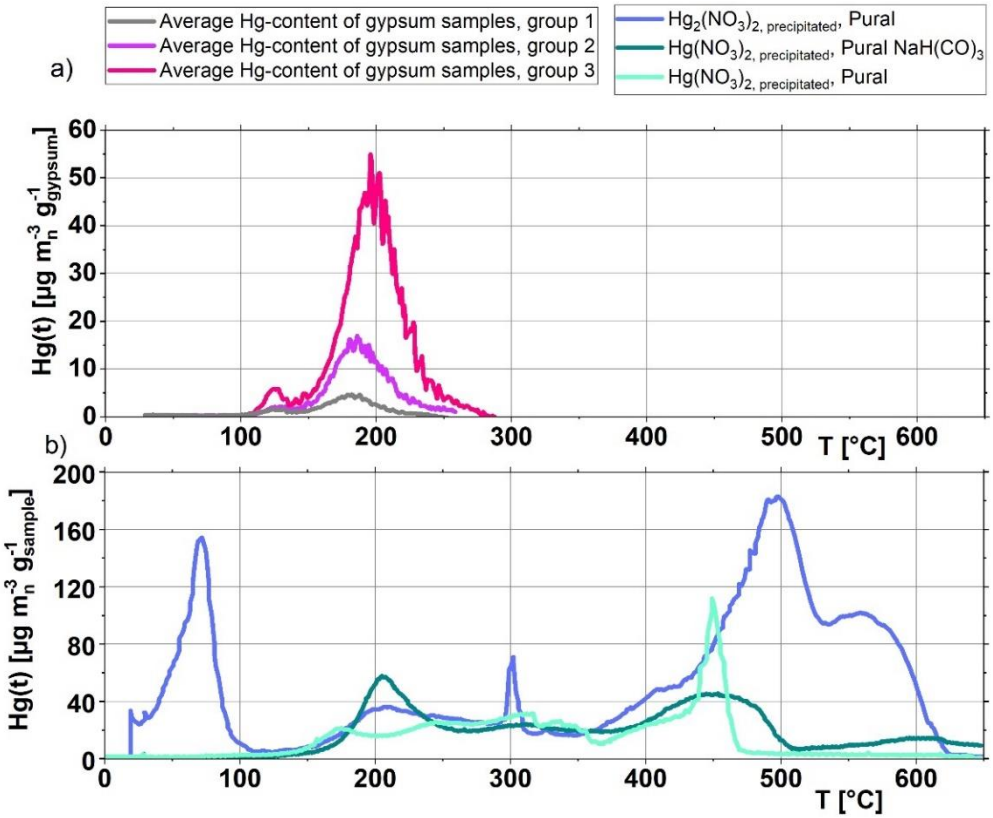

Figure 52 Comparison of $Hg_2(NO_3)_2$, precipitated and $Hg(NO_3)_2$, precipitated (b) with evaporation profile of the gypsum samples (a).

Because $HgBr_2$ as well as the mercury nitrate precipitation products both show not only the searched peak, but also a main evaporation at higher temperatures which is not seen in the curve of the FGD gypsum, an approach with a lower concentration and longer solved species was developed. Only mercury-nitrate species were diluted because of handling and concentration issues.

Solutions

In comparison to the “solid” samples this solution was prepared at least one week before precipitation. According to literature Hg^{2+} as well as Hg_2^{2+} are stable in an acidic pH level.

The aqueous species with an oxidation state of +I showed a greyish color change after the addition of precipitation agent whereas the Hg-solutions with an oxidation state +II did not show any color change, most likely because of the low concentration of mercury in solution (Figure 53).

Figure 53 Picture of the different precipitated samples, from left to right: $Hg_2(NO_3)_2$ (black); $Hg_2(NO3)_{2,aq}$ (grey); $Hg(NO_3)_{2,aq}$ (white); $Hg(NO_3)_2$ (yellow)

The evaporation profiles of the aqueous species showed the expected change. The only evaporation seen is within the searched temperature area.
The Hg^{2+} evaporation starts between 100-150 °C but ends at 300 °C. It covers the evaporation temperature range of the gypsum samples but is much too wide. Interestingly with the change of the precipitant from a strong base such as NaOH to a weaker base as $Ca(OH)_2$ the peak gets shorter, more structured and lies in the temperature ranges searched. Still the starting temperature of the evaporation and the temperature of the maximum of the evaporation is a little bit too low in comparison to the gypsum samples. The Hg_2^{2+}/Hg^+ evaporation profile shows a better fit than Hg^{2+} to the gypsum samples but is still not a perfect fit (Figure 54).

As conclusion following results are set:

- For the precipitation products of the aqueous solution that was prepared one week before precipitation, neither Hg^{2+} nor Hg^+ / Hg_2^{2+} show a evaporation at 400°C. This can be explained with the low concentration of mercury in the sample or a higher disproportionation rate of Hg and NO_3 in solution.
- With a low mercury concentration and an aqueous solution of Hg^+ or Hg_2^{2+}, the precipitation product shows a similar evaporation profile than the mercury species found in the gypsum samples.
- It is problematic, that the precipitation product of Hg_2^{2+}/Hg^+ has the most similar evaporation profile than the gypsum samples because it is not believed to be in the solution due to a fast complex formation with possible ligands. Plausible explanations can be, that the ligand of the gypsum sample is simply not one of the tried species that reacts

similar to Hg_2^{2+}/Hg^+ precipitated. Another explanation can be, that sulfite forces the equilibrium of Hg-Halides to the the equilibrium of Hg^{2+}. It is reported by Van-Loon et al. that dependent on the concentration of sulfite and mercury in solution, Hg_2^{2+}/Hg^+ can be formed. Where it also can be precipitated as such. This must be a very fast reaction because as mentioned Hg_2^{2+}/Hg^+ will form a further complex.

The latter bullet point leads to the conclusion that the most plausible ligand responsible for a precipitation of mercury is sulfite.

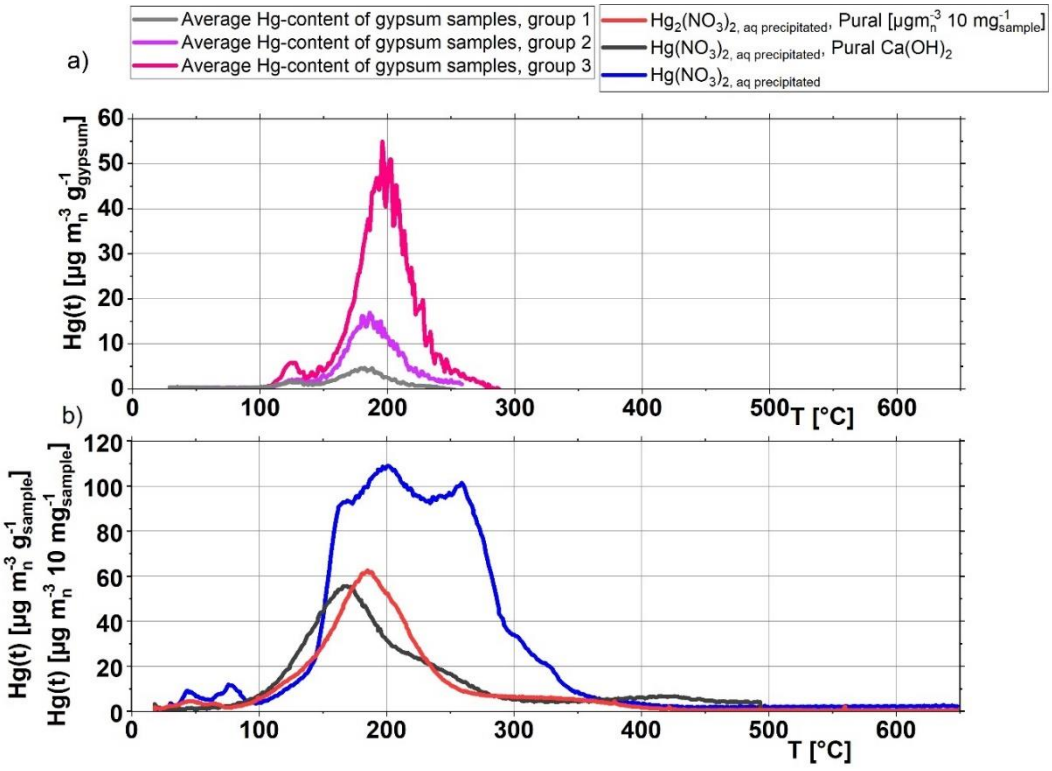

Figure 54 Comparison of $Hg_2(NO_3)_{2,aq\ precipitated}$ and $Hg(NO_3)_{2,aq\ precipitated}$ (b) with evaporation profile of the gypsum samples (a).

Precipitation with sulfite

The last not yet researched mercury species is the precipitation product of $HgSO_3$. Because it is not possible to isolate the species as a solid, an aqueous reaction of Hg^{2+} is used to force the formation of $HgSO_3$. Van Loon et al. showed in their research that sulfite as ligand reduces Hg^{2+} via Hg^{el} to Hg_2^{2+}/Hg^+ with mercury in excess to sulfite. With a 1:1 concentration of sulfite and Hg this should not be the case and mercury should form a one times coordinated complex $HgSO_3$. With an excess of sulfite, the coordination number should be raised to a two times coordinated complex.

The latter should be the most stable coordination in an aqueous solution of mercury with sulfite. To create those three states of the sulfite with mercury, three different concentrations were added to a mercury solution. After a 15 minutes reaction time the solutions were precipitated. Aim was to see if there is any difference in the products as well as if any of the reactions produce a similar peak than the ones that can be measured with the gypsum samples.

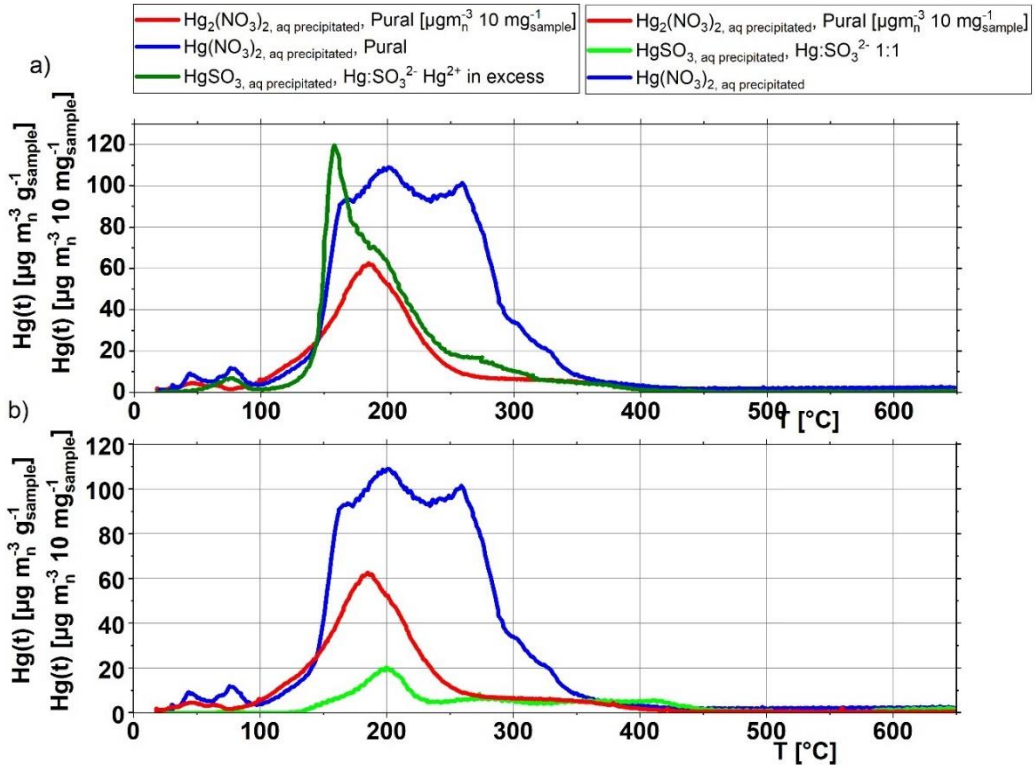

Figure 55 Evaporation profiles of precipitation products of Hg^{2+} with sulfite; a) comparison of $HgSO_{3,aq\ precipitated}$ with mercury in excess to the sample of Hg^{2+} and Hg^{+}/Hg_2^{2+} $_{precipitated}$ b) $HgSO_{3,aq\ precipitated}$ with a $Hg:SO_3^{2-}$ ratio of 1:1 in comparison of Hg^{2+} and Hg^{+}/Hg_2^{2+} $_{precipitated}$.

First point investigated is the comparison of the sulfite sample with excess of mercury to the evaporation profiles of Hg^{2+} (input) and Hg^{2+}/Hg^{+} (suspected output). To see if the theory of van Loon et al. was reproducible and if a reduction of Hg^{2+} to Hg_2^{2+}/Hg^{+} can be forced by the presence of sulfite.

As shown in Figure 55 a) the evaporation of the sample with sulfite starts the evaporation in the same way as Hg^{2+} but shows a much sharper peak than the Hg^{2+} peak without the sulfite dosage. The second part of the peak is similar to the Hg_2^{2+}/Hg^{+} evaporation peak. The peak starts evaporating at the same temperature as Hg^{2+} but ends in the shape of Hg_2^{2+}/Hg^{+}. To conclude is that the first sample containing sulfite with mercury in excess, contains a mixture out of both oxidation states of mercury after precipitation. That can confirm the postulated reaction of van Loon et al. as well as shows a possibility for Hg_2^{2+}/Hg^{+} in solution of FGD.

The second sample (Figure 55 b)) with an equal concentration of sulfite and Hg shows a completely different shape than the other evaporation profiles it is compared to. Clearly a reaction took place, and it is different to the reaction with mercury in excess. In comparison with the gypsum samples (Figure 56), the evaporation profile of the sample with 1:1 Hg:SO_3^{2-} precipitated shows a similar curve than the average of the gypsum samples of group 2. This is a much more likely reaction path for mercury in a FGD than the precipitation of a not coordinated Hg_2^{2+}/Hg^+.

The last sample did not show any evaporation. Possible explanations are that the concentration is too low to be detected by the TDS analysis or that no mercury is left in the sample because all mercury was reduced to Hg^{el} and reemitted before the precipitation.

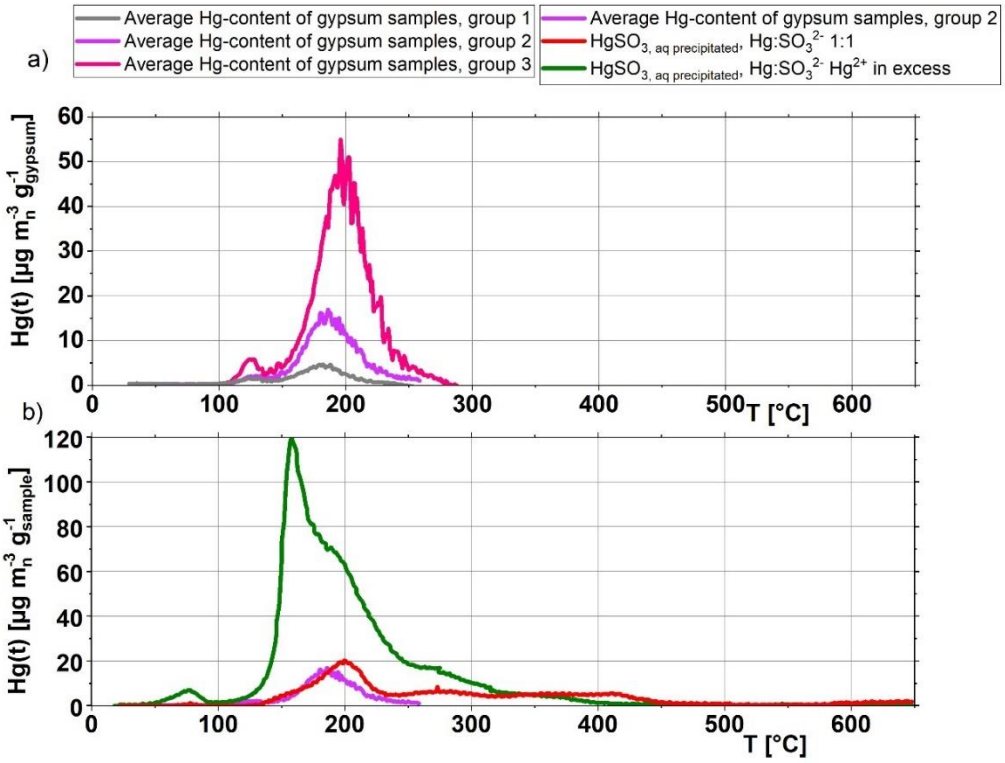

Figure 56 Comparison of the different $HgSO_{3,precipipated}$ samples with the evaporation profile of gypsum sample group 2.

As result of the precipitation experiments three species could be singled out that shown precipitated a signal in the same temperature ranges than the searched profile in the gypsum samples.

These profiles are shown in Figure 57:

- The starting evaporation of HgO(r). This leads to the conclusion that in gypsum the found species is a mercury-oxide.
- The product of the precipitation of $HgBr_2$. With the only difference that no HgO peak at 400-500°C can be seen in the gypsum sample.

- The product of the precipitation of $HgSO_3$.

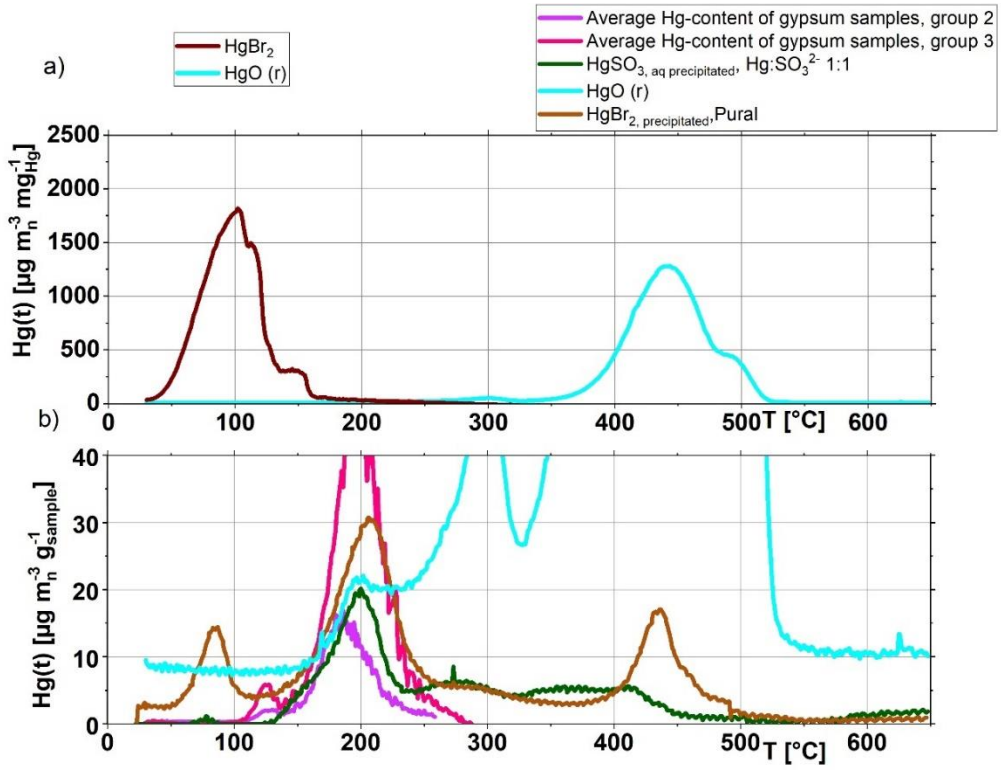

Figure 57 Possible mercury species in gypsum.

4.3.4 RFA and SEM analysis of gypsum samples

An elemental analysis via RFA was conducted for further investigations. Aim of this analysis was to prove, that the chosen matrices were correct and no handling mistake was made. For example, to see that no halide impurity can be found in the samples where no halides were added in the process or metals can be found in the samples where metals were added. Furthermore, the question is, if there is any kind of element that was not considered to have an influence on the precipitation can be identified. Table 23 shows the RFA analysis of different gypsum samples. For some of the samples the mercury content was below the detection limit.

The first batch sample 1-1 in which no halides were added no halides can be found above detection limit. Samples 6-1 and 6-3 (technical FGD solution) show a high variety of impurities. This shows that the matrices changes proved as working. The sample 5-5 where the sulfuric precipitant was added has the highest mercury content. No characteristic element can be singled out to have an influence on mercury. An explanation could be that mercury is a trace element and it is very difficult to analyze its presence as well as its reaction partners with such a method.

There is only one sample where bromine was detected, on the border of the detection limit. No iodine or chlorine was found. The detection limits of the different halides must

be considered here. The detection limits are for Hg around 0.1 ppm, Br 0.1 ppm, Cl 10 ppm and I 1 ppm.

If a mercury(II)halide is adsorbed or if iodine or chlorine is the main species in the gypsum sample the detection limits should be met. Therefore, the results of this measurement are an indication that at least no homoleptic mercury halide complex is present in the solid.

Table 23 RFA analysis of different gypsum samples.

%	1-1	5-3	5-5	6-1	6-3
Ca	20,40	19,97	18,77	18,81	18,86
S	17,35	17	16,73	15,19	14,61
Sr	0,01	0,009	0,008	0,032	0,032
Cu	0,005	0,005	0,005	0,005	0,003
Fe	0,002	0,004	0,006	0,074	0,1
Hg	0	0,001	0,007	0,001	0,001
O	62,23	63,02	64,48	65,16	65,57
Br		0	0,002	0	0
Zn			0	0,002	0,001
Si				0,65	0,75
K				0,06	0,06
Ti				0,009	0,011
Se				0,001	0,001
Rb				0	0
Ni					0,001

With the SEM neither halides nor mercury were detected.

4.3.5 Theoretical calculation of the problem

The next step is the analysis of the possible mercury species calculated with theoretical thermodynamic approaches in the researched conditions. A Pourbaix diagram and Visual MINTEQ Software are used to calculate the possible equilibrium. The Pourbaix diagram was used to see what kind of oxidation states of mercury can be found in the aqueous phase in the conditions of the FGD.

A Pourbaix diagram can be read as following:

- Vertical lines: reaction is only dependent on the pH value (H^+ transition)
- Horizontal lines: reaction is only dependent on the potential (e^- transition)
- Slanted lines are dependent of the pH value and electrical potential.

[52]

Figure 58 shows the Pourbaix diagram for Hg-H_2O at 50 °C. The two dotted lines show the area in which water is stable as H_2O.

The vertical line that separates Hg^{2+} from Hg_2^{2+} describes the reaction:

$$2\,Hg^{2+} + 2e^- \rightleftharpoons Hg_2^{2+} \qquad (4.2)$$

As be seen in Formula 2.32 the reaction is only dependent on the transition of e^-, resulting in a horizontal line between Hg^{2+} and Hg_2^{2+}.

$$HgO + 2H^+ \rightleftharpoons Hg^{2+} + H_2O \qquad (4.3)$$

Formula 2.33 shows that the reaction of HgO to Hg^{2+} is only dependent on the H^+ concentration not a transition of e^-, resulting in a vertical line between Hg^{2+} and HgO.

$$HgO + 2H^+ + 2e^- \rightleftharpoons Hg + H_2O \qquad (4.4)$$

The slanted line between HgO and Hg can be explained with Formula 2.34. It shows the transition of e^- as well as a dependency of H^+. The diagram also shows that all oxidation states of mercury 0, +I, +II can be found in the aqueous phase and inside the experimental conditions. They do not depend directly on the pH value but only on the redox potential. The dependence on the pH value comes with the dependence of the ligand on the pH value, in this case oxygen.

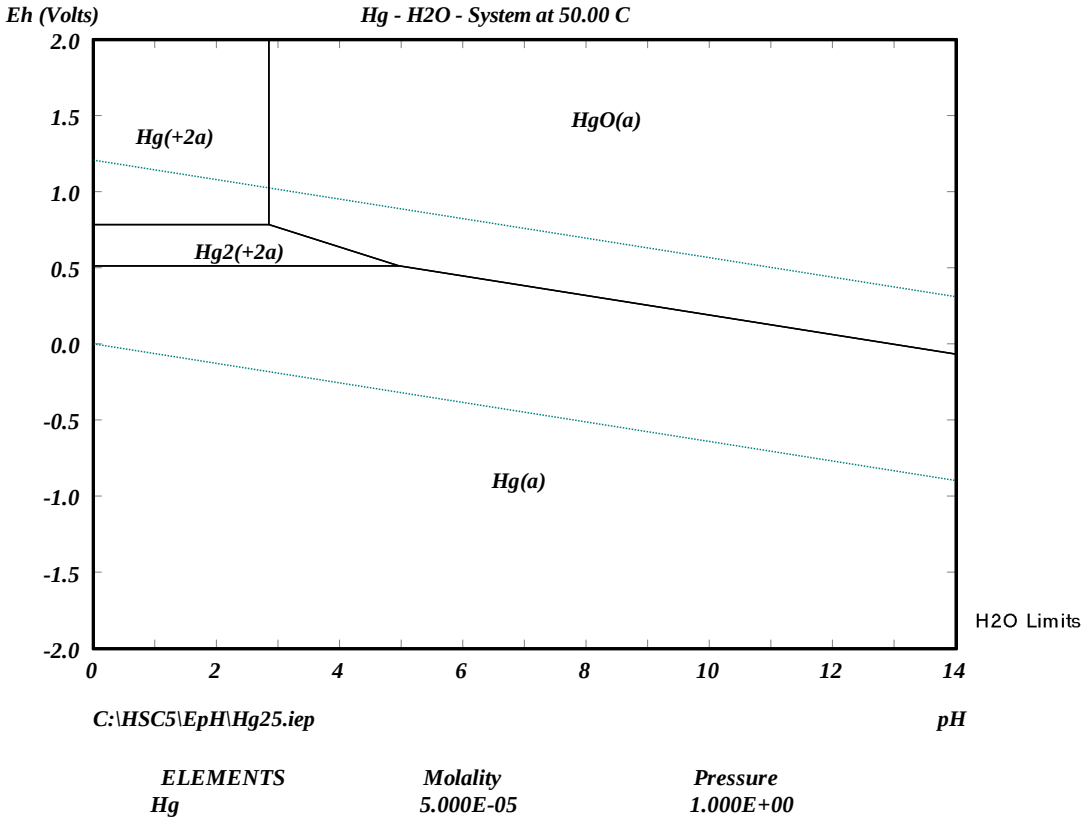

Figure 58 Hg-H_2O Pourbaix diagram created with HSC based on [75].
[52]

Basic calculations via law of mass action were made to see what kind of species theoretically can be precipitated in the system. For this calculation the Visual MINTEQ software was used. Based on the empiric equation of Davies (e.g. chapter 2.1), the activation coefficients are calculated and with the temperature correction of van't Hoff the components for one pH point and a single temperature are determined. With the help of the saturation index calculated with the difference of the ion activity product and the log of the solubility constant possible precipitated species were calculated. A precipitation takes place if the saturation index is positive.

With a mercury concentration of $5*10^{-5}$ mol L^{-1} following calculation were made for pH 5 and pH 8:

Table 24 Visual MINTEQ calculation of possible precipitation species at a pH 5.

Mineral pH 5	log IAP	Sat. index	Stoichiometry	
Calomel	-12.665	3.998	1	Hg_2^{+2}
Coccinite	-32.769	-0.705	1	$Hg(OH)_2$
$Hg(OH)_2(s)$	-12.815	-9.318	1	$Hg(OH)_2$
$Hg_2(OH)_2(s)$	-0.486	-5.747	1	Hg_2^{+2}
$Hg_2Br_2(s)$	-16.67	3.777	1	Hg_2^{+2}
$Hg_2I_2(s)$	-20.441	5.69	1	Hg_2^{+2}
$HgBr_2(s)$	-28.999	-5.602	1	$Hg(OH)_2$
$HgCl_2(s)$	-24.993	-5.192	1	$Hg(OH)_2$
Montroydite	-12.814	-9.442	1	$Hg(OH)_2$

Table 25 Visual MINTEQ calculation of possible precipitation species at a pH 8.

Mineral pH8	log IAP	Sat. index	Stoichiometry	
Calomel	-12.665	3.998	1	Hg_2^{+2}
Coccinite	-32.78	-0.715	1	$Hg(OH)_2$
$Hg(OH)_2(s)$	-6.962	-3.466	1	$Hg(OH)_2$
$Hg_2(OH)_2(s)$	5.514	0.253	1	Hg_2^{+2}
$Hg_2Br_2(s)$	-16.672	3.776	1	Hg_2^{+2}
$Hg_2I_2(s)$	-20.304	5.827	1	Hg_2^{+2}
$HgBr_2(s)$	-29.147	-5.751	1	$Hg(OH)_2$
$HgCl_2(s)$	-25.14	-5.34	1	$Hg(OH)_2$
Montroydite	-6.961	-3.589	1	$Hg(OH)_2$

The only mercury species precipitating in the concentration limits used are Hg(I)-halides or Hg(I)-hydroxides.

None of the suspected mercury species in gypsum can be identified by the program calculation to meet their saturation limit.

This is another strong indication towards the theory that the formed mercury species is not considered or known, like a heteroleptic $(HO)_x$-Hg-SO_3 complex.

The next step is to identify what kind of mercury complexes are the most plausible complexes in the aqueous phase. With concentration limits for halides set as shown in Table 15, similar to the concentration in the FGD experiments with a low halides' concentration. The sulfite concentration was set at a ratio to iodide as 1:1 with $c(SO_3^{2-}) = 1*10\text{-}4$ mol L^{-1}. The results show a huge impact of the pH value on the main mercury species in solution. The main mercury species is $HgI_{2,aq}$ and some

heteroleptic-mercury-halides complexes, like HgClI or HgBrI at a pH of 5. With the change of pH value, the main species still is $HgI_{2,aq}$ but the second is a complex with sulfite $Hg(SO_3)_2^{2-}$. The other remaining species are HgClI with a decrease in its concentration and HgI_3^- with an increase in its concentration. The distribution of possible species can be seen in Table 24 and Table 25 for a pH of 5 and for pH of 8.

4.3.6 Discussion of the investigation of Hg_s

This chapter sums up the results and discuss the findings on the investigation of Hg_s in a FGD scrubber. The focus of this work is to better understand and describe the $Hg_{aq} \rightleftharpoons Hg_s$ equilibrium. Therefore, the main mercury species involved in that equilibrium had to be investigated. To be able to analyze unknown mercury species in a solid sample the method of TDS was implemented. The main suspected mercury species in a gypsum were measured and a template for standard evaporations was created. Because no oxidized mercury emission was found in the evaporation profile of the gypsum samples, the adsorption or inoculation of a Hg_{aq} species as Hg(II)-halides was excluded from the species search.

HgS as well as HgO would not adsorb but precipitate as solid. HgS was excluded because the evaporation profile of the sample with precipitant. $HgSO_4$ and all basic salts created with $HgSO_4$ did not show a right evaporation temperature to be further considered. All Hg(I)-species did not have the right evaporation temperature and even if the temperature was close to the emission profile of calomel a Hg^{ox} emission would be necessary. This made it possible to exclude Hg(I)-halides as possible Hg_s species even though the theoretical approach detected them to be one possibility. HgO was the only species that showed a small evaporation activity at the searched temperature ranges.

The analysis of the influencing parameters and matrix composition showed a positive correlation of Hg_s with:

- Sulfite concentration,
- metal concentration and
- pH value.

The analysis also showed that with these factors sulfite (positive correlation), metals (positive correlation), pH value (positive correlation) and halides (negative correlation) most of the influences of the formation of Hg_s can be explained.

The results point to a heavy metal precipitation via OH^- as main reaction of Hg_{aq} to Hg_s. Depending on those results precipitation experiments were conducted.
The precipitation of Hg(I)-solids led to only one evaporation profile. As described in literature elemental mercury was formed and an evaporation was observed in the temperature ranges of -Hg-O-. The evaporation profiles of $HgCl_2$, HgI_2, $HgSO_4$ precipitated as solids also showed their main evaporation at temperature ranges of Hg-O- species.
The only species that showed similar evaporation profiles as the gypsum samples were:

- $HgBr_{2,\ precipitated}$ and
- $HgSO_{3,\ precipitated}$

These results are coherent with the results in the aqueous solution, that sulfite and bromide have a similar influence on the reaction of mercury (e.g. chapter 4.1).

There are different aspects that seem to exclude $HgBr_{2,\ precipitated}$ as species. One is the fact that not all gypsum samples contain halides, but all show the same evaporation peak.
The theoretical calculation of the most likely mercury species in solution did not show bromide as a relevant ligand for mercury. They did however show sulfite as one of the main ligands in high pH values for mercury.
That would leave $HgSO_{3,\ precipitated}$ as main possible species found in a gypsum sample. It is not possible to isolate $HgSO_3$ as a solid to create a standard evaporation profile for the species for further investigations.

It is very likely that $HgSO_{3,\ precipitated}$ has at least one additional hydroxide group in the complex and forms a heteroleptic HO-Hg-SO_3 complex. Higher coordination is a possibility like $(HO)_3$-Hg-SO_3. A higher coordination with sulfite does not seem plausible because the petri dish with sulfite in excess to the mercury concentration showed no evaporation. This complex would explain the oxygen group and the similarities to the HgO evaporation. The problem is that for this kind of complex no saturation limits are known in literature to make sure it is possible to precipitate as solid in the researched concentration limits.

Another theory can be that sulfites as well as bromides act as some sort of catalyst for the reaction of the same product, with the product being some kind of Hg-O-X, or Hg-OH-X species still not known in detail.

It was not possible to find reported mercury species in literature, for the created FGD gypsum samples. Different reasons can be listed. One reason can be the differences between the analytical methods, for example, the difference in the temperature program and the continuous measurement of Hg. The close temperature range of the evaporations of Hg(II)-halides and the species in the gypsum can overlap with a too-fast temperature ramp or discontinuous measurement. Another possible reason is the differentiation of the two oxidation states of mercury emissions during evaporation. Due to a slow heating ramp and the differentiation of the oxidation states of mercury evaporating, it was possible to show differences in the evaporation behavior of Hg(II)-halides, Hg(I)-halides, and gypsum. As discussed in the results, a too-fast heating ramp can influence the evaporation temperature of the different mercury species. Because of the differentiation of the oxidation states, it was possible to see that mercury-halides all have a Hg(II) evaporation that is not in the evaporation profile of the gypsum samples. The process allowed to use pure mercury samples and no solid mixture was needed or other process steps that could influence the species. Due to the laboratory scaled FGD, it was possible to create standardized gypsum samples with a known input. Similar to Pavlin et al only one mercury species was found with a standardized method.

The reported influences on Hg_s in literature can be confirmed with the gypsum samples.

Metal-, sulfite-, halides concentration as well as pH value all influence the amount of mercury in the gypsum sample. In addition to confirm the known influences, this work was able to show that all those parameter settings or sump matrix changes did not change the species, only the amount of mercury.

It was only possible to create HgS inside the gypsum sample with the addition of a sulfuric precipitant. It is not known if the reported HgS was also created by the addition of a precipitant.
Reasons for missing HgO and $HgSO_4$ can be, that it was not possible to set the ORP level > 700 mV due to the restrictions of the system. Schütze [28] reported that the redox potential has an influence on how mercury is bound in the scrubber solution. Mercury is more thermally stable at redox potentials E_H > 700 mV. He also reported that at those levels' mercury is more stable in aqueous solution. This can be the reason why no statistical influence of the ORP was detected with this system.
It is possible that not all impurities are considered to have an influence. Cyanide as ligand for mercury is also not included in the system.

4.4 The $Hg_{aq} \rightleftharpoons Hg_s$ equilibrium

Based on the scrubber experiments, the following main influences for the $Hg_{aq} \rightleftharpoons Hg_s$ equilibrium were identified:

- Halides concentration: a high ligand/ halides concentration pushes the equilibrium to the side of Hg_{aq}
- pH value: A high pH value forces mercury into the solid
- Sulfite concentration: a high sulfite concentration forces mercury in the solid.
- Metals: Metals act as flocculent for small mercury particles and increase the mercury concentration in Hg_s.
- The ORP did not show an influence but due to restriction of the system the reported influencing high ORP levels were not reachable.
- The time: It was shown that the Hg_s concentration rose over time. This shows that the Hg_{aq}-Hg_s equilibrium is still not met and can be an indication for a slow reaction.

Following hypothesis was developed based on the findings: Mercury is precipitated over sulfite into a solid, this is dependent on the pH value and does not exclude a dissolution.
$HgSO_3$ as a strong ligand for mercury opens a parallel complex row not includable in the Hg-halides system. It seems that sulfite as ligand for mercury is the species responsible for the precipitation of mercury as solid at a high pH value. Metals help to

flocculate the small particles so that they end up in the solid phase. All the influences do not have an influence on the species, only on the amount.
With these new understandings, the Bittig droplet can be further extended by a next point as seen in Figure 59:

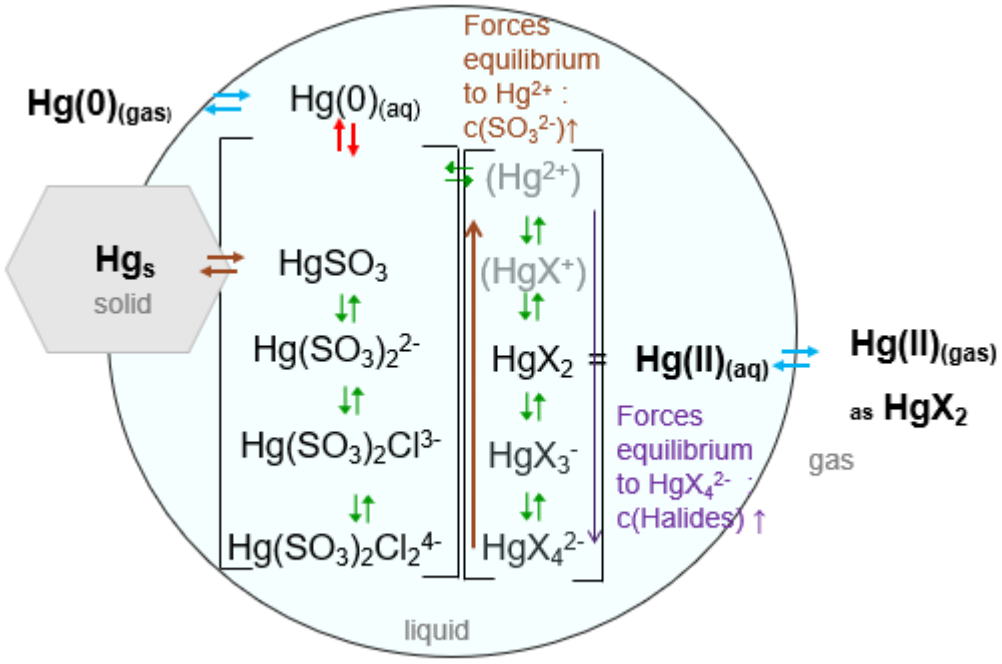

Figure 59 Bittig droplet extended with sulfite as ligand and the solid phase

The red arrows describe the redox reaction to elemental mercury. This equilibrium mainly depends on the mercury concentration, the sulfite concentration, the halides concentration and the temperature; the blue arrows describe the equilibrium with the gas phase depending on the Henry-Law, the temperature and the ligand concentration and mainly on the mercury concentration. The brown arrows stand for the precipitation to Hg_s. This equilibrium depends on the pH value, the sulfite concentration, metal concentration and the halides concentration.

5 Conclusion and Outlook

This work showed the complexity of co-treatment of mercury in a FGD. It was possible to develop a method for the characterization of different mercury species in a solid sample. It was also possible to create standardized gypsum samples via a laboratory scaled FGD.

A lot of phenomenological research was done to find the starting Hg_{aq} species that stands in the Hg_{aq}-Hg_s equilibrium. The analysis of the mercury species in the created gypsum samples showed that the found species is formed via precipitation. The precipitation of different mercury species showed that the most plausible Hg_s species found in gypsum is $HgSO_{3,\ precipitated}$.

Parameter studies for aqueous mercury were conducted to define the main mercury species expected in an aqueous state and the expansion with sulfite of the Hg-Halides-H_2O-System to Hg-Halides-SO_2-H_2O. As result was found that $HgSO_{3,\ aq}$ is precipitated depending on the pH value.

Following hypothesis based on the observations were made:

- It is possible to separate mercury species in a solid by their evaporation profile. Most important factors are:
  - the temperature ramp needs to be as small as possible.
  - The emissions must be measured continuously.
  - The emissions have to be measured as Hg(0) and Hg(t) to better understand the species of mercury in the sample
- Sulfite as ligand needs to be considered outside the Hg-halides system and acts monodental as a Sulfito-S complex. $HgSO_3$ is not comparable as done before with HgX_2 halides but needs to be compared with the stability constants of HgX^+. This was shown with experiments Hg-Br/Cl/I-SO_2-H_2O systems. The formation of $HgSO_3$ is much faster than the ligand changes of Hg-halides and leads to intra-molecular redox reactions, if not enough SO_3^{2-} is in the system. Sulfite is as strong a ligand as iodide for HgX^+ and as strong as bromide as HgX_2. It even has an influence on a HgX_4^{2-} halide system that leads to a raise of Hg(0) reemissions.
- The formation of mercury in a solid is due to a precipitation and not an adsorption or inoculation of mercury in or on the gypsum particle.
- The precipitation forms a heteroleptic Hg-oxide complex most likely over $HgSO_3$. Because the reaction is dependable on the pH value, it is possible that a resolution takes place at lower pH values.

- Metals do not have an influence on the mercury species but on the mercury concentration in gypsum. Concluding that metals act as flocculent not as precipitant for mercury.
- The ORP did not show any influence on the $Hg_{aq} \rightleftharpoons Hg_s$ equilibrium. But the ORP level found in literature were not reached, due to the restrictions of the system.
- The aqueous mercury concentration has no impact on the solid concentration of mercury. That shows that the equilibrium is still not reached yet.
- Because of the high ligand strength sulfite as ligand for mercury is very likely in the system.

This research shows that the evaporation temperature of mercury in gypsum is low and the content is leachable. With those characteristics', mercury can be released during the production process of wallboard gypsum. This would mean a shift of mercury emissions from the coal combustion into the next production step.
To prevent the emission of mercury it is essential to keep mercury out of the gypsum. This can be done by stabilizing it in the aqueous phase of the scrubber or by keeping mercury out of the system.
One possible way to stabilize mercury aqueous in a FGD scrubber is to add chloride into the system. This can keep mercury out of the solid phase and is the main factor investigated to minimize reemissions out of the scrubber. Of cause, the restriction of halides concentration of the wastewater treatment plant and the quality restriction of the gypsum must be considered as well.
Another approach is to reduce the general mercury content in the system. This can be done by systematically targeting and removing mercury in solution or to investigate the mercury content before burning the coal and use only coal with a low mercury content. Same can be done with iodide to keep it out of the scrubber. Bromide showed the strongest reaction with sulfite and should not be added into the scrubber system.
For further research, more specific precipitation experiments with sulfite and controlled pH values in lower concentrations could help to find the one species.
With the theoretical calculation not being able to define the species occurring, it can be suspected that the species is a heteroleptic complex. This can mean that the right species is still not considered and will be very difficult to find.
In different sources, it was reported that $HgCl_2$, HgS as well as $HgSO_4$ was found in gypsum. With the laboratory scaled scrubber system it was not possible to create different kind of mercury species in gypsum. It was also not possible to create an ORP

level E_H> 700 mV. This is the redox potential in which more thermal stable mercury species are reported. None of the other pre-defined influences and scrubber settings were able to change the species. Next step should be to up-scale the laboratory scaled FGD and try to recreate the results and to reach the needed redox potential.

All those results show that mercury is in a constant exchange with its surroundings. If the equilibrium changes it always leads to a reemission of mercury in the cleaned flue gas.
Because the precipitation is also dependable of the pH value and solubility of the species, it is not possible to stabilize mercury in the solid without a precipitation agent. The system also shows how difficult it is to stabilize mercury in a FGD system. All influences can still not describe all the reemissions observed. One of the main problems is still, that not all of the important parameters can be measured continuously or sometimes not even measured at all. To prevent reemissions, aqueous mercury concentrations, halides concentrations and sulfite concentrations need to be available.
One critical weakness of the system is the theoretical calculation of possible reactions. There is a high lack of usable data as input as it can be seen in the complex constants and the right coordination for mercury with sulfite as ligand. Also to calculate the activation coefficients with the empiric equation of Davies needs to be discussed as there can be better approaches, than the chosen one. The calculation can be used as first indicative calculation but could be continued with a more suitable system.

VII. References

[1] **“DIN 1310:1984-02**, Zusammensetzung von Mischphasen (Gasgemische, Lösungen, Mischkristalle); Begriffe, Formelzeichen,” Beuth Verlag GmbH. doi: 10.31030/1082186.

[2] **EU 2017/852**, *Verordnung EU 2017/852 des Europäischen Parlaments und des Rates 17.05.2017*. 2017.

[3] **WHO,** “Fact-sheet-mercury and health,” https://www.who.int/news-room/fact-sheets/detail/mercury-and-health, Mar. 2017. [Online]. Available: https://www.who.int/news-room/fact-sheets/detail/mercury-and-health

[4] **UN Environment**, “Global Mercury Assessment 2018,” UN Environment Programme, Chemicals and Health Branch, Geneva Switzerland, 2019. [Online]. Available: https://www.unenvironment.org/resources/publication/global-mercury-assessment-2018

[5] **UN Environment**, “Minamata Convention on Mercury,” United Nations Environment Program, 2019. [Online]. Available: http://www.mercuryconvention.org/Convention/Text/tabid/3426/language/en-US/Default.aspx

[6] **European Commission**. Joint Research Centre., *Best Available Techniques (BAT) reference document for large combustion plants: Industrial Emissions Directive 2010/75/EU (integrated pollution prevention and control).* LU: Publications Office, 2017. Accessed: Jun. 04, 2023. [Online]. Available: https://data.europa.eu/doi/10.2760/949

[7] **Germany and P.-C. Storm, Eds.**, *Umweltrecht: wichtige Gesetze und Verordnungen zum Schutz der Umwelt: Textausgabe mit ausführlichem Sachverzeichnis und einer Einführung*, 18., Neubearbeitete und erw. Aufl., Stand:1. Oktober 2006. in Beck-Texte im dtv. München: Deutscher Taschenbuch Verlag, 2007.

[8] **B. Heidel,** “Wechselwirkungen bei der Abscheidung von Schwefeldioxid und Quecksilber durch nasse Rauchgasentschwefelungsanlagen,” Dissertation, Universität Stuttgart, Stuttgart, 2015. Accessed: Dec. 10, 2020. [Online]. Available: http://elib.uni-stuttgart.de/handle/11682/2421

[9] **H. Gutberlet, A. Spiesberger, F. Kastner, and J. Tembrink,** “Zum Verhalten des Spurenelementes QUecksilber in Steinkohlefeuerungen mit Rauchgasreinigungsanlagen,” *VGB-Kraftwerkstechnik*, vol. 72, no. 8, pp. 636–641, 1992.

[10] **Schuetze, Jan and Koeser, Heinz,** “Strategies for enhancing the co-removal of mercury in FGD-scrubbers of power plants-opertationg parameters and additives,” *VGB PowerTech*, vol. 03/2012, 2012.

[11] **K. Strauß**, *Kraftwerkstechnik: zur Nutzung fossiler, nuklearer und regenerativer Energiequellen*, 6., Aktualisierte Aufl. in VDI-[Buch]. Berlin: Springer, 2009.

[12] **M. Bittig, S. Haep, and D. Bathen,** “Quecksilber-Abscheidung in Abgaswäschern - über die Wechselwirkung von Chemie und Prozessführung,” *VGB PowerTech*, vol. 96, no. 3, pp. 74–77, 2016.

[13] **F. van Dijen,** “Producing FGD gypsum with low Hg content,” *VGB PowerTech*, vol. 5, pp. 74–79, 2016.

[14] G. Blythe, “Mercury Capture in Wet flue Gas Desulfurization Systems,” in *Mercury Control: for coal-derived gas streams*, Weinheim: Wiley-VCH-Verl, 2015, pp. 261–275.

[15] **M. Schneider, J.-C. Hintzen, and K. Keldenich,** “BREF-eine Herausforderung für den wirtschaftlichen Kraftwerkbetrieb,” in *Emissionsminderung in Kraftwerken, Tagungsband*, Dresden: SAXONIA, 2018, pp. 3–13.

[16] **Bundesverband der Gipsindustrie e.V.**, “Gips schafft Freiräume,” Jul. 10, 2020. https://www.gips.de/wissen/rohstoffe/technischer-gips/

[17] **Richardson and Blythe,** “Field Study of Mercury Partitioning in Wet FGD Byproducts.” Mega Symposium Baltimore M.D. USA, 2008.
[18] **I. Klöfer, M. Bittig, and D. Bathen,** “Speciation of inorganic mercury compounds in solid samples via thermo-desorption experiments,” *Chem. Eng. Technol.*, vol. 44, no. 4, pp. 788–796, 2021, doi: 10.1002/ceat.202000444.
[19] **J. Schuetze, U. Schilling, L. Hilbert, J. H. Strauß, and T. Hörtinger,** “Quecksilber-Abscheidung am Beispiel des Kraftwerkes Lippendorf,” *VGB PowerTech*, vol. 12, pp. 81–87, 2015.
[20] **G. Blythe, J. Currie, and D. W. DeBerry,** “Bench-scale Kinetics Study of Mercury Reactions in FGD Liquors,” Prepared for: National Energy Technology Laboratory U.S Department of Energy, Austin, Final Report DE-FC26-04NT42314, 2008.
[21] **L. Van Loon, E. Mader, and S. L. Scott,** “Reduction of the Aqueous Mercuric Ion by Sulfite: UV Spectrum of $HgSO_3$ and Its Intramolecular Redox Reaction,” *J. Phys. Chem. A*, vol. 104, no. 8, pp. 1621–1626, Mar. 2000, doi: 10.1021/jp994268s.
[22] **L. L. Van Loon, E. A. Mader, and S. L. Scott,** “Sulfite Stabilization and Reduction of the Aqueous Mercuric Ion: Kinetic Determination of Sequential Formation Constants,” *J. Phys. Chem. A*, vol. 105, no. 13, pp. 3190–3195, Apr. 2001, doi: 10.1021/jp003803h.
[23] **U. Spitzer and R. van Eldik,** “Kinetics and mechanisms of the formation, substitution, and aquation reactions of sulfur-bonded (sulfito) amminecobalt (III) complexes in aqueous solution,” *Inorg Chem*, vol. 21, pp. 4008–4014, 1982.
[24] **Z. Sui, Y. Zhang, W. Li, W. Orndorff, Y. Cao, and W.-P. Pan,** “Partitioning effect of mercury content and speciation in gypsum slurry as a function of time,” *J. Therm. Anal. Calorim.*, vol. 119, no. 3, pp. 1611–1618, Mar. 2015, doi: 10.1007/s10973-015-4403-9.
[25] **C. Wu, Y. Cao, Z. Dong, C. Cheng, H. Li, and W. Pan,** “Mercury speciation and removal across full-scale wet FGD systems at coal-fired power plants,” *J. Coal Sci. Eng. China*, vol. 16, no. 1, pp. 82–87, Mar. 2010, doi: 10.1007/s12404-010-0116-7.
[26] **J. Schuetze, D. Kunth, S. Weissbach, and H. Koeser,** “Mercury Vapor Pressure of Flue Gas Desulfurization Scrubber Suspensions: Effects of pH Level, Gypsum, and Iron,” *Environ. Sci. Technol.*, vol. 46, no. 5, pp. 3008–3013, Mar. 2012, doi: 10.1021/es203605h.
[27] **M. Bittig,** *Zum Einfluß unterschiedlicher Liganden auf die Quecksilberabscheidung in absorptiven Abgasreinigungsstufen*. Dissertation, Aachen: Shaker, 2011.
[28] **J. Schütze,** *Quecksilberabscheidung in der nassen Rauchgasentschwefelung von Kohlekraftwerken*. in Beiträge zum Umweltschutz, no. 6., DIssertation Aachen: Shaker, 2013.
[29] **M. Bittig, D. Bathen, and B. Pieper,** “The Mechanism of Mercury Seperation in Wet Flue Gas Cleaning Systems,” *VGB PowerTech*, vol. 90, no. 4, pp. 77–84, 2010.
[30] **R. A. Lidin, L. L. Andreyeva, V. A. Molochko, and R. A. Lidin,** *Constants of inorganic substances: a handbook*, Rev. and augm. Ed. New York: Begell House, 1995.
[31] **R. Gansley,** “Sulfite control of WFGD for Reduced mercury re-emissions and improved trace element removal in waste water,” presented at the Mercury Control Workshop, Presentation, Berlin, 08 June 2017.
[32] **J.-Y. Lee, K. Cho, L. Cheng, T. C. Keener, G. Jegadeesan, and S. R. Al-Abed**, “Investigation of a Mercury Speciation Technique for Flue Gas Desulfurization Materials,” *J. Air Waste Manag. Assoc.*, vol. 59, no. 8, pp. 972–979, Aug. 2009, doi: 10.3155/1047-3289.59.8.972.
[33] **M. Sedlar, M. Pavlin, R. Jaćimović, A. Stergarsek, P. Frkal, and M. Horvat,** “Temperature Fractionation (TF) of Hg Compounds in Gypsum from Wet Flue

Gas Desulfurization System of Coal Fired Thermal Power Plant (TPP)," *Am. J. Anal. Chem.*, vol. 6, pp. 939–956, 2015, doi: 10.4236/ajac.2015.612090.

[34] **M. Rallo, Lopez-Anton, M.A., R. Perry, and M. Maroto-Valer,** "Mercury speciation in gypsums produced from flue gas desulfurization by temperature programmed decomposition," vol. 89, no. 8, pp. 2157–2159, 2010, doi: 10.1016/j.fuel.2010.03.037.

[35] **P. Córdoba *et al.*,** "Unusual Speciation and Retention of Hg at a Coal-Fired Power Plant," *Am. Chem. Soc.*, vol. Environ. Sci. Technol., pp. 7890–7897, 2012, doi: 10.1021/es301106x.

[36] **D. Kunth, J. Schuetze, and H. Koeser,** Eds., "Hg-Emissionen bei der Verarbeitung von Gips aus Rauchgasentschwefelungsanlagen (REA)," in *Emissionsminderung 2012: VDI-Fachtagung mit begleitender Fachausstellung ; Stand, Konzepte, Fortschritte ; Tagung Nürnberg, 19. und 20. Juni 2012*, Nichtred. Ms.-Dr.in VDI-Berichte, no. 2165. Düsseldorf: VDI-Verl, 2012, pp. 61–79.

[37] **M. Rumayor, M. A. Lopez-Anton, M. Díaz-Somoano, and M. R. Martínez-Tarazona,** "A new approach to mercury speciation in solids using a thermal desorption technique," *Fuel*, vol. 160, pp. 525–530, Nov. 2015, doi: 10.1016/j.fuel.2015.08.028.

[38] **D. W. Boening,** "Ecological effects, transport, and fate of mercury: a general review," *Chemosphere*, vol. 40, no. 12, pp. 1335–1351, Jun. 2000, doi: 10.1016/S0045-6535(99)00283-0.

[39] **C. C. Windmöller, N. C. Silva, P. H. Morais Andrade, L. A. Mendes, and C. Magalhães do Valle**, "Use of a direct mercury analyzer® for mercury speciation in different matrices without sample preparation," *Anal. Methods*, vol. 9, no. 14, pp. 2159–2167, 2017, doi: 10.1039/C6AY03041F.

[40] **A. T. Reis, J. P. Coelho, I. Rucandio, C. M. Davidson, A. C. Duarte, and E. Pereira**, "Thermo-desorption: A valid tool for mercury speciation in soils and sediments?," *Geoderma*, vol. 237–238, pp. 98–104, Jan. 2015, doi: 10.1016/j.geoderma.2014.08.019.

[41] **A. Bollen, A. Wenke, and H. Biester**, "Mercury speciation analyses in HgCl2-contaminated soils and groundwater—Implications for risk assessment and remediation strategies," *Water Res.*, vol. 42, no. 1–2, pp. 91–100, Jan. 2008, doi: 10.1016/j.watres.2007.07.011.

[42] **M. Pavlin, A. Popović, R. Jaćimović, and M. Horvat,** "Mercury fractionation in gypsum using temperature desorption and mass spectrometric detection: Mass spectrometric approach to mercury fractionation in FGD gypsum," *Open Chem.*, vol. 16, no. 1, pp. 544–555, Jun. 2018, doi: 10.1515/chem-2018-0046.

[43] **M. Rumayor, M. Diaz-Somoano, M. A. Lopez-Anton, and M. R. Martinez-Tarazona,** "Application of thermal desorption for the identification of mercury species in solids derived from coal utilization," *Chemosphere*, vol. 119, pp. 459–465, Jan. 2015, doi: 10.1016/j.chemosphere.2014.07.010.

[44] **H. Biester, M. Gosar, and G. Müller,** "Mercury speciation in tailings of the Idrija mercury mine," *J. Geochem. Explor.*, vol. 65, no. 3, pp. 195–204, May 1999, doi: 10.1016/S0375-6742(99)00027-8.

[45] **H. Biester, M. Gosar, and S. Covelli,** "Mercury Speciation in Sediments Affected by Dumped Mining Residues in the Drainage Area of the Idrija Mercury Mine, Slovenia," *Environ. Sci. Technol.*, vol. 34, no. 16, pp. 3330–3336, Aug. 2000, doi: 10.1021/es991334v.

[46] **H. Biester and C. Scholz,** "Determination of Mercury Binding Forms in Contaminated Soils: Mercury Pyrolysis versus Sequential Extractions," *Environ. Sci. Technol.*, vol. 31, no. 1, pp. 233–239, Jan. 1997, doi: 10.1021/es960369h.

[47] **M. Rumayor, M. Diaz-Somoano, M. A. Lopez-Anton, and M. R. Martinez-Tarazona,** "Mercury compounds characterization by thermal desorption," *Talanta*, vol. 114, pp. 318–322, Sep. 2013, doi: 10.1016/j.talanta.2013.05.059.

[48] **S.-K. Back *et al.***, “Thermal decomposition characteristics of mercury compounds in industrial sludge with high sulfur content,” *J. Mater. Cycles Waste Manag.*, vol. 20, no. 1, pp. 622–631, Jan. 2018, doi: 10.1007/s10163-017-0630-4.
[49] **L. Sigg and W. Stumm,** *Aquatische Chemie: eine Einführung in die Chemie wässriger Lösungen und in die Chemie natürlicher Gewässer*, 2., Durchges. Aufl. Stuttgart: Teubner [u.a.], 1991.
[50] **Outokumpu,** “Outokumpu HSC Chemistry for WIndows.” Outokumpu, Jun. 28, 2002.
[51] **J. P. Gustafsson,** “Visual MINTEQ.” Royal Institute of Technology, Stockholm, Dec. 21, 2013.
[52] **E. McCafferty,** *Introduction to corrosion science*. New York: Springer, 2010.
[53] **G. Wedler,** *Lehrbuch der physikalischen Chemie*, 5., Vollst. überarb. und aktualis. Aufl., 2. Nachdr. Weinheim: Wiley-VCH, 2010.
[54] **M. Luckas and J. Krissmann,** *Thermodynamik der Elektrolytlösungen: eine einheitliche Darstellung der Berechnung komplexer Gleichgewichte*. Berlin: Springer, 2001.
[55] “**Aqion**_Hydrochemistry & Water Analysis, Mineral Solubility and Saturation Index.” aqion, Nov. 17, 2022. [Online]. Available: https://www.aqion.de/site/168
[56] **E. Fluck,** *Periodensystem der Elemente: unter Berücksichtigung der IUPAC-Empfehlungen bis 2001*. Weinheim: Wiley-VCH, 2002.
[57] **A. F. Holleman, E. Wiberg, and N. Wiberg,** *Lehrbuch der anorganischen Chemie*, 101., verb. Und stark erw. Aufl. Berlin: de Gruyter, 1995.
[58] **R. J. Meyer and E. H. E. Pietsch,** *Gmelins Handbuch der anorgansichen Chemie*, 8. in Quecksilber, Quecksilber-Halogenverbindungen, no. Teil B Lieferung 2. Verlag Chemie GmbH, 1967.
[59] **R. J. Meyer and E. H. E. Pietsch,** *Gmelins Handbuch der anorgansichen Chemie*, 8. in Quecksilber, Verbindungen bis Quecksilber und Stickstoff einschliesslich aller N-haltigen Quecksilberverbindungen, no. Teil B Lieferung 1. Verlag Chemie GmbH, 1965.
[60] **R. J. Meyer and E. H. E. Pietsch,** *Gmelins Handbuch der anorgansichen Chemie*, 8. in Quecksilber,Elektrochemie; chemisches Verhalten; Legierungen, no. Teil A Lieferung 2. Verlag Chemie GmbH, 1962.
[61] **E. Riedel and C. Janiak, *Anorganische Chemie*,** 9. Auflage. in De Gruyter Studium. Berlin ; Boston: De Gruyter, 2015.
[62] **J. P. Hall and W. P. Griffith,** “Vibrational spectra of group VIII sulphito complexes,” *Inorganica Chim. Acta*, vol. 48, pp. 65–71, Jan. 1981, doi: 10.1016/S0020-1693(00)90068-9.
[63] **J. E. Huheey, E. A. Keiter, R. L. Keiter, and R. Steudel,** *Anorganische Chemie: Prinzipien von Struktur und Reaktivität*, 4., Völlig neu bearb. Aufl. in De Gruyter Studium. Berlin: de Gruyter, 2012.
[64] **R. J. Meyer and E. H. E. Pietsch,** *Gmelins Handbuch der anorgansichen Chemie*, 8. in Quecksilber, Verbindungen von Quecksilber und Schwefel bis Quecksilber und Kohlenstoff, no. Teil B Lieferung 3. Verlag Chemie GmbH, 1968.
[65] **J. P. Guthrie,** “Tautomeric equilibria and p K_a values for ‘sulfurous acid’ in aqueous solution: a thermodynamic analysis,” *Can. J. Chem.*, vol. 57, no. 4, pp. 454–457, Feb. 1979, doi: 10.1139/v79-074.
[66] **M. Bittig, S. Haep, and D. Bathen,** “Quecksilber-Abscheidung in Abgaswäschern - über die Wechselwirkung von Chemie und Prozessführung,” *VGB PowerTech*, vol. 96, no. 3, pp. 74–77, 2016.
[67] **J. Munthe and W. J. McElroy,** “Some aqueous reactions of potential importance in the atmospheric chemistry of mercury,” *Atmospheric Environ. Part Gen. Top.*, vol. 26, no. 4, pp. 553–557, Mar. 1992, doi: 10.1016/0960-1686(92)90168-K.

[68] **C. L. Kairies, K. T. Schroeder, and C. A. Cardone**, “Mercury in gypsum produced from flue gas desulfurization,” *Fuel*, vol. Volume 85, no. Issue 17-18, pp. 2530–2536, 2006, doi: 10.1016/j.fuel.2006.04.027.
[69] **W. L. Beatty, K. Schroeder, and C. L. K. Beatty,** “Mineralogical Associations of Mercury in FGD Products,” *Energy Fuels*, vol. 26, no. 6, pp. 3399–3406, Jun. 2012, doi: 10.1021/ef300033u.
[70] “**DIN EN ISO 12846:2012-08**, Wasserbeschaffenheit_- Bestimmung von Quecksilber_- Verfahren mittels Atomabsorptionsspektrometrie (AAS) mit und ohne Anreicherung (ISO_12846:2012); Deutsche Fassung EN_ISO_12846:2012,” Beuth Verlag GmbH. doi: 10.31030/1869854.
[71] **I. Klöfer, M. Bittig, and D. Bathen,** “Quecksilberminderung in der REA-Wäsche, Untersuchungen mit Sulfit als Ligand im Hg-Halogenid-System,” in *Emissionsminderung in Kraftwerken*, Dresden: SAXONIA, 2020, pp. 59–69.
[72] “**DIN 1319-3:1996-05,** Grundlagen der Meßtechnik_- Teil_3: Auswertung von Messungen einer einzelnen Meßgröße, Meßunsicherheit,” Beuth Verlag GmbH. doi: 10.31030/7204542.
[73] **JCGM,** “**JCGM 100:2008** - Evaluation of measurement data- Guid to expression of uncertainty in measurement.” Sep. 2008.
[74] “**DIN 1319-1:1995-01**, Grundlagen der Meßtechnik_- Teil_1: Grundbegriffe,” Beuth Verlag GmbH. doi: 10.31030/2713411.
[75] **M. Pourbaix,** *Atlas of electrochemical equilibria in aqueous solutions*. Houston, Tex.: National Association of Corrosion Engineers, 1974.

VIII. Appendix

Evaluation results of the calculation with Visual MINTEQ

Table A-1 Calculation of the main mercury species in aqueous solution at a pH of 5 with sulfite.

Component	% of total concentration	Species	Component	% of total concentration	Species	Component	% of total concentration	Species	Component	% of total concentration	Species
I^{-1}	12.987	I^{-1}	$Hg(OH)_2$	1.798	$HgCl_2$ (aq)	Br^{1}	99.365	Br^{-1}	Cl^{-1}	99.987	Cl^{-1}
	6.461	HgClI (aq)		1.842	$HgCl_3^{-1}$		0.073	$HgBr_2$ (aq)	SO_3^{-2}	1.061	SO_3^{-2}
	2.358	HgBrI (aq)		0.854	$HgCl_4^{-2}$		0.018	$HgBr_3^{-1}$		0.098	H_2SO_3 (aq)
	1.63	$HgBrI_3^{-2}$		12.923	HgClI (aq)		0.043	HgBrCl (aq)		98.704	HSO_3^-
	1.275	$HgBr_2I_2^{-2}$		0.727	$HgBr_2$ (aq)		0.236	HgBrI (aq)		0.136	$Hg(SO_3)_2^{-2}$
	0.277	$HgBr_3I^{-2}$		0.122	$HgBr_3^{-1}$		0.054	$HgBrI_3^{-2}$			
	69.264	HgI_2 (aq)		0.863	HgBrCl (aq)		0.128	$HgBr_2I_2^{-2}$			
	5.742	HgI_3^{-1}		4.715	HgBrI (aq)		0.083	$HgBr_3I^{-2}$			
Hg_2^{+2}	100	Hg_2^{+2}		1.087	$HgBrI_3^{-2}$						
				1.275	$HgBr_2I_2^{-2}$						
				0.553	$HgBr_3I^{-2}$						
				69.264	HgI_2 (aq)						
				3.828	HgI_3^{-1}						
				0.136	$Hg(SO3)_2^{-2}$						

Table A-2 Calculation of the main mercury species in aqueous solution at a pH of 8 with sulfite.

Component	% of total concentration	Species	Component	% of total concentration	Species	Componen	% of total concentration	Species	Component	% of total concentration	Species
I^{-1}	36.039	I^{-1}	$Hg(OH)_2$	0.026	$Hg(OH)_2$	Br^{-1}	99.233	Br^{-1}	Cl^{-1}	99.998	Cl^{-1}
	1.579	HgClI (aq)		0.158	$HgCl_2$ (aq)		0.052	$HgBr_2$ (aq)	SO_3^{-2}	55.296	SO_3^{-2}
	0.578	HgBrI (aq)		0.162	$HgCl_3^{-1}$		0.013	$HgBr_3^{-1}$		5.143	HSO^{3-}
	3.077	$HgBrI_3^{-2}$		0.075	$HgCl_4^{-2}$		0.031	HgBrCl (aq)		7.136	$Hg(SO_3)_3^{-4}$
	0.871	$HgBr_2I_2^{-2}$		3.158	HgClI (aq)		0.197	HgBrI (aq)		32.425	$Hg(SO_3)_2^{-2}$
	0.068	$HgBr_3I^{-2}$		0.158	HgClOH (aq)		0.062	$HgBrI_3^{-2}$			
	46.957	HgI_2 (aq)		0.064	$HgBr_2$ (aq)		0.124	$HgBr_2I_2^{-2}$			
	10.802	HgI_3^{-1}		0.011	$HgBr_3^{-1}$		0.069	$HgBr_3I^{-2}$			
Hg_2^{+2}	0.029	HgI_4^{-2}		0.076	HgBrCl (aq)		0.219	HgBrOH (aq)			
Hg_2^{+2}	100	Hg_2^{+2}		1.156	HgBrI (aq)						
				2.052	$HgBrI_3^{-2}$						
				0.871	$HgBr_2I_2^{-2}$						
				0.137	$HgBr_3I^{-2}$						
				0.54	HgBrOH (aq)						
				46.957	HgI_2 (aq)						
				7.201	HgI_3^{-1}						
				0.015	HgI_4^{-2}						
				4.757	$Hg(SO_3)_3^{-4}$						
				32.425	$Hg(SO_3)_2^{-2}$						

Multiple regression analysis

Product version:

Minitab® 19.1.1 (64-bit)

Hg(0)

Model Summary

Table A-3 Model summary Hg(0).

S	R-sq	R-sq(adj)	R-sq(pred)
131,383	71,54%	52,56%	4,04%

Analysis of Variance

Table A-4 Analysis of variance Hg(0).

Source	DF	Adj SS	Adj MS	F-Value	P-Value
Regression	6	390486	65081	3,77	0,037
c(Hg) [mg(Hg)*L^-1]	1	196138	196138	11,36	0,008
c(Hal) [mol*L^-1]	1	73317	73317	4,25	0,069
pH	1	21253	21253	1,23	0,296
ORP	1	291	291	0,02	0,900
SO32-	1	49419	49419	2,86	0,125
Metals	1	5105	5105	0,30	0,600
Error	9	155354	17262		
Total	15	545840			

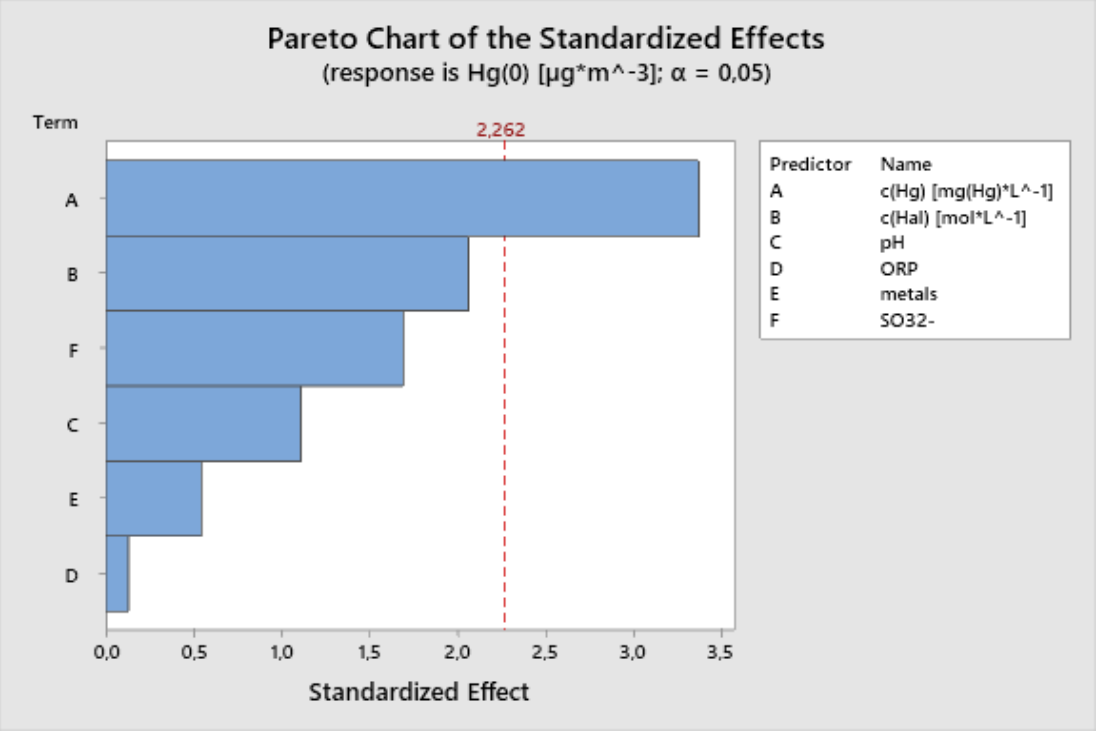

Figure A-1 Pareto chart of standardized effects for Hg(0).

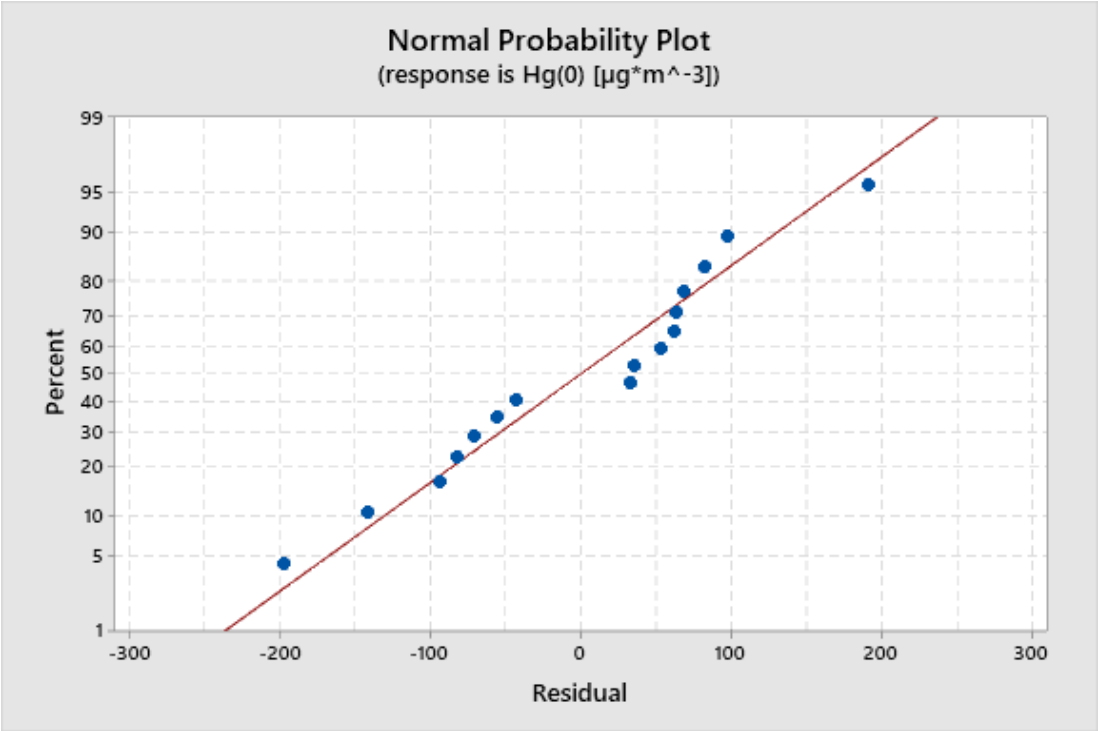

Figure-A-2 Normal probability plot Hg(0).

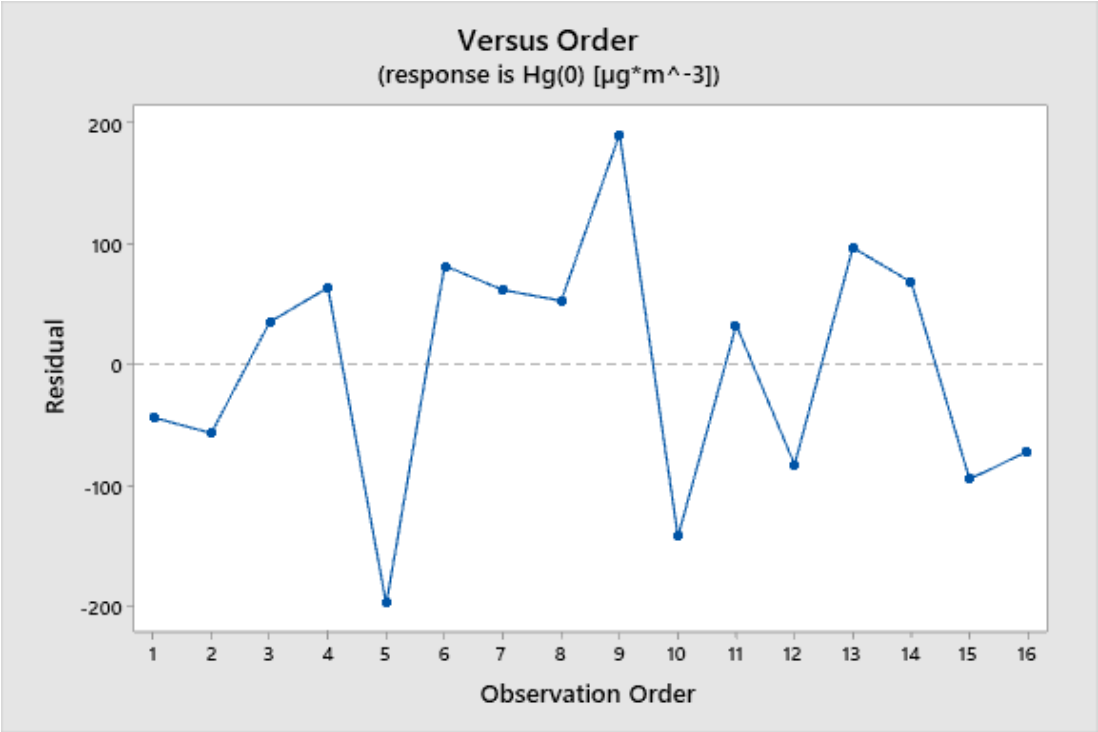

Figure A-3 Versus order Hg(0).

Hg(t)

Coefficients

Table A-5 Coefficients Hg(t).

Term	Coef	SE Coef	T-Value	P-Value	VIF
Constant	776	661	1,17	0,270	
c(Hg) [mg(Hg)*L^-1]	37,1	11,0	3,39	0,008	1,81
c(Hal) [mol*L^-1]	-361	213	-1,69	0,125	1,88
pH	-152	128	-1,18	0,267	1,37
ORP	0,189	0,906	0,21	0,839	1,51
SO32-					
Yes	-113,8	65,1	-1,75	0,114	1,05
Metals					
Yes	60,0	98,2	0,61	0,557	1,79

Model Summary

Table A-6 Model summary Hg(t).

S	R-sq	R-sq(adj)	R-sq(pred)
127,039	70,98%	51,63%	2,56%

Analysis of Variance

Table A-7 Analysis of variance Hg(t).

Source	DF	Adj SS	Adj MS	F-Value	P-Value
Regression	6	355284	59214	3,67	0,040
c(Hg) [mg(Hg)*L^-1]	1	184999	184999	11,46	0,008
c(Hal) [mol*L^-1]	1	46125	46125	2,86	0,125
pH	1	22634	22634	1,40	0,267
ORP	1	702	702	0,04	0,839
SO32-	1	49361	49361	3,06	0,114
Metals	1	6016	6016	0,37	0,557
Error	9	145250	16139		
Total	15	500534			

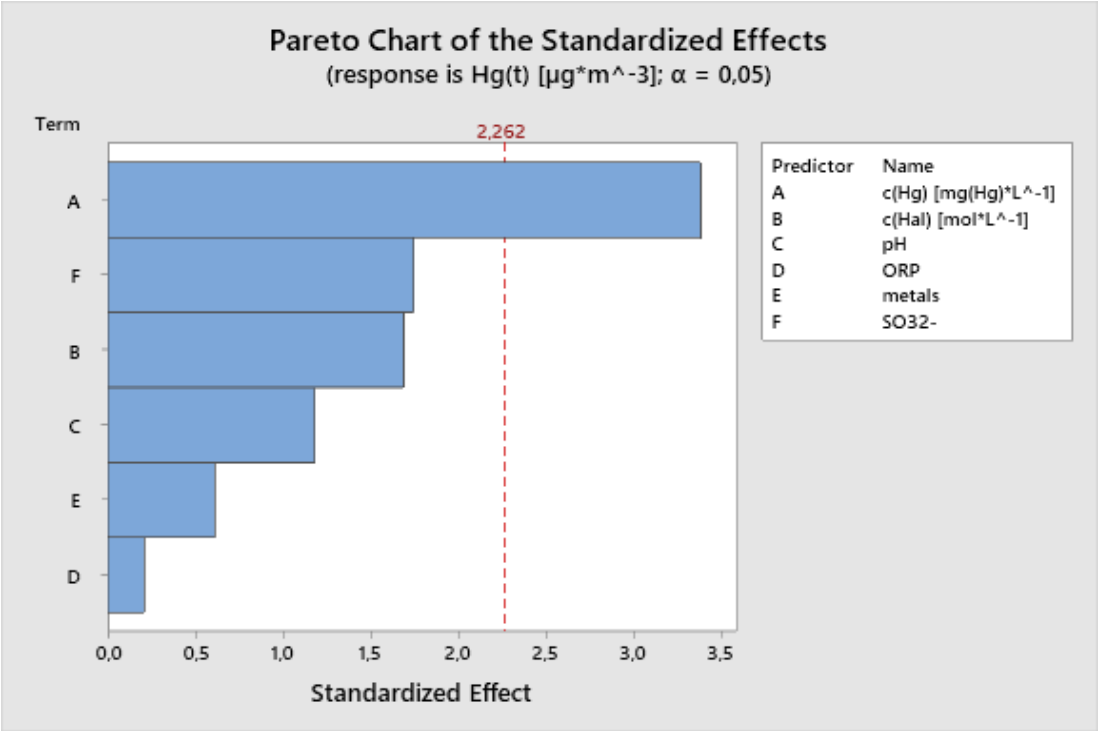

Figure A-4 Pareto chart of the standardized effects Hg(t).

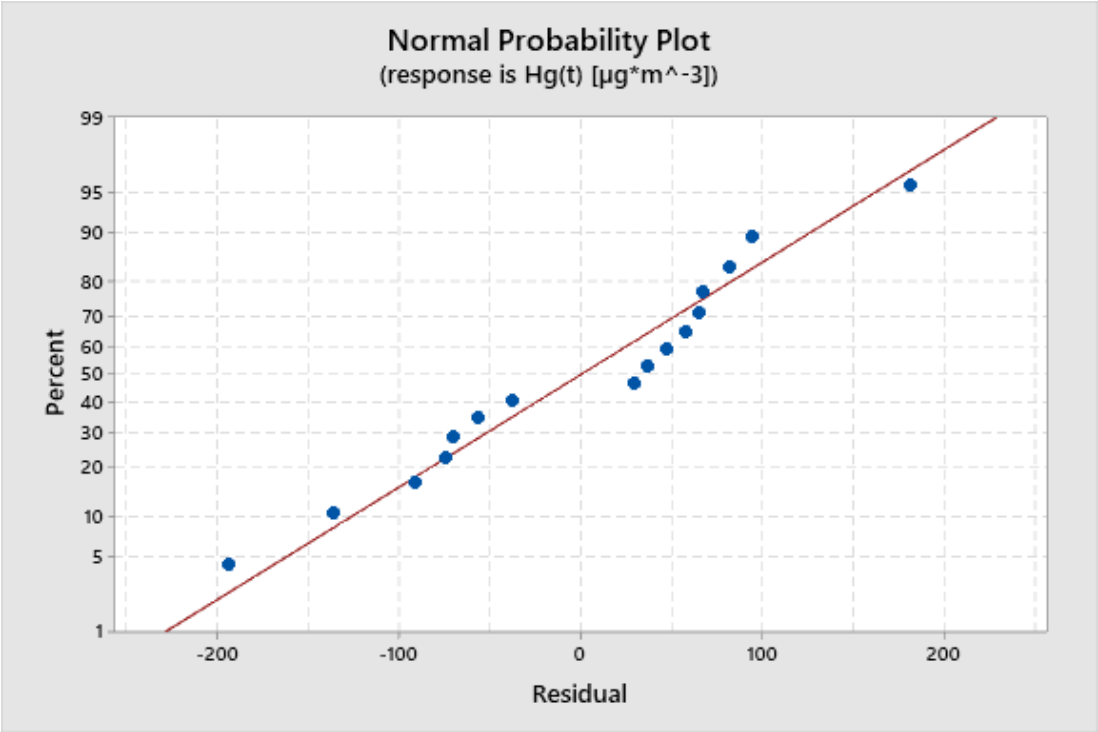

Figure A-5 Normal probability plot Hg(t).

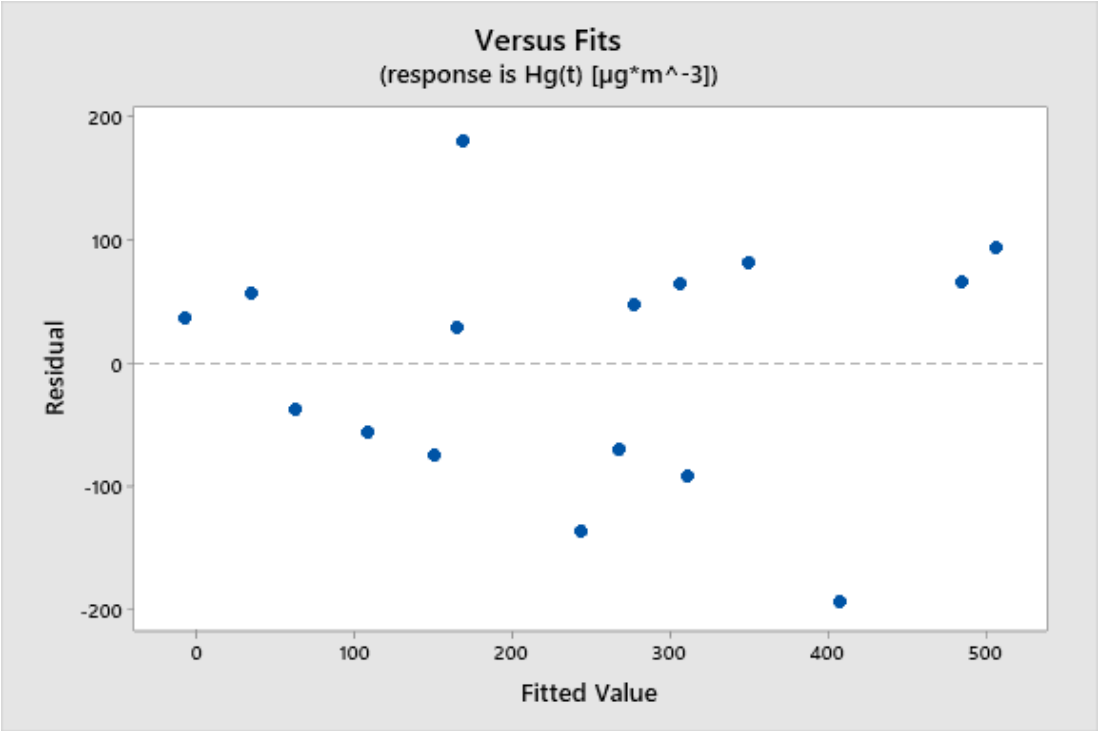

Figure A-6 Versus fits Hg(t).

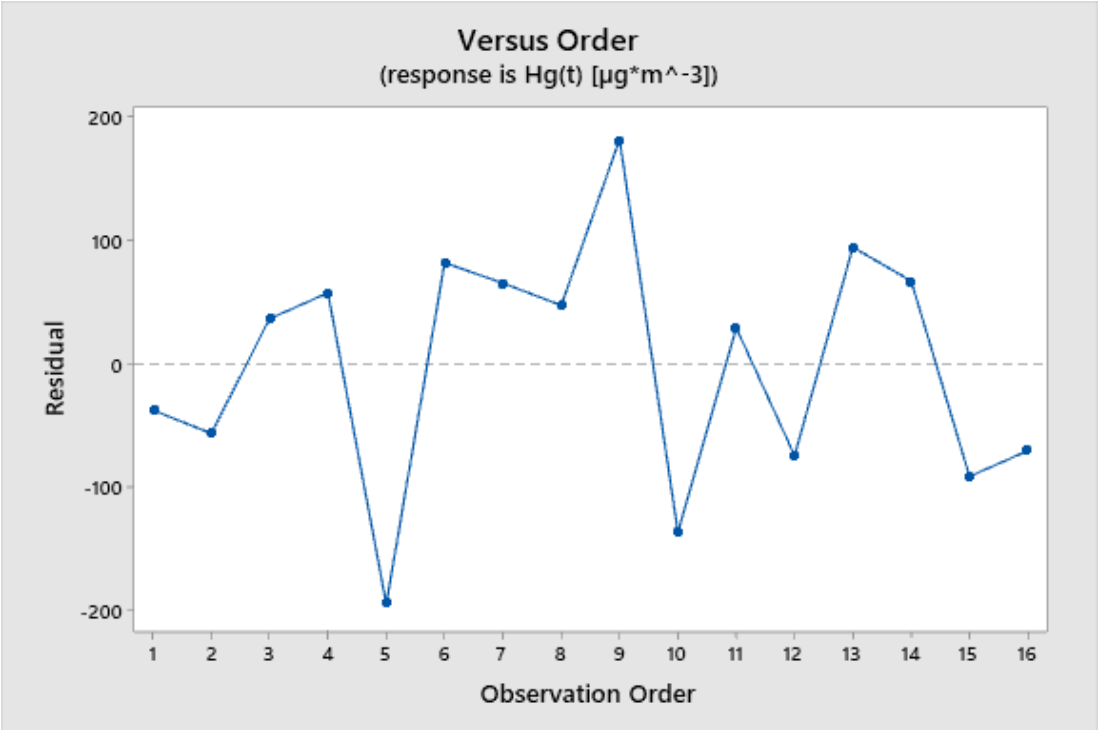

Figure A-7 Versus order Hg(t).

Hg(II)

Coefficients

Table A-8 Coefficients Hg(II).

Term	Coef	SE Coef	T-Value	P-Value	VIF
Constant	4,3	31,5	0,14	0,894	
c(Hg) [mg(Hg)*L^-1]	-1,059	0,523	-2,03	0,074	1,81
c(Hal) [mol*L^-1]	92,4	10,2	9,08	0,000	1,88
pH	-4,00	6,10	-0,66	0,529	1,37
ORP	0,0670	0,0432	1,55	0,155	1,51
SO32-					
Yes	0,13	3,10	0,04	0,967	1,05
Metals					
Yes	4,30	4,68	0,92	0,382	1,79

Model Summary

Table A-9 Model summary Hg(II).

S	R-sq	R-sq(adj)	R-sq(pred)
6,05339	94,27%	90,46%	80,36%

Analysis of Variance

Table A-10 Analysis of variance Hg(II).

Source	DF	Adj SS	Adj MS	F-Value	P-Value
Regression	6	5429,44	904,91	24,69	0,000
c(Hg) [mg(Hg)*L^-1]	1	150,27	150,27	4,10	0,074
c(Hal) [mol*L^-1]	1	3023,63	3023,63	82,51	0,000
pH	1	15,73	15,73	0,43	0,529
ORP	1	88,34	88,34	2,41	0,155
SO32-	1	0,07	0,07	0,00	0,967
Metals	1	30,90	30,90	0,84	0,382
Error	9	329,79	36,64		
Total	15	5759,24			

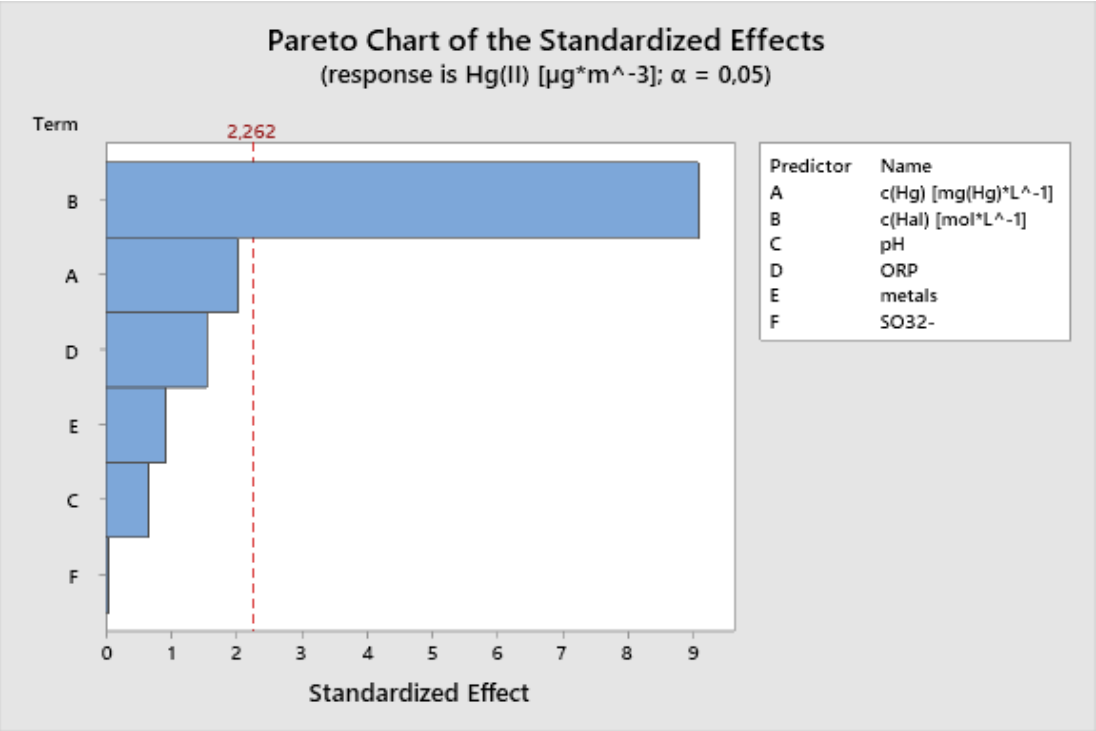

Figure A-8 Pareto chart of the standardized effects Hg(II).

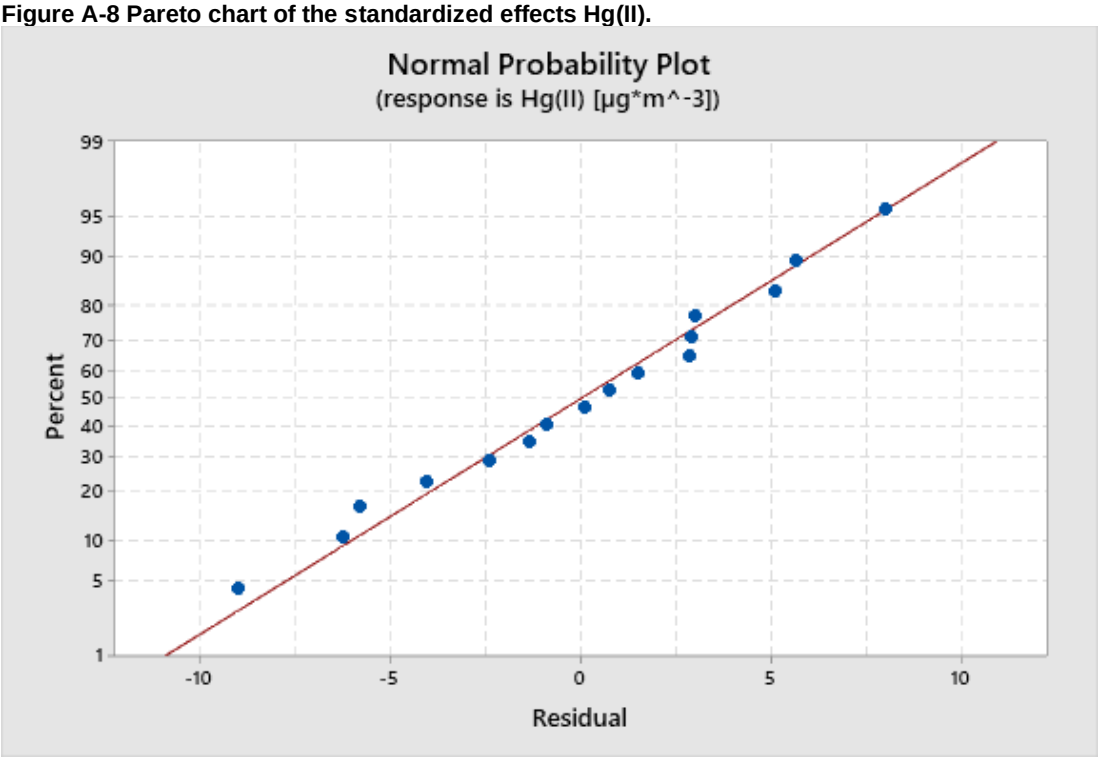

Figure A-9 Normal probability plot Hg(II).

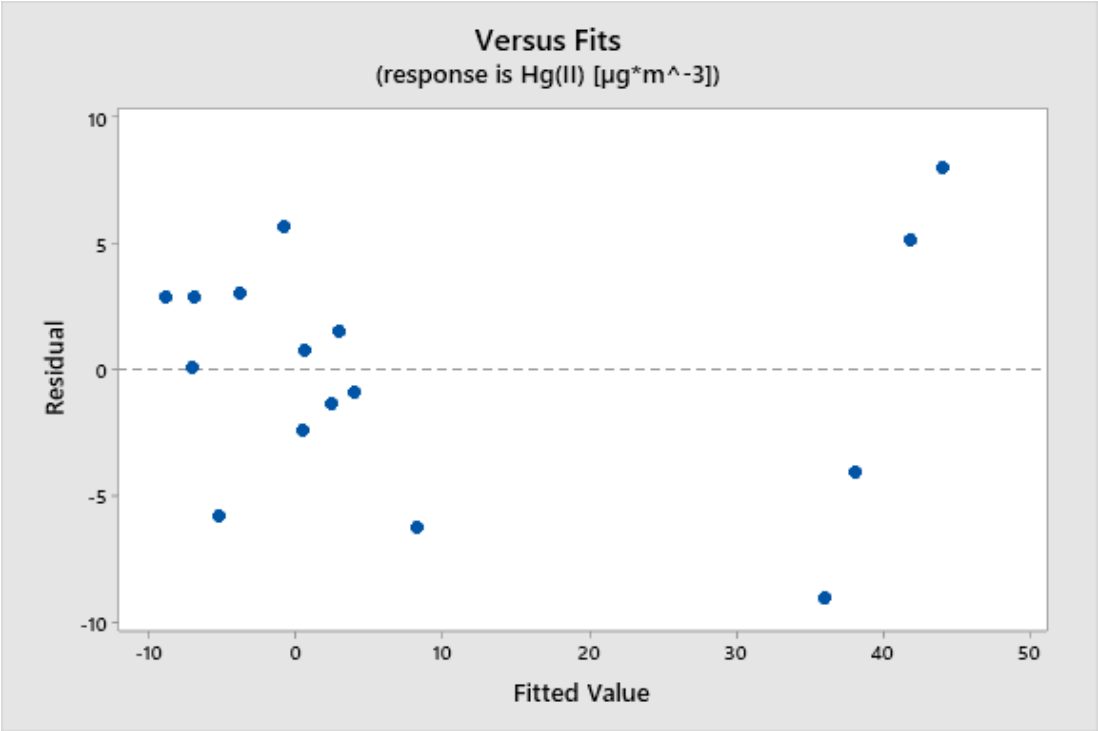

Figure A-10 Versus fits Hg(II).

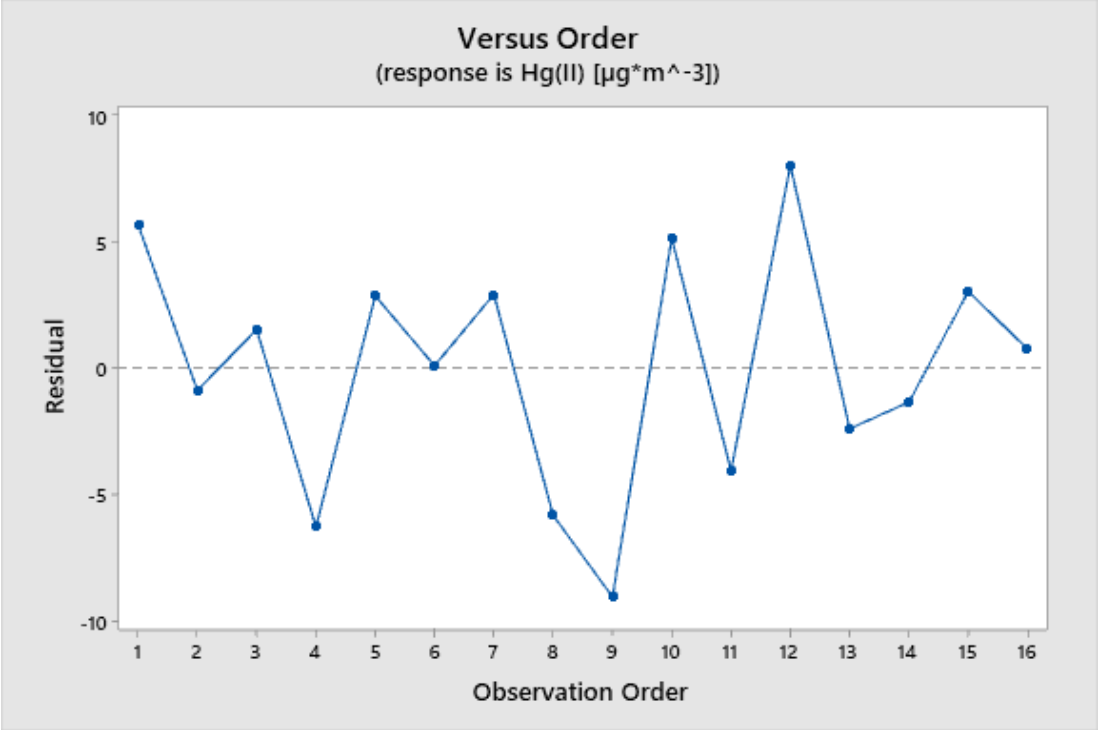

Figure A-11 Versus order Hg(II).

Hg_{aq}

Coefficients

Table A-11 Coefficients Hg_{aq}.

Term	Coef	SE Coef	T-Value	P-Value	VIF
Constant	2,95	5,63	0,52	0,613	
c(Hg) [mg(Hg)*L^-1]	0,4495	0,0935	4,81	0,001	1,81
c(Hal) [mol*L^-1]	3,06	1,82	1,68	0,127	1,88
pH	-0,07	1,09	-0,06	0,951	1,37
ORP	-0,00648	0,00772	-0,84	0,423	1,51
SO32-					
Yes	-2,264	0,555	-4,08	0,003	1,05
Metals					
Yes	-0,891	0,837	-1,06	0,315	1,79

Model Summary

Table A-12 Model summary Hg_{aq}.

S	R-sq	R-sq(adj)	R-sq(pred)
1,08278	88,49%	80,81%	65,05%

Analysis of Variance

Table A-13 Analysis of variance Hg_{aq}.

Source	DF	Adj SS	Adj MS	F-Value	P-Value
Regression	6	81,1097	13,5183	11,53	0,001
c(Hg) [mg(Hg)*L^-1]	1	27,0986	27,0986	23,11	0,001
c(Hal) [mol*L^-1]	1	3,3153	3,3153	2,83	0,127
pH	1	0,0046	0,0046	0,00	0,951
ORP	1	0,8253	0,8253	0,70	0,423
SO32-	1	19,5399	19,5399	16,67	0,003
Metals	1	1,3283	1,3283	1,13	0,315
Error	9	10,5517	1,1724		
Total	15	91,6614			

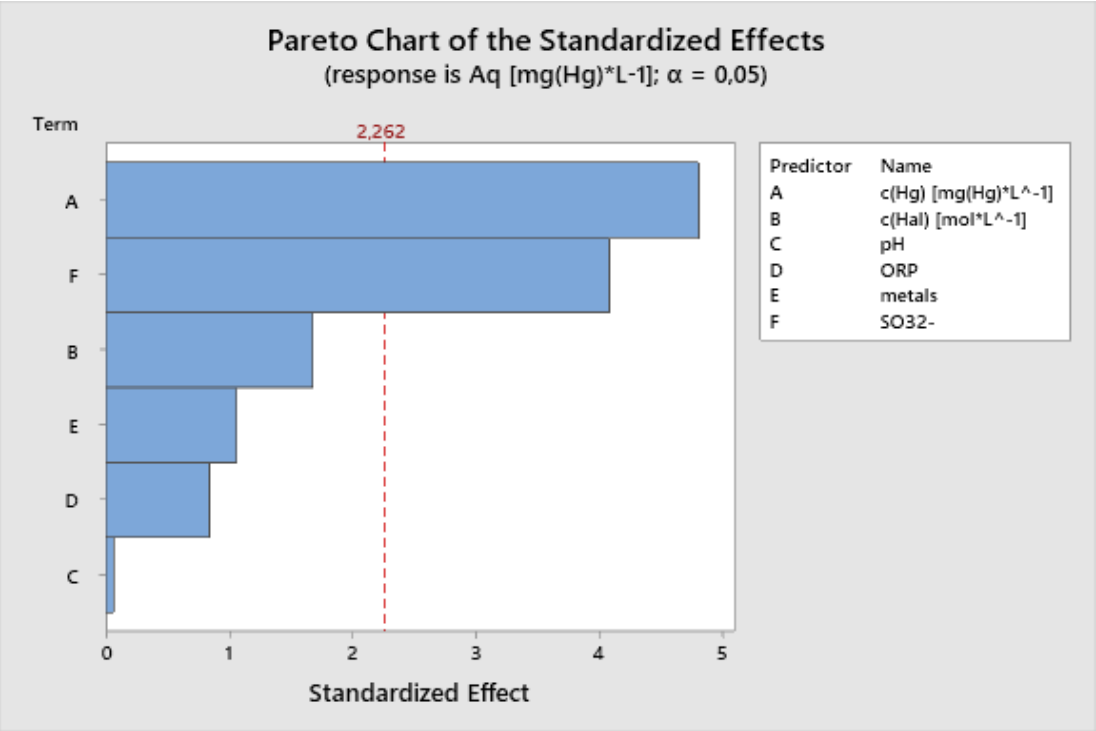

Figure A-12 Pareto chart of the standardized effects Hg_{aq}.

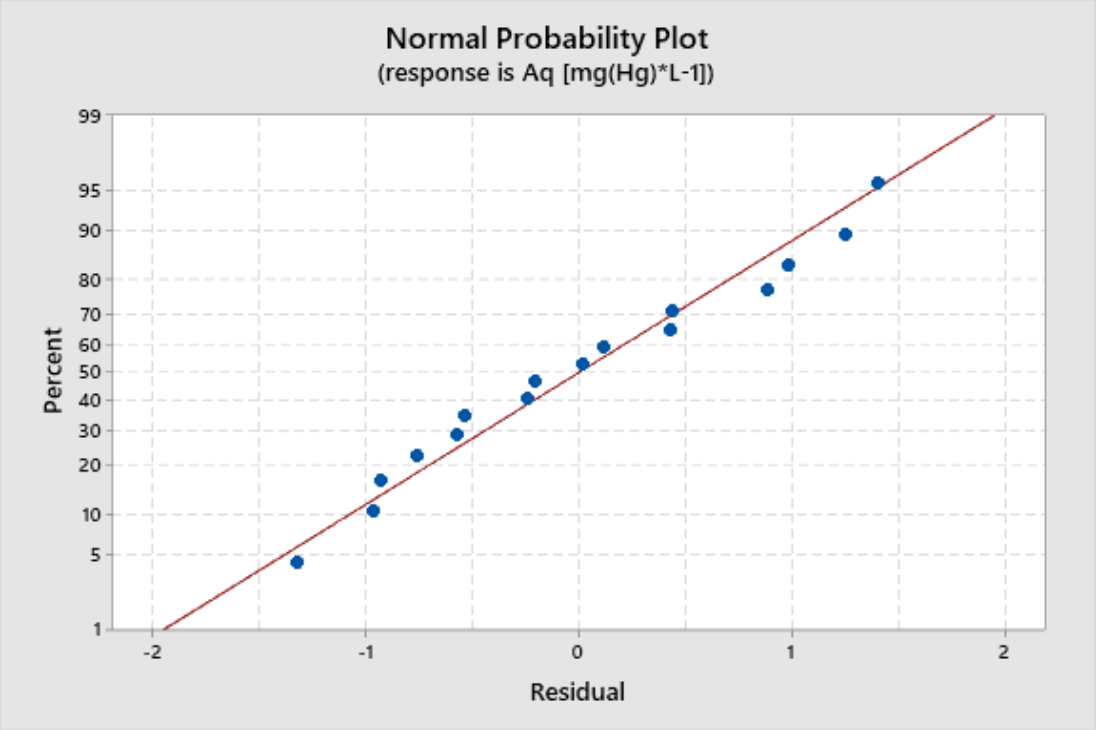

Figure A-13 Normal probability plot Hg_{aq}.

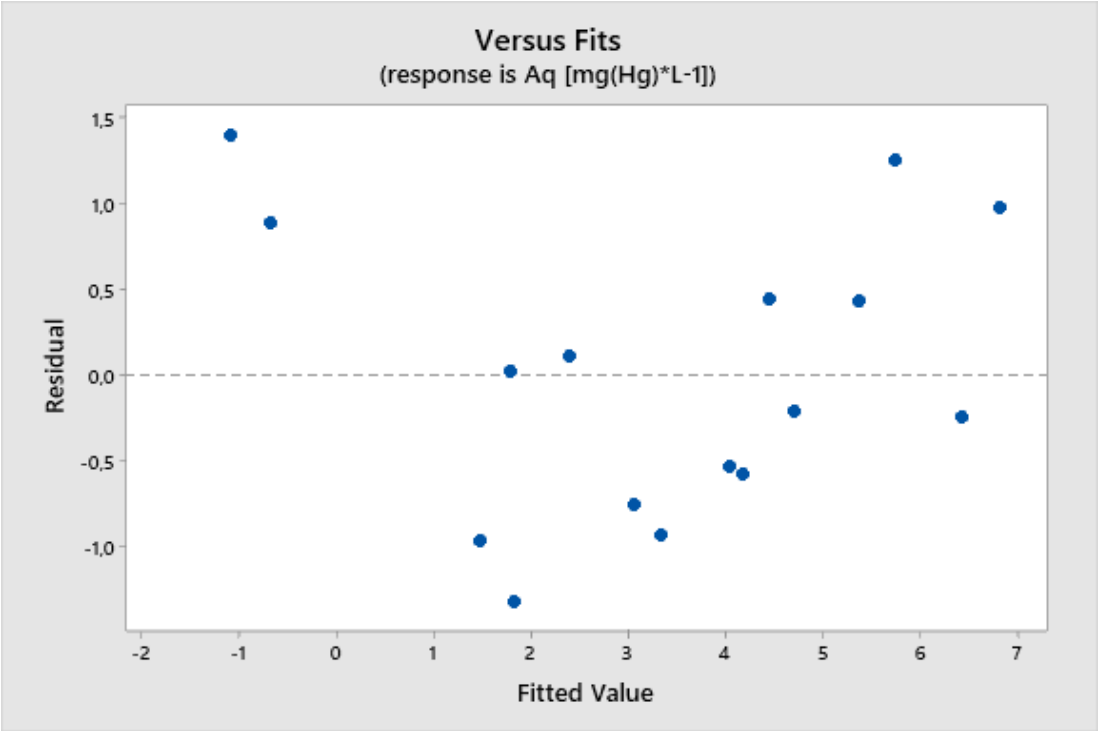

Figure A-14 Versus fits Hg_{aq}.

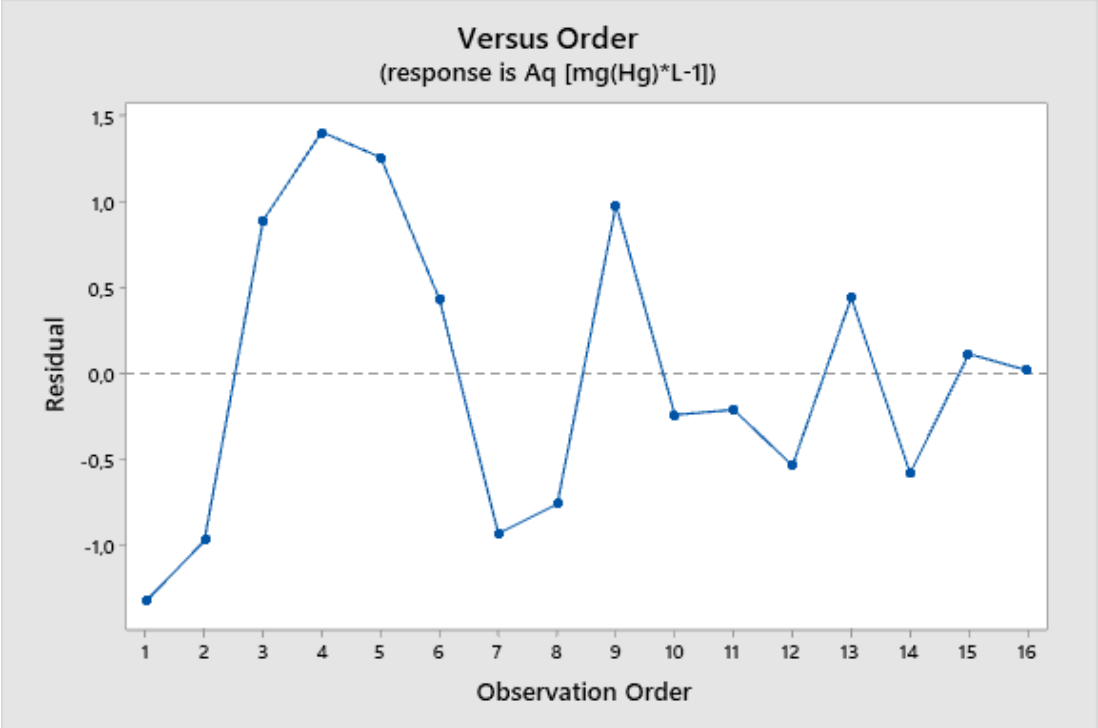

Figure A-15 Versus order Hg_{aq}.

$Hg_{s,\ cumulated}$

Coefficients

Table A-14 Coefficients $Hg_{s,\ cumulated}$.

Term	Coef	SE Coef	T-Value	P-Value	VIF
Constant	-49,2	11,2	-4,39	0,002	
c(Hg) [mg(Hg)*L^-1]	0,060	0,186	0,32	0,753	1,81
c(Hal) [mol*L^-1]	-8,36	3,62	-2,31	0,046	1,88
pH	9,40	2,17	4,33	0,002	1,37
ORP	0,0096	0,0154	0,62	0,549	1,51
SO32-					
Yes	4,96	1,10	4,49	0,002	1,05
Metals					
Yes	4,77	1,67	2,86	0,019	1,79

Model Summary

Table A-15 Model summary $Hg_{s,\ cumulated}$.

S	R-sq	R-sq(adj)	R-sq(pred)
2,15534	91,00%	85,00%	72,82%

Analysis of Variance

Table A-16 Analysis of variance $Hg_{s,\ cumulated}$.

Source	DF	Adj SS	Adj MS	F-Value	P-Value
Regression	6	422,763	70,4605	15,17	0,000
c(Hg) [mg(Hg)*L^-1]	1	0,487	0,4874	0,10	0,753
c(Hal) [mol*L^-1]	1	24,747	24,7470	5,33	0,046
pH	1	87,038	87,0384	18,74	0,002
ORP	1	1,802	1,8020	0,39	0,549
SO32-	1	93,715	93,7150	20,17	0,002
Metals	1	38,063	38,0634	8,19	0,019
Error	9	41,809	4,6455		
Total	15	464,572			

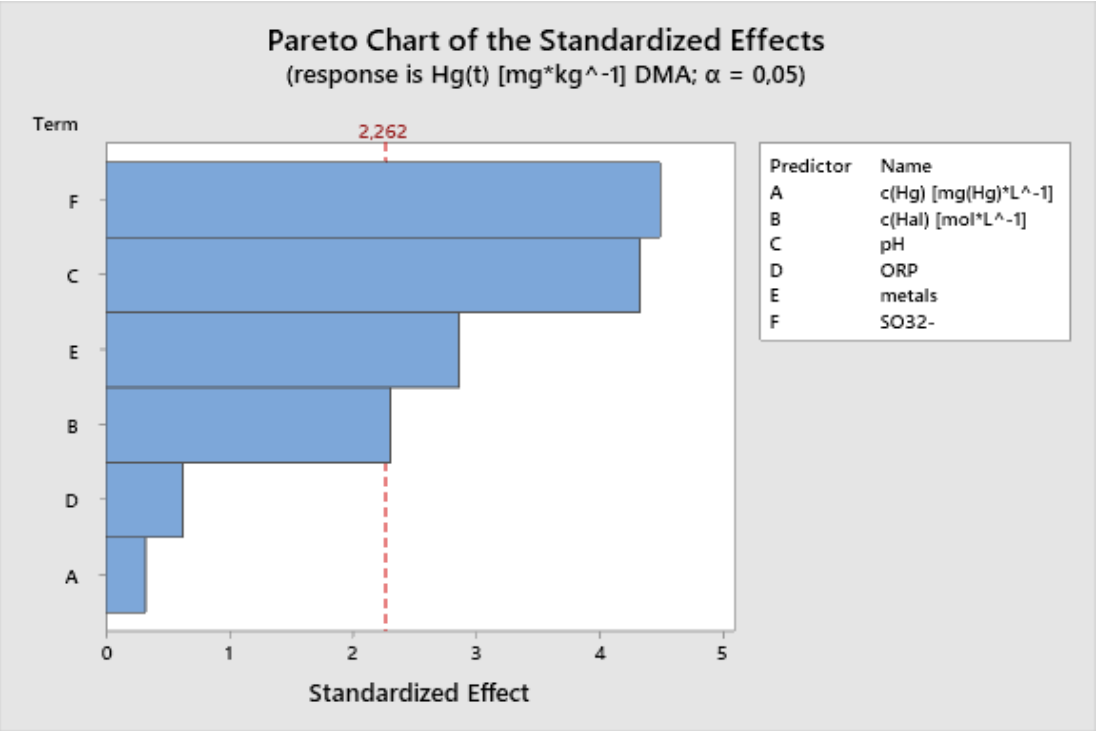

Figure A-16 Pareto chart of the standardized effect $Hg_{s,\ cumulated}$.

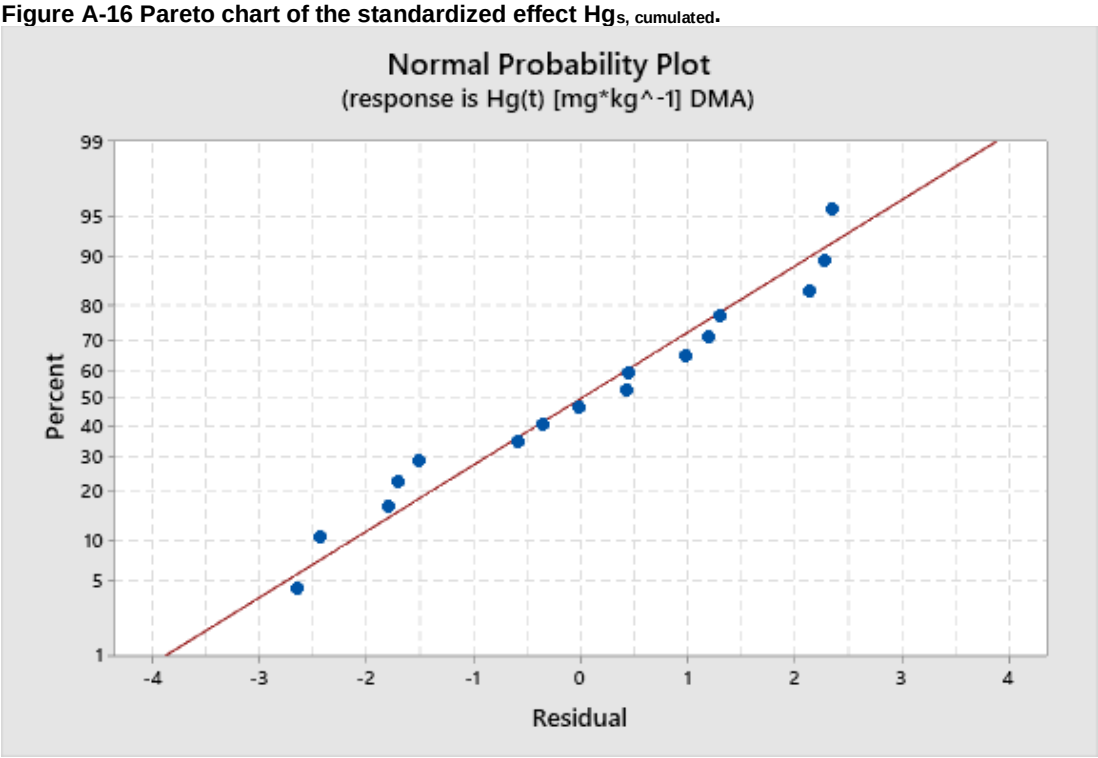

Figure A-17 Normal probability plot $Hg_{s,\ cumulated}$.

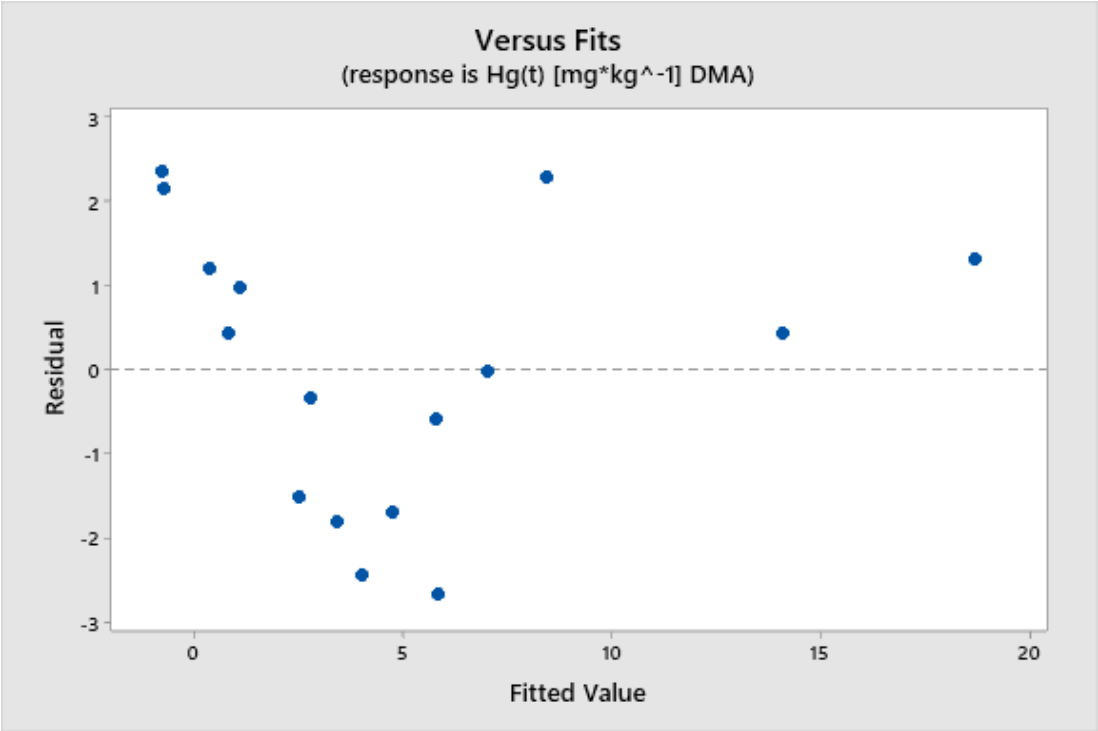

Figure A-18 Versus fits $Hg_{s,\ cumulated}$.

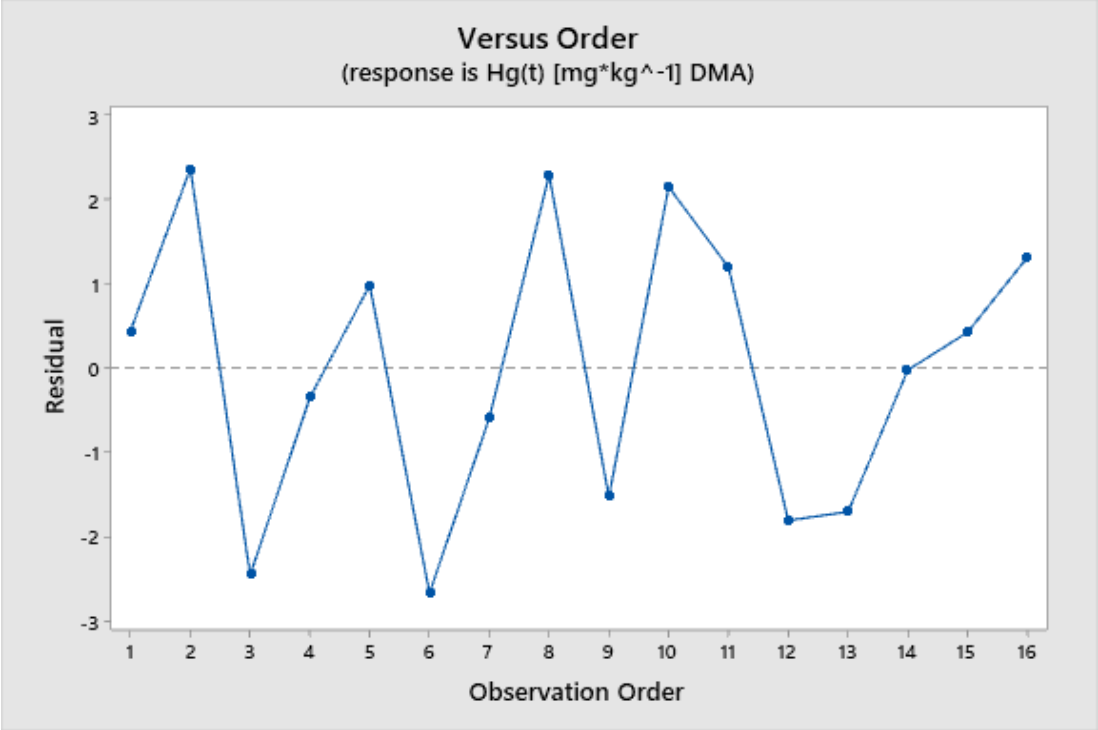

Figure A-19 Versus order $Hg_{s,\ cumulated}$.

$Hg_{s,\ difference}$

Coefficients

Table A-17 Coefficients $Hg_{s,\ difference}$.

Term	Coef	SE Coef	T-Value	P-Value	VIF
Constant	-8,57	6,61	-1,30	0,227	
c(Hal) [mol*L^-1]	-3,91	2,14	-1,83	0,100	1,88
ORP	-0,00686	0,00907	-0,76	0,469	1,51
pH	2,09	1,28	1,63	0,138	1,37
Metals					
Yes	2,469	0,983	2,51	0,033	1,79
c(Hg) [mg(Hg)*L^-1]	0,159	0,110	1,45	0,181	1,81
SO32-					
Yes	1,259	0,651	1,93	0,085	1,05

Model Summary

Table A-18 Model summary $Hg_{s,\ difference}$.

S	R-sq	R-sq(adj)	R-sq(pred)
1,27113	81,72%	69,54%	44,61%

Analysis of Variance

Table A-19 Analysis of variance $Hg_{s,\ difference}$.

Source	DF	Adj SS	Adj MS	F-Value	P-Value
Regression	6	65,0206	10,8368	6,71	0,006
c(Hal) [mol*L^-1]	1	5,4203	5,4203	3,35	0,100
ORP	1	0,9250	0,9250	0,57	0,469
pH	1	4,2910	4,2910	2,66	0,138
Metals	1	10,1988	10,1988	6,31	0,033
c(Hg) [mg(Hg)*L^-1]	1	3,3979	3,3979	2,10	0,181
SO32-	1	6,0361	6,0361	3,74	0,085
Error	9	14,5420	1,6158		
Total	15	79,5626			

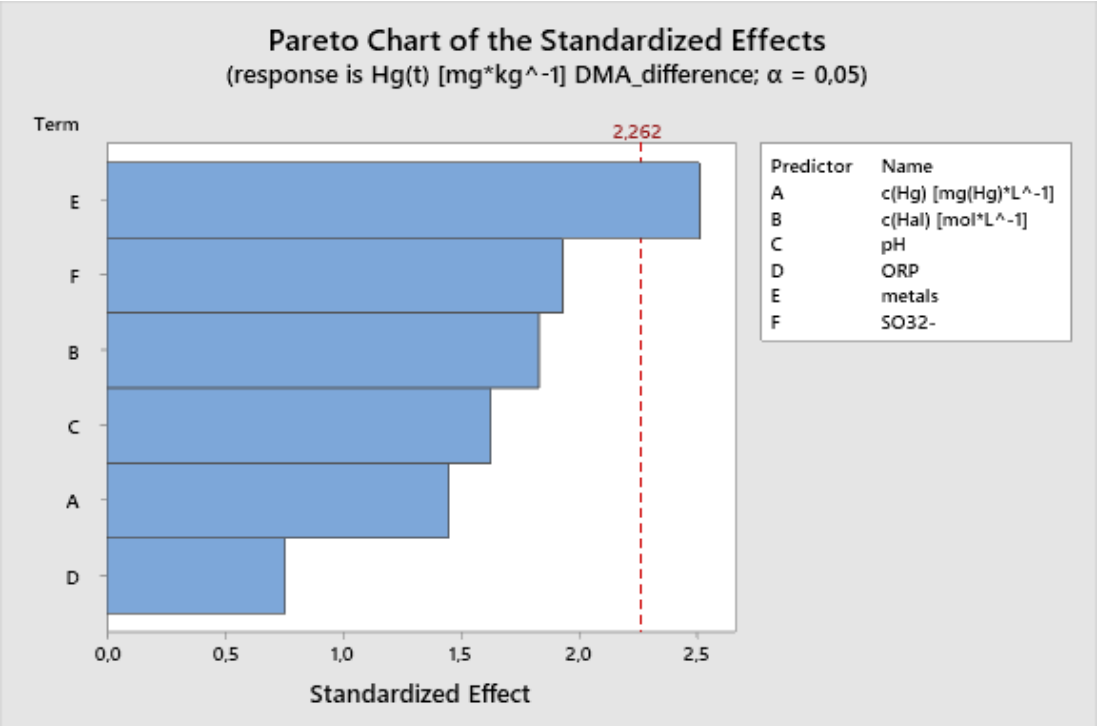

Figure A-20 Pareto chart of the standardized effects $Hg_{s,\ difference}$.

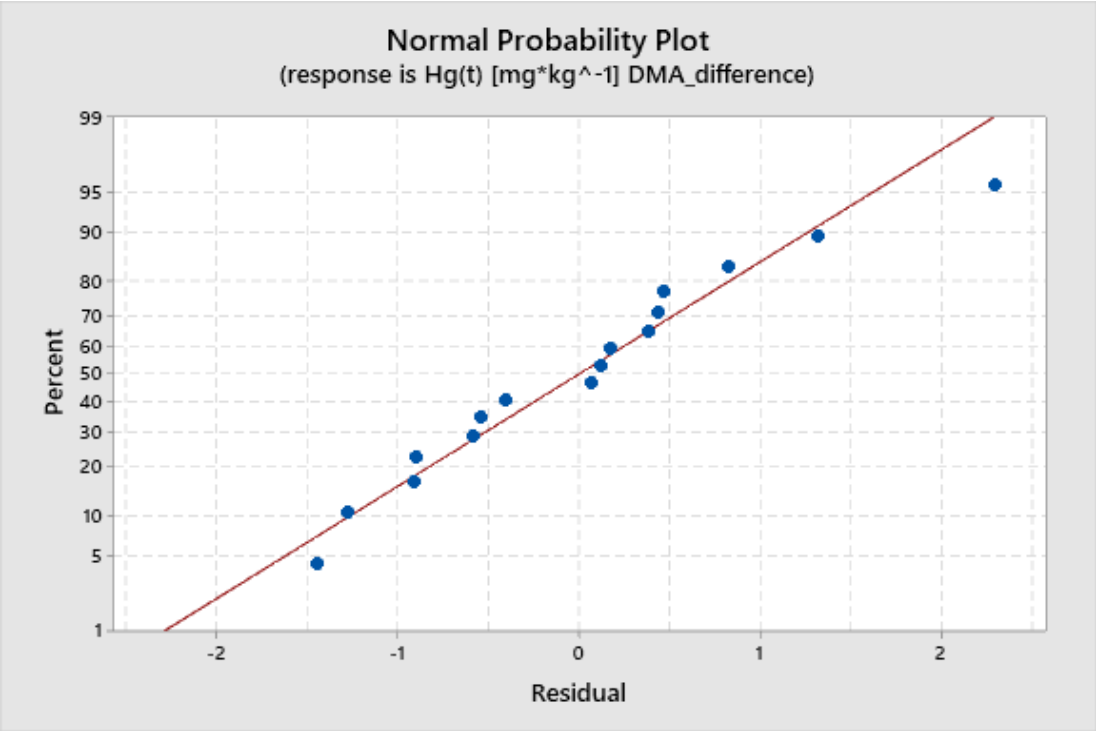

Figure A-21 Normal probability plot $Hg_{s,\ difference}$.

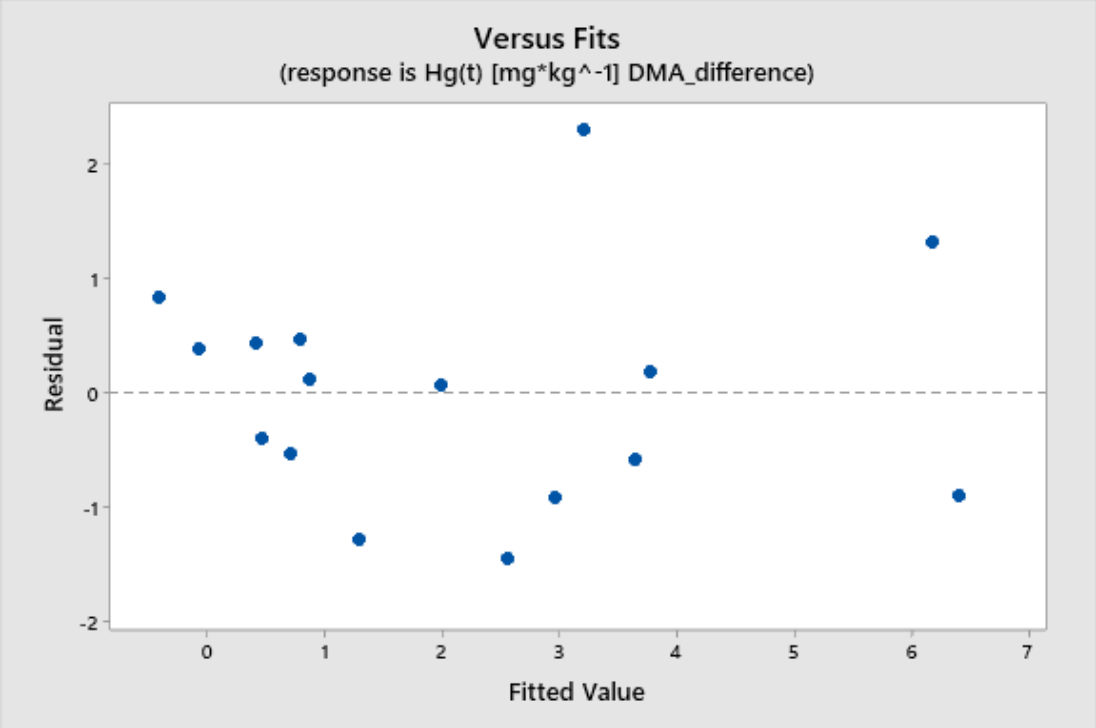

Figure A-22 Versus fits $Hg_{s,\ difference}$.

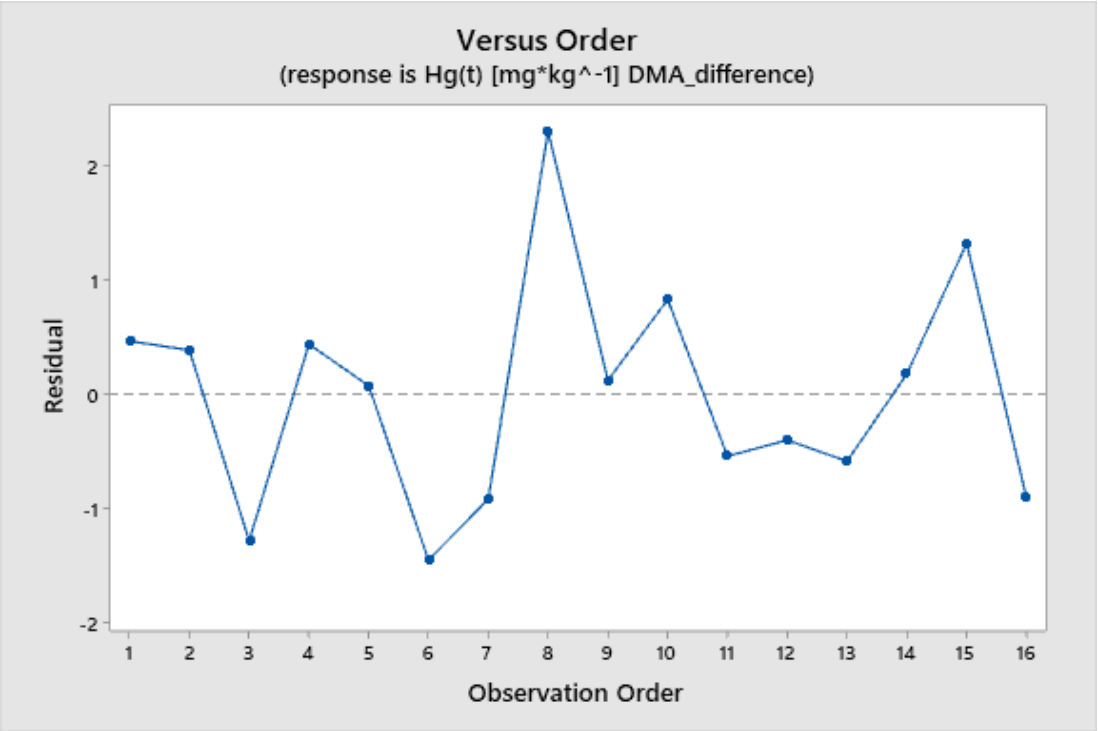

Figure A-23 Versus order $Hg_{s,\ difference}$.

DOI: 10.17185/duepublico/81414
URN: urn:nbn:de:hbz:465-20240126-131759-7